Proceedings of the I·R·E

A Journal of Communications and Electronic Engineering

(Including the WAVES AND ELECTRONS Section)

February, 1948

Volume 36 Number 2

Airborne Instruments Laboratory

AIRCRAFT-ANTENNA PATTERN MEASURING SYSTEM

ectional antenna of special design (on right) is pointed at aircraft under test by dified SCR-584 automatic tracking radar (antenna at left). Antenna provides dis- nination against ground-reflected wave, and provides separate outputs for vertically d horizontally polarized field components, making possible direct plotting of aircraft enna patterns.

PROCEEDINGS OF THE I.R.E.

Waves and Electrons Section

TABLE OF CONTENTS FOLLOWS PAGE 32A

1948 I.R.E. NATIONAL CONVENTION—MARCH 22-25

The Institute of Radio Engineers

NEW!

Commercial Grade Components

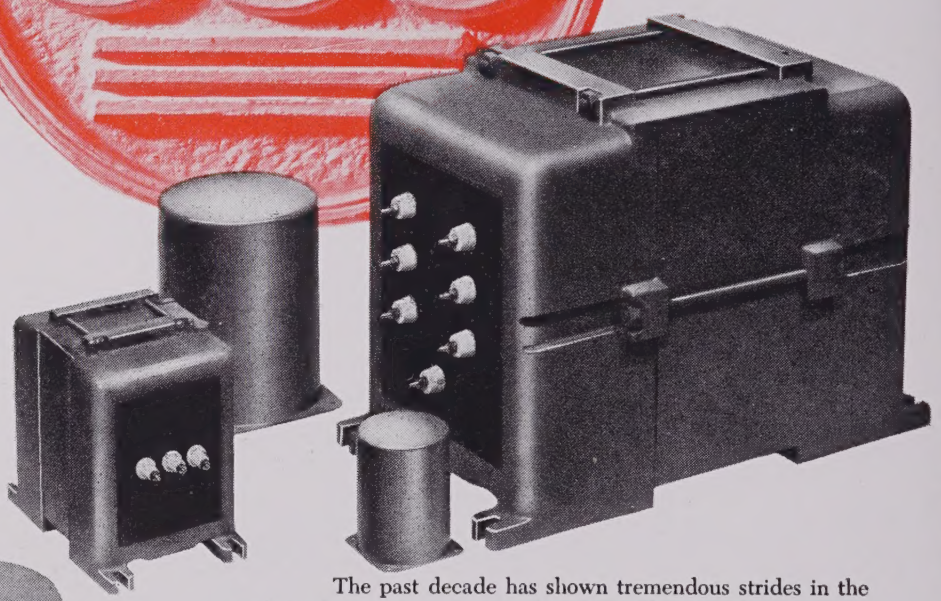

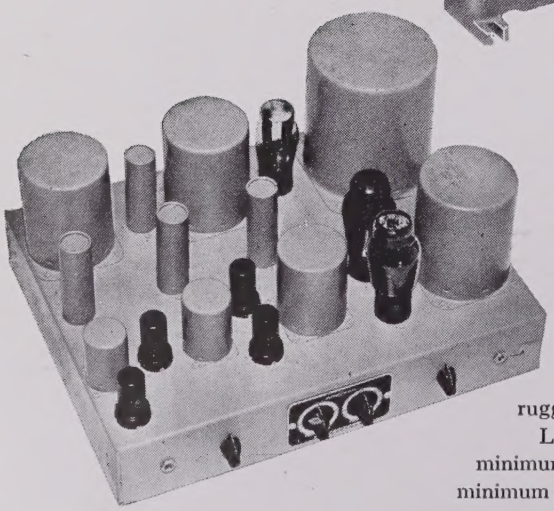

The past decade has shown tremendous strides in the adaptation of electronics to the industrial field. The new UTC Commercial Grade Series of transformers was developed to meet the requirement of this field as well as that of the discriminating amateur and public address man.

CG units are conservatively designed with low temperature rise and good insulation factors to assure dependability in continuous service. All coil structures are vacuum impregnated, and cases are poured with special sealing compounds to assure stability under adverse climatic conditions.

The mechanical construction is rugged. Audio units and power units up to 300 V.A. are housed in heavy drawn steel cases with rugged lugs on moisture-proof bakelite, arranged for chassis mounting. Large power and audio components employ cast aluminum shells for minimum weight, and support the lamination in vertical position to occupy minimum chassis space. CG units are finished in light grey enamel and result in unusual professional appearance on equipment in which they are used.

The CG line includes audio components for all applications ranging from low level... humbucking... multiple alloy shielded input transformers to 600 watt Varimatch modulation transformers. Power and filament components range up to those required for a 3,000 volt 1 Amp. plate supply.

For full details on this new line, write for catalogue PS-408.

United Transformer Corp.

150 VARICK STREET • NEW YORK 13, N. Y.

EXPORT DIVISION: 13 EAST 40th STREET, NEW YORK 16, N. Y. CABLES: "ARLAB"

PROCEEDINGS OF THE I.R.E.

(Including the WAVES AND ELECTRONS Section)

Published Monthly by

The Institute of Radio Engineers, Inc.

VOLUME 36 — *February, 1948* — NUMBER 2

PROCEEDINGS OF THE I.R.E.

INSTITUTE NEWS AND RADIO NOTES SECTION

WAVES AND ELECTRONS SECTION

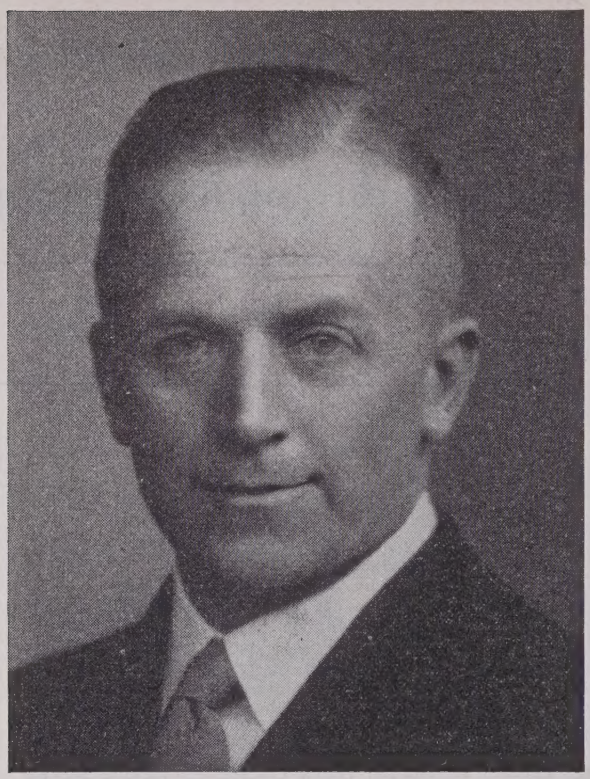

Reginald L. Smith-Rose

VICE-PRESIDENT, 1948

Reginald L. Smith-Rose was born in London, England, in 1894. He received his scientific and technical education at the Imperial College of Science, London University, where he obtained his B.Sc. degree with first class honors in physics in 1914, and the diploma of the Imperial College in electrical engineering in 1915. These courses were followed by four years' practical experience in the works of Messrs. Siemens Brothers, and Company, Limited, where he was engaged in experimental work on automatic telephone systems and the application of valve amplifiers to line communication.

He was one of the earliest members of the London Wireless Club in 1913. This later became the Radio Society of Great Britain, to which Dr. Smith-Rose was elected an Honorary Member in 1942. He joined the scientific staff of the National Physical Laboratory at Teddington, Middlesex, as a member of the Electricity Department in 1919, and later formed the nucleus of the Wireless Division of that department. He has been associated with the work of the Radio Research Board of the Department of Scientific and Industrial Research, London, since the formation of the Board in 1920, and he has been responsible for conducting extensive investigations in radio direction finding, the electrical properties of soil and sea water, and the propagation of radio waves over the ground and through the lower atmosphere. The results of these investigations have been described in numerous papers published in the *Proceedings of the Royal and Physical Societies*, the *Journal of the Institution of Electrical Engineers*, the *Wireless Engineer*, and in the official reports published by H. M. Stationery Office, England. In the course of this research work, he received the degrees of Doctor of Philosophy and Doctor of Science at London University.

In 1939, Dr. Smith-Rose was appointed superintendent of the Radio Division of the National Physical Laboratory and is responsible for both the Slough and Teddington sections of that division. He is a member of the British National Committee for Scientific Radiotelegraphy, and has attended numerous international conferences, including those of U.R.S.I. and C.C.I.R., in Brussels, Bucharest, Copenhagen, London, Paris, Rome, Venice, and Washington.

Dr. Smith-Rose is a member of the Institution of Electrical Engineers, London, was chairman of the Radio Section in 1943, and is the recipient of five Premiums for original papers read before the Institution. He was awarded the Fellowship of The Institute of Radio Engineers in 1945 "in recognition of his pioneer work in the field of direction finding and radio propagation allied to his leadership of an outstanding radio research group"; and it was during his visit to New York in the preceding year that he was instrumental in arranging a closer co-operation between the British Institution of Electrical Engineers and the I.R.E. He is a member of the Liaison Committee of the two bodies. In August 1947, he was awarded the United States Medal of Freedom with Silver Palm for exceptionally meritorious service in scientific research and development, and for his advice, experience and helpful co-operation among English and American scientists.

Dr. Smith-Rose has just been appointed to a new post as director of radio research in an enlarged organization to be established by the Department of Scientific and Industrial Research, in Great Britain.

Technological methods, as recently applied to problems of peace and war, have shown extraordinary, and indeed alarming, capabilities. As a result, engineers and other thoughtful members of the community have begun to question the adequacy of an earlier viewpoint that engineers are concerned solely with the production of equipment and services, but not with their social significance and mode of use.

If engineers desire a voice in the selection and control of the uses of their professional products, they must seriously consider entering the arena of politics and the sphere of government, with all that is thus implied.

The following guest editorial forcefully presents one proposal along these lines. It is from the pen of a skilled communications engineer who has been the editor of a journal in that field, a President of The Institute of Radio Engineers and the mayor of a town of good size.—*The Editor.*

The Engineer's Role in Government

DONALD McNICOL

It has been demonstrated in several instances that engineers are well equipped intellectually to resolve problems of government; local, state, and national. This, because they are trained in resolving engineering problems through the procedures of analyses, blueprints, plans, and estimates. We know, of course, that being equipped to engage in an undertaking may require also knowledge peculiar to the particular undertaking if success is to be attained. There are reasons why in the past not many engineers have looked with favor upon the holding of public office.

The business of politics, which deals with the attainment of and holding of public office, unfortunately has attached to it much that is branded as sordid. Having choice, engineers are averse to being involved in unsavory surroundings. And, as is the experience of the novitiate in most callings, it is necessary for the beginner to serve in a minor capacity, and without money compensation; all of which means that serving the public contains little if any attraction for men whose waking hours appear to be already fully occupied with professional work.

However, there are arriving now new governmental and social concepts that form a background against which, perhaps, engineers' traditional habits of thought may perforce have to undergo orientation. Engineers may not much longer safely remain on the sidelines while events on the national and international levels relentlessly intrude to confuse the capacities of provincial politicos too often thinking mainly in terms of home-town new postoffices. It may be significant that in the press one comes across declarations such as: "Scientists must quit their ivory towers and assume responsibility or stand convicted in the court of public opinion."

In a recent address, Professor W. A. Noyes, of the American Chemical Society, said: "Present leaders of political, social and economic thought are not likely to extend to us gold-edged invitations to join them in developing the master plan for the world of tomorrow, other than to assign to us the usual role of supplying strictly scientific advances. This role we reject. Today scientists recognize that they have greater responsibilities than mere discovery, and are determined to see that what they develop for the betterment of mankind shall not be used for its destruction."

In all of this there is immediate challenge for radio engineers.

The Visibility of Small Echoes on Radar PPI Displays*

RUBY PAYNE-SCOTT†

Summary—**A theory of visibility on an intensity-modulated display is developed. From it is derived a mathematical formula for visibility on a PPI display, and this formula is confirmed by experimental investigations. It is shown that, under favorable conditions, received signals whose power is 15 db below noise level can be observed. Replacement of a linear detector in the receiver by a square-law detector will, under some conditions, produce a further improvement of 3 db. In the visibility formula all the system variables have been grouped into four parameters, and thus it has been possible to provide nomograms enabling the rapid calculation of the minimum visible signal under any set of conditions.**

Introduction

DETECTION OF AN object by radar depends ultimately on the ability of an observer to pick out a small change, in brightness or position, of part of the pattern on the screen of a cathode-ray tube. This ability depends on the one hand on physiological and psychological factors, and on the other, on the parameters of the whole radar system, which determine the nature of the change to be detected. In order to design systems of predictable performance or to compute the effect of any proposed change in a given system, we need to know the laws governing visibility.

A general theory of visibility for an isolated echo on an intensity-modulated display, in particular on that type known as a plan-position indicator or PPI, is developed in this paper. By making certain simplifications, this theory is put in a mathematical form enabling the least visible signal under given conditions to be calculated. The predictions of the theory have been checked on an artificial radar system and found to be generally true. Finally, a series of nomograms are provided, from which the least visible signal under any set of conditions can be read off.

Notation

$P_{\min}$ = minimum visible signal, in terms of available signal power at antenna output terminals (watts)

P_n = available noise power, referred to receiver input terminals, i.e., $MkT\Delta f$ (watts)

N = receiver noise factor

k = boltzmann's constant (watts seconds $^{-1}$ degree^{-1})

T = ambient temperature (°K)

Δf = bandwidth at radio frequency, i.e., $(\int_0^\infty G_f df)/G_0$, where G_f is the gain of the amplifier at frequency f, and G_0 the gain at signal frequency (cycles per second).

τ = pulse duration (microseconds)

r = pulse-repetition frequency (seconds^{-1})

r_c = repetition frequency beyond which noise background is always uniform for given speed of rotation

θ_h = antenna beamwidth in direction of scan (radians)

S = antenna speed of rotation (revolutions per second)

s = rate of time-base sweep (millimeters per microsecond)

d = spot diameter along radius (millimeters)

θ_s = angular spot diameter along arc (radians)

Φ_s = angle subtended by spot at observer's eye (steradians)

I = average brightness of noise on screen

ΔI = r.m.s. deviation of noise brightness from I

δI = peak increment in brightness due to signal

$(\delta I/I)_0$ = minimum visible value of $\delta I/I$

$(\Delta I/I)_0$ = minimum visible value of $\Delta I/I$

$V, \Delta V, \delta V$ = detector output voltages corresponding to $I, \Delta I, \delta I$

n = number of noise pulses averaged on PPI screen

n_c = value of n required to make the noise background uniform

$k_1 = i_p \propto V^{k_1}$, where i_p is the beam current of the indicator tube, and V the driving voltage on the grid

$k_2 = V \propto P^{1/k_2}$, where P is the input receiver power and V the output voltage from the detector; 2 for a linear detector and 1 for a square-law detector.

a, b = constants of long-persistence screen; in time t after sweep, intensity has decayed by $(1+at)^{-b}$; for P7 screen, illuminated to about 0.02 effective foot-candles and excited once per second, $a = 0.15$ second^{-1}, $b = 1.2$

$\alpha = 0$ when $(\tau_s/d) > 2\tau\Delta f$ or background is uniform, $\frac{1}{2}$ otherwise

$\beta = 1$ when $\tau_s/d < 1$, p when $\tau_s/d > 1$

$\gamma = 1$ when $\theta_h/\theta_s < 1$, p when $\theta_h/\theta_s > 1$

$\epsilon = 0$ for uniform backgrounds, $\frac{1}{2}$ for discontinuous background

$p = 2/3$ when $\Phi < \Phi_c$; 0 when $\Phi > \Phi_c$; Φ being solid angle subtended by echo at observer.

The Plan-Position Indicator—A General Theory of Visibility

In a PPI display, the receiver output intensity-modulates a trace that travels out from the center of the cathode-ray-tube screen each time the transmitter

* Decimal classification: R537.131×R116. Original manuscript received by the Institute, January 13, 1947; revised manuscript received, August 6, 1947.

† Council for Scientific and Industrial Research, Chippendale, N.S.W., Australia.

emits a pulse. The trace at the same time rotates in synchronism with the antenna. The screen is made of long-persistence fluorescent material, so that a certain proportion of the brightness produced by the trace at any one bearing persists throughout a revolution of the antenna. Thus the area looked at by the radar is exhibited on the screen as an illuminated map centered on the radar station, any small reflecting object appearing as a bright arc at the appropriate range and bearing. When observing faint echoes, the gain of the receiver is high; so that, in addition to the echoes, there is a background illumination produced by the receiver noise.

Fig. 1 shows graphically how the PPI picture is built up. The wave forms (a) (traced from photographs in a report by Goldstein and Bates)[1] are of single sweeps on a deflection-modulated or class-A display, and may be considered as graphs of the receiver output voltage against time. On each sweep there is one signal pulse, several db above the mean noise level and always occurring at the same time after the start of the sweep. The remaining peaks are due to the receiver noise. This noise originates as a series of impulses (due to Johnson noise in circuit components or shot noise in tubes) which, after passing through the r.f. amplifier, appears as a series of peaks of varying amplitude with characteristic shape. Their shape varies a little with the type of amplifier, but always shows a fast rise and slower fall; its form for an amplifier consisting of five cascaded single-tuned circuits is shown in Fig. 2. The signal pulse also changes its shape on passing through the r.f. amplifier; for a given type of amplifier, the final shape depends only on the product of receiver bandwidth and pulse duration. Fig. 2 also shows the resultant shape of an originally square pulse after passing through five cascaded single-tuned stages. A comparison of the relative shapes of pulse and impulse in Fig. 2 shows that (except when the bandwidth/pulse-duration product is large) the signal and noise pulses are not distinguishable by any difference in shape—a conclusion borne out by the traces in Fig. 1.

The receiver output is next used to intensity-modulate the beam current of the cathode-ray tube (c.r.t.), producing a beam current varying with time as shown in Fig. 1(b). The resulting variation in charge falling on the screen of the c.r.t. gives rise to a proportional variation in the light emitted by the screen. The beam at any instant illuminates a finite area of the screen, having, say, a radial length d and angular width θ_s (see upper part of Fig. 1(c)). Since the time between sweeps is too short for any appreciable decay in light intensity to occur, the brightness at any point is, to a first approximation, the mean of the brightnesses produced by all the sweeps occurring in an angle $\pm\frac{1}{2}\theta_s$, the brightness contributed by each sweep being in turn its average brightness over a distance $\pm d/2$ on either side of the point. Fig. 1(c) shows the brightness resulting from averaging over all sweeps in an angle θ_s and over a distance d along the trace; when d is less than the

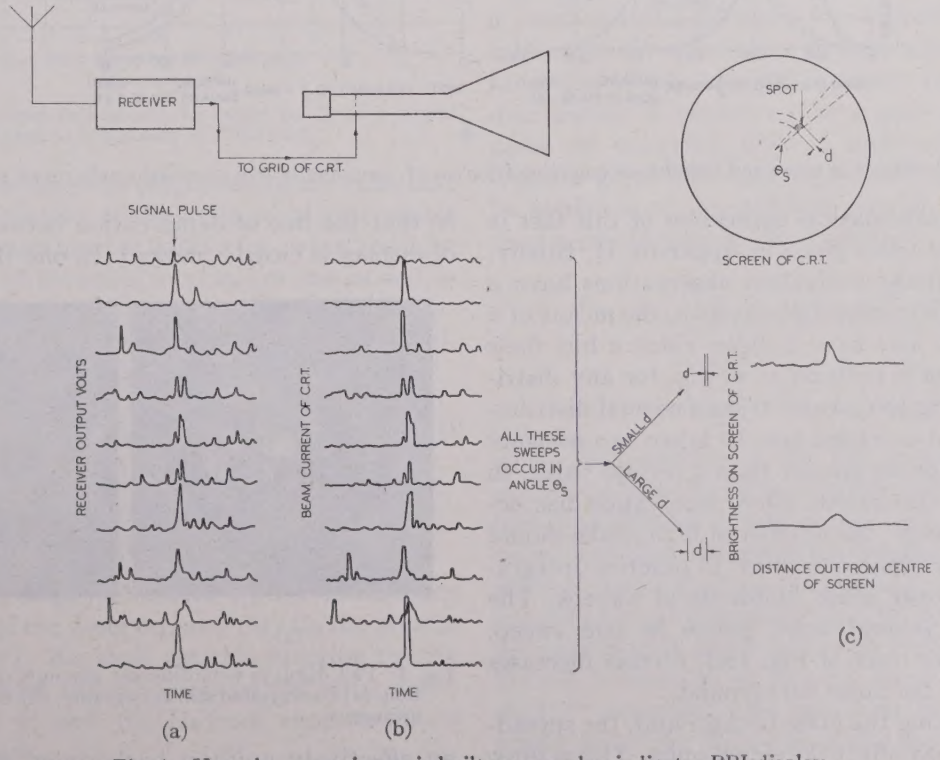

Fig. 1—How the screen image is built upon a plan-indicator PPI display.

length of a pulse (upper trace) its effect is small, but when it is longer than a pulse length (lower trace) its

[1] H. Goldstein and P. D. Bates, "Preliminary Report on the Fluctuations of Radar Signals," *M.I.T. Rad. Lab. Rep.* 569, 1944.

effect is large. A further integrating effect from sweep to sweep is produced by the long persistence of the screen, so that the brightness at a point is built up not only by sweeps occurring in the present revolution but also by sweeps occurring in past revolutions; this effect may be taken into account by increasing by an appropriate factor the number of sweeps integrated in the step from Fig. 1(b) to Fig. 1(c).

It is apparent that in the original receiver output (Fig. 1(a)), it is often very difficult to distinguish the signal pulse from the higher noise pulses, though its power is several decibels above the mean noise power. On the other hand, during integration (Fig. 1(c)) the signal pulse is added at the same position each time, while, owing to the random occurrence of noise peaks, they only coincide at rare intervals, so that the number of high noise peaks diminishes and the possibility of confusing these with the signal pulse correspondingly will occur if the beam width θ_h is less than θ_s, so that a signal pulse only occurs on some of the integrated sweeps; the angular width of the echo will be increased from θ_h to θ_s, with a proportional decrease in brightness.

Fig. 3 shows photographs of two PPI displays, identical except for the amount of background integration. In display (a) the background is still very grainy, while in (b) there is sufficient overlapping of pulses to produce a practically uniform background. This particular display has many defects, but the photographs illustrate the improved visibility of synchronized over random phenomena as integration increases. Not only are small echoes more easily seen on Fig. 3(b) but so are the striations (due to friction in the selsyn drive) and the dark circle (due to a negative kick from the range marker).

It is well known that there is a definite threshold limit to the ability of the eye to distinguish contrast,

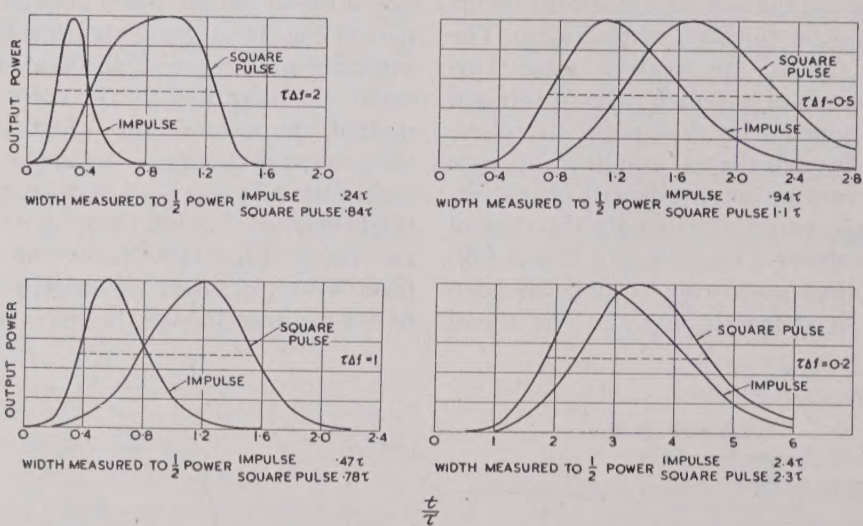

Fig. 2—Shape of pulse and impulse on emerging from an r.f. amplifier of five cascaded single-tuned stages.

decreases. The mathematical expression of this fact is the theorem in statistics given in Appendix II. Briefly, this states that, if the individual observations have a mean value a and a standard deviation σ, the means of n such observations also have a mean value a but their standard deviation is reduced to $\sigma/\sqrt{n}$, for any distribution not differing too greatly from a normal distribution. The standard deviation may be taken as a measure of the number of peaks greater than a certain value, so that in the case illustrated, where integration has occurred over 10 sweeps, the number of high peaks should be reduced by more than one-third. In practice, integration may occur over some hundreds of sweeps. The integration over several noise pulses in one sweep, shown in the lower trace of Fig. 1(c), further increases the uniformity of the noise background.

As well as affecting the noise background, the spreading of the beam may affect the signal pulse. This is illustrated in the lower trace of Fig. 1(c), in which a signal pulse shorter than the spot diameter is spread out with a proportional decrease in brightness. A similar effect so that the line of demarcation between the two types of display is clearly marked. In one (Fig. 3(b)) there is

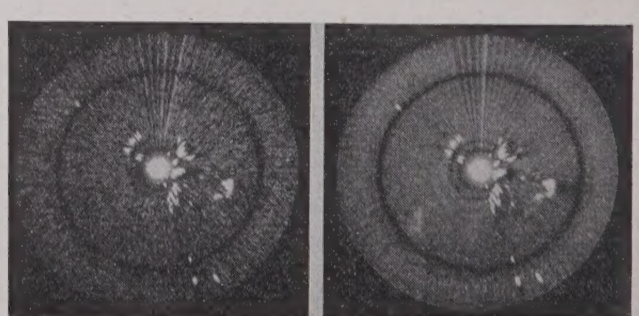

(a) (b)

Fig. 3—PPI displays with different amounts of background integration. (a) Background still very grainy, (b) Background practically uniform.

an effectively uniform background against which the operator is required to detect a bright patch corresponding to the signal; in the other (Fig. 3(a)) the background is still discontinuous and the operator has to

recognize a particular bright patch, the signal, against an aggregate of patches of varying brightnesses due to the noise. The theory of visibility developed here is based on accepting this division, setting up criteria of visibility for each type, and then determining mathematically the way in which these criteria and the type of display depend on the system parameters.

The criteria of visibility for the uniform background are, from physiological experiments, known to be the contrast of the echo against the background ($\delta I/I$), the area of the echo, and the background brightness. Experiments on visibility under conditions somewhat resembling ours were made by Langmuir and Westendorp.[2] A white screen 1.5 meters square could be illuminated at any brightness from that of moonlight (0.023 effective foot-candles (e.f.c.)) down to zero. This maximum brightness is of the order of that used in a PPI display. In the screen were holes of various areas that could be illuminated to any brightness by flashing lamps on and off. From the data given in their paper we have computed the curve of Fig. 4; in this the contrast ($\delta I/I$,

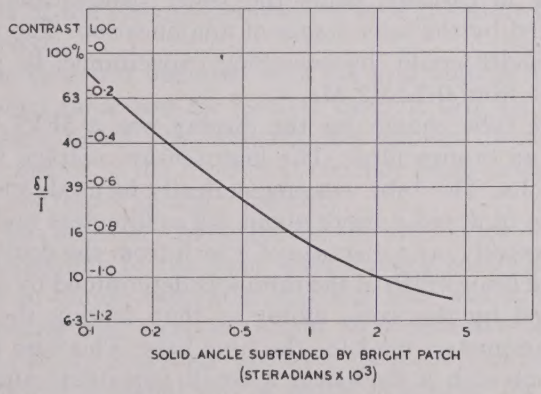

Fig. 4—Contrast required to just see the bright patch on a screen illuminated to brightness of 0.023 e.f.c.

assuming that it is the peak brightness of the echo that counts) required for one of the holes to be just visible against a background level of 0.023 e.f.c., when the light is flashed on and off for equal intervals of one second, is plotted against the solid angle subtended by the hole at the observer's eye. The curve of Fig. 2 may be approximately represented by the function

$$\frac{\delta I}{I} = \left(\frac{\Phi}{\Phi_c}\right)^{-p} \cdot \left(\frac{\delta I}{I}\right)_0 \qquad (1)$$

where

$$p = 2/3 \text{ when } \Phi < \Phi_c$$
$$= 0 \quad \text{when } \Phi > \Phi_c,$$

Φ being the solid angle subtended by the illuminated patch at the eye of the observer, and $(\delta I/I)_0$ the asymptotic value of $\delta I/I$. We shall use this function to give the effect of contrast and echo area on visibility, deriving the values of Φ_c and $(\delta I/I)_0$ from experiments on actual PPI displays.

The background brightness has been assumed unimportant for the following reasons. Langmuir and Westendorp found that decreasing background brightness increased the visibility for a given contrast when they used very small screens; other observers using larger sources and higher background brightness have found the opposite to hold; the size of source and brightness used in PPI displays are about intermediate between these two extremes. In a PPI display the operator is usually allowed to adjust brightness to suit himself, and it is found that the optimum appears to be very flat. It was hence concluded that brightness can be excluded as an important parameter affecting visibility, so long as adequate illumination is available.

The display with a nonuniform background presents the problem of picking out one particular bright patch from a collection usually similar in shape to the one required, a problem apparently not investigated by physiologists, so that we have been forced here to establish our own criteria of visibility. We have assumed that the visibility of the echo (i.e., the reciprocal of the signal power required for detection) is proportional to its brightness relative to that of the unwanted noise peaks, each measured above the mean noise brightness; i.e., that it is proportional to $\delta I/\Delta I$ where ΔI is the standard deviation of the noise. This criterion replaces the contrast $\delta I/I$ in the case of a uniform background. The other criterion is still taken to be the area of the echo.

A Formula for Visibility

In Appendix I the above theory is applied to produce a mathematical formula for visibility, using simple mathematical expressions as approximations to certain functions which actually are very complex (e.g., the distribution of intensity over a spot or the shape of a pulse on emerging from a receiver). The resulting formula gives the least signal power $P_{\min}$ that must be available at the antenna output terminals to produce a visible echo on the display as

$$P_{\min} = \left(\frac{k_2}{k_1}\right) \cdot \frac{P_n}{(1 - e^{-2\tau\Delta f})^2} \cdot \left(\frac{\tau_s}{d}\right)^{-\beta} \cdot \left(\frac{\theta_h}{\theta_s}\right)^{-\gamma} \cdot \left(\frac{\Phi_s}{\Phi_c}\right)^{-p} \cdot \left(\frac{n}{n_c}\right)^{-\epsilon} \cdot \left(\frac{\delta I}{I}\right)_0. \qquad (2)$$

where the meaning of the symbols is set out in the section on notation. The significance of the various factors is as follows: k_1 and k_2 represent the effects of detector law and the grid-bias/beam-current characteristics of the c.r.t.; P_n is the available noise power at the antenna output terminals, i.e., $NkT\Delta f$; $(1-e^{-2\tau\Delta f})$ is the decrease in peak amplitude of the pulse produced by the limited bandwidth of the r.f. amplifier; $(\tau s/d)^{-\beta}$ and $(\theta_h/\theta_s)^{-\gamma}$ represent the reduction in pulse brightness produced by the finite size of the spot and the effect of the echo area; $(n/n_c)^{-\epsilon}$ represents the smoothing of the noise background due to the superposition of pulses; and $(\delta I/I)_0$ is a physical constant of the human eye.

[2] I. Langmuir and W. F. Westendorp, "A study of light signals in aviation and navigation," *Physics I*, p. 273; 1931.

An alternative form of this formula is

$$P_{\min} = \frac{k_2}{k_1} \cdot P_n \cdot \frac{(2\tau\Delta f)^{-\alpha}}{(1 - e^{-2\tau\Delta f})^2} \cdot \left(\frac{\tau_s}{d}\right)^{\alpha-\beta} \cdot \left(\frac{\theta_h}{\theta_s}\right)^{-\gamma} \cdot \left(\frac{r}{r_c}\right)^{-\epsilon} \cdot \left(\frac{\Phi_s}{\Phi_c}\right)^{-p} \cdot \left(\frac{\delta I}{I}\right)_0 \quad (3)$$

where r_c is the pulse-repetition frequency above which, for a given c.r t. and antenna speed, the background is always uniform whatever the values of the other system constants, and is given by

$$r_c = \left(\frac{k_1}{k_2}\right)^2 \cdot \left(\frac{I}{\Delta I}\right)_0^2 \cdot \frac{2\pi S}{\theta_s} \cdot \frac{1 - (1 + a/S)^{-b}}{1 + (1 + a/S)^{-b}} \cdot \quad (4)$$

The condition for the background to be uniform is

$$r > r_c \quad \text{if} \quad \tau s/d > 2\tau\Delta f,$$
$$r \cdot \frac{2\Delta f d}{s} > r_c \quad \text{if} \quad \tau s/d < 2\tau\Delta f. \quad (5)$$

Before discussing this formula in detail, we shall describe the experiments undertaken to check it. At this stage we may observe that, in either form of the equation for visibility, the ratio $P_{\min}/P_n$ is expressed in terms of only four parameters, other than the multipliers k_1 and k_2: $(\delta I/I)_0$ is a physical constant independent of the radar system, as is Φ_c; while for a given type of electron gun Φ_s remains constant, the observer moving backward as the diameter of the tube, and hence the spot size, increases in order to keep the whole field in view. The four parameters may be variously chosen, one convenient group being $\tau\Delta f$, $\tau s/d$, θ_h/θ_s and r/r_c. It is this reduction from the large number of system variables that has permitted the construction of nomograms for calculating the level of signal power required for visibility.

Experimental Arrangement Used to Test Theory

Artificial echoes on a normal noise background were produced by the system shown in Fig. 5. The apparatus allowed a wide range of values of system parameters to be arranged in any desired combination. Fading was not simulated.

The receiver consisted of the following:

(a) A standard preamplifier with damping resistors across the tuned circuits, having an over-all bandwidth of about 4 Mc., followed by (b) a special variable-bandwidth preamplifier, with two stages that could be switched to give the required bandwidth, feeding into (c) a standard radio-frequency channel, having 5 stages with an over-all bandwidth of 3.2 Mc., followed by a linear detector, video amplifier, and cathode follower.

All receiver circuits were single-tuned. The heavily damped initial stages were found necessary to ensure that the noise factor of the receiver was not affected by the bandwidth switching. The gain of the output stages was also switched, so that the receiver noise output was constant, and hence the same part of the detector curve was always used. A variable bandwidth in at least two stages was considered necessary to give a fair comparison with actual receivers. Even then the selectivity curves for the various bandwidths were not geometrically similar, as the narrow bandwidths were produced effectively by only the two variable bandwidth stages in cascade, while the wider bandwidths were affected by the later stages of amplification. The video bandwidth could, by switching capacitance, be given values from 0.2 to 2 Mc.

The tube chosen for the display was a 5FP7, used with an orange filter. The high-tension voltage was 6 kilovolts. The tube was magnetically focused, and the values of d and θ_s were about 0.6 millimeters and 1.1° respectively, at a distance of 1 inch from the center.

The beamwidth of the echo was determined by a cam rotated by the same motor as that driving the sine potentiometers used for the time base. This cam made contact with a stud over a small adjustable angle in each rotation. The bearing angle at which contact was made could be varied.

The whole system was set up in a small darkened cubicle. As it has been shown that general illumination of the same order as the trace brightness does not affect visibility and is less tiring for the operators, most of the measurements were made with a low general illumination provided by diffused light from a low-power lamp near the ceiling. The face of the c.r.t. was shielded

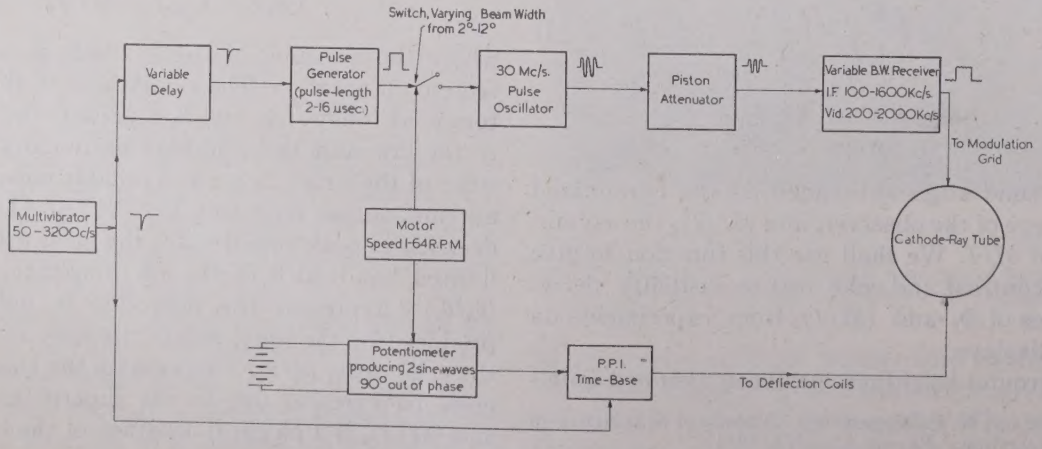

Fig. 5—Block diagram of an artificial radar set.

by a hood. The observer was seated with his head on a level with the tube and about 15 inches from its face.

To make an observation, the system variables were set to the required values, and the attenuator turned back until the echo was no longer visible. The bearing of the echo was altered to some value unknown to the observer, and he was then asked to turn the attenuator up until he was just certain that he saw the echo. The echo was always placed 1 inch from the center of the tube. Thus the problem was to pick out an echo of known shape and range but unknown bearing; lack of knowledge of bearing precluded guessing. In any one sequence the observations were taken in random order, so that any variations with time in equipment or observer should not have a systematic effect. Readings were taken by three observers—the writer, and two Royal Australian Air Force operators whose experience had been mainly with deflection-modulated (class-A) displays. After a learning period of a few observational hours, the average absolute difference between readings from any two of the observers was less than 1 db and the effects of the various parameters were the same for all observers.

The tube was operated with the grid voltage at cut-off when there was no receiver output, this being the optimum bias.[3] The observer was allowed to set the gain control to the level he preferred; small deviations were not found to affect visibility.

It was necessary to determine the attenuator reading corresponding to the noise level at each bandwidth in order to obtain the ratio P_{min}/P_n. This was achieved by feeding the receiver output to a deflection-modulated display at a high repetition frequency, measuring the height of signal and of signal plus noise for some convenient attenuator setting, and calculating the ratio of signal-to-noise power from the known detector law. This method may give rise to an error of the order of 1 db.

Comparison of Theory and Experiment

Using the equipment and procedure described in the preceding section, each of the available parameters was varied through its range of values and the consequent variation in visibility compared with that predicted from (3). Usually only one parameter at a time was varied, but in investigating the effects of pulse length and sweep rate, it was convenient to vary bandwidth at the same time to keep the product $\tau\Delta f$ constant. Finally, the signal power required for visibility under the best conditions that could be attained was measured.

Fig. 7 shows typical experimental observations, together with the corresponding theoretical curves, and is discussed in detail below. In this figure, results for the variation in visibility with bandwidth give the value of P_{min}, the input signal power required, in decibels above an arbitrary level that may vary from one set of curves to the next (but is the same for all the curves of one set). For all other parameters the quantity plotted is the ratio P_{min}/P_n. As mentioned in the previous section, this ratio is not known to better than 1 db. Also, there may be a further slight variation between different curves, because only for the results on ultimate visibility (Fig. 7.7) were the measurements of noise power made at the same time as the observations; at other times values measured perhaps a few days previously were used.

1. Effect of R.F. Bandwidth (Pulse Duration and Sweep Rate Constant).

Equation (3) gives, setting P_n equal to $kT\Delta f$,

$$P_{min} \propto \frac{(\tau\Delta f)^{1-\alpha}}{(1-e^{-2\tau\Delta f})^2} \text{ for constant } \tau,$$

$$P_{min} \propto \frac{\tau\Delta f}{(1-e^{-2\tau\Delta f})^2} \text{ when the background is uniform or when } \tau s/d > 2\tau\Delta f; \quad (6)$$

otherwise,

$$P_{min} \propto \frac{\sqrt{\tau\Delta f}}{(1-e^{-2\tau\Delta f})^2}. \quad (7)$$

Graphs of these two functions of $\tau\Delta f$, expressed in decibels below an arbitrary level, are shown in Fig. 6. The curve for the relative visibility under any given conditions as a function of $\tau\Delta f$ is then made up from the appropriate parts of these curves. This has been done in Fig. 7.1, in which observations on the experimental system and the corresponding predicted curves are plotted. The agreement is fairly good; some error will be introduced by the previously mentioned variation in shape of the receiver selectivity curve with bandwidth.

The optimum value of $\tau\Delta f$ varies slightly with the parameters, lying between 0.63 and 1.17, the maxima of the two curves shown in Fig. 6. The optimum is flat, and

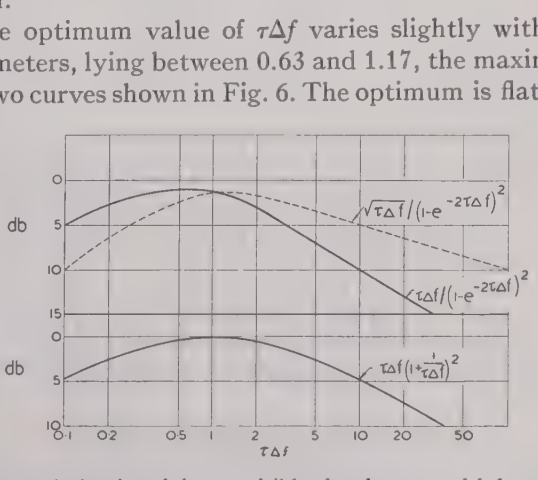

Fig. 6—Variation in minimum visible signal power with bandwidth versus pulse-duration product.

the loss resulting from making $\tau\Delta f$ equal to unity is never more than 0.4 db.

The empirical function $\tau\Delta f[1+(1/\tau\Delta f)]^2$, found by Haeff[4] to fit his measurements on deflection-modulated (class-A) displays, is also shown in Fig. 6. It is apparent that it gives the same results as the present

[3] W. B. Nottingham, "Conference on P7 Cathode-Ray Tubes," *M.I.T. Rad. Lab. Rep.* 62-7, 1943.

[4] A. V. Haeff (unpublished work), Naval Research Laboratory, Washington D. C., 1943.

theory if P_{min} varies as in (7) for values of $\tau\Delta f$ between 0.5 and 10 and as in (6) outside these limits; such displays are the most common, corresponding to a pulse length about equal to the spot diameter and a background discontinuous except for very large bandwidths.

2. Effect of Pulse Duration and Sweep Rate ($\tau\Delta f$ constant).

When the length of the pulse on the screen would be less than the pulse diameter,

$$P_{min} \propto \frac{(\tau s)^{-1}}{\tau}$$

when the background is uniform or $(\tau s/d) > 2\tau\Delta f$; otherwise,

$$P_{min} \propto \frac{(\tau s)^{-1/2}}{\tau}.$$

otherwise,

$$P_{min} \propto \frac{(\tau s)^{-p+1/2}}{\tau}. \qquad (9)$$

It is apparent that, under all circumstances, the visibility improves with increasing pulse duration; at least uniformly as the pulse duration, and under some circumstances as the square of the pulse duration. This is due to the decreased noise accepted by the narrow bandwidths that can be used with long pulses.

Let us now consider the effect of altering sweep rate, i.e., altering the length of the pulse on the screen, for a given pulse duration.

As long as the pulse length (τs) would be less than the spot diameter, the visibility improves as the pulse length if the background is uniform or if $\tau s/d > 2\tau\Delta f$, and otherwise improves as the square root of the pulse length.

A little consideration of the conditions when the pulse length is greater than the spot diameter shows that,

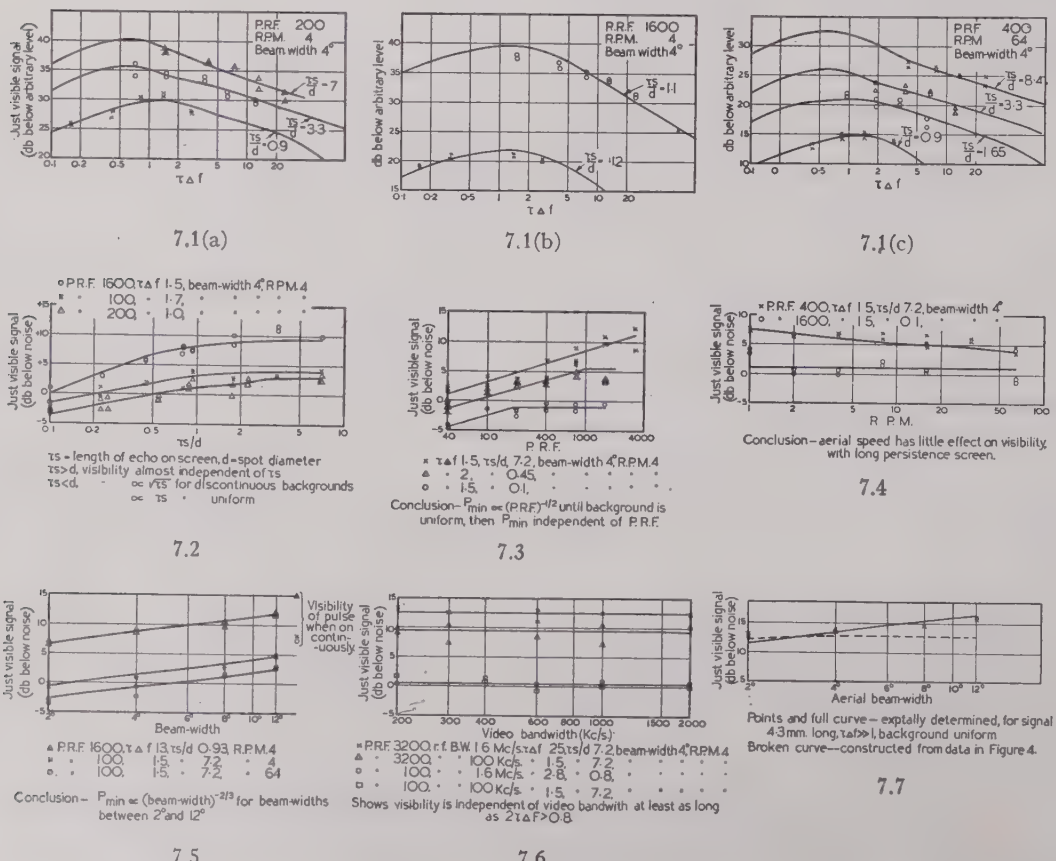

Fig. 7—Effect of various system parameters on visibility (curves are theoretical, points are experimental). 7.1—Effect of r.f. bandwidth. 7.2—Effect of pulse-length. 7.3—Effect of pulse repetition frequency. 7.4—Effect of antenna speed. 7.5—Effect of antenna beamwidth. 7.6—Effect of video bandwidth. 7.7—Ultimate limit of visibility.

For pulse lengths greater than the spot diameter,

$$P_{min} \propto \frac{(\tau s)^{-p}}{\tau} \qquad (8)$$

when the background is uniform, or $(\tau s/d > 2\tau\Delta f)$; when the conditions for (8) obtain, p is usually zero, while when those for (9) obtain, p is usually $\frac{2}{3}$, so that the visibility is almost independent of pulse length.

In Fig. 7.2 the ratio P_{min}/P_n has been plotted against τs. Then

$$P_{min}/P_n \propto (\tau_s)^{\alpha-\beta} \quad \text{for constant} \quad \tau\Delta f.$$

and the effect of changing pulse length can be conveniently examined. The experimental points are in conformity with the theory.

3. Effect of Pulse-Repetition Frequency

The theory states that

$$P_{\min} \propto r^{-1/2}$$

until the background becomes uniform; thereafter $P_{\min}$ is independent of r.

The frequency at which the change-over occurs is proportional to the length of the average noise pulse ($s/2\Delta f$) when this is less than the spot diameter; otherwise it is independent of Δf and s. It is, of course, independent of τ. It is a function of the antenna speed and the characteristics of the second detector and the indicator tube.

Fig. 7.3 shows that the experimental results confirm the theory. On plotting the change-over frequency against the length of a noise pulse a straight line is obtained; on extrapolating this, the frequency corresponding to a noise pulse one spot diameter in length (i.e., the frequency r_c) is found to be 6000; we predict that, whatever the other system parameters, as long as the antenna speed remains at 2 revolutions per minute the visibility will always be independent of repetition frequency when this exceeds 6000. Unfortunately, the experimental system could not reach this frequency.

The values of n_c and $(\Delta I/I)_0$ may be calculated from this critical frequency. Using (36) and (35), we have

$$n_c = r_c \times \frac{\theta_s}{360} \times \frac{1}{S} \times \frac{1+(1+a/S)^{-b}}{1-(1+a/S)^{-b}} \quad (\theta_s \text{ in degrees})$$

$$= 6000 \times \frac{1.1}{360} \times 30 \times \frac{1.129}{0.871}$$

$$= 710$$

and

$$\left(\frac{\Delta I}{I}\right)_0 = \frac{k_1}{k_2} \cdot \frac{1}{\sqrt{n_c}} = \frac{3}{2} \cdot \frac{1}{\sqrt{710}} = 0.06.$$

Thus about 700 superimposed pulses are required to make the noise background uniform, and a ratio of brightness deviation to r.m.s. brightness of 6 per cent cannot be detected. The latter figure agrees well with the threshold visible contrast given by Fig. 4.

4. Effect of Antenna Speed

When the background is uniform,

$$P_{\min} \text{ is independent of } S.$$

When it is discontinuous,

$$P_{\min} \propto \sqrt{S \cdot \frac{1-(1+a/S)^{-b}}{1+(1+a/S)^{-b}}} \qquad \text{(see equation 27, Appendix I)}$$

where $\propto \sqrt{S}$ when $S \ll a$, independent of S when $S \gg a$, a and b being constants of the screen material.

For a P7 tube a is 0.15 seconds^{-1} and it will be of the same order for other long-persistence screens, so that $S=a$ for a speed of about 10 revolutions per minute.

The upper curve in Fig. 7.4 shows the above expression and experimental points; owing to build-up, the effect of antenna speed is seen to be small. The lower curve and points show the constancy with uniform backgrounds.

5. Effect of Antenna Beamwidth

$$P_{\min} \propto \theta_h^{-1} \quad \text{when} \quad \theta_h < \theta_s$$

$$P_{\min} \propto \theta_h^{-p} \quad \text{when} \quad \theta_h > \theta_s.$$

The smallest beamwidth that could be obtained (2°) was twice θ_s, so that the behavior for $\theta_h < \theta_s$ could not be investigated. The experimental observations (Fig. 7.5) agree with the prediction that $P_{\min}$ is inversely proportional to the 2/3 power of the beamwidth when the pulse first becomes larger than the spot diameter, but show a continuance of this law to much larger beamwidths than anticipated from Fig. 4. This might be expected, as the characteristic arc shape of the echo is of great aid in distinguishing it from noise pulses. The asymptotic values inserted on the margin of the graph (pulse on continuously) show that the 2/3-power law does not continue much further.

It must be remembered that an increase in $P_{\min}$ with decreasing beamwidth does not necessarily mean a decreased range in the target, as the range varies directly as the square root of aerial gain, as well as inversely as the fourth power of $P_{\min}$, and the decrease in beamwidth may be accompanied by a more than compensating increase in aerial gain.

6. Effect of Video Bandwidth

This is not taken into account in the theory. The experimental results (Fig. 7.6) show that, over a range of pulse-duration versus video-bandwidth product of 0.4 to 32, the visibility is unaffected by video bandwidth. Similar results have been obtained on deflection-modulated displays.

7. Ultimate Visibility on a PPI Display

From (3) we see that the least value of signal above noise that can be seen on a PPI display is given by

$$\frac{P_{\min}}{P_n} = \frac{k_2}{k_1} \cdot \left(\frac{\delta I}{I}\right)_0$$

and that this occurs when the background is uniform, neither dimension of the echo is determined by the spot diameter and its total area is at least a_c, and the bandwidth is wide enough not to appreciably limit the power in the pulse.[5] For a pulse of any area greater than the

[5] Since $1-e^{-2\tau\Delta f} > 0.98$ when $\tau\Delta f > 2$, this condition can be readily attained.

spot size, the corresponding equation is

$$\frac{P_{\min}}{P_n} = \frac{k_2}{k_1} \cdot \frac{\delta I}{I}.$$

In Fig. 7.7 is plotted the above equation using values of $\delta I/I$ from Fig. 4, together with experimental points. The theoretical and experimental curves almost coincide initially, but the experimental curve shows the continued improvement with beamwidth already mentioned. One reason for this divergence may be that the screen brightness chosen by operators (about 0.04 effective foot-candles) is twice that used in the observations from which the theoretical curve was derived. Another reason, previously mentioned, is the greater importance of dimensions along the arc than radial dimensions in distinguishing the echo from noise pulses.

The fact that signals up to 18 db below noise can be seen under favorable conditions is most striking.

Some Other Aspects of the Theory

1. The Effect of Second-Detector Law and Grid-Voltage Versus Beam-Current Characteristic of the Indicator Tube

These occur as k_1 and k_2 in (3) and (4), so that

$$P_{\min} \propto \frac{k_2}{k_1} \cdot \left(\frac{k_1}{k_2}\right)^{2\epsilon}$$

i.e.,

$$P_{\min} \propto \frac{k_2}{k_1} \text{ for uniform backgrounds,}$$

but independent of k_2 and k_1 with discontinuous backgrounds.

Thus, *when once the background is uniform*, a system with a square-law detector should have a visibility 3 db better than the same system with a linear detector, while an indicator tube for which $i_p \propto e_g^3$ should give a visibility 2 db better than one for which $i_p \propto e_g^2$. Attempts to obtain improved visibility by using a square-law detector have been made by various workers and proved unsuccessful; the reason presumably is that the noise backgrounds were always discontinuous—as they are in most practical PPI displays.

Our experimental system did not provide facilities for altering k_1 or k_2.

2. Improvement to be Expected from Integrating Systems

As long as the background is still nonuniform ($n < n_c$), an increase in the number of integrated pulses produces improved visibility, but once $n > n_c$ further integration gives no improvement. It sometimes may be more convenient to use some integrating system other than the screen of a cathode-ray tube, but the integration will be no more efficient than that obtainable by using high repetition frequencies and low antenna speeds with a PPI display. However, the real advantage of electrical integrating systems lies not in their superior powers of integration or of display (the limit of detectability of a change in a meter reading, for example, is of the same order as that of a change in screen brightness), but in the possibility of removing the d.c. level; if, in such a system, voltages V, δV, and ΔV are obtained corresponding to the I, δI, and ΔI for the screen, then it is possible to arrange to apply the voltage V (the mean noise voltage) to bias the system, so that instead of detecting a change δV in a voltage V we are detecting a change δV in a system whose mean voltage is zero but which suffers random fluctuations of r.m.s. value ΔV, where ΔV can be made as small as desired by increasing the integration time. Any system that could remove the average brightness on a long-persistence screen without affecting the incremental values (e.g., scanning such a screen and biasing the resultant voltages) should be as efficient as a purely electrical integrator.

The above discussion applies, of course, only to post-detector integrators, predetector integrating systems being of quite a different nature.

3. Greater Variability in Results with Discontinuous Backgrounds

As well as increasing the mean signal power required to see an echo, a discontinuous noise background causes the signal power required to vary widely from time to time, in accord with the random occurrence of bright noise pulses. The standard deviation of the mean signal power required for visibility will be inversely proportional to the square root of the number of integrated pulses. This variability was particularly noticeable in the experimental tests at repetition frequencies of about 50 c.p.s., where a large number of observations had to be made to obtain a satisfactory average value.

Display Design, and the Calculation of Losses

1. The Optimum Display

To design a display for optimum visibility, when there are no limitations except those of permissible peak and average power set by the transmitter tube, the foregoing analysis indicates that the procedure should be as follows:

(1) Use the maximum available peak power in the pulse.
(2) Use as long a pulse duration as possible.
(3) Make the over-all bandwidth of the receiver equal to the reciprocal of the pulse duration.
(4) Use a time-base sweep to produce a pulse length tween one and two spot diameters. (When long ranges are required, this may be achieved by delaying the sweep relative to the transmitter pulse.)
(5) Use the highest pulse-repetition frequency that, with the pulse duration chosen, will not necessitate exceeding the permissible tube dissipation.

(6) Make the antenna gain as high as possible.
(7) Having decided on the antenna gain, make the beamwidth in the direction of scan as large as possible, consistent with this gain and requirements of bearing accuracy.
(8) Use as slow a speed of antenna rotation as possible. (This condition is less important than any of the others.)

2. *Calculation of Losses*

Usually operational requirements make it impossible to fulfill all the above conditions, and it is required to know what losses are thereby incurred. Or, we may want to know what change in visibility occurs when we make some alteration in an existing system. For this purpose, nomograms have been drawn, using (3), to give the value of P_{min}/P_n, the signal power above noise power required for visibility, for any radar system in terms of the system parameters $\tau\Delta f$, $\tau s/d$, θ_h/θ_s, and r/r_c.

These nomograms are given in Fig. 10 (a, b, and c); which of the three is to be used in a particular case is determined by criteria that will be given below. Subsidiary nomograms of use in calculation are given in Figs. 8 and 9. Fig. 8 gives $\tau s/d$ in terms of the pulse duration, tube spot diameter, and range and radius of the display on the c.r.t.; Fig. 9, which is a nomogram of equation (4), gives the value of r_c in terms of the angular spot diameter and the antenna speed for tubes with a P7 screen.

In all the nomograms it is assumed that the second detector of the receiver is linear (i.e., $k_2=2$) and alternative scales are given for two types of c.r.t., those for which $i_p \propto e_g^2 (k_1=2)$ and those for which $i_p \propto e_g^3 (k_1=3)$. It is also assumed that the echo area remains small enough for p to be 2/3, and that the ratio Φ_s/Φ_c does not vary.

The method of using the nomograms is best illustrated by an example, one of which follows and is worked out in detail in Table I. The form used in this figure has been found convenient, and supplies of blank forms are available from this laboratory. The method of use, obvious from the example, is as follows:

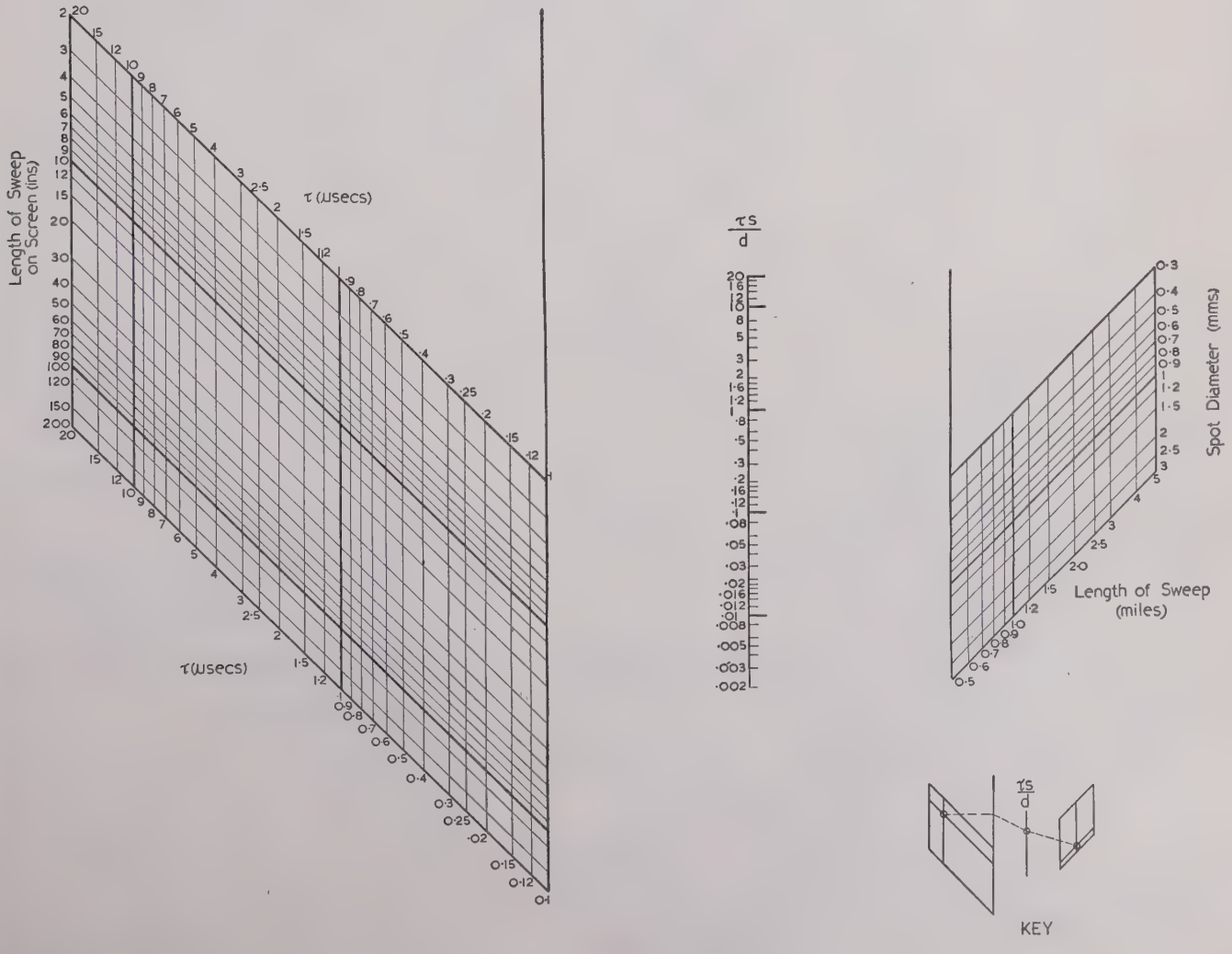

Fig. 8—Calculation of $\tau S/d$.

(1) Fill in the values of the system variables in the first column.
(2) From these data and the nomograms of Figs. 8 and 9, complete the second column.
(3) Determine from the third column which of Figs. 10(a), (b), or (c) should be used.
(4) Turn to this chart and, using the quantities in the second column marked (1), (2), (3), and (4),

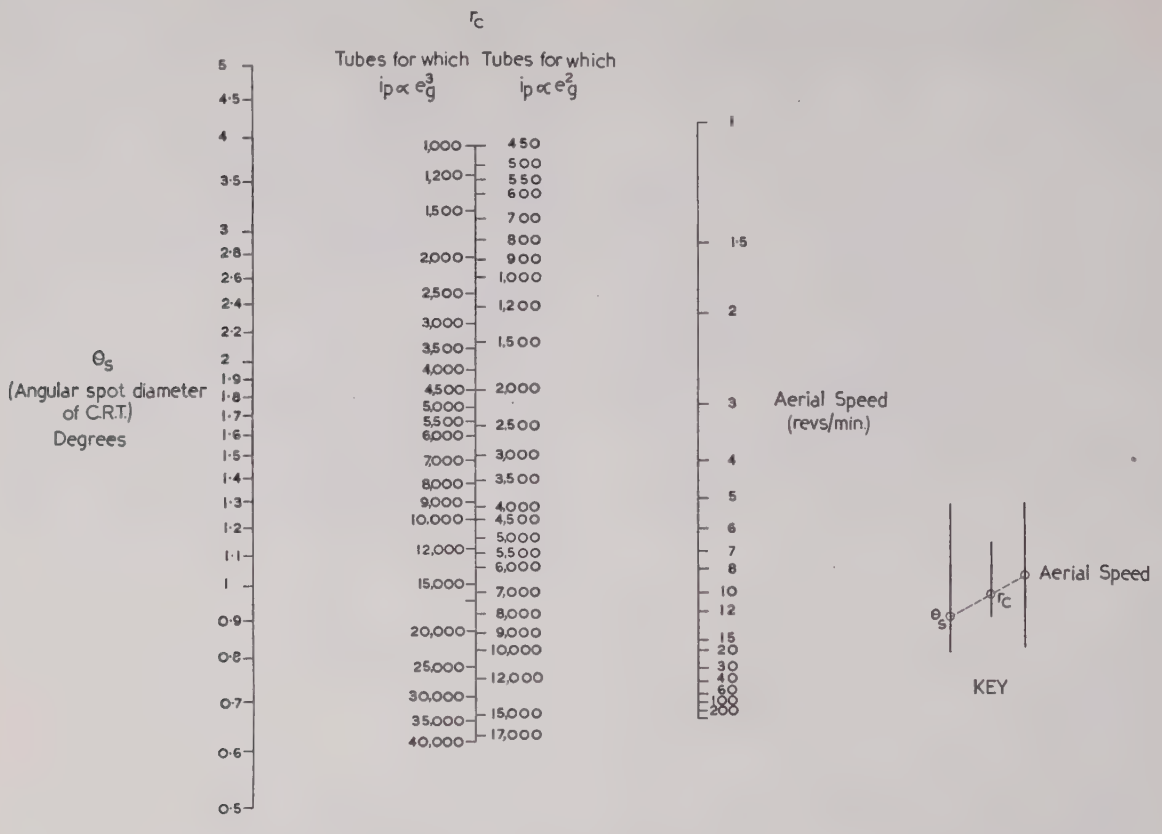

Fig. 9—Calculation of r_c for cathode-ray tube with P7 screens.

TABLE I
Example of Use of Nomograms to Calculate Minimum Visible Signal

System Variables	Calculations	Choice of Charts	Minimum Visible Signal
Pulse duration = 2 μsec. Length of sweep in miles = 100 miles Length of sweep on screen = 2.25 inches Spot diameter along radius = 0.6 mm.	From Fig 8, (1) $\frac{\tau s}{d}=0.178$ $R=\frac{2\tau\Delta f}{\tau s/d}$ $=4/0.178$ $=22.5$ which >1 ~~or <1.~~		From Fig. 10(a), minimum visible signal power $=+3.3$ db below noise
Pulse duration τ = 2 μsec. Receiver bandwidth Δf = 1 Mc.	(2) $\tau\Delta f=2$	$R<1$ { if $\frac{r}{r_c}>1$ use Fig. 10(a); ~~if $\frac{r}{r_c}<1$ use Fig. 10(c)~~	or, expressed in terms of available signal power in the antenna circuit, $=$ above $+P_n$ $=+3.3+130.8$ $=+134$ db below 1 watt (i.e., 4.0×10^{-14} watt)
Antenna beamwidth in direction of scan, θ_h = 3.5° Angular spot diameter of tube θ_s = 0.6°	(3) $\frac{\theta_h}{\theta_s}=6.0$		
Angular spot diameter θ_s = 0.6° Antenna speed of rotation = 2 r.p.m. Law of tube { ~~$ip=eg^2$~~ or $iz=eg^3$	$r_c=11{,}000$ pulses/sec. (from Fig. 9 if c.r.t. with P7 screen is used.)	$R>1$ { if $\frac{r}{r_c}\times R>1$ use Fig. 10(a); ~~if $\frac{r}{r_c}\times R<1$ use Fig. 10(b)~~	
Pulse-repetition frequency $r=500$ pulses/sec.	(4) $\frac{r}{r_c}=\frac{500}{11{,}000}$ $=0.045$ If $R>1$, calculate $\frac{r}{r_c}\times R$ $=0.045\times22.5$ $=1.01$		
Receiver bandwidth Δf = 1 Mc. Receiver noise factor N = 13 db	Available noise power P_n in antenna circuit $=-N-10\log\Delta f+143.8$ $=-13-0+143.8$ $=+130.8$ db below 1 watt		

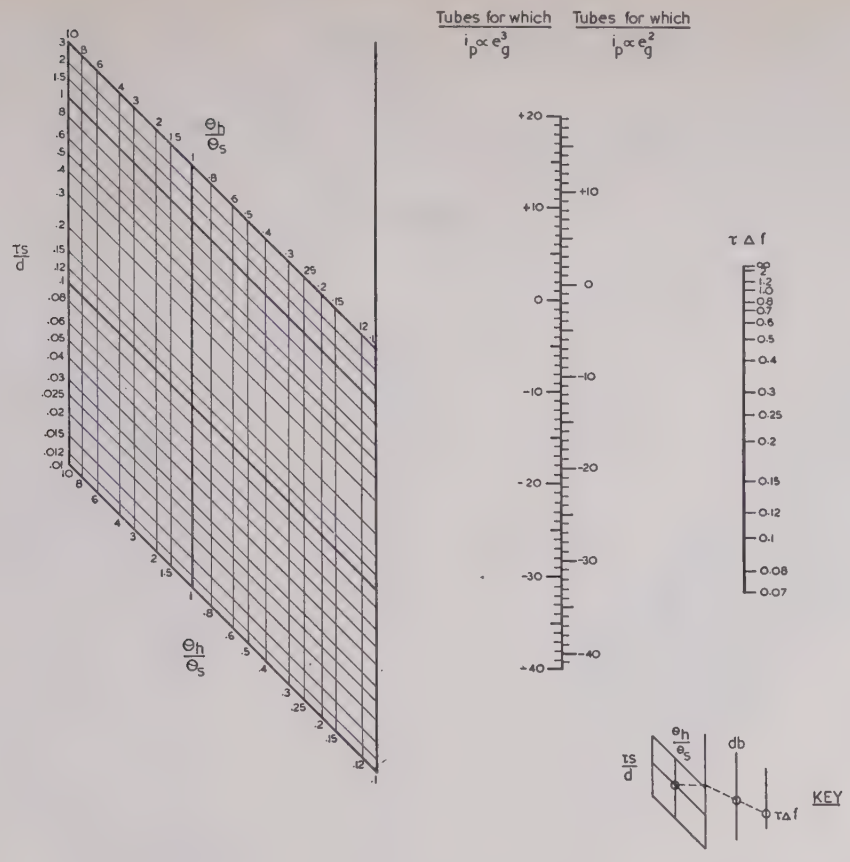

Fig. 10—(a) Minimum visible signal on PPI display. $R<1$, $(r/r_c)>1$, or $R>1$, (r/r_c) X $R>1$.

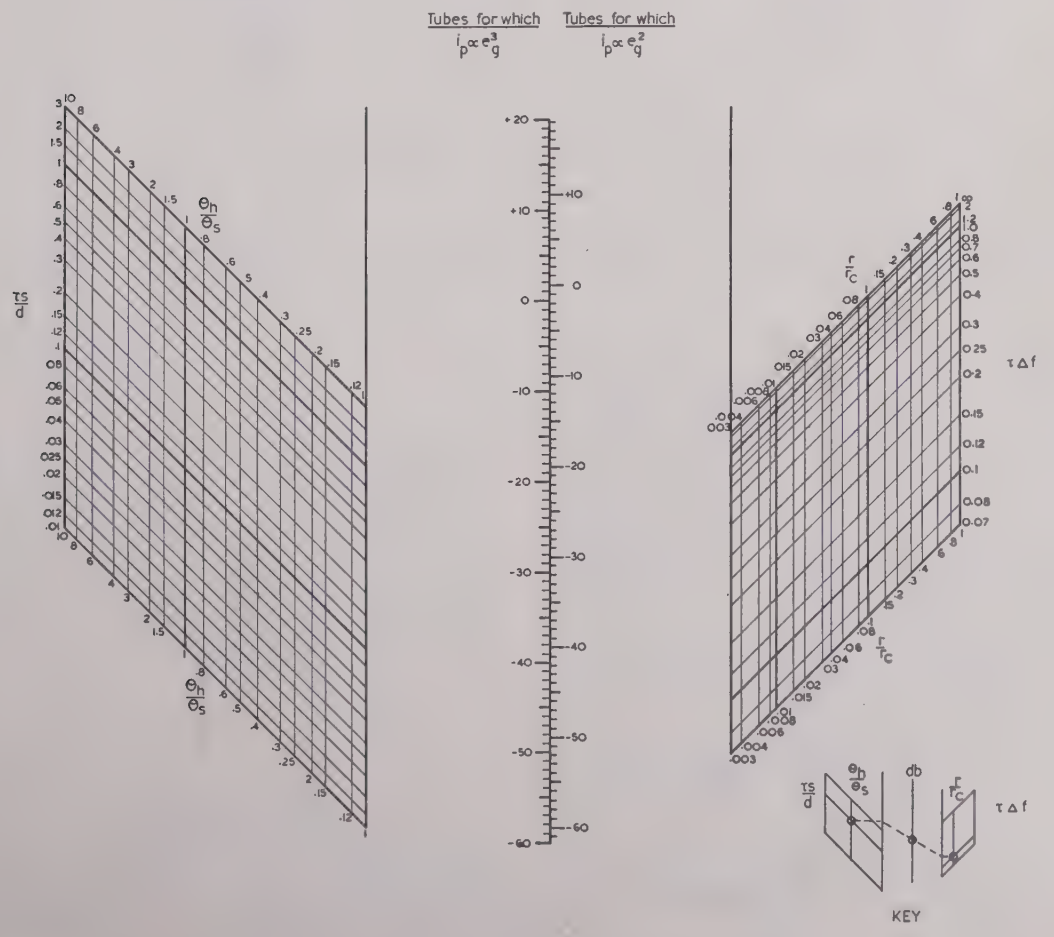

Fig. 10—(b) Minimum visible signal on PPI display. $R<1$ $(r/r_c)<1$.

read off the value of the minimum visible signal power below noise. (Use the scale appropriate to the type of tube used.)

If the value of the minimum visible signal in terms of the available signal power in the antenna circuit is giving for a P7 screen the loss in visibility when the echo builds up over only a few scans instead of over an infinite number; e.g., when the target is moving or the antenna is nodding as it scans.

From it we see that, if in the example of the previous

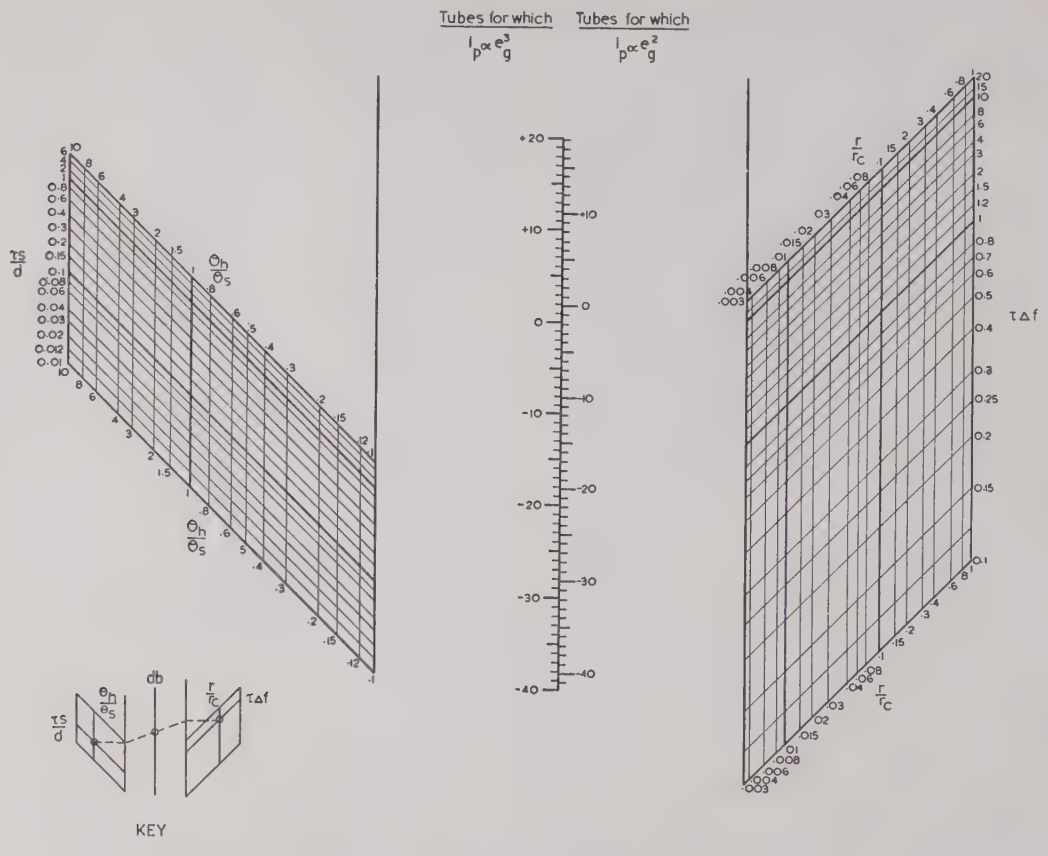

Fig. 10—(c) Minimum visible signal on PPI display. $R>1$, (r/r_c) X $R<1$.

preferred, add to the above the value of P_n from the second column, obtaining the result in decibels below 1 watt.

Example

A system with a PPI display, using a 5FP7 tube, has a beamwidth of 3.5 degrees (to the 1½-db points)[6] in the direction of scan, an antenna speed of 2 r.p.m., a pulse-repetition frequency of 500 pulses per second, a pulse duration of 2 microseconds, and a 100-mile sweep occupying 2¼ inches on the face of the cathode-ray tube. The receiver has a noise factor of 13 db and a bandwidth of 1 Mc. What is the value of the least signal that can be seen on the display?

This example is worked out in Table I, and the least visible signal is found to be 134 db below 1 watt available at the antenna output terminals.

3. *A Nomogram for Obtaining Loss when Echoes are Returned on Only a Few Scans*

Fig. 11 is a nomogram, based on (37) of Appendix I,

[6] The 1½-db points measured for transmission or reception only correspond to a 3-db decrease in power for radiation transmitted and received by the same aerial.

section the echo had built up over only two antenna rotations, there would have been a decrease in visibility

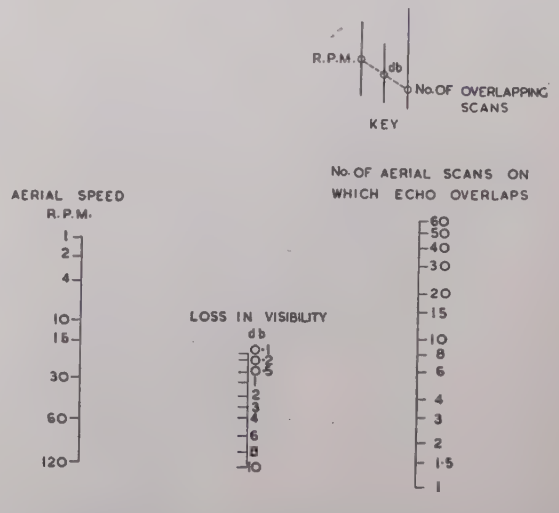

Fig. 11—Loss in visibility due to movement of the target, or to change in antenna elevation between successive scans.

of 0.1 db. The loss is small because there is very little build-up on the 2-r.p.m. scan. If the original speed had

been not 2 but 60 r.p.m., and still only 2 scans were superposed, the loss would be $5\frac{1}{2}$ db, i.e., the build-up is now very important. The nomogram illustrates the behavior mentioned at the end of Appendix I; for speeds greater than 10 r.p.m. ($S>a$), the visibility depends only on the total time of looking at the target; for speeds less than 4 r.p.m. ($S \ll a$), the loss under any circumstance is never more than 1 db.

Acknowledgment

This work has been carried out as part of the research program of the Division of Radiophysics, Council for Scientific and Industrial Research, Commonwealth of Australia.

The author would like to acknowledge her indebtedness to the discussion by Andrew and Langford[7] of the problems of deflection-modulated (class-A) displays, and also to many conversations with B. Y. Mills of this laboratory.

APPENDIX I

A Mathematical Formula for Visibility

The principles outlined in Section 3 are here applied to derive a mathematical formula for visibility. For some of the factors affecting visibility the exact mathematical expressions are too cumbersome to be useful, while for others they are not exactly known, so that a number of approximations have been made; these are indicated as they occur. As a considerable amount of material is involved, it is presented in note form. First, the various factors involved are set out in their mathematical form, and from these the formula for visibility is developed step by step. The notation is that given in Section 2.

(*1*) *Available Power at Antenna Output:*

Peak signal power—$P_{\min}$
Mean noise power—$P_n = NkT\Delta f$.

(*2*) *Output from R.F. Amplifier*

Peak signal power—$P_{\min}' = G_0 \cdot A^2 \cdot P_{\min}$

where G_0 is the gain at the center of the amplifier passband and A is the reduction in peak voltage of a square pulse caused by the selectivity of the r.f. amplifier. Fig. 12 shows the reduction in peak voltage suffered by a square pulse when passed though an amplifier consisting of 1, 2, 5, or 10 cascaded single-tuned stages. None of the curves diverge greatly from that for one circuit, for which

$$A = 1 - e^{-2\tau\Delta f},$$

and hence we have taken this value for A, so that

$$P_{\min}' = G_0 \cdot (1 - e^{-2\tau\Delta f})^2 \cdot P_{\min}. \qquad (10)$$

[7] E. R. Andrew and B. A. Langford, "An Interim report on an Investigation of the Dependence of the Visibility of Signals in Noise on the Parameters of Radar Equipment and on Certain other Factors," A.D.R.D.E. Research Report No. 207, 1943. (Limited circulation.)

Duration of Signal Pulse: Fig. 3 shows that, so long as $\tau\Delta f \ll 0.5$, the pulse duration is not affected significantly

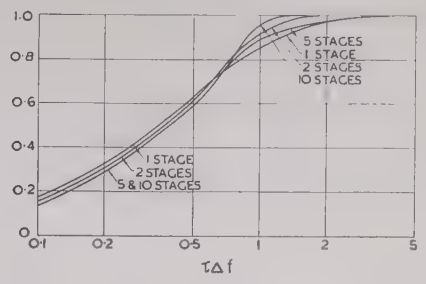

Fig. 12—Reduction in peak voltage of square pulse duration τ on passing through an r.f. amplifier of over-all bandwidth Δf comprising 1, 2, 5, or 10 cascaded single-tuned stages.

by the receiver bandwidth, but that for narrower bandwidths the pulse becomes longer, its duration eventually being inversely proportional to bandwidth. However, in so doing the pulse loses its characteristic shape, and inspection of Fig. 2 shows that, for $\tau\Delta f < 0.5$ the signal and noise pulses have almost identical shapes and durations; this effect will offset any improved visibility due to the greater area of the pulse. Hence, we have assumed

$$\text{duration of output pulse} \doteq \tau. \qquad (11)$$

$$\text{mean noise power } P_n' = G_0 \cdot NkT\Delta f. \qquad (12)$$

$$\text{duration of noise pulse} \doteq (1/2\Delta f) \text{ (from Fig. 3).} \qquad (13)$$

(*3*) *Output from Detector*

Amplitude of Signal and Noise: It has been shown by R. E. Burgess, a member of the staff of the Radio Division of the National Physical Laboratory of England, that

$$\begin{aligned} V &= 1.25\sqrt{P_n'} && \text{for a linear detector} \\ &= 2P_n' && \text{for a square-law detector} \\ \Delta V &= 0.63\sqrt{P_n'} && \text{for a linear detector} \\ &= 2P_n' && \text{for a square-law detector} \\ \frac{\delta V}{\Delta V} &= \frac{P_{\min}'}{P_n'} && \text{for either detector.} \end{aligned}$$

Hence, substituting from (10) and (12),

$$\frac{\delta V}{V} = \frac{(1 - e^{-2\tau\Delta f})^2}{2} \cdot \frac{P_{\min}}{P_n} \quad \text{for a linear detector}$$

$$= (1 - e^{-2\tau\Delta f})^2 \cdot \frac{P_{\min}}{P_n} \quad \text{for a square-law detector,}$$

or

$$\frac{\delta V}{V} = \frac{(1 - e^{-2\tau\Delta f})^2}{k_2} \cdot \frac{P_{\min}}{P_n}, \qquad (14)$$

while

$$\frac{\delta V}{\Delta V} = (1 - e^{-2\tau\Delta f})^2 \cdot \frac{P_{\min}}{P_n} \quad \text{for either detector.} \qquad (15)$$

Pulse Durations: Still as in equations (11) and (13).

(4) *Beam Current in Terms of Receiver Output*

$$i_p \propto V^{k_1} \tag{16}$$

where

$k_1 = 3$ for magnetically focused tubes of the single-crossover type (e.g., 5FP7, 7BP7).

$= 2$ for electrostatically focused tubes of the double-crossover type (e.g., 5CP7)[8]

(5) *Brightness of Screen for Zero Spot Size and Screen Persistence*

$$I \propto i_p{}^k$$

where k is slightly greater than unity when the screen is complete deactivated between sweeps, and slightly less than unity when the screen is allowed to build up with an interval of 1 second between sweeps,[8,9] so that for the conditions in which we are interested it is sufficient to take

$$I \propto i_p,$$

and hence, from (16),

$$I \propto V^{k_1}. \tag{17}$$

Hence,

$$\frac{\delta I}{I} = k_1 \frac{\delta V}{V},$$

and thus, from (14),

$$\frac{\delta I}{I} = \frac{k_1}{k_2}(1 - e^{-2\tau\Delta f})^2 \cdot \frac{P_{\min}}{P_n}. \tag{18}$$

It can be shown that, within wide limits, the value of $\delta V/\Delta V$ is independent of the detector law, and hence as, according to (17), the change from voltage to brightness is equivalent to multiplying the exponent of the detector law by k_1, we have

$$\frac{\delta I}{\Delta I} = \frac{\delta V}{\Delta V} = (1 - e^{-2\tau\Delta f})^2 \cdot \frac{P_{\min}}{P_n} \tag{19}$$

from equation (15).

(6) *Effect of Spot Size on Screen Picture*

1. Area of signal and noise pulses:

$$\text{signal length} = \tau s \text{ when } \tau_s > d$$
$$= d \text{ when } \tau_s < d$$

$$\text{signal width} = \theta_h D \text{ when } \theta_h > \theta_s \tag{20}$$
$$= \theta_s D \text{ when } \theta_h < \theta_s$$

where D is the distance out from the center of the screen.

$$\text{Noise length} = \delta/2\Delta f \text{ when } \delta/2\Delta f > d$$
$$= d \text{ when } \Delta/2\Delta f < d \tag{21}$$
$$\text{Noise width} = \theta_s D.$$

2. Brightness of Signal and Noise: Mean noise background I: unaffected by spot size.

Signal: peak brightness reduced when either length or width is increased by spreading of beam.

Hence, from (20) and (18),

$$\frac{\delta I}{I} = \frac{k_1}{k_2}(1 - e^{-2\tau\Delta f})^2 \cdot \left(\frac{\tau_s}{d}\right)^l \cdot \left(\frac{\theta_h}{\theta_s}\right)^m \cdot \frac{P_{\min}}{P_n} \tag{22}$$

where

$$l = 0 \text{ when } \tau_s > d$$
$$= 1 \text{ when } \tau_s < d$$
$$m = 0 \text{ when } \theta_h > \theta_s$$
$$= 1 \text{ when } \theta_h < \theta_s.$$

Noise: R.m.s. deviation of the noise is reduced by the square root of n_s, the number of overlapping pulses, i.e., the number of sweeps occurring in an angle θ_s multiplied by the number of pulses occurring in the length d when this is greater than the length of a pulse.

$$n_s = \frac{r\theta_s}{2\pi S} \cdot \left(\frac{2\Delta f d}{s}\right)^{2q} \tag{23}$$

where

$$2q = 0 \text{ when } \frac{s}{2\Delta f} > d$$
$$= 1 \text{ when } \frac{s}{2\Delta f} < d.$$

Hence, decreasing If by $\sqrt{u_s}$ and using the value of δI given by (22), (19) becomes

$$\frac{\delta I}{\Delta I} = (1 - e^{-2\tau\Delta f})^2 \cdot \left(\frac{\tau_s}{d}\right)^l \cdot \left(\frac{\theta_h}{\theta_s}\right)^m \cdot \sqrt{n_s} \cdot \frac{P_{\min}}{P_n}. \tag{24}$$

(7) *Effect of Long Persistence of Screen*

Area of pulse: Unaffected (provided target does not move appreciably between successive antenna rotations).

Brightness:

(a) $\delta I/I$. As stated in Section (5) of this appendix, we may assume that the proportional change in intensity $\delta I/I$ remains equal to the corresponding change in beam current $\delta i_p/i_p$, irrespective of the screen persistence and rate of antenna rotation.

[8] G. F. J. Garlick, "Report of Tests Made of the Afterglow Characteristics of American Cathode-Ray Tubes of Electrostatically Focused and Deflected Type with P7 Screens," Telecommunications Research Establishment, Report T1668, 1944.

[9] G. F. J. Garlick, "A Study of the Screen Characteristics of C.R.T. 16QDEZ21 with G.E.C. 'P' Screen under Conditions Simulating those of Operational P.P.I. Equipment," Telecommunications Research Establishment, Report T1678, 1944.

(b) $\Delta I/I$ obviously *is* affected by the screen-persistence, which acts as a further integrating agency smoothing out variations in the noise and thus decreasing $\Delta I/I$; i.e., the effect of screen persistence is to increase n, the number of pulses averaged on the PPI screen.

To obtain a value of the factor by which n is increased for long-persistence screens, we shall assume that in each antenna rotation a constant average increment I' of brightness is added, while between each rotation the brightness decays by a factor $(1+at)^{-b}$, t being the time since the last increment (in this case $1/S$, the time of a rotation), b being a constant of the screen, and a another constant depending on the screen material and the screen brightness. Since only past notations whose brightness still appreciably persists are of importance, we are greatly interested only in intensities about the final value I, so that it is sufficient to take the value of a appropriate to this final brightness. For the same reason, the assumption of equal average increments from each rotation is reasonable. Then we have

$$\begin{aligned} I &= I'[1 + (1 + a/S)^{-b} + (1 + a/S)^{-2b} \\ &\quad + (1 + a/S)^{-3b} + \cdots \text{ to infinity}] \\ &= I'/[1 - (1 + a/S)^{-b}], \end{aligned} \tag{25}$$

i.e., the average brightness exceeds that produced in the present rotation by a factor $1/[1-(1+a/S)^{-b}]$. Now the average increments I' will themselves vary with a certain standard deviation. Applying the theorem of Appendix II, the standard deviation of I will exceed that of I' by the

$$\sqrt{1 + (1 + a/S)^{-2b} + (1 + a/S)^{-4b} + \cdots \text{ to infinity}},$$

i.e.,

$$1/\sqrt{1 - (1 + a/S)^{-2b}}.$$

Hence the effect of long persistence of the screen causes the ratio $\Delta I/I$ (and hence the ratio $\Delta I/\delta I$) to be multiplied by

$$[1 - (1 + a/S)^{-b}]/\sqrt{1 - (1 + a/S)^{-2b}}$$

i.e.,

$$\sqrt{[1 - (1 + a/S)^{-b}]/[1 + (1 + a/S)^{-b}]} \tag{26}$$

which, as anticipated, is less than unity.

We may express this by saying that the number of integrated pulses is effectively increased from n_s to n, where

$$n = n_s \cdot \frac{1 + (1 + a/S)^{-b}}{1 - (1 + a/S)^{-b}}, \tag{27}$$

and thus (24) becomes

$$\frac{\delta I}{\delta I} = (1 - e^{-2\tau\Delta f})^2 \cdot \left(\frac{\tau_s}{d}\right)^{l} \cdot \left(\frac{\theta_h}{\theta_s}\right)^{m} \cdot \sqrt{n} \cdot \frac{P_{\min}}{P_n}. \tag{28}$$

It has been shown by several workers,[8] that the rate of decay of long-persistence screens depends on the past history of the screen. This means that the value of a in (27) is a function of S. Since the effect of antenna speed is anyhow small (see Fig. 7.4), it has seemed sufficient to take a as the value appropriate for cyclic excitation at those speeds for which persistence is important. The value given in the notation is for a speed of 1 r.p.m.

(*8*) *Formula for Visibility*

(a) *Uniform background*

From equation (22),

$$P_{\min} = \frac{k_1}{k_2} \cdot \frac{P_n}{(1 - e^{-2\tau\Delta f})^2} \cdot \left(\frac{\tau S}{d}\right)^{-l} \cdot \left(\frac{\theta_h}{\theta_s}\right)^{-m} \cdot \frac{\delta I}{I}. \tag{29}$$

The variation of $\delta I/I$ with echo area is given by

$$\frac{\delta I}{I} = \left(\frac{\Phi}{\Phi_c}\right)^{-p} \cdot \left(\frac{\delta I}{I}\right)_0 \tag{1}$$

where Φ is derived from (20), so that

$$\frac{\delta I}{I} = \left(\frac{\tau_s}{d}\right)^{-u} \cdot \left(\frac{\theta_h}{\theta_s}\right)^{-v} \cdot \left(\frac{\Phi_s}{\Phi_c}\right)^{-p} \cdot \left(\frac{\delta I}{I}\right)_0 \tag{30}$$

where

$u = p$ when $\tau s > d$
$= 0$ when $\tau_s < d$,
$v = p$ when $\theta_h > \theta_s$
$= 0$ when $\theta_h < \theta_s$,
Φ_s = solid angle subtended by spot.

Substituting this in (29), the minimum signal visible on a uniform background is given by

$$P_{\min} = \frac{k_2}{k_1} \cdot \frac{P_n}{(1 - e^{-2\tau\Delta f})^2} \cdot \left(\frac{\tau_s}{d}\right)^{-\beta} \cdot \left(\frac{\theta_h}{\theta_s}\right)^{-\gamma} \cdot \left(\frac{\Phi_s}{\Phi_c}\right)^{-p} \cdot \left(\frac{\delta I}{I}\right)_0 \tag{31}$$

where

$\beta = 1$ when $\tau_s < d$, p when $\tau_s > d$
$\gamma = 1$ when $\theta_h < \theta_s$, p when $\theta_p > \theta_s$.

(b) *Discontinuous Background:* The equation corresponding to (29) is (28), i.e.,

$$P_{\min} = \frac{P_n}{(1 - e^{-2\tau\Delta f})^2} \cdot \left(\frac{\tau_s}{d}\right)^{-l} \cdot \left(\frac{\theta_h}{\theta_s}\right)^{-m} \cdot \frac{1}{\sqrt{\bar{n}}} \cdot \frac{\delta I}{\Delta I}. \tag{32}$$

There is no equation corresponding to (1) giving the numerical values of $\delta I/\Delta I$ required to make a certain bright patch of given area visible. However, we shall assume that the variation with echo area in the value of $\delta I/\Delta I$ required for visibility is of the same form as that with $\delta I/I$, and that when the number n of overlapping noise pulses reaches a certain critical value n_c such that the noise background is just uniform, the values of $P_{\min}$ for uniform and discontinuous backgrounds are identical. The first condition transforms (32) into

$$P_{\min} = \frac{P_n}{(1 - e^{-2\tau\Delta f})^2} \cdot \left(\frac{\tau_s}{d}\right)^{-\beta} \cdot \left(\frac{\theta_h}{\theta_s}\right)^{-\gamma} \cdot \left(\frac{\Phi_s}{\Phi_c}\right)^{-p} \cdot \frac{1}{\sqrt{n}} \cdot \left(\frac{\delta I}{\Delta I}\right)_0 \tag{33}$$

where β, γ, p, etc., have the same values as in (31). The second condition requires that

$$\left(\frac{\delta I}{\Delta I}\right)_0 = \frac{k_2}{k_1} \cdot \sqrt{n_c} \left(\frac{\delta I}{I}\right)_0. \tag{34}$$

It is worth noting that this implies that

$$n_c = \left(\frac{k_1}{k_2}\right)^2 \cdot \left(\frac{I}{\Delta I}\right)_0^2, \tag{35}$$

$(\Delta I/I)_0$ being the highest ratio of the standard deviation of the background brightness to its mean value that produces an apparently uniform background.

(c) *A General Formula*: Using (34), we can combine (31) and (33) into one formula

$$P_{\min} = \frac{k_2}{k_1} \cdot \frac{P_n}{(1 - e^{-2\tau\Delta f})^2} \cdot \left(\frac{\tau_s}{d}\right)^{-\beta} \cdot \left(\frac{\theta_h}{\theta_s}\right)^{-\gamma} \cdot \left(\frac{\Phi_s}{\Phi_c}\right)^{-p} \left(\frac{n}{n_c}\right)^{-\epsilon} \cdot \left(\frac{\delta I}{I}\right)_0 \tag{2}$$

where $\epsilon = \frac{1}{2}$ for discontinuous backgrounds
$= 0$ for uniform backgrounds.

The background is uniform when $r > r_c$ if $\tau s/d > 2\tau\Delta f$ or $r \cdot (2\Delta f d/s) > r_c$ if $\tau s/d < 2\tau\Delta f$.

Equation (2) can be expressed in a more useful form by defining a critical pulse-repetition frequency r_c given by

$$r_c = n_c \cdot \frac{2\pi S}{\theta_s} \cdot \frac{1 - (1 + a/S)^{-b}}{1 + (1 + a/S)^{-b}} \tag{36}$$

$$= \left(\frac{k_1}{k_2}\right)^2 \cdot \left(\frac{I}{\Delta I}\right)_0^2 \cdot \frac{2\pi S}{\theta_s} \cdot \frac{1 - (1 + a/S)^{-b}}{1 + (1 + a/S)^{-b}} \tag{4}$$

using equation (35).

The physical significance of r_c is that it is the pulse-repetition frequency above which, for a given cathode-ray tube and given antenna speed of rotation, the background is always uniform whatever the values of the other system constants.

Then, from (23), (27), and (35),

$$\frac{n}{n_c} = \left(\frac{2\Delta f d}{s}\right)^{2q} \cdot \frac{r}{r_c}$$

and

$$\left(\frac{n}{n_c}\right)^{-\epsilon} = \left(\frac{2\Delta f d}{s}\right)^{-\alpha} \cdot \left(\frac{r}{r_c}\right)^{-\epsilon} = (2\tau\Delta f)^{-\alpha} \cdot \left(\frac{\tau_s}{d}\right)^{\alpha} \cdot \left(\frac{r}{r_c}\right)^{-\epsilon}$$

where

$\alpha = 0$ when $(s/2\Delta f) > d$ or the background is uniform
$= \frac{1}{2}$ otherwise.

Then (2) can be written

$$P_{\min} = \frac{k_2}{k_1} \cdot P_n \cdot \frac{(2\tau\Delta f)^{-\alpha}}{(1 - e^{-2\tau\Delta f})^2} \cdot \left(\frac{\tau_s}{d}\right)^{\alpha-\beta} \cdot \left(\frac{\theta_h}{\theta_s}\right)^{-\gamma} \cdot \left(\frac{r}{r_c}\right)^{-\epsilon} \cdot \left(\frac{\Phi_s}{\Phi_c}\right)^{-p} \cdot \left(\frac{\delta I}{I}\right)_0. \tag{3}$$

(9) *When Echoes are Returned on Only a Few Scans*

The target may be moving, or the antenna may alter its elevation between successive rotations (the process of "scanning"), so that, although noise occurs on every scan, a return from the target may occur on only one or a few scans. Then I and ΔI are unaltered by δI will be reduced.

We shall assume that the simplified picture of build-up processes given in Section (7) of this Appendix can still be used, this time to give the incremental intensity due to an echo. We pointed out in Section (7) that the picture is close to the truth so long as the *total* light intensity does not vary much, and this is true here as long as δI is not too large compared with I. Then, if δI_q is the value of δI when the echo builds up over only q rotations, and δI_∞ the value when it has built up over so many rotations that further build-up has a negligible effect,

$$\frac{\delta I_q}{\delta I_\infty} = \frac{1 + (1+a/S)^{-b} + (1+a/S)^{-2b} + \cdots + (1+a/S)^{-(q-1)b}}{1 + (1+a/S)^{-b} + (1+a/S)^{-2b} + \cdots \text{ to infinity}} = 1 - (1+a/S)^{-qb}, \tag{37}$$

giving the reduction in visibility.

For $S > a$, the reduction factor is approximately $ab \cdot q/S$; i.e., for high speeds the reduction depends only on the time, q/S, during which the antenna looks at the target. When $S \ll a$, the factor approaches unity; i.e., at very low speeds the number of hits on the target is not important, obviously because build-up hardly enters at these speeds.

APPENDIX II

A Relevant Theorem in Statistics

If $x_1, x_2 \cdots, x_n$ are each distributed normally with means $a_1, a_2 \cdots, a_n$ and standard deviations $\sigma_1, \sigma_2 \cdots, \sigma_n$, then any linear function of the x's, $l_1x_1 + l_2x_2 \cdots + l_nx_n$ is also normally distributed with a mean $\sum_1^n l_r a_r$ and a standard deviation $\sqrt{\sum_1^n l_r^2 \sigma_r^2}$.

In particular, if the x's are individual observations on a normal population of mean value a and standard deviation σ, then the means of sets of n such observations form another normal population whose mean is a and whose standard deviation is $\sigma/\sqrt{n}$.

Although these theorems apply exactly only to normal populations, they are adequate for the populations encountered in this paper, for the fairly high values of $n (> 10$, and often some hundreds) encountered.

Results of Microwave Propagation Tests on a 40-Mile Overland Path*

A. L. DURKEE†

Summary—**This paper gives the results of a series of microwave radio propagation tests over an unobstructed 40-mile overland path. The purpose of the tests was to investigate the transmission characteristics of such a path at centimeter wavelengths over a long period of time. Statistics on the transmission results at wavelengths ranging from 1.25 to 42 cm. are given. The tests extended over a period of about two years.**

THIS PAPER presents the results of a series of microwave radio propagation tests over an unobstructed 40-mile overland path. The purpose of these tests was to study the characteristics of propagation over such a path at centimeter wavelengths, and to investigate the practicability of using microwaves for radio relaying under conditions calling for a high degree of circuit reliability. The nature of the test program was such as to provide statistical data on the performance of a typical microwave circuit over a long period of time. The program included studies of the variation of transmission characteristics with time of day, season, wavelength, polarization, path length, and path clearance. The tests covered a period of about two years.

The Test Circuit

The transmission path over which the measurements were made extended from New York City to Neshanic, N. J., a distance of 40.1 miles. The New York terminal of the test circuit was located on the roof of the New York Telephone Company building at 140 West Street. The antennas at this location were approximately 500 feet above mean sea level. At Neshanic, the antennas were mounted on top of a 50-foot wooden tower located on a ridge having an elevation of about 550 feet above sea level. A profile of the transmission path is shown in Fig. 1.

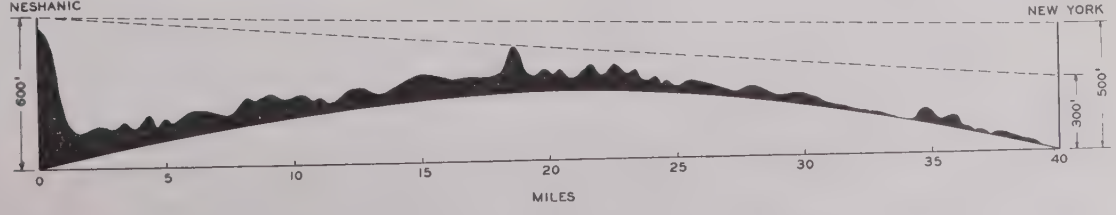

Fig. 1—Profile of test path from Neshanic to New York (true earth radius).

Measurements were made on continuous carrier signals transmitted from New York and received at Neshanic. The transmitters employed reflex-oscillator tubes giving output powers up to 100 milliwatts. The receivers were connected to Esterline-Angus recorders which produced continuous records of the transmission variations. In most of the tests, antennas of the parabolic-reflector type, horizontally polarized, were used at both ends of the circuit. Means were provided for measuring the power delivered to the transmitting antennas, and for calibrating the receiver outputs in terms of power delivered by the receiving antennas. The range of calibration of the equipment varied somewhat with the wavelength employed, but except at the shortest wavelength (1.25 cm.) it covered receiver inputs corresponding to received field intensities from about 10 db[1] above to about 20 db below the calculated free-space values.

Scope of the Data and Method of Analysis

Continuous transmission on a wavelength of 6.5 cm. was started late in July, 1943. This circuit was operated until February, 1945, with only a few interruptions, and its performance was taken as a standard against which the results at other wavelengths were compared. In the fall of 1943 a circuit was put into operation on 3.2 cm., and measurements were made at this wavelength until February, 1945. A 10-cm. circuit was operated intermittently from September, 1943, until August, 1944, when it was replaced by a 42-cm. circuit. The latter was kept in operation for about two months. Finally, a series of measurements at 1.25 cm. was made during August and September of 1945. The 3.2-cm. system was used as the comparison circuit during the 1.25-cm. tests.

With continuous graphical recording of the receiver outputs, large amounts of data were accumulated in the course of the tests. Certain sections of particular interest were examined in detail, but the bulk of the record was condensed into a form suitable for statistical analysis. The reduction process consisted in the tabulation of maximum and minimum received field intensities for each interval of one hour, together with an estimate of the average field for the hour. The ratio of maximum-to-minimum field for a one-hour period, expressed in decibels, was called the fading range for the hour. Similarly,

* Decimal classification: R112.×R113. Original manuscript received by the Institute, April 21, 1947.

† Bell Telephone Laboratories, Inc., New York 14, N. Y.

[1] The ratio of any field intensity E_1 to the free-space field intensity E_0, expressed in decibels, is $20 \log_{10}(E_1/E_0)$.

the ratio of maximum-to-minimum field for a 24-hour period was called the fading range for that day.

A summary of the data for all of the tests except those at 1.25 cm. is given in Fig. 2. This is a plot of daily fading range for each circuit for each day on which a complete record was obtained. It can be seen that the fading ranges were generally greater on summer days than on winter days. Also, there was a tendency for the fading ranges to be greater at the shorter wavelengths. These trends will be more apparent in later figures. Since the calibration range of the test equipment was limited to about 30 db, this is the maximum value of fading range shown in Fig. 2, although the records indicated that the range exceeded 30 db on some days.

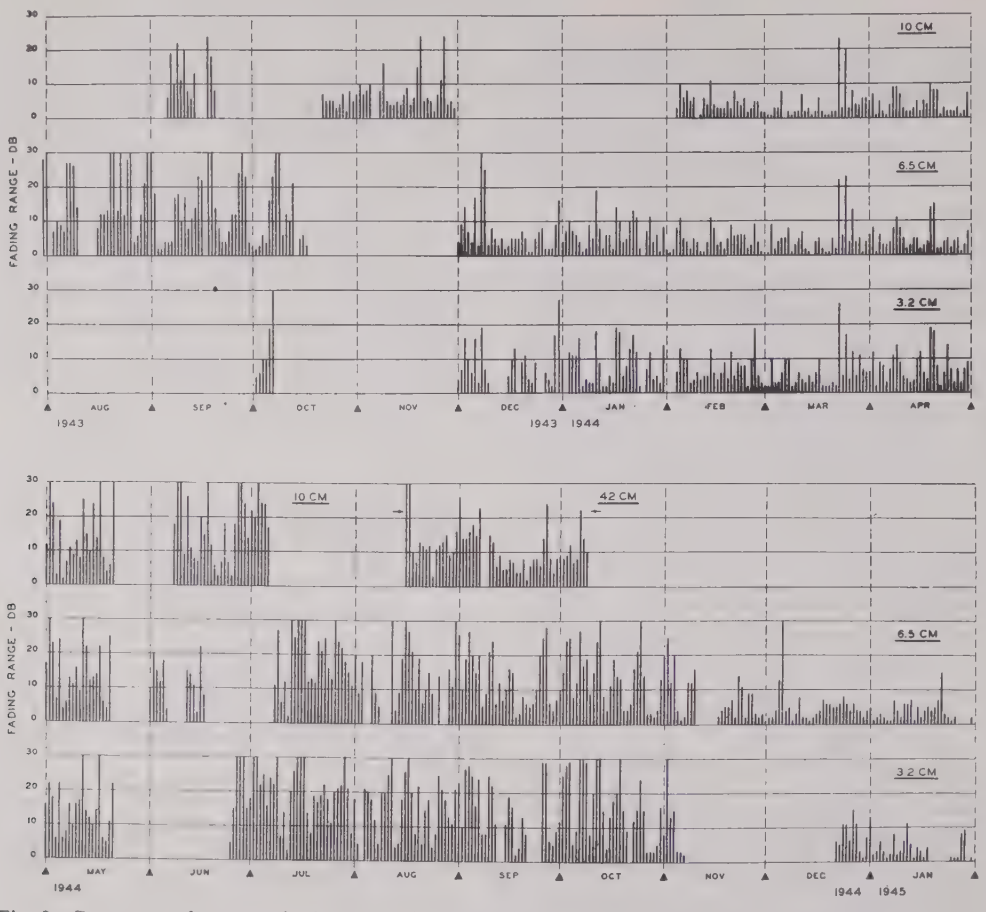

Fig. 2—Summary of test results in terms of daily fading ranges from August, 1943, to January, 1945

The wavelengths used in the tests were 1.25, 3.2, 6.5, 10, and 42 cm. The 1.25-cm. data are not included in Fig. 2 because the character of the record obtained on that circuit necessitated a somewhat different method of analysis. As a result of the limited amount of transmitter power available and the relatively large atmospheric loss factor at this wavelength, the signal was obscured by the receiver noise a substantial fraction of the time, and a satisfactory value for the daily fading range frequently was unobtainable.

Diurnal and Seasonal Trends

Fig. 3 shows the average daily fading range at 6.5-cm. for each month of the year 1944. The greater variability of transmission in the summer than in the winter is clearly evident in this figure. A striking feature is the abrupt rise in the average fading range from April to May. The reduction from May to June may perhaps be accounted for by the fact that complete records on 6.5 cm. were obtained on only 12 days in June, due to special tests and work on the equipment. With respect

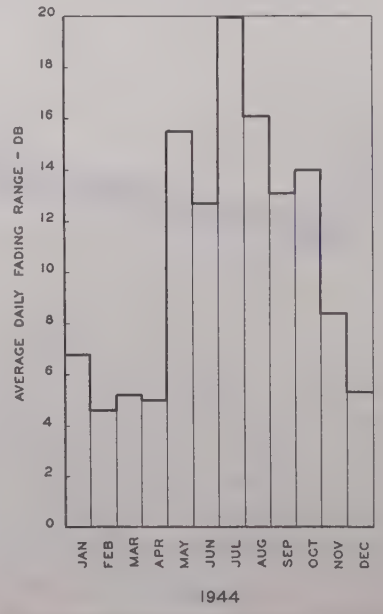

Fig. 3—Seasonal variation of fading at 6.5 cm.

to diurnal and seasonal trends, the results at 6.5 cm. are typical of those at the other wavelengths used in the tests.

The diurnal variation of fading at 6.5 cm. for typical summer and winter months is illustrated in Fig. 4. This figure shows average fading range for each hour of the day for the months of August, 1943, and February, 1944. The diurnal trend is much more pronounced in the summer than in the winter. Throughout the summer months, transmission almost invariably was stable for

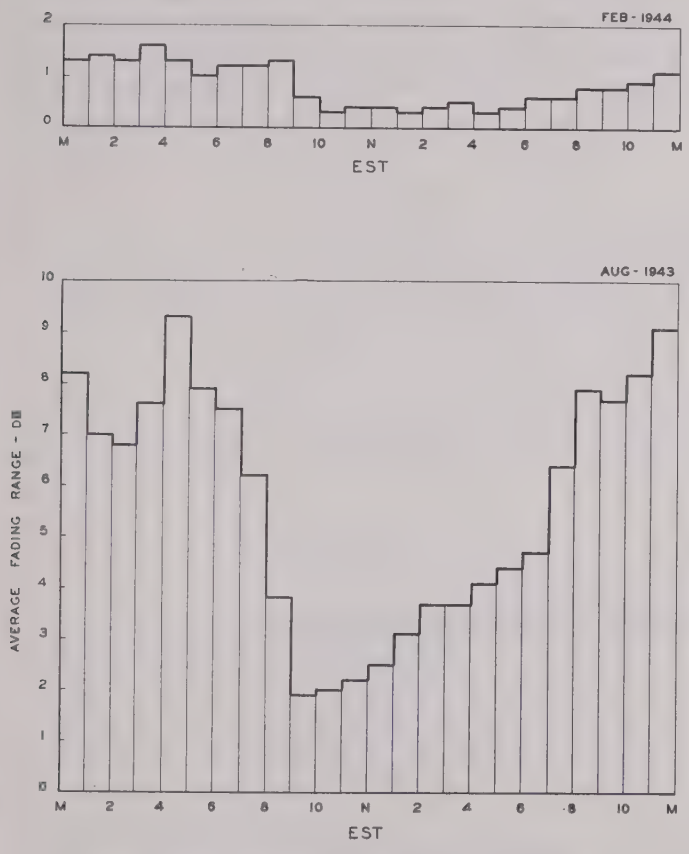

Fig. 4—Diurnal variation of fading at 6.5 cm. in winter and summer months.

several hours around midday, even on days marked by extreme fading at other hours. The period of greatest fading extended from about midnight to sunrise. After sunrise, the fading range decreased rapidly to a minimum at about 10 A.M.

Another illustration of the seasonal difference in propagation characteristics is given in Fig. 5. This figure shows distribution curves of instantaneous field intensity at 6.5 cm. for two selected days, August 1, 1943, and February 14, 1944, which were the days of greatest fading in the respective summer and winter months. On August 1 the received field was more than 20 db below the free-space value for a total time of about 7 minutes. On February 14, on the other hand, the field never was more than 6 db below free-space.

The curves of Fig. 5 illustrate the difference between relatively severe fading conditions in summer and winter. Many days during the summer showed considerably less field variation than that indicated by curve 1 and, similarly, on most winter days the variability was less than that represented by curve 2. In fact, during the winter there were a number of days on which the maximum variation of received field intensity did not exceed 2 db.

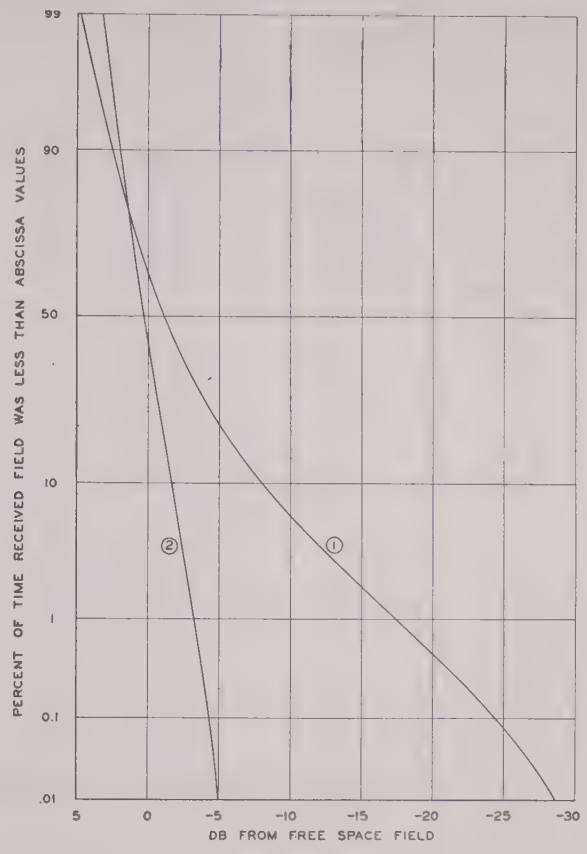

Fig. 5—Instantaneous field-intensity distributions at 6.5 cm. for a typical summer and a typical winter day. (1) August 1, 1943. (2) February 14, 1944.

Wavelength Comparisons

In the discussion of Fig. 2, attention was called to a tendency for the fading range to be somewhat greater at the shorter wavelengths. This effect is shown more clearly in Fig. 6. In this figure, percentage distributions of the hourly fading ranges at 3.2, 6.5, and 10 cm. are plotted for a period of one month, during which the three circuits were operated simultaneously. In the region where the ranges are greater than a few decibels, there is a definite increase in fading range with decreasing wavelength.

For some purposes, field-intensity minima are of more interest than fading ranges. Accordingly, in Fig. 7 are plotted percentage distribution curves of the hourly minima of field intensity for all of the transmission records summarized in Fig. 2. It is evident that the deepest fades occurred at the shortest wavelength, but the over-all spread between the 3.2- and 42-cm. curves is not very great. It should be noted, however, that the 42-cm. data cover only two months at a time of year when fading is severe, while the data for the other wavelengths cover much longer periods of time and a wide range of fading conditions.

A comparison of the records taken on the various circuits revealed several interesting characteristics. In the first place, when there was no fading the received fields at wavelengths from 3.2 to 10 cm. were usually within a few decibels of the calculated free-space values. Secondly, close inspection of the records showed that there was a marked tendency for the fading variations at 3.2, 6.5, and 10 cm. to be synchronous much of the time. It was also found that fading was generally synchronous on two receivers with antennas separated about 25 feet vertically and tuned to the same 6.5-cm. signal. From these observations it was concluded that ground reflections did not play an important part in the propagation of 3- to 10-cm. waves over the New York–Neshanic path.

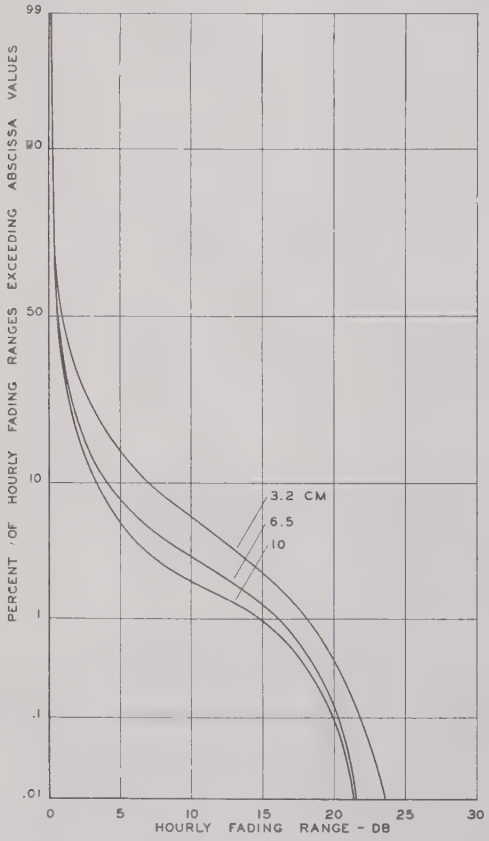

Fig. 6—Distributions of hourly fading range at 3.2, 6.5, and 10 cm., April 15 to May 15, 1944.

Types of Fading

It was found that the transmission records obtained were of four distinct types, examples of which are shown in Fig. 8. Type 1 represents a condition of stable transmission with very little fading. This condition was quite common in the winter, sometimes lasting for several days at a time. It was comparatively rare in the summer, and when it did occur it seldom continued for more than a few hours. Type 2 consists of a rapid small-amplitude variation superposed on a steady average value or on a slow, irregular variation. It was fairly common in the summer and almost nonexistent in the winter. Type 3 is characterized by comparatively slow variations of irregular amplitude and period. This is the kind of fading most frequently encountered in the summer, and practically the only kind observed in the winter. Type 4 represents the most violent fluctuations experienced on the circuits. It occurred only in the summer and fall, and then only on rare occasions. The duration of these periods of extreme fading ranged from 1 to 5 hours, and they usually occurred between midnight and sunrise.

All four types of fading were encountered at 3.2, 6.5, and 10 cm. In fact, the records for 3 to 10 cm. were generally very much alike, except that the fading was somewhat greater at the shorter wavelengths. At 42 cm., however, the records obtained were noticeably different. The transmission variations, which at times were comparable in magnitude to those at the shorter wavelengths, usually were considerably slower. There was no occurrence of the type-2 rapid scintillation, nor were there any fluctuations as violent as those classified as type 4. On a number of occasions the 42-cm. field was observed to be abnormally high and fairly steady, while the 3.2- and 6.5-cm. circuits were fading considerably. A comparison of 42- and 6.5-cm. records taken during a period of moderately severe fading is shown in Fig. 9.

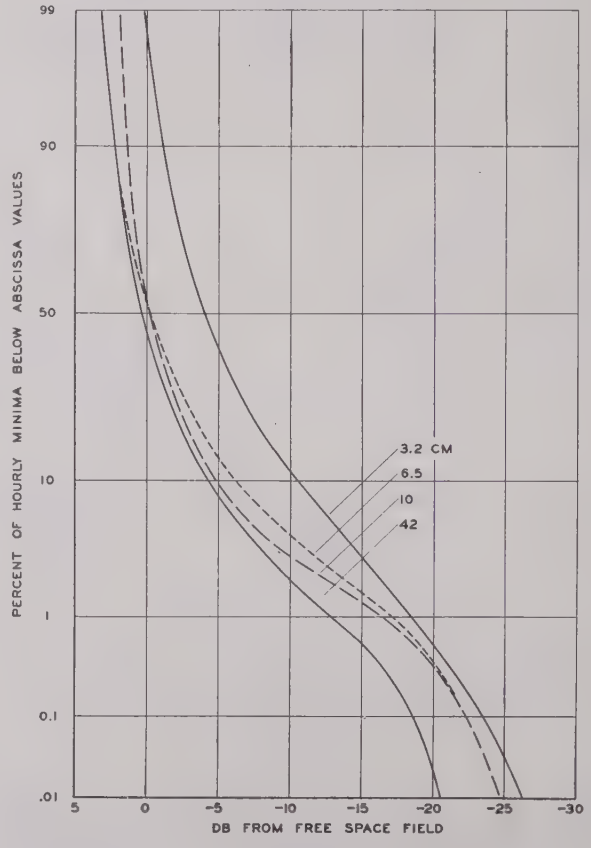

Fig. 7—Distributions of hourly minima of field intensity at 3.2, 6.5, 10, and 42 cm., August 1, 1943, to February 1, 1945.

Polarization

Some comparisons of the fading of horizontally and vertically polarized waves were made at 6.5 cm. by setting the polarization of the New York transmitting antenna at 45 degrees and recording the signal at Neshanic on two receivers, one arranged to accept the horizontal component and the other the vertical component. These

tests covered a period of 10 days and included a wide range of fading conditions. After making allowance for minor dissimilarities in the receiver characteristics, no significant differences in the two records could be found.

Path Length

About halfway between New York and Neshanic, the transmission path crossed a ridge located in Plainfield, N. J. From the top of a 25-foot tower on this ridge there was an unobstructed view of the New York and Neshanic test sites. A temporary field station was set up at this point in November, 1943, for the purpose of making comparisons of transmission on the over-all 40-mile path and the two 20-mile half sections. The complete setup for these tests consisted of a 6.5-cm. transmitter at New York which was received both at Plainfield and at Neshanic, and another transmitter at Plainfield on a slightly different wavelength which was received on a second receiver at Neshanic. Observations were made during the winter, when transmission was generally stable, but they included several periods of moderate fading which produced some interesting results.

Fig. 10 shows distribution curves of the hourly minima of field intensity for the month of December, 1943. The curves for the two 20-mile sections are very similar, while the one for the over-all path shows a considerably greater range of field minima. In fact, the depth of fading on the 40-mile path was consistently about twice as great, in decibels, as that on either of the two half sections. The similarity of the distributions for the two 20-mile circuits is interesting in view of the different character of the two transmission paths. The New York–

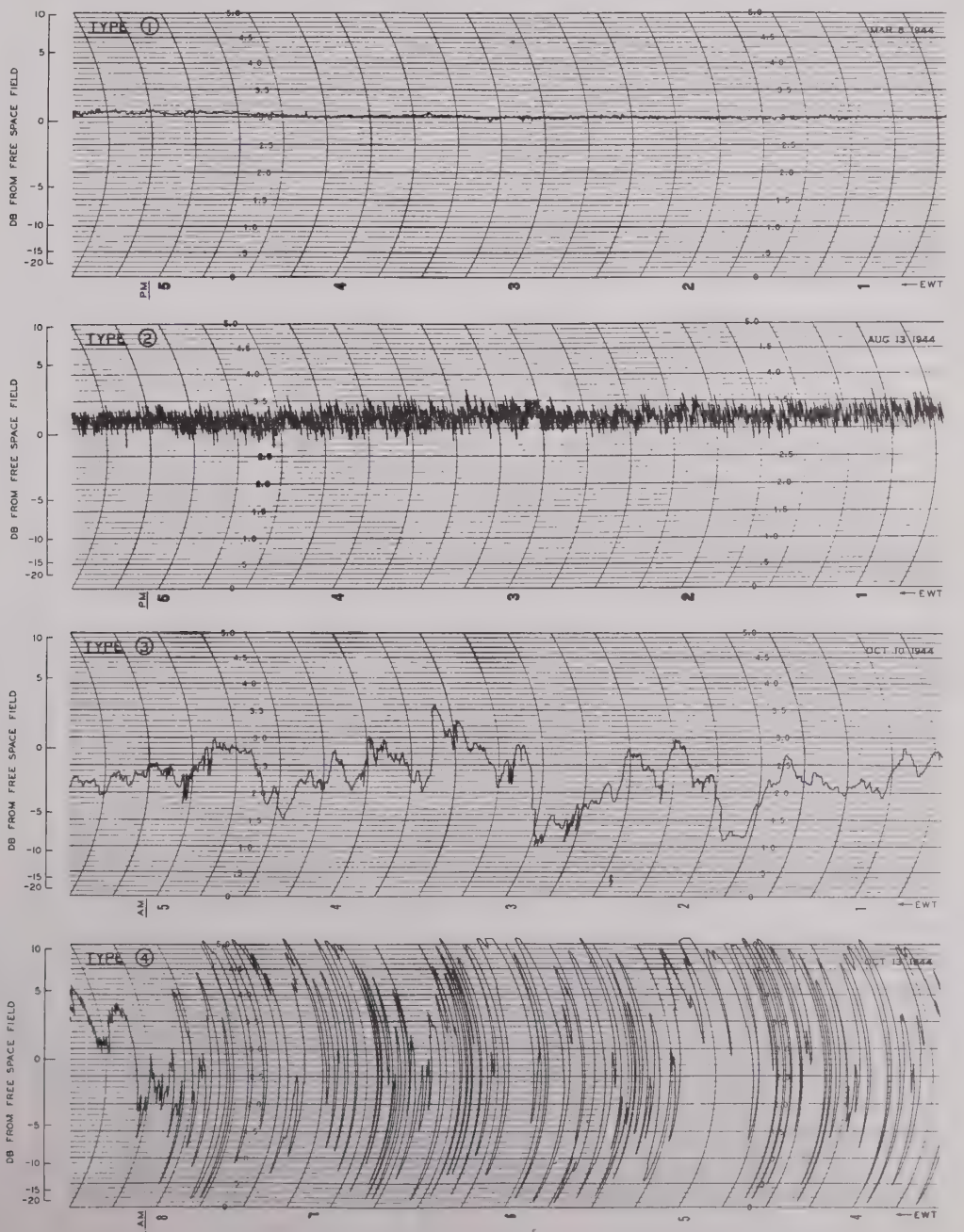

Fig. 8—Examples of four types of fading at 6.5 cm. Time shown is Eastern War Time.

Plainfield path was largely over an industrial and urban area, whereas the Plainfield–Neshanic path crossed a region of woods and fields.

A careful examination of the records for periods of fading revealed no evidence of any correlation between instantaneous variations on the over-all path and those on either of the half sections. When fading occurred, however, all three circuits invariably were affected. There were a few occasions when differences of the order of 30 minutes to an hour were observed in the times at which fading began or ended on the two 20-mile paths, indicating a rather slow movement of the atmospheric conditions responsible for the fading.

Path Clearance

In all of the tests described so far, the transmitting antennas at New York were located on the roof of the Telephone Building at 140 West Street. The transmission path from this point to the top of the tower at Neshanic cleared the ground level on the ridge at Plainfield by about 100 feet, assuming no atmospheric refraction. Actually, this 100-foot clearance was reduced somewhat by scattered trees and small buildings on top of the ridge.

The existence of a number of setbacks at different levels on the West Street building made it possible to vary the transmitting antenna height over a wide range, and thus to investigate transmission over the 40-mile path with different amounts of clearance at the midpoint. As a first step, a 6.5-cm. transmitter was installed

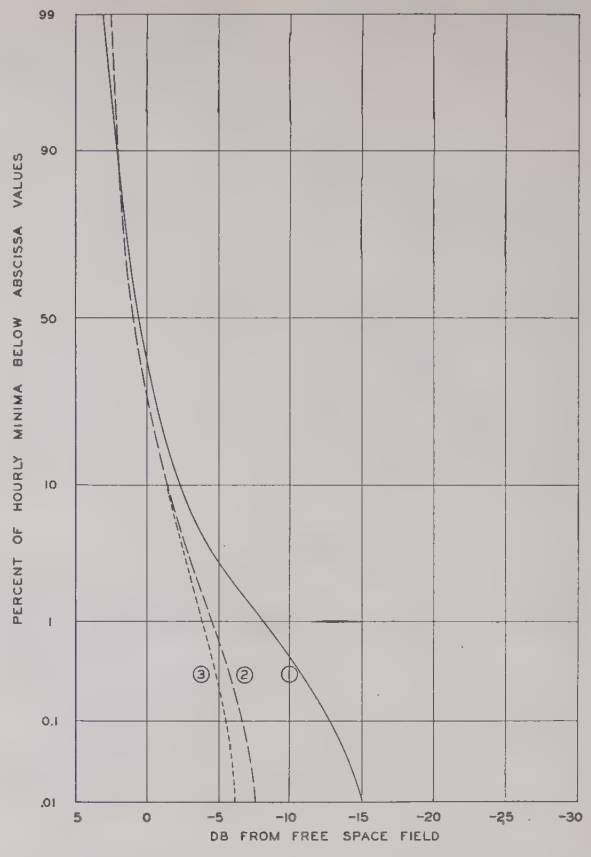

Fig. 10—Comparison of fading on over-all 40-mile path and two half sections, December, 1943. (1) New York–Neshanic. (2) New York–Plainfield. (3) Plainfield–Neshanic.

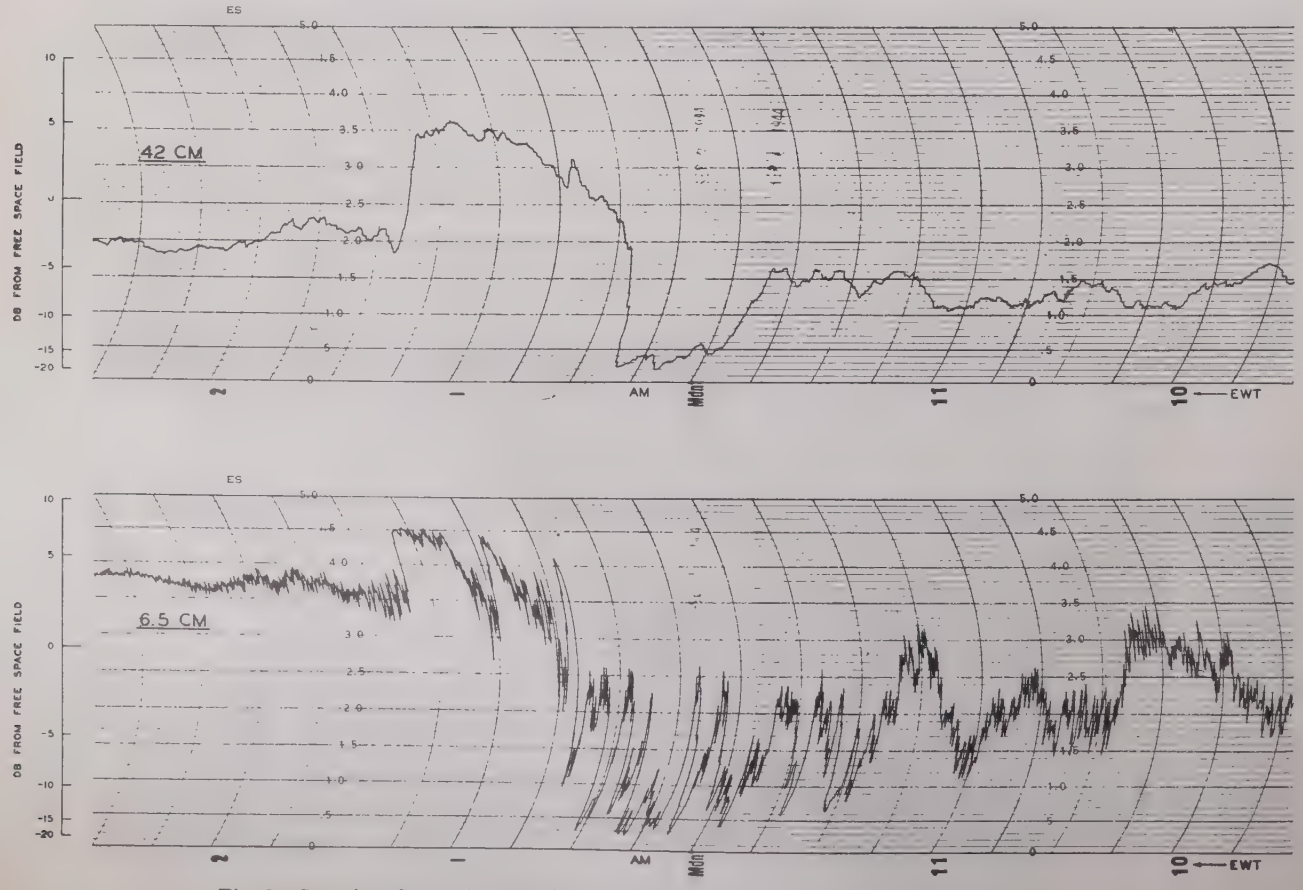

Fig. 9—Samples of record taken simultaneously at 6.5 and 42 cm., September 6–7, 1944.

at an elevation of 175 feet at West Street, and comparisons were made with a similar transmitter on the roof. The ridge at Plainfield extended some 60 feet above the straight-line path between the lower transmitter and its receiver at Neshanic. It was found that the received fields on this obstructed path ran 12 to 15 db below the free-space value when the circuit was stable, and fluctuated violently during periods of fading. It was concluded that such paths should be avoided if the objective is to provide a reliable communication circuit.

Following the tests at the 175-foot level, the lower transmitter was raised to a height of about 300 feet. From this point the path to Neshanic was very nearly grazing at ground level on the Plainfield ridge, again assuming no refraction. In the absence of fading, the average received field on this grazing path was found

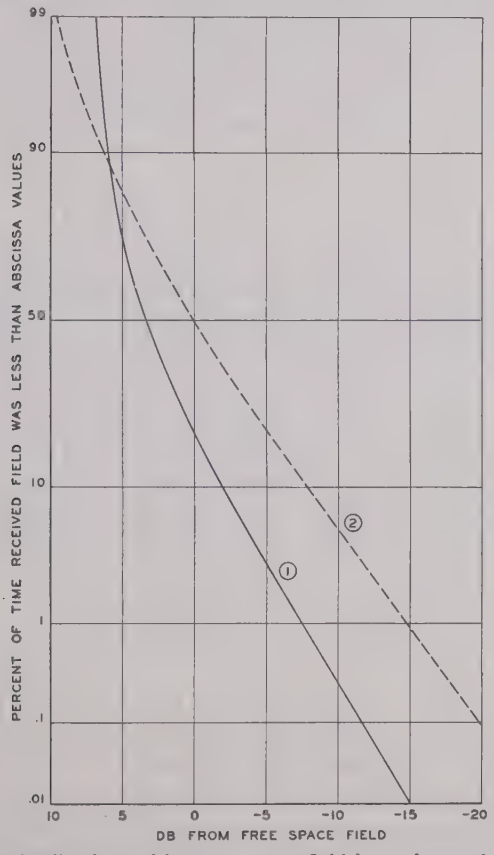

Fig. 11—Distributions of instantaneous field intensity at 6.5 cm. on clear and grazing paths, June 2, 1944. (1) Clear path. (2) Grazing path.

to be 3 to 5 db below the free-space value, while the variations during periods of fading were considerably greater than those on the clear path. No evidence of synchronism in the fading on these two circuits was discernible in the records. At times the average field intensity was considerably above the normal steady value on the grazing path when it was below normal on the clear path.

Fig. 11 gives distribution curves of the instantaneous field intensities on the two paths for a 24-hour period characterized by moderately severe fading. These curves illustrate the great variability of transmission on the lower path. It is interesting to note that the maximum field intensity recorded on the grazing path during this day was about 12 db above the free-space value, whereas on the clear path it was only about 7db above free-space. On the other hand, the fading minima were considerably lower on the grazing path. Distribu-

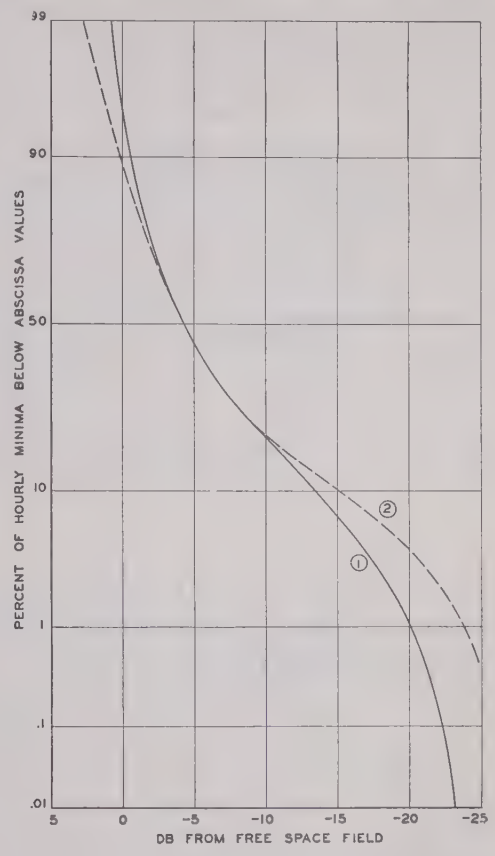

Fig. 12—Distributions of hourly minima of field intensity at 6.5 cm. on clear and grazing paths, July, 1944. (1) Clear path. (2) Grazing path.

tions of the hourly minima of field intensity on the two circuits during the month of July, 1944, are shown in Fig. 12. Again the data for the grazing path show the greater spread. The desirability of some additional clearance over the grazing condition is evident from these curves.

Test at 1.25 Centimeters

Late in July, 1945, the installation of equipment for making tests at 1.25 cm. was completed. Continuous transmission and recording at this wavelength was carried on through August and September. The transmitter power was approximately 25 milliwatts, and the antennas at both ends of the circuit consisted of metal-plate lenses with horn feeds. The receiving equipment was capable of measuring field intensities ranging from about 0 db to about −30 db with respect to the calculated free-space value. For comparison purposes the 3.2-cm. circuit was operated throughout the period of the 1.25-cm. tests.

The performance of the 1.25-cm. circuit was found to be very sensitive to atmospheric conditions. The average path loss varied widely with the water-vapor content of the atmosphere. During rainstorms, even of moderate intensity, the signal was lost completely. In

addition to these relatively slow changes, the received signals were subject to the same types of fading observed in the 3- to 10-cm. range. The maximum instantaneous field intensity at 1.25 cm. during the entire two-month test period was 5 db below the calculated free-space value. Most of the time, however, the fields were 15 db or more below free space. The similarity of the general character of the fading at 1.25 and 3.2 cm. is illustrated by the two sections of record reproduced in Fig. 13.

Fig. 14 summarizes the test results for a period of one week during which the transmission at 1.25 cm. was relatively good. The vertical lines show hourly ranges of received field intensity for both the 1.25- and 3.2-cm. circuits. The large reductions from free-space transmission at 1.25 cm. are typical of the performance at this wavelength. There was no rain during the period in Fig. 13, but on September 25 the relative humidity at New York was very high, ranging between 80 and 100 per cent.

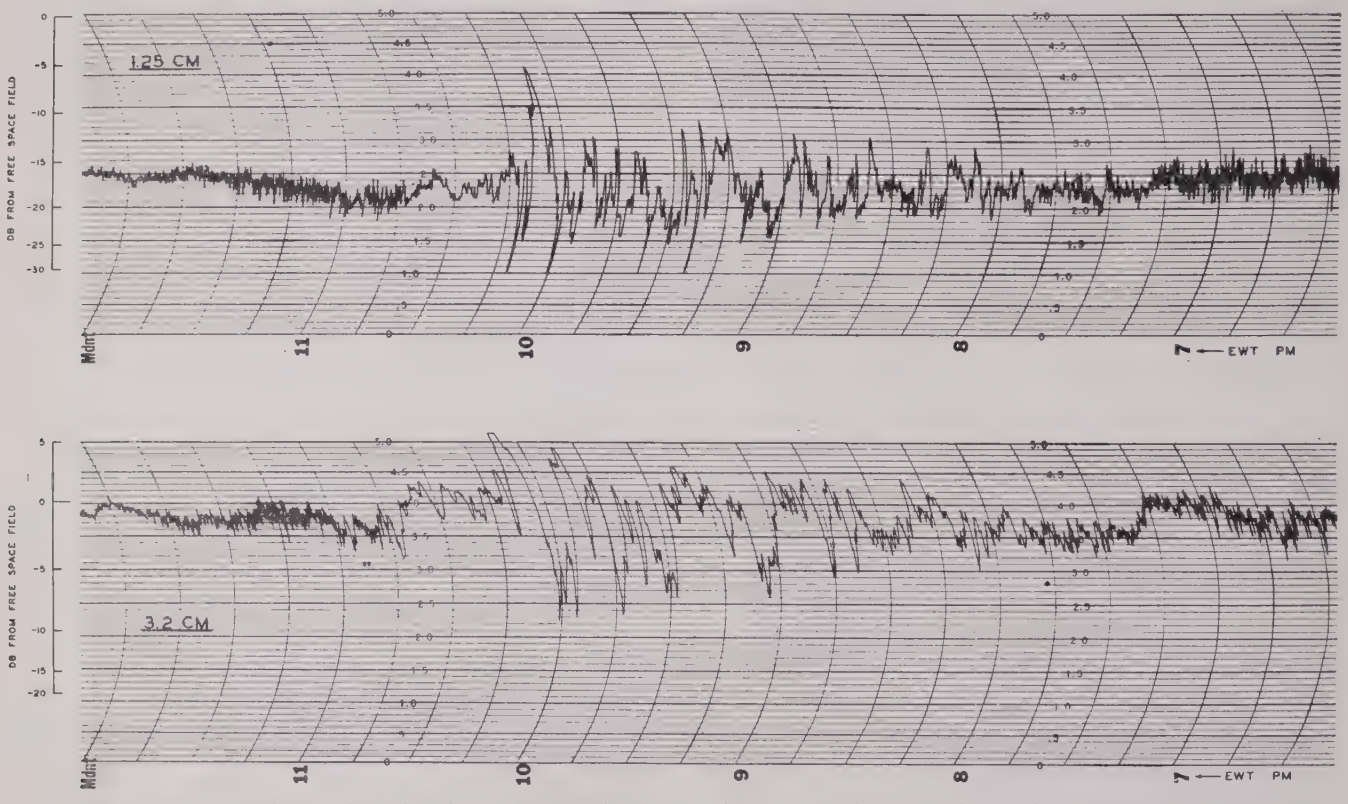

Fig. 13—Samples of record taken simultaneously at 1.25 and 3.2 cm., August 7, 1945.

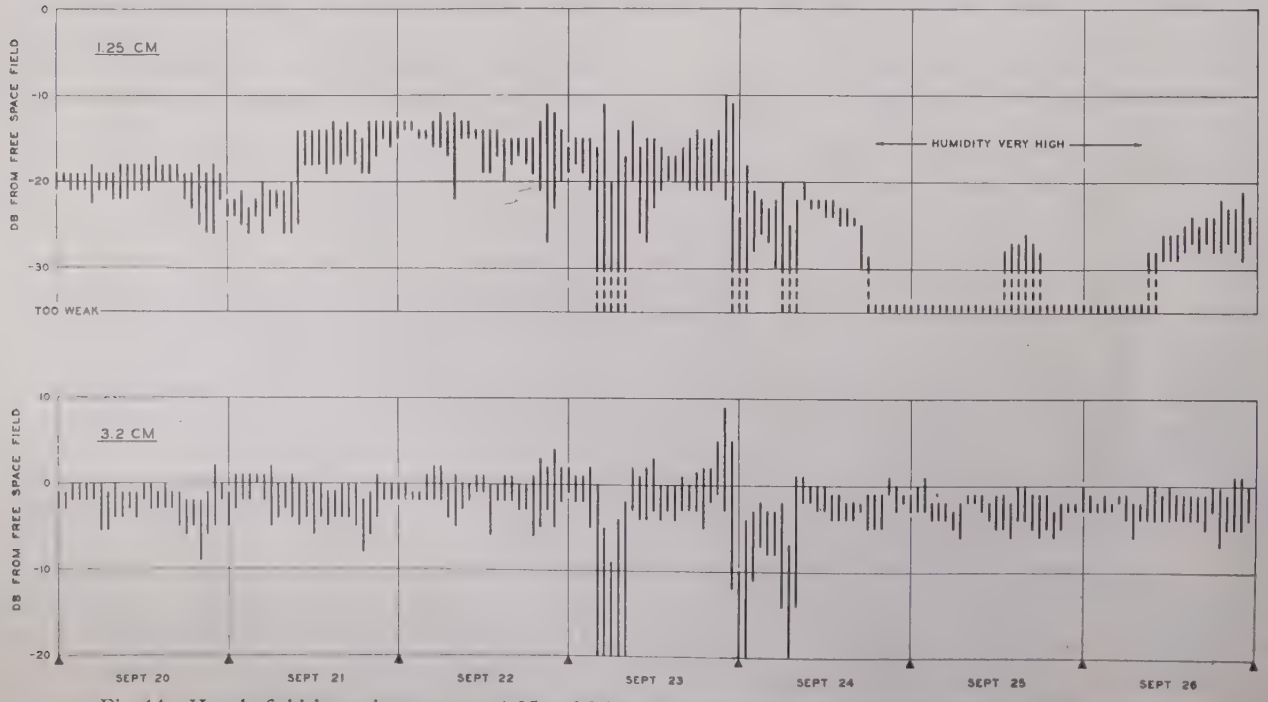

Fig. 14—Hourly field-intensity ranges at 1.25 and 3.2 cm. for a period of one week, September 20 to 26, 1945.

Distribution curves of the hourly maximum and minimum fields at 1.25 cm. for the whole test period are given in Fig. 15. These data show that about 40 per cent of the total hours of transmission had field intensity minima below −30 db, the lower limit of the measurement range. They also show that during 10 per cent of the hours the field never came up to the −30 db level. Although some difficulty was experienced in maintaining the 1.25-cm. equipment in good operating condition, a total of 867 hours of satisfactory transmission record was obtained during the test period of two months.

Meteorological Aspects

It was found that the performance of all of the test circuits was affected considerably by changes in the physical state of the atmosphere over the transmission path. As stated previously, the purpose of these tests was primarily to obtain statistics on the performance of this particular path over a long period of time, rather than to investigate the causes of the transmission variations. Consequently, no attempt was made to include in this test program any extensive meteorological studies, but some of the broader aspects of the relation between transmission variability and local weather conditions were noted.

In general, transmission was steady when the air was well mixed, as in windy or rainy weather. Under these conditions the vertical distributions of temperature and humidity are such as to yield a refractive index which decreases uniformly with height above ground. In such a medium the waves travel along paths which have uniform curvature and which tend to be stable. It was also found, as pointed out in the discussion of Fig. 4, that steady signals almost always were received around midday even on calm days. This may be accounted for by the mixing which normally occurs at this time of day, resulting from convection currents in the lower atmosphere due to the heating of the earth's surface by the sun.

Severe fading of the received signals frequently occurred when the air was calm and still, a condition favorable to stratification and duct formation. It was shown in Fig. 4 that fading was generally worse at night than during the daytime, particularly in the summer months. On calm nights the cooling of the earth by radiation tends to produce a temperature inversion in the lower atmosphere. Moreover, evaporation from the earth's surface produces a decrease of moisture content with height which, with the temperature inversion, may result in the formation of a duct. Under these conditions transmission is generally unstable, and may be subject to wide fluctuations. The lower average temperatures and the greatly reduced moisture content of the air during the winter months tend to reduce the severity of fading in the winter as compared with summer.

At the wavelengths above 3.2 cm. used in these tests there was no indication of any appreciable loss due to rainfall over the transmission path. There was some evidence of rain attenuation at 3.2 cm., although no accurate measurements of its magnitude were attempted. At 1.25 cm. a general rainfall of moderate intensity over the path introduced enough loss (15 to 20 db, at least) to obliterate the signal at the receiver.

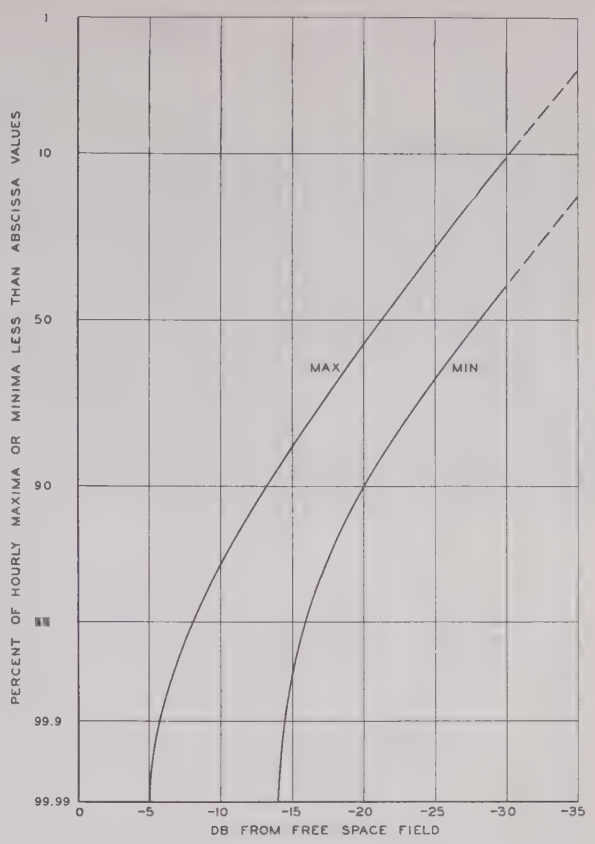

Fig. 15—Distributions of hourly maxima and minima of field intensity at 1.25 cm., August 1 to October 1, 1945.

Conclusion

The results of these tests give further assurance that the use of centimeter waves for communication circuits requiring a high degree of reliability is entirely practicable, provided due allowance is made for the variability of the transmission medium. It was shown that there was a tendency for fading to be somewhat greater at the shorter wavelengths employed in these tests, although the difference was not large enough to be a controlling factor in the choice of an operating wavelength. For continuous, reliable operation day after day in such applications as extensive relay networks, however, wavelengths well above 3 cm. are to be preferred. The usefulness of the shorter wavelengths is affected by rain attenuation and by absorption by certain gases present in the atmosphere (principally water vapor and oxygen). To insure optimum performance, it is desirable to avoid grazing-path conditions and to select transmission paths having ample clearance over intervening obstructions.

Acknowledgment

The tests described represent the co-operative efforts of a number of engineers and assistants of Bell Telephone Laboratories, including members of the Holmdel group. The author expresses appreciation to all who had a part in providing the material for this paper.

Wavelength Lenses*

GILBERT WILKES†

Summary—**The operation of a polyrod antenna can be considered as that of a lens having cross-section dimensions of the order of a wavelength. The sides of this lens are shown to be responsible for the concentration of energy, and this gathering action continues with increasing length up to a point where the energy inside the lens traveling slower than light falls out of phase with the external energy. The velocity of energy inside the lens is a function primarily of the lens dimension in the *E* plane of the wave. There exists an optimum length for each lens at which the energy is maximum. If these maxima are plotted against the lens aperture, a well-defined minimum is obtained at an aperture of one square wavelength. Below this point energy increases with decreasing cross section in the wavelength lens region, and above this point energy increases with increasing cross section in the optical lens region.**

Introduction

IF A ROD of dielectric is held in front of a receiver antenna, the received signal increases. When the rod dimensions are properly chosen, a maximum increase is obtainable. Certain laws of this behavior that have been found at the Applied Physics Laboratory of The Johns Hopkins University will be discussed in this paper.

Hertz appears to have been the first experimenter to observe the lens-like action of blocks of pitch on his newly discovered radiation. In the study of dielectric rods, one has constantly to consider their index of refraction, which is a function of their dimensions as well as their orientation with respect to the incident wave. It is also evident that they actually act somewhat like optical lenses as energy concentrators. Finally, the power of these wavelength lenses blends smoothly into that of optical lenses of large aperture. The term "lens" is capable of interpreting satisfactorily this physical behavior, whereas the terms "polyrod antenna" or "dielectric antenna" do not. The term "wavelength lens" for these devices is suggested as more appropriate than "polyrod antenna."

These lenses lie in the transition zone between radio antennas and optical lenses. The writer prefers considering only their relative power, or concentrating action, while others more familiar with radio terms prefer directive gain, as referred to an isotropic oscillator. Both will occur in the following as convenience may require.

A 3-cm. or "X"-band wavelength was used in the experimental work, so as to limit the size of equipment and space requirements.

* Decimal classification: R326.8. Original manuscript received by the Institute, June 2, 1947; revised manuscript received, September 2, 1947. Presented, joint meeting, International Scientific Radio Union and American Section I.R.E., May 7, 1947, Washington, D. C.

Extracted from "Wave Length Lenses," Bumblebee Series, Report 59, The Johns Hopkins University Applied Physics Laboratory.

† Applied Physics Laboratory, The Johns Hopkins University, Silver Spring, Md.

Fundamental Lens Behavior

If we take a series of dielectric blocks having a uniform cross section of the order of a wavelength, and place them in front of a receiving horn in such a way as to obtain an increasing length of dielectric or lens in front of the horn, the gain is found to vary periodically with the lens length. If the steps by which the length is increased are made sufficiently small, a second-harmonic variation of small intensity is found superimposed on the fundamental variation. Fig. 1 shows these characteristics for two different lenses. The harmonic is found to correspond to Snell's law for the reflection from thin sheets, and can be eliminated by the use of pointed lenses. It has no practical importance, therefore, but did lead to the determination of a wavelength individual to each lens, which permitted the determination of the velocity at which energy travels through the lens; this, in turn, gives an explanation of the characteristic variation with length of the fundamental gain of lenses.

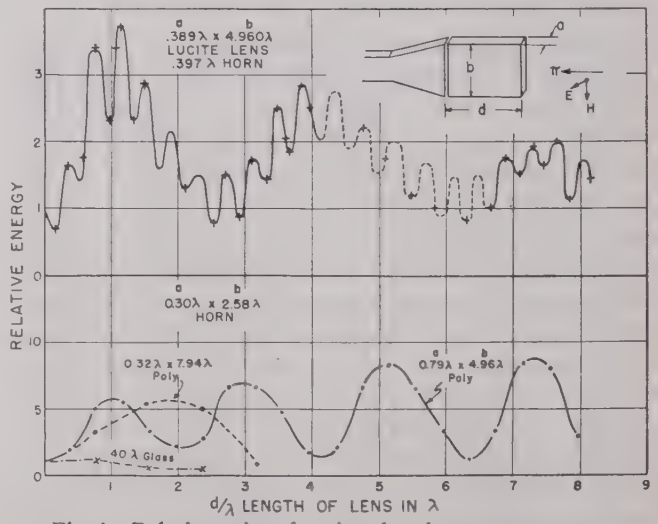

Fig. 1—Relative gains of various lens horn arrangements (preliminary experiments).

Apparent Index of Refraction

The harmonic variation of Fig. 1 passes through minima at lengths equal to about 0.4λ. The dielectric constant of lucite is about 2.55, and its index of refraction is 1.6. If the lens behaved according to this index, its wavelength would be 0.635λ, and the minima would occur at every 0.31λ. The discrepancy between this and the observed data exceeds any possible experimental error and the existence of a characteristic wavelength λ_L must be postulated.[1,2] This wavelength im-

[1] This phenomenon was first reported by G. C. Southworth, "Some fundamental experiments with wave guides," Proc. I.R.E., vol. 25, pp. 807–823; July, 1937.

[2] Peter Mallach, "Dielectric Radiators for DM and CM Waves," Intelligence Interrogation Report, Berlin, Combined Intelligence Objectives Subcommittee, Item 1, File No. xxx1–83.

plies characteristic lens velocities v_L and indices of refraction n_L that are all interrelated by the same types of equation as the more usual constants for large masses of dielectric.

To visualize lens behavior, it is helpful to realize that there is no critical or cutoff dimension for a bare dielectric rod, and also that the energy traveling in a dielectric rod is mainly concentrated toward the center of the rod. These ideas have been discussed theoretically by many authors, particularly Schelkunoff.[3] The latter gives the general expressions for waves in dielectric wires that substantiate the above statement, and from which at least an approximate form of the expression of the lens index of refraction may be obtained.

The variations of energy observed in Fig. 1 may be explained by Fig. 2, where a plane wave is shown sweeping over a lens. Admitting that the lens has a wave-

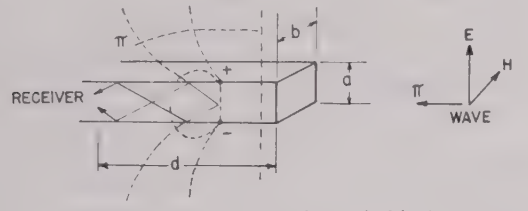

Fig. 2—Wake over a dielectric block.

length λ_L, Snell's law for normal incidence gives the transmission through a thin dielectric sheet[4] as

$$T = 1 - R = 1 - \frac{(r_{12} + r_{23})^2 - 4r_{12}r_{23}\sin^2 \alpha d}{(1 + r_{12}r_{23})^2 - 4r_{12}r_{23}\sin^2 \alpha d} \tag{1}$$

with
$$r_{jk} = \frac{\sqrt{\mathcal{E}_j} - \sqrt{\mathcal{E}_k}}{\sqrt{\mathcal{E}_j} + \sqrt{\mathcal{E}_k}} \tag{2}$$

$$\alpha = \frac{2\pi}{\lambda_L}, \quad \lambda_L = \text{wavelength in lens.} \tag{3}$$

If each side of the dielectric is looking at the same impedance, which is only an approximation in the present case, (2) gives

$$r_{12} = -r_{23} = r$$

and (1) becomes

$$T = 1 - \frac{4r^2 \sin^2 \alpha d}{(1 - r^2)^2 + 4r^2 \sin^2 \alpha d}, \tag{4}$$

which goes through minima for

$$|\sin \alpha d| = 1 \qquad \alpha d = (2K + 1)\frac{\pi}{2} \tag{5}$$

or

$$d = \frac{(2K + 1)\lambda_L}{4} = \frac{\lambda_L}{4}, \quad \frac{3}{4}\lambda_L, \quad \frac{5}{4}\lambda_L. \tag{6}$$

[3] S. A. Schelkunoff, "Electromagnetic Waves," D. Van Nostrand Co., New York, N. Y., 1943; pp. 425–428.
[4] J. A. Stratton, "Electromagnetic Theory," McGraw-Hill Book Co., New York, N. Y., 1941; p. 514.

The harmonic minima of Fig. 1 therefore define a lens wavelength λ_L. This lens wavelength must correspond to an index of refraction n_L and energy velocity v_L in the lens:

$$n_L = \frac{\lambda}{\lambda_L} \qquad v_L = \lambda_L \nu = \frac{\lambda_L}{\lambda} c = \frac{c}{n_L} \tag{7}$$

where v, c, ν are the frequency, velocity, and wavelength of the radiation in free space.

A wave flowing over the dielectric of Fig. 2 will excite displacement currents inside the dielectric. These, in turn, will radiate energy, a large part of which will be totally reflected inside the dielectric. Neglecting losses and external field depletion, this action will continue down the dielectric until the internal and external energies are one-half cycle out of phase, after which the internal energy will feed back into the external field until the two are again in phase, when the process will be repeated.

The transit time of the internal and external energies are, respectively,

$$t_L = \frac{d}{v_L} = \frac{n_L}{c} d \qquad t = \frac{d}{c}. \tag{8}$$

The peak gain will occur when these two times differ by an odd number of half periods, or

$$t_L - t = \frac{(2K + 1)}{2\nu} = \frac{d}{c}(n_L - 1), \tag{9}$$

or the first optimum lens length is

$$d \max = \frac{c}{2\nu(n_L - 1)} = \frac{\lambda}{2(n_L - 1)}, \tag{10}$$

and so on. This then corresponds to the fundamental variation of energy of Fig. 1.

In simple lenses that have no matching device inside the horn or waveguide, the value of optimum length from (10) is always verified. The apparent index of refraction may be obtained either directly from a phase meter or calculated. We note for future reference that the apparent indexes vary with dimensions. Thus, the larger polystyrene lens of Fig. 1 would have an index of 1.5, and the smaller one an index of 1.25. When a lens is extended into a waveguide for matching purposes, the optimum position is influenced slightly by the length in the guide. However, after the best match is obtained, the lens length can be adjusted so as to again verify (10). Referring to Fig. 3, a single piece of dielectric is slid in a waveguide so that one end acts as matching slug and the other as lens. The experimental apparent index of refraction is 1.09, indicating an optimum length of 5.55λ. The slug, however, moved the peak gain back to 5.5λ. At this point a slight additional gain would have been available by increasing the length of lens by 0.05λ and leaving the matching slug at its original length.

The most important characteristic of a wavelength lens is its apparent index of refraction. Reference has already been made to Schelkunoff's treatment of waves in dielectric wires.[3] The equations are involved and space does not permit their reproduction here. Suffice it to say that they indicate an approximate form of the transmission constant, and that from this work and our many experimental determinations we have adopted the expression

$$n_L - 1 = (n - 1)e^{-(\lambda/\lambda' c)^2} \qquad (11)^5$$

in which λ_c' is a characteristic wavelength akin to the cutoff wavelength of guides. However, it is found experimentally that the dimension of preponderant influence in lenses is the one in the E plane or "a" of Fig. 2, while the dimension in the H plane plays only a minor role that may be neglected.

The expression for λ_c' is, therefore,

$$\lambda' c = 2na \quad \text{(rectangular lenses)}$$

$$\lambda' c = \frac{n\pi a}{1.84} \quad \text{(cylinder lenses)}$$

(a = diameter).

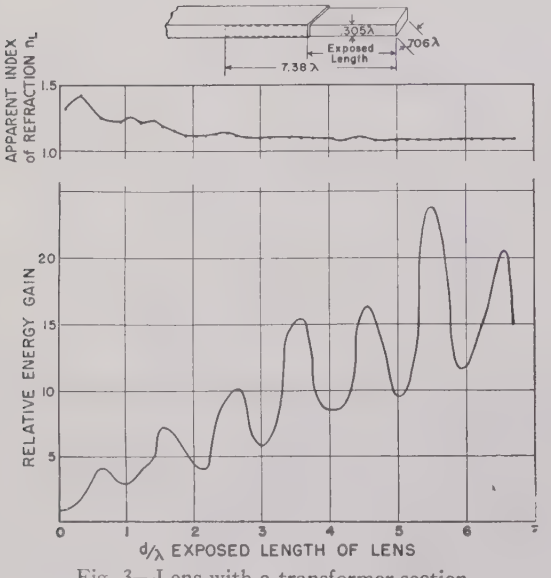

Fig. 3—Lens with a transformer section inside wave guide.

In obtaining (11), dielectric losses, field depletion, and the proximity of metal surfaces were neglected. Reference to Figs. 3 and 4 will show that the apparent index of refraction passes from the true index in the vicinity of the metal mouth to an almost constant value a wavelength away from the mouth, and from this point on it decreases only very slowly. This slow decrease is believed due to field depletion, and will be discussed in the following. A few experimental points are plotted against (11) in Fig. 5.

[5] Equation (11) above is semiempirical. It is found to check closely experimental data on rectangular lenses, and only approximately cylindrical lenses. D. W. Horton, of the University of Texas, has communicated graphical solutions he has worked out for the transcendent expression for waves in cylindrical rods given by Stratton on page 526 of footnote reference 4. These solutions appear to be better for cylindrical lenses than (11), which, however, remains the most accurate expression known for rectangular lenses. The writer also wishes to acknowledge Dr. Horton's kind co-operation in establishing (14) in the following section.

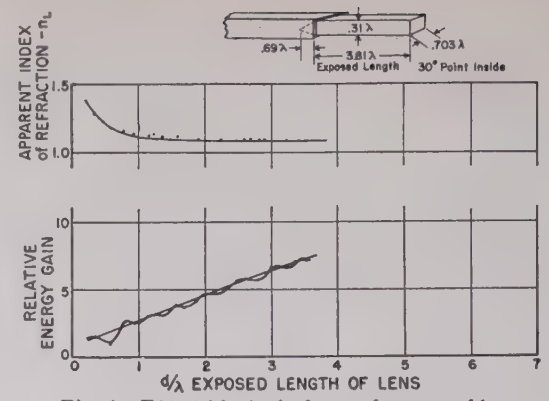

Fig. 4—F1114 blocks in front of wave guide.

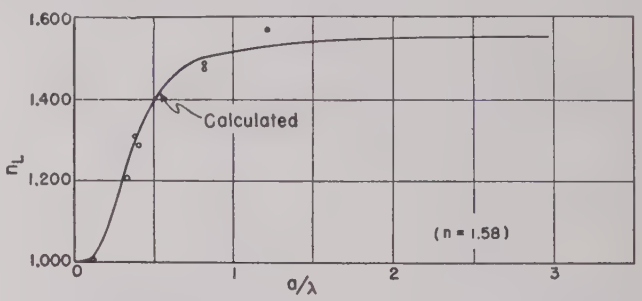

Fig. 5—Experimental verification of $n_L - 1 = (n-1)e^{-(\lambda/\lambda_c')^2}$. For rectangular lenses, $\lambda_c' = 2na$. For cylindrical lenses, $\lambda_c^1 = \frac{\eta\pi a}{1.84}$.

The energy velocities given by (11) explain the operation of the dielectric depolarizer or circular polarizer of Fig. 6. If a flat dielectric plate is mounted at a slant of 45 degrees in front of a crystal, its length can be so adjusted as to transform a plane-polarized wave to

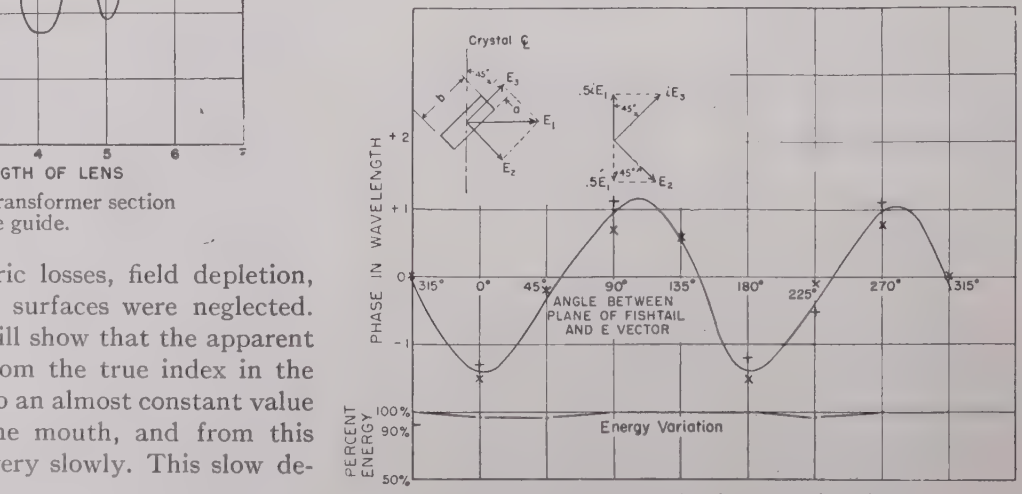

Fig. 6—Phase variation from rotation of a fish-tail depolarizer.

circular polarization at the crystal. For example, suppose that a plane wave E_1 normal to the crystal is fed onto this assembly. It will be decomposed into a wave E_2 normal to the dielectric and E_3 parallel to the dielectric. According to (11), the former will not be de-

layed appreciably, while the latter will be strongly retarded. These two waves will have components in the crystal plane equal to half the original amplitude but opposed in space. If the length of the dielectric plate is such that the phase between these two is one-quarter period, the crystal becomes sensitive to their resultant, or 0.7 of the original amplitude or 0.5 of the original energy. This resultant is, then, in reality a circularly polarized wave, rotating counterclockwise in the case of Fig. 6, and the crystal is insensitive to a change in the angle of polarization of the received wave. The device becomes a depolarizer to receive a constant signal with a rolling receiver. It is generally made by flattening the end of the lens sticking into a circular wave guide to resemble a fish tail, by which name it is often called.

Relative Gain

The relative gain of a lens is the optimum energy received on the optical axis of a lens-receiver combination referred to the energy received by the receiver alone. It is the characteristic of practical significance in lens work, and unfortunately the one least reducible to a simple quantitative expression. The relative gain of a lens is affected by the nature of the receiver, the directivity or beam width of the combination, whether the lens intercepts all the received energy or only part of it, how well the lens is matched to the receiver, and on field depletion. For short, stubby lenses there does not appear to exist a reliable expression for gain. However, the optimum length can be calculated from (10), and the power of the lens can be determined experimentally without trouble.

For less than wavelength apertures, optimum lenses are always long. Under these conditions all the oscillators along the lens can be considered in phase and their contributions to gain can be added. This results in the simple expression for relative energy:

$$G_{REL} = 1 + \frac{d \max}{\lambda} = 1 + \frac{1}{2(n_L - 1)}, \qquad (12)$$

which, it is repeated, is only an approximation on the conservative side for long lenses in which no special matching is used between lens and receiver. Where the dimensions in either plane are such as to influence the beamwidth, the directivity of the lens-receiver combination acts to increase the apparent relative energy on optical axis.

This influence is marked on Fig. 1 and less noticeable on Fig. 4. Where a matching slug is used, as in Fig. 3, the effect of this device is important. In Fig. 4 the end of the lens in the waveguide was made and placed so as to obtain a fixed mismatch between the waveguide and atmosphere. The lens of Fig. 3, identical in all other respects, was intended to afford a variable matching device such that the maximum reflected energy would be 50 per cent of the total. The minima of Fig. 3 lie, therefore, on Fig. 4, and the maxima lie on a line twice as high. The harmonic of Fig. 4 will be recognized as Snell's reflection, and that of Fig. 3 as the characteristic of a matching slug which is so great that it hides almost entirely Snell's reflection.

Equation (12) would indicate the possible construction of an infinitely powerful lens by making n_L approach unity. This is very nearly obtained in thin lenses, and the drooping characteristic of Fig. 7 is obtained. The falling off of the relative energy from the straight line indicated by (12) can be analyzed approximately as follows:

Adapting Schelkunoff's treatment for the pattern of an array of sources of amplitude M to the relative gain of a lens, (12) can be written

$$G_R = 1 + \left| \frac{R(d)_R}{M_0} \right|^2 \qquad (13)$$

where

$$R(d) = \int_0^d M \sin (K_L z + \delta) e^{iKz} dz \qquad (14)$$

with

$$K_L = \frac{2\pi}{\lambda_L} \qquad K = \frac{2\pi}{\lambda}. \qquad (15)$$

If we suppose n_L to approach unity, then

$$K_L \to K \qquad \delta \to 0 \qquad d \to \infty,$$

and, neglecting losses, Fig. 7 suggests that

$$M^2 = M_0^2 e^{-2Kmz}. \qquad (16)$$

On integrating (14), (13) becomes

$$\lim_{} G_R \to 1 + \frac{1}{4K^2 m^2}, \qquad (17)$$

which is finite, although large.

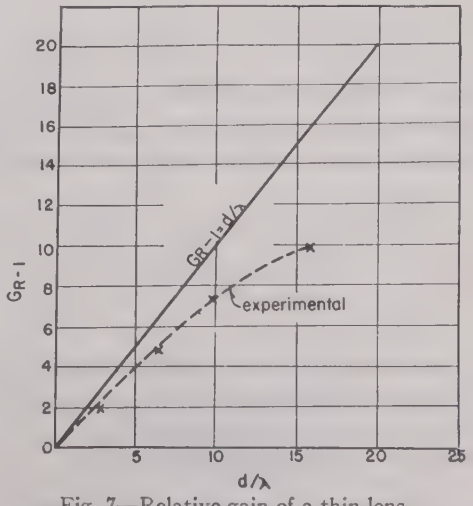

Fig. 7—Relative gain of a thin lens.

If, in Fig. 7, each increment wavelength gathers an energy fraction α of the preceding one, the total energy is

$$E = E_0 + \alpha E_0 + \alpha^2 E_0 + \cdots + \alpha^{d/\lambda - 1} E_0$$
$$= E_0 \frac{1 - \alpha^{d/\lambda}}{1 - \alpha}, \tag{18}$$

and this equals

$$7.5 \quad \text{for} \quad \frac{d}{\lambda} = 10.$$

The values of α and M are related by

$$e^{-2mK} = \alpha, \tag{19}$$

and solving, the limit relative energy becomes

$$\lim_{G_R} \to 1 + \frac{1}{0.14^2} \simeq 50.$$

The particular lens cross section used in Fig. 7 was $0.2\lambda^2$, so that the maximum energy an ideal lens is capable of gathering appears to be that contained in $10\lambda^2$. The ideal aperture of such a lens would be 3λ, and the minimum beam half-power point would be a third of a radian, or 19 degrees, which checks the sharpest patterns obtained with lenses of less than a wavelength aperture.

Equation (12) is the roughest kind of an approximation of the relative energy of a lens. It is of interest, however, as it confirms the experimentally proven fact that more powerful wavelength lenses can be made with dielectric materials of low indexes than with those of high indexes, such as glass. However, as the dielectric constant tends to unity, there must occur a point at which the lens ceases to function. Our experiments have not extended into this region, but only down to F1114 ($\mathcal{E}$ 2.1) which gives better lens operation than polystyrene ($\mathcal{E} = 2.5$).

Lens Patterns

Usable expressions for lens patterns can be derived from metallic-array theory. The computations are, however, too long to repeat here, and only the case of the cylindrical lenses will be discussed, as the expressions obtained can give qualitative information on the directivity of lenses.

The expression for the distant field of a linear array[6] is

$$E^2 = A^2 F_0^2 F_1^2 F_2^2 \tag{20}$$

where

A = function of received energy and aperture
F_0 = form factor of aperture
F_1 = form factor of single element
F_2 = factor of linear array of elements.

If a circular wave guide is filled with a piece of dielectric flush with the end, this dielectric will be the seat of displacement currents that, in the aggregate, resemble the current distribution of a half-wavelength oscillator in the E plane for which

$$F_0 = \frac{\cos \frac{\pi}{2} \cos\theta}{\sin\theta}, \tag{21}$$

experimentally checked on graph A of Fig. 8.

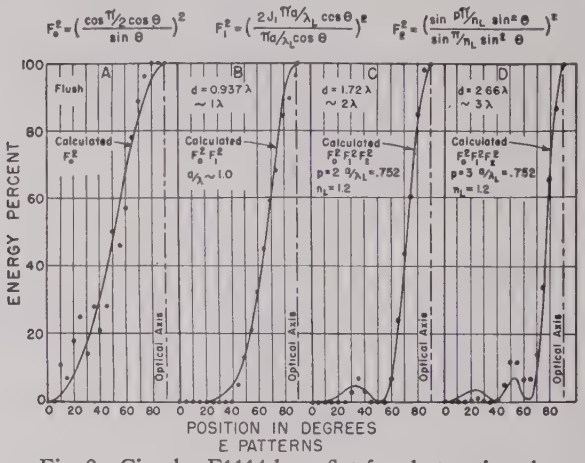

Fig. 8—Circular F1114 lens, flat-faced at each end.

As the lens walls are powerful absorbers of energy, its pattern may be compared to that of an orifice in an absorbing screen, and factor F_1 becomes[7]

$$F_1 = \frac{2J_1 \frac{\pi a}{\lambda_L} \cos\theta}{\frac{\pi a}{\lambda_L} \cos\theta} \tag{22}$$

experimentally checked on graph B of Fig. 8, for a lens one wavelength long. Side lobes will only occur if F_1 passes through zero. As long as

$$\frac{\pi a}{\lambda_L} < 3.8$$

this cannot occur, so that generally lenses of one wavelength are free from side lobes.

The factor

$$F_2 = \frac{\sin p \frac{\gamma}{2}}{\sin \frac{\gamma}{2}} \tag{23}$$

where p = number of lens wavelengths in length of lens departs from unity as p increases from unity. The classical value of γ in (23) is[8]

$$\gamma = \frac{2\pi l}{\lambda} \cos\psi - \alpha \tag{24}$$

[6] See page 451 of footnote reference 4.

[7] See page 356 of footnote reference 3.
[8] See page 342 of footnote reference 3.

with

l = spacing between oscillators, one lens wavelength
$\psi = \pi/2 - \theta$
α = phase lag from one oscillator to next $= 2\pi$.

Equation (11) shows that the wavelength in a lens is an inverse function of the dimension of the E plane. While this function may be quite complex, satisfactory E patterns are obtained if

$$l \sim \frac{1}{\alpha} \sim \lambda_L \sin\theta,$$

and, after simplifying, (23) becomes

$$F_2 = \frac{\sin\left(\frac{\pi p}{n_L}\sin^2\theta\right)}{\sin\left(\frac{\pi}{n_L}\sin^2\theta\right)}, \qquad (25)$$

which after introduction in (20), is verified in graphs C and D of Fig. 8.

It may be noted that p, the number of oscillators in a metallic array, is required to vary by integer lengths, whereas in lenses p can vary continuously and the side lobes represented by F_2 vary smoothly from one lens length to the next.

The actual patterns are seen to check the above expression closely in the main beam, while the side lobes do not check nearly so well.[9]

Gain From Patterns

Returning now to (20), consider only the energy received on the axis, for which

$$\theta = \frac{\pi}{2}$$

$$E^2 = A^2\left[\frac{\sin\frac{p\pi}{n_L}}{\sin\frac{\pi}{n_L}}\right]^2. \qquad (26)$$

Now consider only optimum lenses for which

$$p\ \max = \frac{d\ \max}{\lambda_L} = \frac{n_L}{2(n_L - 1)} \geqq 1. \qquad (27)$$

If the equals sign is used,

$$p\ \max = 1,$$

and the corresponding n_L is found to be equal to 2, corresponding to short, thick glass lenses for which the lens energy from (26) is equal to the energy of the aperture without the lens. Setting aside this rather inefficient case and letting

$$1 < n_L < 2,$$

and replacing in (26) p by $p_{\max}$ drawn from (27),

$$E^2 = A^2\left[\frac{\sin\left(\pi p - \frac{\pi}{2}\right)}{\sin\left(\pi - \frac{\pi}{2p}\right)}\right]^2.$$

If only large integer values of p are considered, the expression becomes simply

$$E^2 = A^2\left(\frac{2p}{\pi}\right)^2. \qquad (28)$$

To arrive at a qualitative expression of the energy on the axis in the function of aperture "a," "p" is replaced by its value from (27) and n_L from (11):

$$p = \frac{n_L}{2(n_L - 1)} = \frac{1 + (n-1)e^{-(\lambda/2na)^2}}{2(n-1)e^{-(\lambda/2na)^2}} \sim e^{(\lambda/2na)^2},$$

and introducing

$$A \sim \frac{a^2}{\lambda^2},$$

the expression of (28) is seen to assume the form

$$E^2 \sim B\left(\frac{\lambda}{a}\right)^z \qquad z > 1,,$$

which qualitatively expresses the energy of the lens proper on the axis.

In (12), for the relative energy of a receiver-lens combination, the unit represents the signal of the receiver without the lens, which is a function to the fourth power of the aperture. The total signal received by a lens-receiver combination is, qualitatively,

$$G_{ABS} = \left(\frac{a}{\lambda}\right)^4 + B\left(\frac{\lambda}{a}\right)^z, \qquad (29)$$

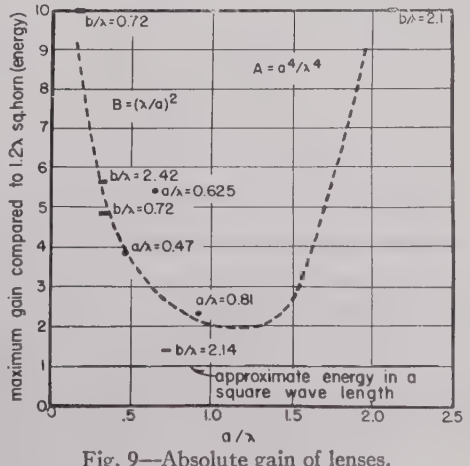

Fig. 9—Absolute gain of lenses.

consisting of two terms, one of which is negligible for small or large apertures. The curve is cusped at

[9] Peter Mallach developed pattern expressions which give good results for small ratios of a/λ. They do not seem to apply for $a/\lambda \leq 1$, which is usual in this country.

$$\frac{a}{\lambda} = 1.$$

Below this value, the wavelength lens region extends to zero, and the optimum energies are limited by the phase and field depletion discussed previously. Above this value, lenses approach the optical region where the energy is only a function of aperture.

Several experimental values have been plotted on Fig. 9 against the signal received by a square horn of approximately one-square-wavelength effective aperture. To arrive at an idea of the directive gains shown on this curve, the ordinates can be multiplied by 4π.

ACKNOWLEDGMENT

The writer wishes to acknowledge the co-operation of The Johns Hopkins University and the help of the Applied Physics Laboratory in preparing this note. It is to be hoped that others eventually will arrive at rigorous data were only qualitative information derived from experimental evidence has here been indicated.

A Method of Determining and Monitoring Power and Impedance at High Frequencies*

J. F. MORRISON†, SENIOR MEMBER, I.R.E., AND E. L. YOUNKER†, ASSOCIATE, I.R.E.

Summary—A method and newly developed devices for determining and monitoring power and impedance levels in transmission lines at high frequencies are explained. Practical considerations influencing accurate determination of power and impedance levels are analyzed, and the previous and newly developed methods of monitoring these important quantities under changing conditions of load are compared.

THE MEASUREMENT of power delivered at radio frequencies, as well as the impedance presented by the transmission line over which it is delivered, presents increased difficulties as we go to higher and higher frequencies. The work reported in this paper was directed primarily toward the measurement of power and impedance at the output terminals of radio transmitters operating at frequencies of about 100 megacycles. However, as will be seen, the methods and techniques developed are not necessarily limited to that application or frequency region.

At radio frequencies slight changes in the physical structure of antennas, transmission lines, or networks often cause a substantial change in their impedance. This effect is accentuated as the frequency is increased, and uncertainties regarding impedance values are usually reflected in the accuracy of power measurements. We therefore desire to indicate, with good accuracy, the power being dissipated in a load regardless of any changes, accidental or otherwise, that may occur in the load impedance, and also to indicate the magnitude of a transmission-line mismatch if any should occur during operation. To give such a power indication, it is practically necessary that some form of radio-frequency wattmeter be provided. In addition, some form of impedance indicator or standing-wave detector which can be used under power is essential to fulfill the second desire. Both of these facilities are provided by the circuit arrangements to be described.

Consider Fig. 1(a), where a transmission line with an inductive impedance L in series with the line and a capacitive impedance C across the line is shown. The voltage produced across the inductance L by the line current I causes a small sample current i_1 to flow through the resistance R and the crystal rectifier. If the resistance is made large compared with the reactance of the inductance, this sample current is proportional to and in phase quadrature with the line cur-

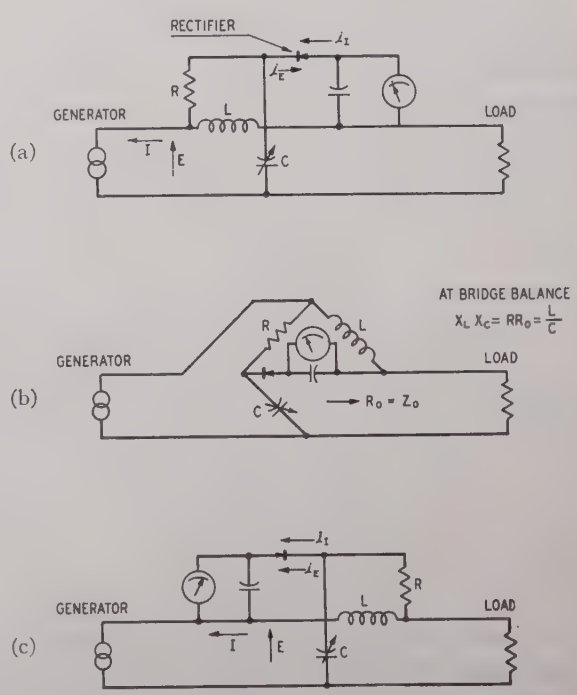

Fig. 1—Basic circuits used in the power and impedance monitor.

* Decimal classification: R245×R244. Original manuscript received by the Institute, March 10, 1947. Presented, 1947 I.R.E. National Convention, March 3, 1947, New York, N. Y.

† Bell Telephone Laboratories, Inc., Whippany, N. J.

rent. The voltage E across the transmission line causes another sample current i_E to flow through the capacitance C and the crystal rectifier. If the reactance of the capacitance is made large compared with the impedance of the rectifier, this sample current is proportional to and in phase quadrature with the line voltage. When the line is terminated in a load resistance equal to its characteristic impedance, the sample currents will flow through the rectifier in opposite phase. The capacitance C is then adjusted so that these sample currents are equal in amplitude, which is indicated by zero current through the meter. A change in the transmission-line load impedance will now cause an inequality and generally a phase displacement of the two sample currents. Their resultant, which is no longer zero, flows through the rectifier and provides a meter indication which is related to the magnitude of the impedance change.

The performance of this circuit can also be explained if it is drawn as shown in Fig. 1(b), where it is seen to constitute a Maxwell bridge, the transmission-line input impedance providing one of the resistance arms. When the bridge is balanced, the meter is not, of course, responsive to changes in the generator output. However, changes in the transmission-line input impedance will upset the bridge balance and will cause a meter indication which is related to the magnitude of the impedance change. The conditions for balance with this bridge require that the product of the reactances equal the product of the resistances, i.e.,

$$X_L X_C = RR_0.$$

A change in frequency causes the reactance of the inductance and the capacitance to change in such manner that their product remains constant, i.e., $RR_0 = L/C$. From this it is readily seen that the circuit balance is independent of frequency.

From another point of view, when the circuit of Fig. 1(a) is balanced, it may be said to be unresponsive to energy in a wave traveling from the generator to the load, left to right, while the circuit of Fig. 1(c) is unresponsive to energy in a wave traveling from right to left because this circuit is merely Fig. 1(a) reversed; i.e., the generator and load are interchanged. Each circuit is in effect a "directional coupler"[1] responsive only to energy flowing in a particular direction.

We will now consider the application of this circuit to power and impedance monitoring. If the circuit is first balanced, and then the resistance R and rectifier meter transposed as shown in Fig. 1(c), the sample currents i_E and i_I will be equal in amplitude and will add in phase. Their sum will cause a current to flow through the meter which permits it to be calibrated as a wattmeter, the indication being responsive to both line-current and line-voltage variations. If the calibration is carried out with a matched-line termination, the calibration holds with good accuracy for considerable departures from a matched load condition, as compared with the large errors involved when using the customary transmission-line ammeter or voltmeter to measure power absorbed by the load.

The relative accuracies of power monitoring by means of the circuit of Fig. 1(c) and by the ammeter or voltmeter method, as functions of transmission-line standing-wave ratio, are shown in Fig. 2. The ammeter or

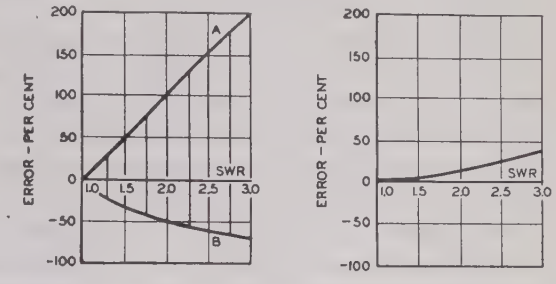

Fig. 2—Inherent error in power measurement due to transmission line mismatch. (a) Current or voltage monitor, and (b) combined current and voltage monitor.

voltmeter method involves a wide range of uncertainty between curves A and B in Fig. 2(a), depending on the position of the standing wave (phase of the reflection coefficient). The error will lie on a vertical line between curves A and B that intersects the abscissa at a standing-wave ratio corresponding to the mismatch. A derivation of these curves is given in Appendix I.

The inherent error in the combined current and voltage circuit is shown by the curve of Fig. 2(b). A derivation of this curve is given in Appendix II. It will be seen that the error in this case is much smaller than that shown on Fig. 2(a) and does not depend on the position of the standing wave. It is specific for a given standing-wave ratio and always of one sign (positive). We will show later that even this relatively small error can be eliminated from our power measurement.

The reason for this error may be explained with the aid of Fig. 1. When a transmission-line mismatch occurs, energy will be reflected back toward the generator, but the meter in Fig. 1(c) will not be cognizant of this reflection because the device is insensitive to energy propagated in the reverse direction. Accordingly, the indication will be in error relative to the power dissipated in the load by the amount of energy reflected from the load. This error, in per cent, is precisely equal to that shown in Fig. 2(b).

Now, if a second circuit is also provided in series with the transmission line, but connected as in Fig. 1(a), it will indicate any energy reflected from the load impedance, and this indication corresponds exactly to the error in the other connection. Hence, by subtracting the power reading afforded by the arrangement of Fig. 1(a) from that afforded by the arrangement of Fig. 1(c), we eliminate the error and have a precise means

[1] W. W. Mumford, "Directional couplers," Proc. I.R.E., vol. 35, pp. 160–165; February, 1947.

of measuring the power dissipated in the load regardless of its impedance. In addition to measuring the power dissipated in the load by subtracting the reflected from the incident power, the ratio of these two power readings is a measure of the amount by which the transmission line is misterminated by the load impedance. The standing-wave ratio on the transmission line can be computed from the following expression:

$$\text{S.W.R.} = \frac{1 + \sqrt{P_R/P_I}}{1 - \sqrt{P_R/P_I}}.$$

The two d.c. circuits could be connected in series and poled so that their currents would be subtractive. The meter would then indicate directly the power dissipated in the load. However, to accomplish this it would be necessary for the rectifier to have a linear relation between radio-frequency power and d.c. response. The present application for this device does not appear to justify the extra apparatus and circuit complexities required to obtain this linear characteristic, particularly since the same answer can be obtained by merely throwing a switch and mentally subtracting the readings.

An arrangement of the two radio-frequency circuits in a section of coaxial transmission line, together with the d.c. switching and metering circuits, is shown in Fig. 3. These sampling circuits are arranged back-to-back on a coaxial line and in a shielded enclosure. Each includes a transverse slot cut in the outer conductor of the coaxial line which constitutes an inductive impedance in series with the line, and a circular plate which forms a capacitive impedance to the center conductor. The switch S_2 associated with the meter transfers the meter from one sampling circuit to the other, so that the incident and reflected powers can be observed on a single meter. This circuit arrangement also provides for a transmission-line protective device. A relay is connected in series with the d.c. portion of the circuit that samples the reflected wave, so that, if the reflection exceeds a safe operating limit, the relay closes. This relay can be made to de-energize the transmitter or, if preferred, to energize a warning device.

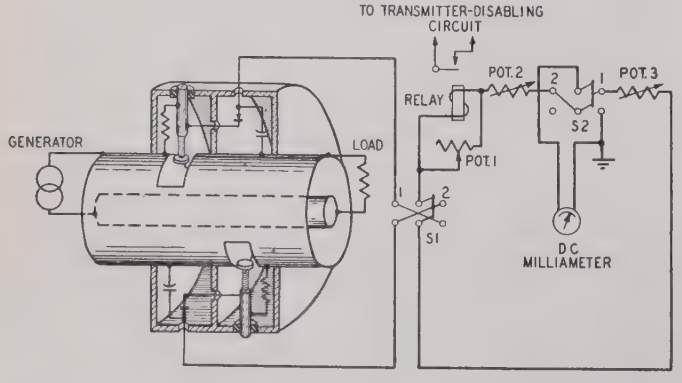

Fig. 3—Schematic diagram of the power and impedance monitor.

The initial wattmeter calibration is accomplished by first determining the amount of radio-frequency power being delivered to a matched load at the operating frequency. With the desired power being delivered and switches S_1 and S_2 in position 1, the potentiometer (*Pot. 3*) is adjusted so that the meter indicates the true power being delivered to the load *Pot. 3* is then sealed and not changed unless an apparatus change or operating-frequency shift is made. Switches S_1 and S_2 are then thrown to position 2, and *Pot. 1* and *Pot. 2* adjusted until the meter again indicates the power being delivered, and the relay sensitivity is properly set. This completes the calibration, and switches S_1 and S_2 are thrown to position 1 for normal operation.

A matched pair of germanium-crystal rectifiers is used in the metering circuit. With this type of rectifier and a d.c. circuit resistance of about 1000 ohms, the characteristics shown in Fig. 4 were obtained. Fig. 4(a) shows the relation of the d.c. current and radio-frequency power, and Fig. 4(b) shows the calibrated meter scale corresponding to this relation. It will be noted that this scale is expanded in the lower power region, which is convenient because we are interested in observing both high and low powers with about the same accuracy.

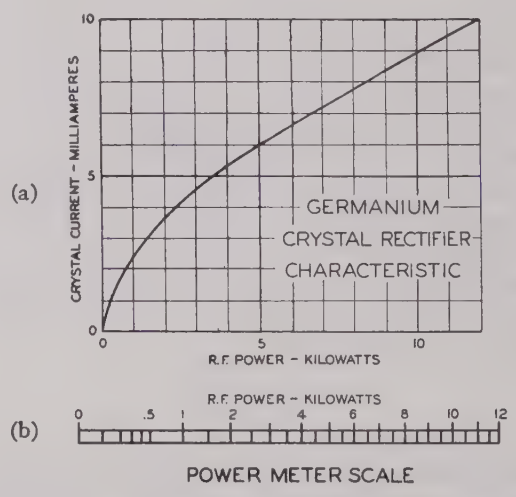

Fig. 4—Crystal-rectifier characteristic and corresponding power-meter scale.

Convenient devices for use during the initial adjustment of the line load impedance, and for determining the power flow during calibration of the wattmeter, have also been developed and incorporated as a part of this monitor. They consist of the items shown in Fig. 5. Fig. 5(a) is a small Wheatstone bridge arranged so that it can be plugged into the end of a coaxial transmission line. It is connected as shown in the schematic. The ratio arms R_2, R_3 and the standard arm R_1 are high-frequency resistors each equal to the characteristic impedance of the line. (Throughout this paper it is assumed that low-loss lines are used so that the phase angle of the characteristic impedance is negligible.) A small amount of radio-frequency power is supplied

through the input jack, and the load impedance at the far end of the transmission line is adjusted for a bridge balance. Owing principally to the compactness of the circuit, it is possible to adjust the input impedance of the line to the desired value with an accuracy better than 5 per cent at frequencies in the region of 100 megacycles and possibly higher.

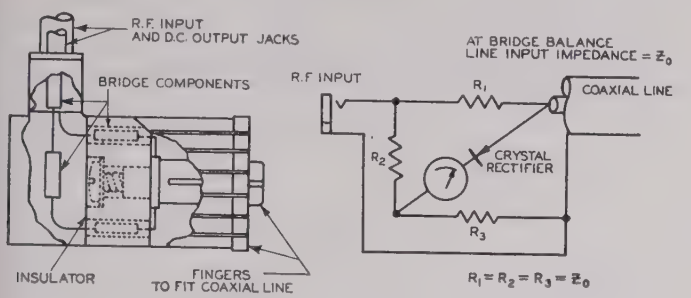

Fig. 5—(a) R.f. Wheatstone bridge, and (b) capacitance voltage divider.

A capacitance voltage divider, as shown in Fig. 5(b), has been included in the assembly for use during the calibration of the wattmeter. The small cylinder, supported close to but insulated from the outer conductor, provides a capacitance C_1 to the inner conductor of about 1 $\mu\mu$fd. The sum C_2 of the capacitance between this cylinder and the outer conductor, plus the voltmeter input capacitance, and an adjustable external capacitance is made to equal about 100 $\mu\mu$fd. This voltage divider affords a convenient range for a vacuum-tube voltmeter with high-power transmitters. It also permits the insertion of the voltmeter without affecting the line impedance or power, as would be the case if a voltmeter probe having 5 or 10 $\mu\mu$fd. were connected directly to the inner conductor. The divider can be calibrated by determining either the ratio of the capacitances C_2/C_1 or the ratio of the voltages V_1/V_2 at much lower frequencies where high accuracies can be obtained.

The accuracy of power and impedance measurements, as made with this power and impedance monitor, was checked experimentally by inserting it into a line between the output of a 100-Mc. transmitter and a water-cooled resistance load (Fig. 6). This load was shunted by a transmission-line stub which was adjusted in length, thereby changing the terminal impedance to effect standing-wave ratios from unity to about 6 to 1.

The power dissipated in the load was measured by the calorimeter method and the calorimeter checked by a

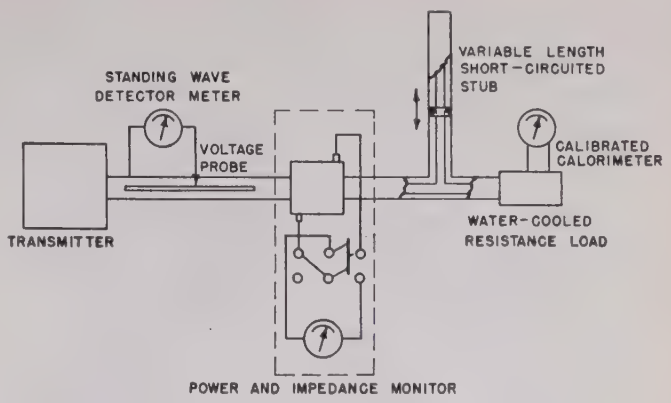

Fig. 6—Experimental arrangement for testing the power and impedance monitor.

known 60-cycle power dissipation. A comparison of the power measurements made with the monitor and the calorimeter showed that they agreed to within 5 per cent

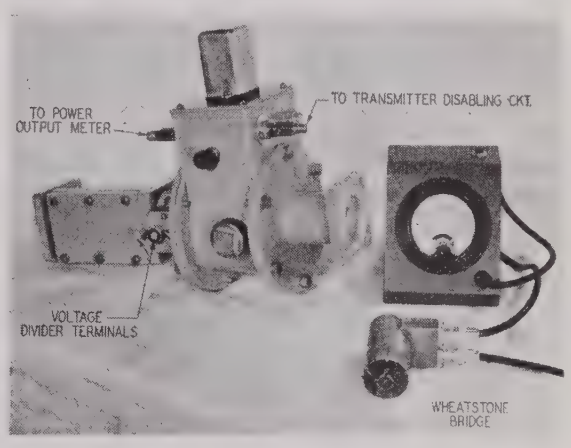

Fig. 7—Experimental model of the power and impedance monitor with Wheatstone bridge.

for standing-wave ratios up to about 2.5 to 1 and to better than 10 per cent for standing-wave ratios up to 6 to 1. The standing-wave ratio on the line, as measured with the monitor, agreed closely with the values known

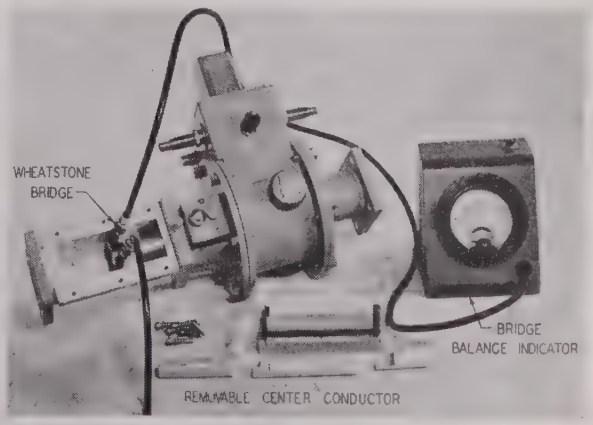

Fig. 8—The power and impedance monitor with Wheatstone bridge inserted into transmission line.

to exist from a knowledge of the line terminal impedance.

This monitor has been assembled into a section of coaxial line together with the capacitance voltage divider and a port for the insertion of the small Wheatstone bridge. Photographs of this assembly and the small bridge, as they will be supplied with high-power f.m. transmitters, are shown in Fig. 7 and Fig. 8. Fig. 9

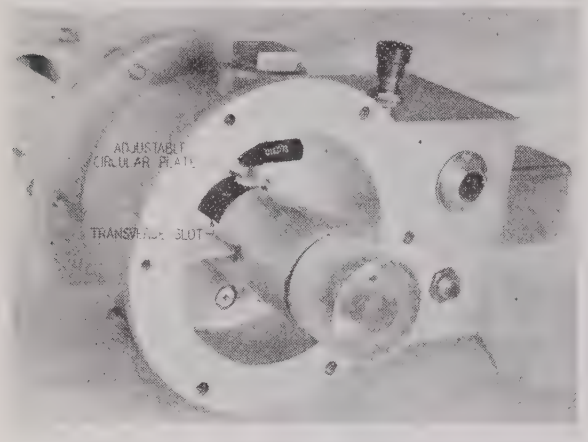

Fig. 9—An internal view of the power and impedance monitor.

is an internal view showing the voltage and current pickups.

The authors wish to acknowledge the valuable assistance of their associates at the Bell Telephone Laboratories.

Appendix I

Consider a transmission line of characteristic impedance Z_0 terminated by a load impedance Z_L. If Z_L does not equal Z_0, standing waves will appear on the line in which the line voltage (and line current) will vary periodically between maximum and minimum values. The standing-wave ratio (s.w.r.) is defined as follows:

$$\text{s.w.r.} = \frac{E_{\max}}{E_{\min}} = \frac{I_{\max}}{I_{\min}}.$$

The power in the load Z_L is given by the expression

$$P_{\text{load}} = \frac{E_{\max}E_{\min}}{Z_0} = \frac{E_{\max}^2}{Z_0} \times \frac{1}{\text{s.w.r.}} = \frac{E_{\min}^2}{Z_0} \times \text{s.w.r.}$$

Suppose that the power in the load is calculated from a measurement of line voltage. If the voltage probe is at a voltage maximum, the computed power is

$$P_{\max} = \frac{E_{\max}^2}{Z_0}.$$

The error in power determination (relative to the true power in the load) is

$$\frac{P_{\max} - P_{\text{load}}}{P_{\text{load}}} = \frac{\dfrac{E_{\max}^2}{Z_0} - \dfrac{E_{\max}^2}{Z_0} \times \dfrac{1}{\text{s.w.r.}}}{\dfrac{E_{\max}^2}{Z_0} \times \dfrac{1}{\text{s.w.r.}}}$$

$$\frac{P_{\max} - P_{\text{load}}}{P_{\text{load}}} = \text{s.w.r.} - 1.$$

This errror, in per cent, is shown by curve A in Fig. 2(a). When the probe is at a voltage minimum, the computed power is

$$P_{\min} = \frac{E_{\min}^2}{Z_0}.$$

The error in power determination is then

$$\frac{P_{\min} - P_{\text{load}}}{P_{\text{load}}} = \frac{\dfrac{E_{\min}^2}{Z_0} - \dfrac{E_{\min}^2}{Z_0} \times \text{s.w.r.}}{\dfrac{E_{\min}^2}{Z_0} \times \text{s.w.r.}}$$

$$\frac{P_{\min} - P_{\text{load}}}{P_{\text{load}}} = \frac{1}{\text{s.w.r.}} - 1.$$

This error, in per cent, is shown by curve B in Fig. 2(a). A similar analysis, involving the line current rather than voltage, yields identical results.

If the voltage or current probe is not at a maximum or minimum point, the error in power measurement will be less than that shown by curve A or B in Fig. 2(a). Accordingly, vertical lines are drawn between curves A and B to indicate that the actual error may fall any place between limits given by these curves.

Appendix II

It has been shown that, when the combined voltage and current circuit is used as a wattmeter, it is sensitive only to energy incident upon the load. Let the incident power be P_I and the power reflected by the load be P_R. Then

$$P_{\text{measured}} = P_I,$$

$$P_{\text{load}} = P_I - P_R,$$

The error in power determination (relative to the true power in the load) is

$$\frac{P_{\text{meas}} - P_{\text{load}}}{P_{\text{load}}} = \frac{P_R}{P_I - P_R} = \frac{1}{\dfrac{P_I}{P_R} - 1},$$

and since

$$\frac{P_I}{P_R} = \left[\frac{\text{s.w.r.} + 1}{\text{s.w.r.} - 1}\right]^2,$$

$$\frac{P_{\text{meas}} - P_{\text{load}}}{P_{\text{load}}} = \frac{(\text{s.w.r.} - 1)^2}{4\ \text{s.w.r.}}.$$

This error, in per cent, is plotted in Fig. 2(b).

Resistor-Transmission-Line Circuits*

PAUL I. RICHARDS†, ASSOCIATE, I.R.E.

Summary—**Necessary and sufficient conditions are derived for a function to be the driving-point impedance of a physically realizable network consisting (essentially) of lumped resistors and lossless transmission lines. The circuits so developed are thoroughly practical for pure reactances and in many other special cases, but, in general, ideal transformers are sometimes required. A rigorous correspondence between lumped-constant circuits and line-resistor circuits is established. This correspondence immediately extends the usefulness of a wealth of theorems and techniques.**

I. Introduction

THROUGHOUT this paper we shall consider networks which are composed of lumped resistors and of lossless transmission lines whose electrical lengths are commensurable. Our goals are (1) to find a method of recognizing physically realizable driving-point impedance functions for such networks, and (2) to construct at least one such circuit having a prescribed driving-point impedance. We shall thus be concerned with an extension of the well-known results of Brune[1] in the field of lumped constants. The word "impedance" will be used throughout only in the sense of "driving-point impedance," unless otherwise stated. Except for the purely reactive circuits, it has, unfortunately, not yet been possible to eliminate ideal transformers in general, so that these, too, must be allowed in the class of circuits to be studied.

As is usual in this type of analysis,[1,2] we shall find it convenient to introduce a complex frequency variable $s=\gamma+j\omega$. The "real-frequency" axis is then the imaginary s axis, and it is on this line that the truly significant values of the network functions are assumed. The use of the entire complex plane, however, with the consequent extension of the functions involved, enables the use of the powerful methods of the theory of functions of a complex variable.

II. Necessary Conditions

It has been shown[1,3] that any physical impedance whatever must have a positive real part in the right half-plane, $\gamma \geqq 0$. Then our first necessary condition is

$$R \geqq 0 \text{ in } \gamma \geqq 0 \tag{1}$$

where R = real part of Z.

Since only transmission lines and lumped resistors (and ideal transformers) are involved in the circuit, Z will be a rational function of factors of the form e^{bs}. Moreover, the restriction that the line electrical lengths be commensurable insures that only terms of the form $e^{nas}=(e^{as})^n$ will appear, where a is an appropriate fundamental phase parameter, and n is an integer. Hence, our second necessary condition is

$$Z(s) = \text{rational function of } e^{as}. \tag{2}$$

III. Change of the Frequency Variable

Let us define a new frequency variable by the equation

$$S(s) = \tanh(as/2) = \frac{e^{as}-1}{e^{as}+1} = \Gamma + j\Omega. \tag{3}$$

We can then solve for $e^{as}=(1+S)/(1-S)$; if we substitute this value for e^{as} into the impedance function, we obtain from (2)

$$Z = \text{rational function of } S. \tag{4}$$

Moreover, it is easily verified that the complex function S has a positive real part Γ whenever $\gamma \geqq 0$. In other words, (3) maps the right-half of the s plane into the right-half of the S plane. Thus, from (1),

$$R \geqq 0 \text{ in } \Gamma \geqq 0. \tag{5}$$

Of course, this mapping is not one-to-one, but the multiple-valuedness of the inverse corresponds merely to the periodicity of Z by (2).

IV. Sufficiency of (1) and (2)

Consider the new variable S as the independent frequency variable. The conditions (4) and (5) have been shown by Brune[1] to be both necessary and sufficient for Z to be a physically realizable lumped-constant impedance.

Using Brune's method, let us develop this lumped-constant impedance. This development will, in general, yield a circuit containing inductive tees with one negative element (equivalent to a pair of perfectly coupled coils). These may be replaced, however, with inductances and ideal transformers by means of the equivalences shown in Fig. 1. The lumped circuit will then contain only positive L, R, C, and ideal transformers.

Now replace each inductance L by the input of a short-circuited line of electrical length $ac/2$ (c = velocity

* Decimal classification: R117.11×R143. Original manuscript received by the Institute, March 12, 1947. This paper contains a portion of the author's doctor's thesis, the research for which was carried on under the direction of Dr. P. LeCorbeiller at Harvard University.

† Brookhaven National Laboratory, Upton, L. I., N. Y.

[1] O. Brune, "Synthesis of a finite two-terminal network whose driving-point impedance is a prescribed function of frequency," *Jour. Math. and Phys.*, vol. 10, pp. 191–236; October, 1931.

[2] H. W. Bode, "Network Analysis and Feedback Amplifier Design," D. Van Nostrand Co., New York, N. Y., 1945.

[3] P. I. Richards, "General impedance-function theory," *Quart. Appl. Math.*, scheduled for publication, January, 1948.

of light) and of characteristic impedance L, and replace each capacitance C by an open-circuited line of electrical length $ac/2$ and of characteristic impedance $1/C$. The result will be to replace the impedances Ls and $1/Cs$ by the impedances $L \tanh (as/2) = LS$ and $1/CS$. Thus the lumped-constant circuit will go over into a network having exactly the required impedance, and sufficiency of (1) and (2)—or their equivalents, (4) and (5)—has been proved.

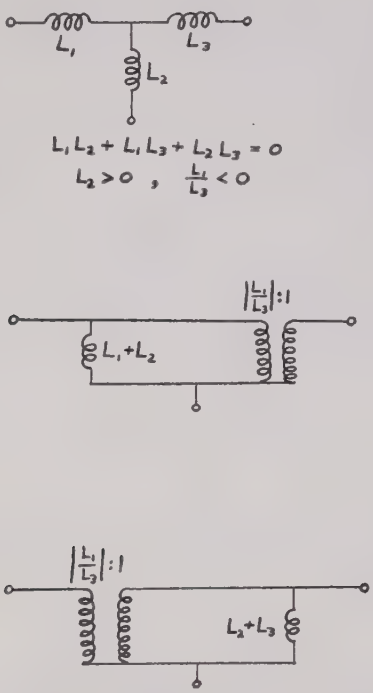

Fig. 1—Equivalents of perfectly coupled coils.

The circuit produced by the above procedure will, in general, involve the eminently impractical ideal transformer. For pure reactances and in other special cases these may be eliminated, as will be discussed later. However, no completely successful general method of elimination has yet been found.

V. Correspondence With Lumped Circuits

The last section shows that a completely rigorous correspondence exists between the driving-point impedances of circuits of the type under consideration and those of lumped constants. This immediately makes available a wealth of material. By use of the correspondences

S-plane (lumped nets)	s-plane (line-resistor nets)
$S = \infty$	$s = j\pi/a$
$S = 0$	$s = 0$
$j\omega$	$j \tan (\omega a/2)$
$d\omega$	$\dfrac{a\,d\omega}{2\cos^2(\omega a/2)}$

(6)

many lumped-constant theorems may be "translated" into theorems about line-resistor networks. For example, Bode's well-known "phase-area law"[2] becomes, for line-resistor circuits,

$$\int_{\omega=0}^{\omega=\pi/2} X d\left(\log \tan \frac{\omega a}{2}\right) = \frac{\pi}{2}\left(R\left(\frac{\pi}{a}\right) - R(0)\right). \tag{7}$$

Again, if the circuit is purely reactive,

$$\frac{dX}{d\omega} \geqq a\left|\frac{X}{\sin a\omega}\right|. \tag{8}$$

This correspondence may also be extended to side-circuit or transfer properties. The appropriate equivalence is shown in Fig. 2. (The line length (ac) appears, instead of $(ac/2)$ as before, because transfer properties are only singly periodic in line lengths while input properties are doubly periodic.) The only restriction to be imposed is that the line section must be run in the balanced condition, where the currents in the two conductors are equal and opposite. Thus, for coaxial lines, there must be no current traveling on the outer surface of the shield. With this restriction, any of our line-resistor networks can be replaced by an exactly equivalent lumped circuit. A conventional circuit analyzer may then be used, and the results translated back into terms of the true frequency merely by means of a table of tangents.

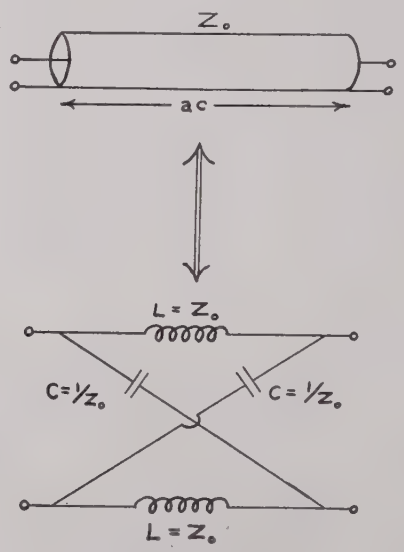

Fig. 2—Side-circuit equivalence properties.

VI. Reactive Circuits

From the work of Brune and Foster, it is known that the equivalent lumped circuit (and hence the final network) will not contain ideal transformers if the circuit is purely reactive. This removes the greatest practical objection to the method of Section IV, but the circuit

may not yet be in a form enabling completely shielded construction. This objection may also be removed.

Consider the impedance reduction represented by Fig. 3(a), where

$$\left.\begin{aligned} Z' &= \frac{Z - SZ_1}{1 - \frac{Z}{Z_1}S} \\ Z_1 &= (\text{the value of } Z \text{ at } S = 1) \end{aligned}\right\}. \qquad (9)$$

It may be shown[4] that Z' will again satisfy (1) and (2) or their equivalents, (3) and (4). Moreover, it may also be shown[4] that Z' is of lower degree than Z. Thus a repetition of (9) will eventually lead to an impedance which is merely a multiple of S or $1/S$.

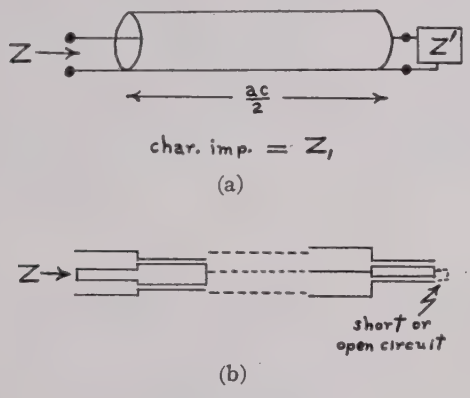

Fig. 3.—(a) Fundamental step in reactance realization. (b) Canonical form for reactances.

Any rectance of the type considered can be realized in the canonical form shown in Fig. 3(b).

In actual calculation, Z' will at first appear to be of higher degree than Z. However, the factor (S^2-1) will always cancel from numerator and denominator. This cancellation can be performed in a single step by the following device. To obtain a given coefficient in the result, add the corresponding coefficient of the original to the previous coefficient of the result. For example,

$$\frac{S^7 + 3S^5 - 2S^3 - 2S}{S^6 + 2S^4 - 2S^2 - 1} = \frac{S^5 + 4S^3 + 2S}{S^4 + 3S^2 + 1}.$$

The rule may be proved by observing the results of the process of synthetic division.

Of course, the canonical form of Fig. 3(b) is not the only shielded circuit which has the prescribed reactance. For instance, a zero of Z may be removed at any stage in the procedure. The resulting circuit will then have several stubs connected in shunt across the main line. This flexibility may be of considerable assistance in meeting mechanical or other practical requirements.

[4] P. I. Richards, "A special class of functions with positive real part in a half-plane," *Duke Math. Jour.*, September, 1947.

An interesting reciprocity theorem applies to the canonical form of Fig. 3(b). Namely, it is easily seen from (9) that if we are required to realize a new reactance equal to R_0^2/Z, where Z is the old reactance and R_0 a (real) constant, then the new canonical circuit can be obtained from that for Z by (a) reciprocating each characteristic impedance with respect to R_0, and (b) changing the final short- (open-) circuited to an open- (short-) circuited termination.

VII. Eliminating Ideal Transformers

It is known[4] that the procedure of (9) and Fig. 3(a) will always yield a physically realizable Z' of no higher degree in S than Z. (A factor $(S-1)$ will always cancel.) Moreover, $Z'(S)$ will be of lower degree than $Z(S)$ if, and only if, $Z(-1) = -Z(1)$.

In view of this fact, if for all ω

$$R \geqq R_0 \equiv \tfrac{1}{2}(Z(1) + Z(-1)) \geqq 0,$$

then we may remove a series resistor R_0 and apply (9) to obtain a Z' of lower degree than Z. If this is not possible, it may be that the same method can be applied to $Y = 1/Z$ (removal of a shunt conductance). In general, however, both may fail. Occasionally either may succeed after a few applications of (9), but again this will not always happen. Despite the lack of generality, however, these methods are often of considerable assistance.

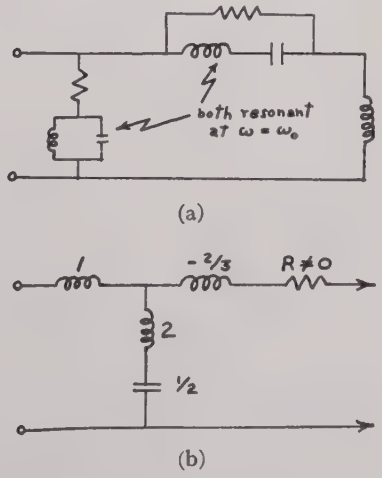

Fig. 4—(a) A minimum-resistance–minimum-reactance circuit. (b) The first section of the Brune development of (a) if all elements there are given the value of unity.

The above devices will almost never be applicable to "minimum-resistance–minimum-reactance" functions; that is, functions that have no resonances but which have zero resistance at some frequency. These functions will always require mutual coupling in the Brune representation. This does not mean, however, that such

coupling is inevitable. For example, the circuit of Fig. 4(a) has an input impedance of the minimum-resistance–minimum-reactance type. The first section of its Brune development is shown in Fig. 4(b). While the latter form would require ideal transformers in the line-resistor equivalent, the former goes into the very practical circuit shown in Fig. 5.

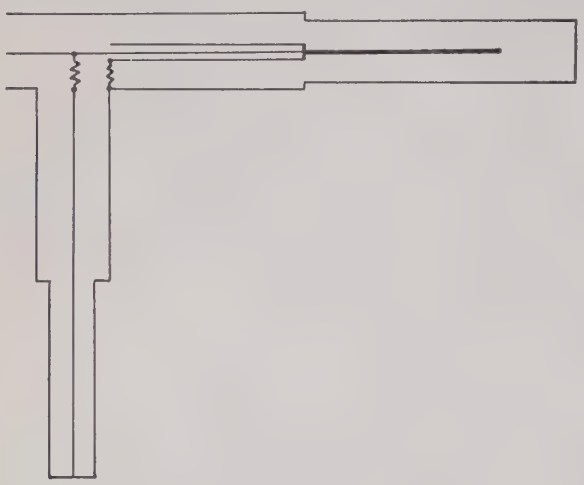

Fig. 5—Line-resistor equivalent of Fig. 4(a).

Thus it appears that there may be hope of eventually finding a general way of eliminating ideal transformers. The principal difficulty appears to be that the presence of an ideal transformer does not affect the mathematical form of the impedance in any easily detectable manner.

VIII. Discussion

The reader has undoubtedly noticed that the present theory derives its simplicity from two postulates defining the class of circuits studied. Without these postulates the simple statements (2) and (4) cannot be made.

The assumption that the lines are lossless is no great bar to practical application. First, these losses are well known to be extremely small and, for a host of practical problems, may be entirely neglected. Second, the following device for including small losses may be carried over from the theory of lumped circuits: Let r, l, g, c be the series resistance, series inductance, shunt conductance, and shunt capacitance, all per unit length, for a given line. Assume, as a first approximation, that for all lines in the circuit $(g/c) = (r/l) = d$ and that d has the same value for all the lines. Then the propagation constants and characteristic impedances may be written:

$$\sqrt{(r + ls)(g + cs)} = (s + d)\sqrt{lc}$$

$$\sqrt{\frac{r + ls}{g + cs}} = \sqrt{\frac{l}{c}}.$$

Thus the circuit behavior can be reduced to the lossless case by the familiar device of changing the frequency variable. Note that this change must be made in the (true frequency) s plane and not in the (equivalent) S plane.

Our second fundamental postulate requires that the electrical lengths of the lines be commensurable. Although most engineers will feel that this is not a serious practical consideration, it ought to be mentioned that application of the theory to a noncommensurable circuit assumes not only convergence but *uniform* convergence.[5]

The reader will note immediately that the restriction is an "unnatural" one. In truth, given two actual lines it would be impossible to determine whether their lengths were commensurable; ever-present experimental error would always limit us to a finite range of ratios, within which there would always lie both rational and irrational numbers. The reason why the mathematical theory asks a question which experiment cannot answer lies, of course, in the fact that the simple theory ignores the "smoothing" effect of discontinuity reactances arising at the junction of dissimilar lines. In general, probably no actual physical impedance will be periodic in frequency.

Yet our theory is rooted in an assumption of periodicity. The author feels that this is no serious objection to its physical meaning. A similar situation arises in lumped-circuit theory, where lead inductance, distributed capacitance, and radiation are neglected. This is unimportant for most purposes, but at the same time insures that the impedance function will not be correct for high frequencies. Yet the mathematical theory treats Z as having physical meaning beyond the frequency of visible light and, indeed, at $s = \infty$. As usual, a theory both tractable and useful has been achieved by idealizing the physical facts in such a way that there are no heuristic difficulties or internal contradictions. It is felt that the same is true of the present theory.

[5] This was pointed out by P. LeCorbeiller.

Currents Excited on a Conducting Plane by a Parallel Dipole*

BEVERLY C. DUNN, JR.†, ASSOCIATE, I.R.E., AND RONOLD KING†, SENIOR MEMBER, I.R.E.

Summary—An analysis is made of the distribution of magnetic field and of current on the plane surface of a perfectly conducting infinite sheet due to a driven half-wave dipole parallel to the sheet. The analysis is based upon the following assumptions: (a) the axial distribution of the amplitude of the current in the dipole is cosinusoidal with respect to the midpoint; (b) the relative phase of the current in the dipole is constant; and (c) the interaction between currents on the conducting plane and in the dipole does not significantly alter the assumed distribution of the current along the dipole as this is moved relative to the plane. It is found that, independent of the distance of the dipole from the surface, the tangential magnetic field at the plane surface is everywhere perpendicular to the direction specified by the axis of the dipole, while the current in the plane is everywhere parallel to this direction. Expressions are derived for the relative amplitude and phase of the magnetic field and the current in the plane referred to the input current of the dipole. A fairly complete set of graphs is included showing the behavior of these expressions for six different distances b of the dipole from the surface; namely, $b=0.02\lambda$, 0.05λ, 0.125λ, 0.25λ, 0.5λ, and λ. The validity of the initial assumptions when applied to physically possible dipoles is discussed briefly.

Introduction

THE DISTRIBUTIONS of current on conducting surfaces driven by various devices such as dipoles, slots, etc., are largely unknown. As a step in their determination, a relatively simple problem has been solved; namely, that of calculating the distribution of the magnetic B field and the surface-current density on a perfectly conducting surface of infinite extent excited by a half-wave dipole mounted parallel to the surface.

I. Theory

In setting up the problem it is noted that the magnetic B vector amplitude in the space surrounding an isolated dipole has only a θ component (Fig. 1):

$$\vec{B} = B_\theta \hat{\theta}. \tag{1}$$

Under the assumptions (a) that the length of the dipole is exactly one-half wavelength ($2h=\lambda/2$); and (b) that the instantaneous current at any point along the dipole is given by

$$\begin{aligned} i &= I_m \cos \beta_0 z \cos \omega t \\ &= \text{Real part } [I_m \cos \beta_0 z \exp (j\omega t)], \end{aligned} \tag{2}$$

B_θ is given by[1]

$$B_\theta = \frac{jI_m}{4\pi\nu_0 r} \{\exp (-j\beta_0 R_{1h}) + \exp (-j\beta_0 R_{2h})\}. \tag{3}$$

In these expressions ν_0 is the reluctivity of space and equals $1/4\pi \times 10^7$ meters/henry; r is the cylindrical radial co-ordinate of the point P at which B_θ is evaluated; R_{1h} and R_{2h} are the distances between the extremities of the dipole and P; β_0 is the phase constant for free space and equals $2\pi/\lambda$. The current amplitude in the dipole is cosinusoidally distributed with a maximum value

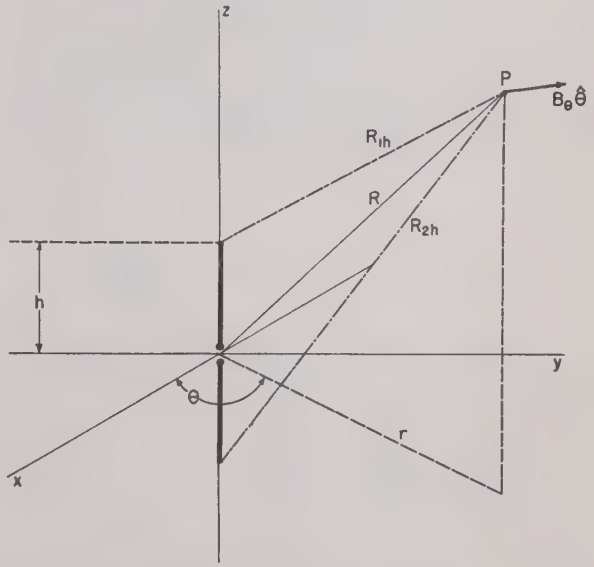

Fig. 1—Intermediate-zone geometry for the half-wave dipole. a=radius of dipole. d=distance between input terminals.

I_m at the center ($z=0$), and the value zero at the extremities ($z=\pm h=\pm\lambda/4$). The relative phase of the instantaneous current i is constant along the conductor and equal to the phase of the instantaneous current at the midpoint. Henceforth the relative phase of current and magnetic field on the conducting surface will be referred to the constant phase of the current in the dipole.

It is important to note that (3) is perfectly general for a half-wave dipole with the assumed current distribution. For a point P in the radiation zone defined by

$$\beta_0 R \gg 1$$

* Decimal classification: R120. Original manuscript received by the Institute, April 5, 1947. The research reported in this document was made possible through support extended Cruft Laboratory, Harvard University, jointly by the Navy Department (Office of Naval Research) and the Signal Corps, U. S. Army, under ONR Contract No. N5ori-76, T.O.1.

† Cruft Laboratory, Harvard University, Cambridge, Mass.

[1] An as-yet-unpublished formula due to R. W. P. King. The corresponding expression for half the antenna is given by G. H. Brown, "Directional antennas," PROC. I.R.E., vol. 25, p. 145, Eq. (193); January, 1937. In the Brown formula it is necessary to set $B=0$, $G=\pi/2$.

where R is the radial distance to P in spherical coordinates, (3) can be simplified to give the usual approximate expression for the radiation B field of a half-wave dipole. In the form given, however, it is valid in the induction and intermediate zones for which R is too small to satisfy the above inequality. Since the present analysis will inquire into the behavior of the B field at points within a few wavelengths of the dipole, the exact expression (3) is required.

The problem can be set up with the aid of Fig. 2. The infinite, perfectly conducting surface is taken to be the y-z plane, and the half-wave dipole is parallel to the z axis with its center at the point $(b, 0, 0)$. In calculating the surface density of current on the conducting plane at a point such as $P(0, y, z)$, the magnetic B vector is first determined at P. The surface current is then determined from the boundary conditions obeyed by the B vector at the surface of a perfect conductor. It is assumed that the mutual coupling between the perfectly conducting plane and the dipole does not alter the assumed current distribution along the dipole given by (2) as the distance between the dipole and the plane is varied. A discussion of this assumption, together with those regarding the distribution of current along the dipole, will be given at the end of this paper.

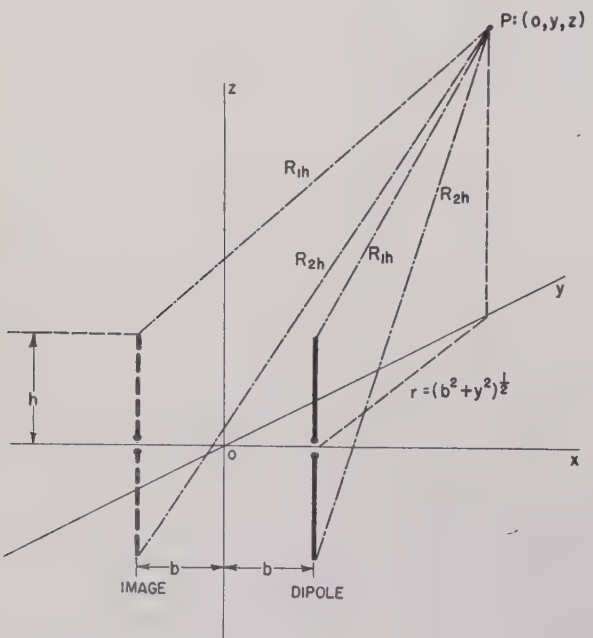

Fig. 2—Intermediate-zone geometry for the half-wave dipole mounted parallel to an infinite, perfectly conducting plane.

In computing the B vector at P, use is made of the theory of images, which proves that the combination of the perfectly conducting y-z plane and the dipole is equivalent at all points in the infinite half-space defined by $(0 \leqq x \leqq \infty, y, z)$ to the situation actually shown in Fig. 2. Here the infinite surface has been replaced by an image dipole exactly like the actual dipole in physical dimensions and orientation but with its center at the point $(-b, 0, 0)$. Furthermore, the currents at corresponding points in the dipole and its image are equal in amplitude but 180° out of phase.

Thus, for any point $P(0, y, z)$ in the y-z plane of Fig. 2, a vector diagram can be drawn similar to that

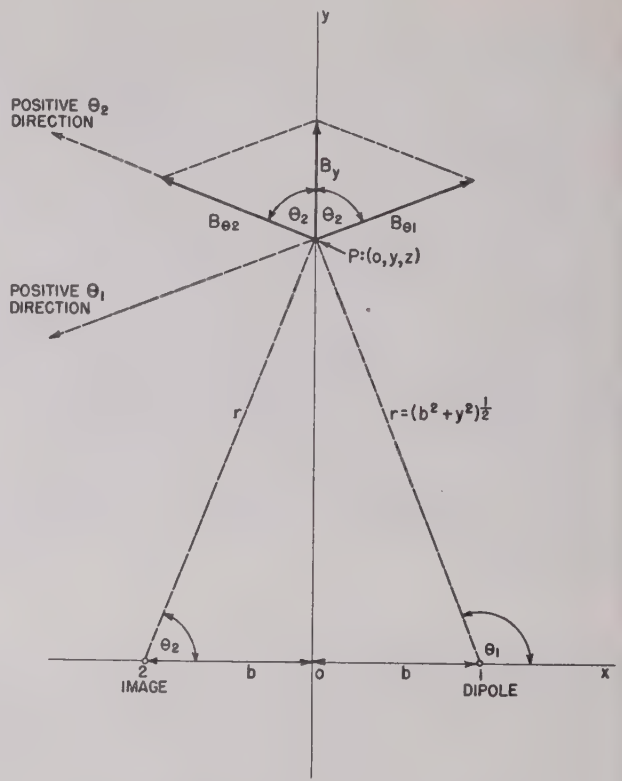

Fig. 3—Vector diagram at a point P in the y-z plane of Fig. 2.

in Fig. 3, where the x-y plane is shown. The positive z axis is directed upward from the paper at 0. Although drawn in the x-y plane at $(0, y, 0)$ in the figure, the vector diagram actually belongs at the point $(0, y, z)$ at a distance z above the plane of the paper. The individual B vectors are oriented correctly to take account of the 180°-out-of-phase relationship of the currents on the antennas. The magnitudes $B_{\theta 1}$ and $B_{\theta 2}$ are equal as shown, since the dipoles carry currents of equal magnitude and P is equidistant from corresponding points on the two dipoles.

It is clear from Fig. 3 that at any point in the y-z plane the resultant B-vector amplitude is given by

$$\begin{aligned} B_x &= B_{x1} + B_{x2} = 0 \\ B_y &= B_{y1} + B_{y2} = 2B_{y1} \\ B_z &= 0. \end{aligned} \tag{4}$$

Since $B_{\theta 1}$ is drawn in the negative θ_1 direction in Fig. 3,

$$B_{y1} = B_{\theta 1} \cos \theta_1 = - B_{\theta 1} \cos \theta_2 = - B_{\theta 1} \frac{b}{r} \tag{5}$$

with $B_{\theta 1}$ as given by (3). Noting from Figs. 2 and 3 that, in (3),

$$\left.\begin{matrix} R_{1h} \\ R_{2h} \end{matrix}\right\} = [r^2 + (z \mp h)^2]^{1/2} = [b^2 + y^2 + (z \mp h)^2]^{1/2}, \quad (6)$$

and using (4) and (5),

$$B_y = -\frac{jI_m b}{2\pi\nu_0 r^2}\left[\exp(-j\beta_0 R_{1h}) + \exp(-j\beta_0 R_{2h})\right]$$

$$= -\frac{jI_m b}{2\pi\nu_0(b^2+y^2)}\left\{\exp\left[-j\beta_0(b^2+y^2+(z-h)^2)^{1/2}\right]\right.$$

$$\left.+\exp\left[-j\beta_0(b^2+y^2+(z+h)^2)^{1/2}\right]\right\}. \quad (7)$$

The instantaneous value of B_y is then given by

$$(B_y)_{\text{inst}} = \text{Real part}\left[B_y \exp(j\omega t)\right]$$

$$= \frac{I_m b}{2\pi\nu_0(b^2+y^2)}\left\{\sin\left[\omega t - \beta_0(b^2+y^2+(z-h)^2)^{1/2}\right]\right.$$

$$\left.+\sin\left[\omega t - \beta_0(b^2+y^2+(z+h)^2)^{1/2}\right]\right\}. \quad (8)$$

By means of familiar trigonometric identities and some rearranging, (8) can be put in the form

$$(B_y)_{\text{inst}} = \frac{I_m}{2\pi\nu_0\lambda} A \cos(\omega t - \phi) \quad (9)$$

with the relative amplitude A and relative phase angle ϕ given by the dimensionless expressions

$$A = \frac{2b\lambda}{b^2+y^2}\cos\tfrac{1}{2}\left[\beta_0(b^2+y^2+(z+h)^2)^{1/2}\right.$$

$$\left.-\beta_0(b^2+y^2+(z-h)^2)^{1/2}\right] \quad (10)$$

$$\phi = \tfrac{1}{2}\left[\beta_0(b^2+y^2+(z+h)^2)^{1/2}\right.$$

$$\left.+\beta_0(b^2+y^2+(z-h)^2)^{1/2}\right] + \frac{\pi}{2}. \quad (11)$$

Having thus obtained (4) and (9), which define the properties of the B vector at the perfectly conducting surface (y-z plane), the boundary condition on the tangential component of the B vector may be applied in order to determine the surface density of current on the surface. Since the B vector is wholly tangential to the surface and is directed parallel to the y axis at all points, the boundary condition can be written in a suitably specialized form as follows:[2]

$$\nu_0[-\hat{x}, (B_y)_{\text{inst}}\hat{y}] = -\vec{l}_{\text{inst}} \quad (12)$$

where $\vec{l}_{\text{inst}}$ is the instantaneous vector density of surface current. Hence,

$$\vec{l}_{\text{inst}} = \nu_0(B_y)_{\text{inst}}[\hat{x}, \hat{y}] = \nu_0(B_y)_{\text{inst}}\hat{z} = l_z\hat{z}, \quad (13)$$

or, with (9),

$$l_z = \nu_0(B_y)_{\text{inst}} = \frac{I_m}{2\pi\lambda} A \cos(\omega t - \phi). \quad (14)$$

Thus it has been shown that at all points on the conducting plane the positive directions for $\vec{B}_{\text{inst}}$ and $\vec{l}_{\text{inst}}$ are respectively the positive y and z directions. Furthermore, these two quantities are characterized by the same relative amplitude A and angle of relative phase lag ϕ with respect to the current on the dipole.

[2] The notation, $[\vec{A}, \vec{B}]$, is used for the vector or cross product of $\vec{A}$ and $\vec{B}$. $\hat{x}$ and $\hat{y}$ are unit vectors.

II. Graphical Results

In the graphs which follow, the relative amplitude A and the relative phase angle ϕ of $\vec{B}_{\text{inst}}$ and $\vec{l}_{\text{inst}}$ (see (10) and (11)) have been plotted against y and z in terms of the distance of the point P in wavelengths from the origin. The curves are shown only in the first quadrant of the y-z plane, since, according to (10) and (11), A and ϕ, and consequently $\vec{B}_{\text{inst}}$ and $\vec{l}_{\text{inst}}$, are symmetrical in both the y and z axes and hence in the origin.

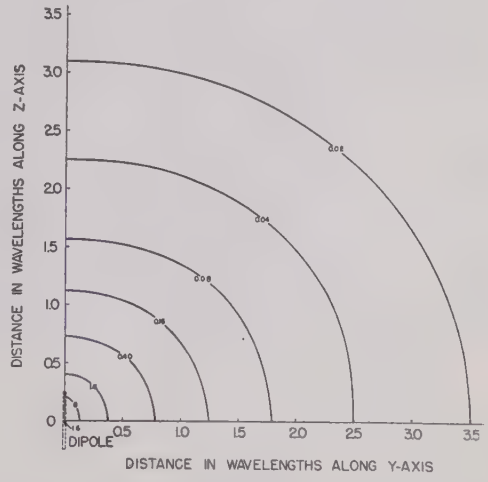

Fig. 4—Contours of constant relative amplitude for surface current density and magnetic field on the surface; $b = 0.125\lambda$.

A somewhat more extensive set of curves was computed for a dipole spaced one-eighth wavelength ($b = 0.125\lambda$) from the conducting plane than for other spacings. These are shown in Figs. 4 through 7, in addition to being represented in the figures following Fig. 7. Contours of constant relative amplitude and phase (in de-

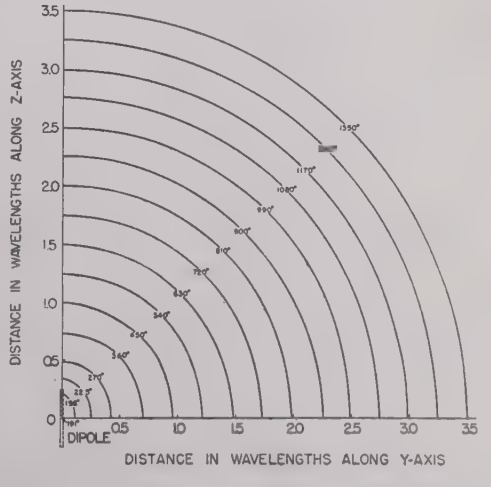

Fig. 5—Contours of constant relative phase for surface current density and magnetic field on the surface; $b = 0.125\lambda$.

grees) are plotted in Figs. 4 and 5. The half-wave dipole is shown schematically, and the values of the relative amplitude and phase at the origin are given. It is of interest here to note that the amplitude contours have an approximately elliptical shape, the major axis shifting from the z axis to the y axis as one moves away from the origin. The phase contours have approximately the same shape as the amplitude contours close to the origin but become very nearly circular within a distance of somewhat over two wavelengths.

Referring to (9) and (14), the expression $A\cos(\omega t-\phi)$ was computed for $b=0.125\lambda$ and for two values of t,

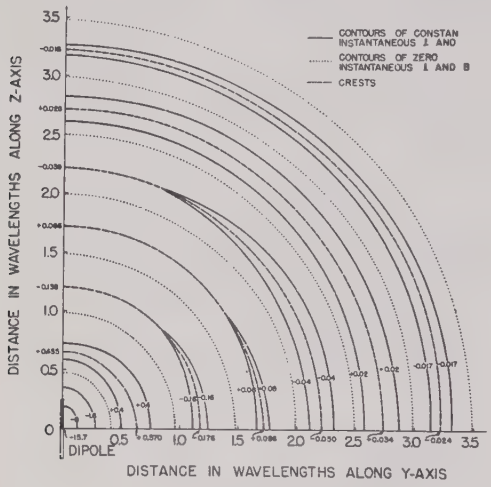

(a)

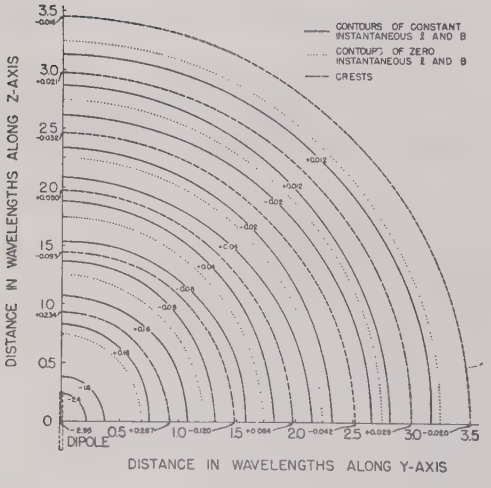

(b)

Fig. 6—Contours of constant, instantaneous surface current density and magnetic field on the surface at (a) $t=0$, and (b) $t=T/4$; $b=0.125\lambda$.

namely, $t=0$ and $t=T/4$, where T is the period. The curves obtained are shown in Figs. 6 and 7; they represent the behavior of the relative instantaneous magnetic B field, $\vec{B}_{inst}$, and current, $\vec{I}_{inst}$, on the surface. The plus and minus signs which appear on the figures indicate the sense of $\vec{B}_{inst}$ and $\vec{I}_{inst}$ with reference to the positive y and z directions, respectively.

A wave motion along the surface is clearly indicated by these figures. Thus, by means of appropriate contours, Fig. 6 represents instantaneous pictures of this wave motion at two time instants a quarter-period apart; i.e., Fig. 6(a) for $t=0$, and Fig. 6(b) for $t=T/4$. The contours of constant $\vec{I}_{inst}$ and $\vec{B}_{inst}$ are shown as solid lines, with small numerals to indicate the relative magnitudes represented by the contours. In addition, the nodal and antinodal (crest) contours are indicated by the dotted and dashed lines, respectively. It is noteworthy that along the loci defining the antinodes the peak absolute value increases from a minimum on the z axis to a maximum on the y axis, these values being indicated by small numerals along the co-ordinate axes. It is for this reason that in three instances in Fig. 6(a) pairs of solid-line contours meet to form cusps whose apexes are located on antinode contours. It might be added that sufficiently close to the origin the variation of peak absolute value along the antinode contours is just the reverse of that described above; i.e., the maximum peak value lies on the z axis, and the minimum on the y axis. (This phenomenon is apparent from an inspection of Fig. 10, which will be described later.)

For $b=0.125\lambda$, $t=0$, and $t=T/4$, the expression $A\cos(\omega t-\phi)$ is shown plotted along the z axis in Fig. 7 where the plus and minus signs have the same meaning as before. A curve which forms the envelope of the crests is shown dotted. This curve is simply a plot of A along the z axis; it appears again on Fig. 8 together with five similar curves for other values of b. Fig. 9 shows a similar set of curves representing the variation of the relative amplitude along the y axis. As indicated on these two figures, the curves correspond to six different spacings of the dipole from the conducting plane, these spacings lying in the range $\lambda/50\leqq b\leqq\lambda$. In comparing the curves it should be noted that the input current amplitude I_m is the same for all curves on Figs. 8 and 9.

It appears that the relative amplitude factor A decreases much more rapidly with distance from the origin along the y axis than along the z axis. In order to compare the curves in Figs. 8 and 9 more accurately in this respect, they are shown replotted in Fig. 10 under the assumption that I_m in the dipole is so adjusted in each case that the amplitude product I_mA in (9) has the same value at the origin on the conducting plane for each value of b. It can be seen that while the relative amplitude decreases, at first, most rapidly along the y axis, the rate of decrease also falls off more rapidly. For each pair of curves there is a definite point of intersection which approaches the origin as b increases.[3] The location of a given point of intersection along the distance scale corresponds to the approximate radius of curvature of a nearly circular contour of constant amplitude (cf. Fig. 4) for the given value of b. It was mentioned in the dis-

[3] The fact that the point of intersection for $b=0.125\lambda$ does not follow this tendency is due to small errors in drafting, resulting from the fact that the curves have nearly equal slopes.

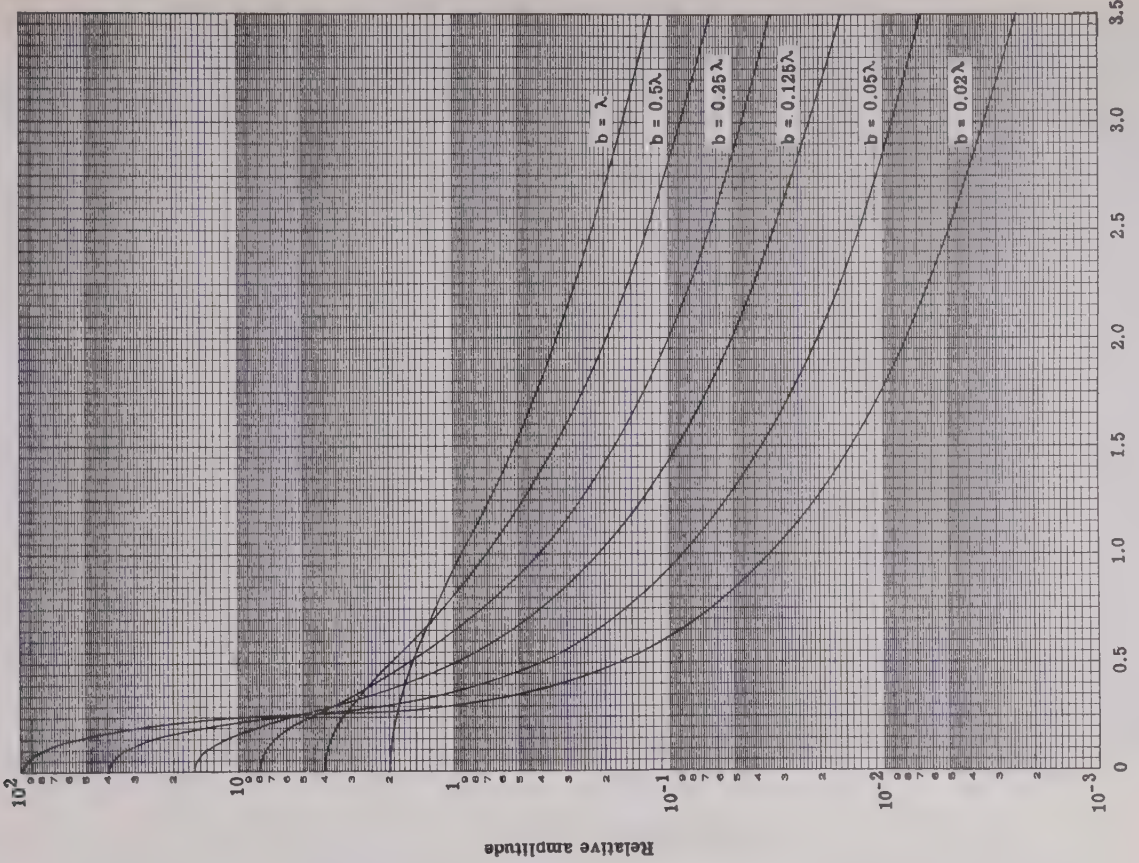

Fig. 8—Relative amplitude of surface current density and magnetic field along the z axis for six values of b.

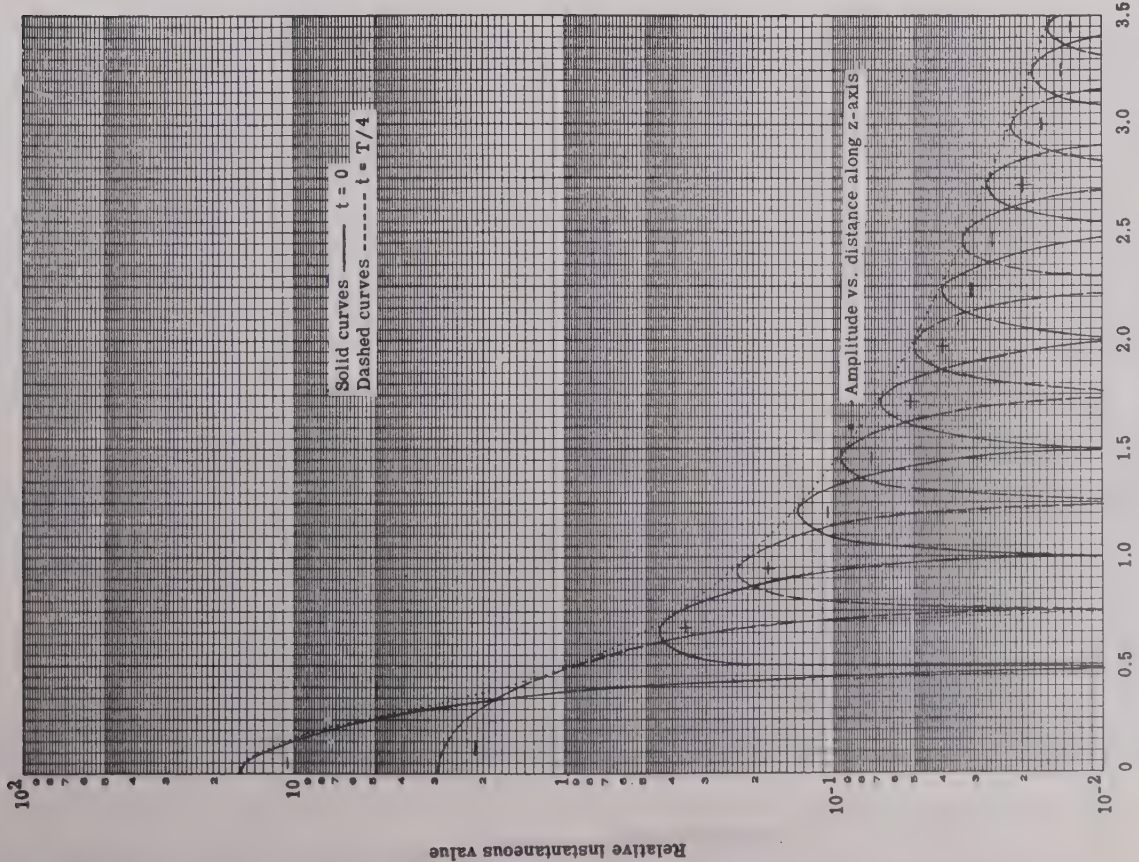

Fig. 7—Instantaneous surface current density and magnetic field along the z axis at $t=0$ and $t=T/4$; $b=0.125\lambda$. (The "solid" curve begins near 16; the "dashed" curve near 3.)

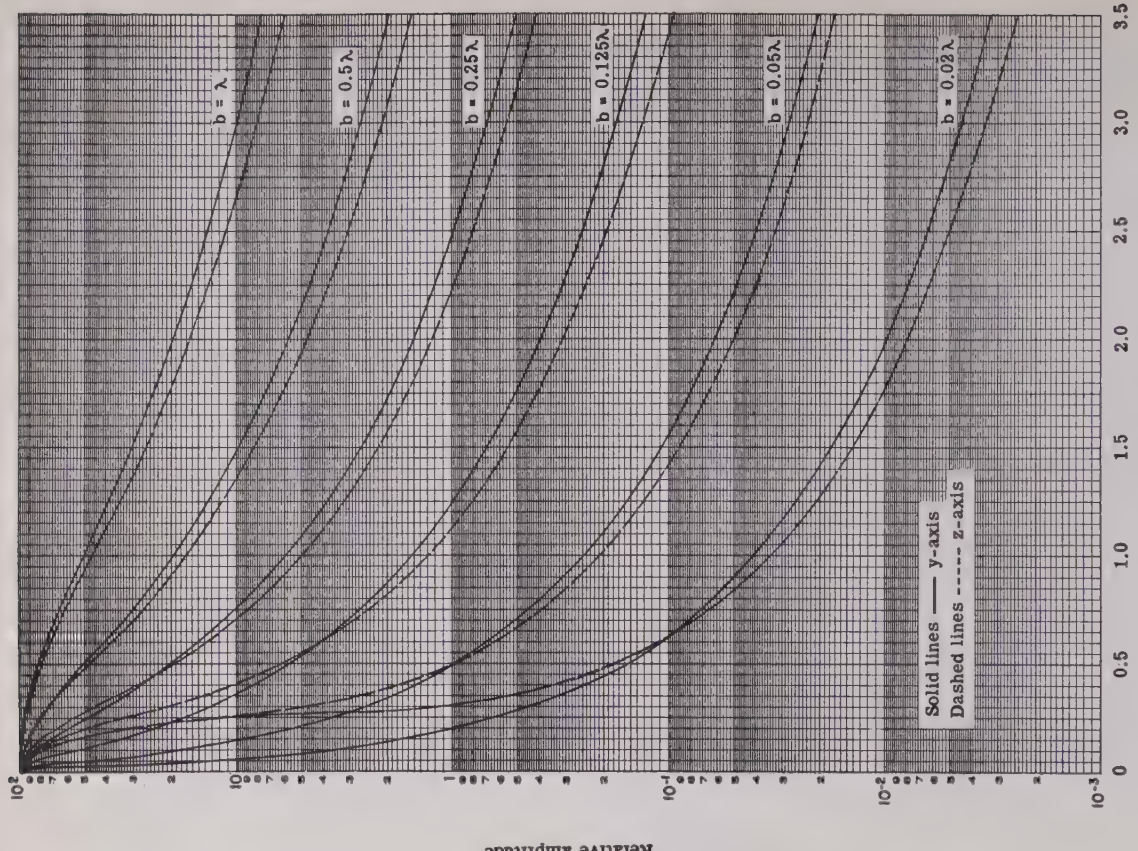

Fig. 10—Comparison of the relative amplitudes of surface current density and magnetic field along the y and z axes for six values of b. (For each value of b the "dashed" line lies below the "solid" line on the right.)

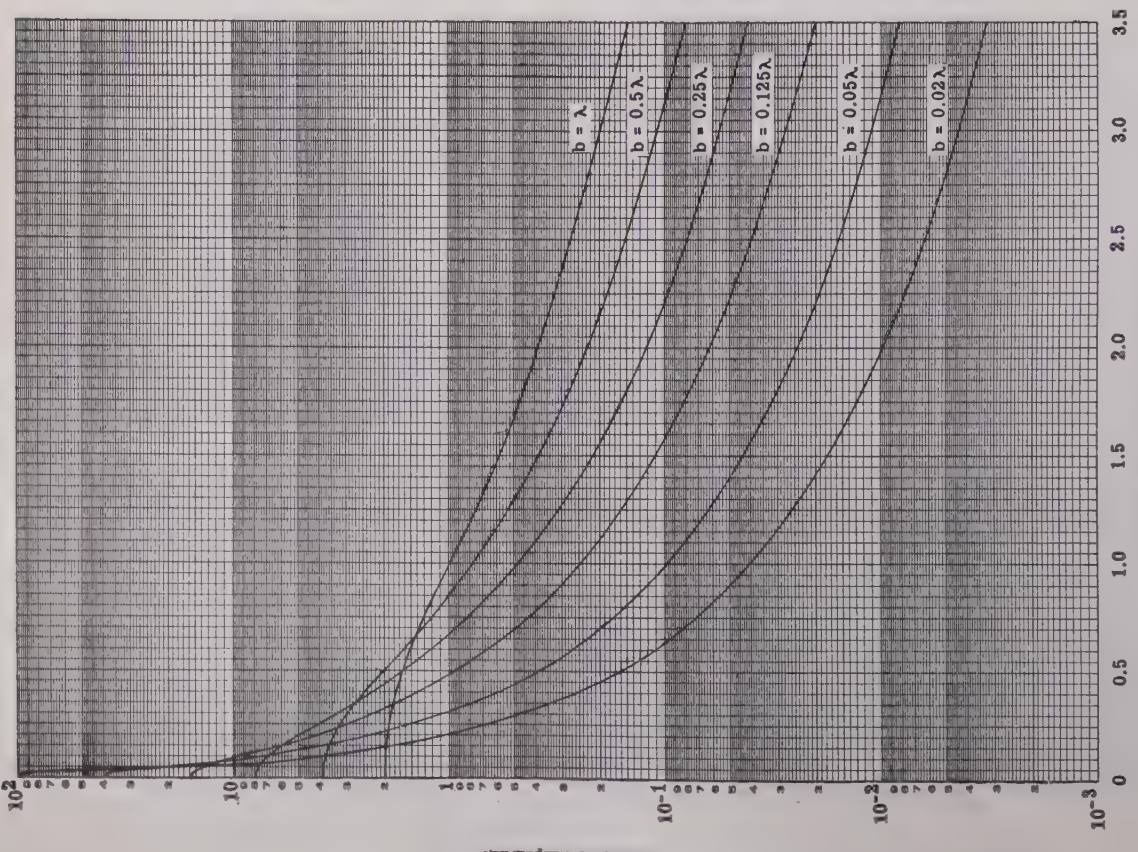

Fig. 9—Relative amplitude of surface current density and magnetic field along the y axis for six values of b.

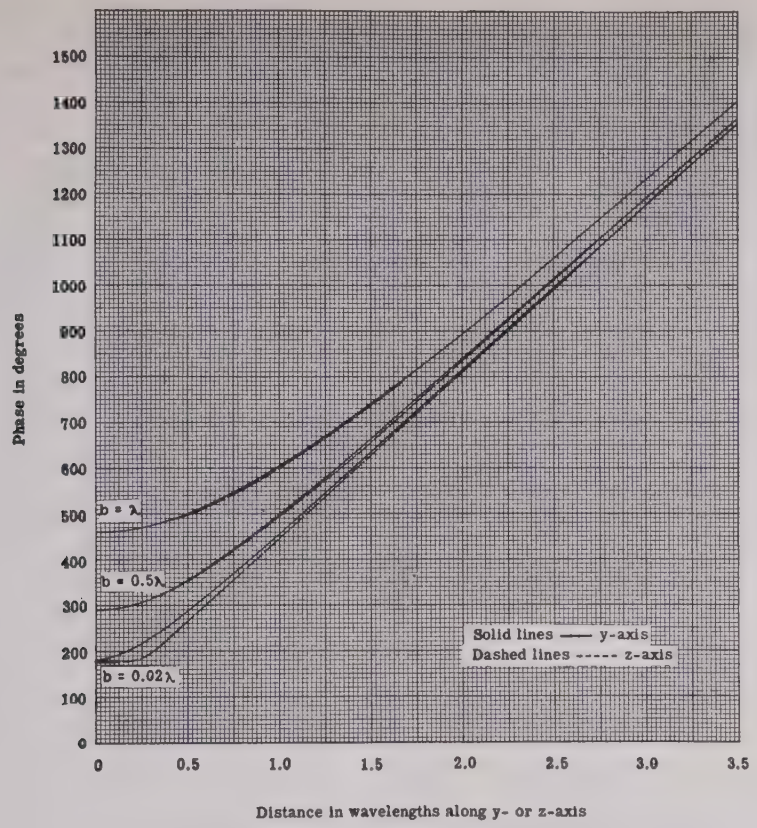

Fig. 11—Relative phase of surface current density and magnetic field along the y and z axes for three values of b. (For each value of b the "dashed" line lies below the "solid" line.)

cussion of Fig. 4 that the contours of constant amplitude are of an approximately elliptical shape, with the major axis oriented along the z axis for the contours near the origin, and then along the y axis for the contours further out. Therefore, the nearly circular contour mentioned here represents the transition between these two effects.

The behavior of the relative phase (11) along the y and z axes is shown in Figs. 11 and 12. Here again curves are plotted for the same six values of b mentioned before. However, for clarity, the pairs of curves for only three values of b are shown on Fig. 11; while on Fig. 12, all six pairs of curves are plotted to an expanded scale which covers only the region within one wavelength of the origin.

It appears that all curves approach each other as the distance from the origin increases. As would be expected, it can be shown quite easily from (11) that all of the curves approach from above the asymptotic line given by

$$\phi = \frac{2\pi}{\lambda} d + \frac{\pi}{2}, \qquad (15)$$

d being the distance in wavelengths from the origin along either the y or z axes. Clearly the curves approach this asymptote the more rapidly, the smaller the value of b.

The fact that the slopes of all curves decrease as the

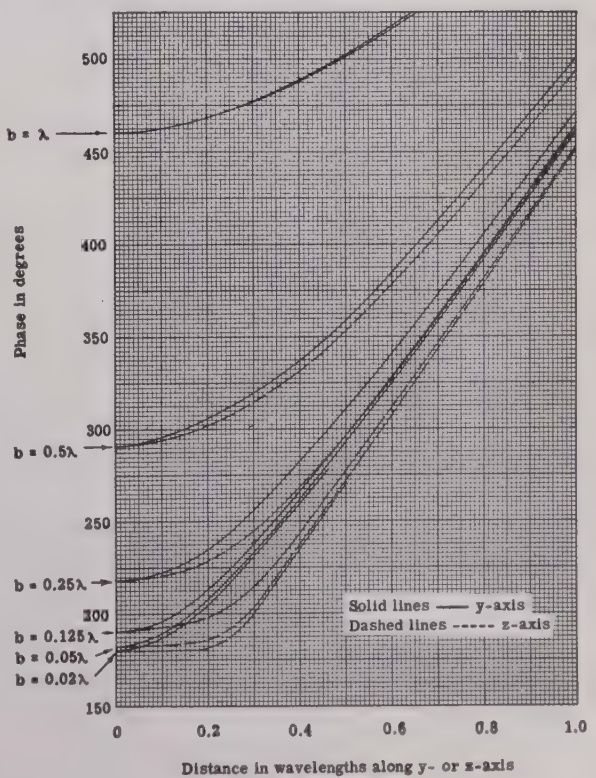

Fig. 12—Relative phase of surface current density and magnetic field along the y and z axes in the vicinity of the origin; for six values of b. (For each value of b the "dashed" line lies below the "solid" line.)

origin is approached can be attributed to a phase velocity greater than the velocity of light, which increases as the origin is approached, and which becomes theoretically infinite at the origin. This can be shown quite simply in the following way. Referring to either (9) or (14), it is evident that a contour of constant phase behaves in time according to the relation

$$\omega t - \phi = \text{constant}. \tag{16}$$

Differentiating with respect to t,

$$\frac{d\phi}{dt} = \omega. \tag{17}$$

If $d\phi/dt$ is evaluated from (11) in terms of dy/dt along the y axis ($z=0$), and then in terms of dz/dt along the z axis ($y=0$); and if the resulting expressions are substituted in (17), and the latter is solved first for dy/dt and then for dz/dt, expressions of the following form are obtained:

$$(V_p)_y = \frac{dy}{dt} = c \cdot \frac{(b^2+y^2+h^2)^{1/2}}{y} \tag{18}$$

$$(V_p)_z = \frac{dz}{dt} = c \cdot \frac{2}{\dfrac{z+h}{(b^2+(z+h)^2)^{1/2}} + \dfrac{z-h}{(b^2+(z-h)^2)^{1/2}}} \tag{19}$$

where $(V_p)_y$ and $(V_p)_z$ are the phase velocities along the y and z axes, and c is the velocity of light or ω/β_0. It is at once evident that, while both expressions approach c asymptotically as y or z becomes large, they are considerably greater than c for sufficiently small values of y or z and become infinite at the origin.

To obtain expressions for the slopes of the curves appearing in Figs. 11 and 12, note that

$$\frac{d\phi}{dy} = \frac{d\phi/dt}{dy/dt} = \frac{\omega}{(V_p)_y} \tag{20}$$

and

$$\frac{d\phi}{dz} = \frac{d\phi/dt}{dz/dt} = \frac{\omega}{(V_p)_z}. \tag{21}$$

Therefore, as the origin is approached the phase velocity along the y or z axis increases, and the slope of the curve decreases, becoming zero at the origin. It is interesting to note that the z-axis curve for the case $b=0.02\lambda$ has an effectively zero slope almost out to $z=0.2\lambda$. This is a necessary consequence of (19), for, when $b^2 \ll h^2$, $(V_p)_z$ remains effectively infinite out to a value of z which lies in the range $0<z<h$ but which no longer satisfies the inequality

$$b^2 \ll (z-h)^2.$$

Thus, as b approaches zero, the z-axis curve in Figs. 11 and 12 has a sharper and sharper elbow; and the position of this elbow approaches $z=h$. This effect is discussed later from a physical point of view.

It is also evident from Fig. 12 that as b approaches zero the relative phase ϕ approaches π at the origin. In order to bring out this effect even more clearly, ϕ from (11) is plotted as a function of b in Fig. 13 for $y=z=0$.

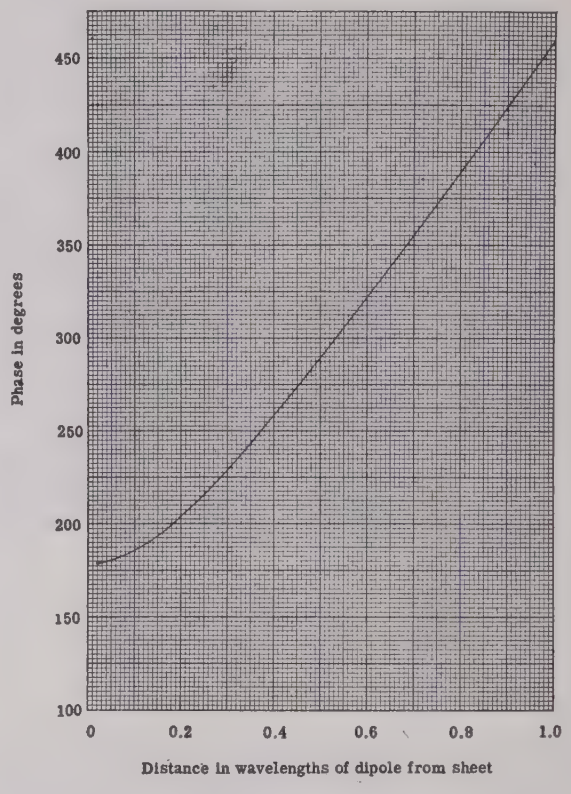

Fig. 13—Relative phase of surface current density and magnetic field at the origin as a function of the distance of the dipole from the conducting plane.

As before, it can be shown that this curve approaches from above the asymptote

$$\phi = \frac{2\pi}{\lambda} b + \frac{\pi}{2}, \tag{22}$$

as b becomes large.

A corresponding plot at the origin of the relative amplitude A as a function of b is not included since such a curve would simply represent an inverse-first-power decrease, as is evident from (10) on setting $y=z=0$.

The discussion of the graphical results is essentially complete at this point, but a few further remarks will be made on the interesting behavior of the relative amplitude A and relative phase ϕ along the z axis in the small interval $-h \leqq z \leqq +h$, which represents that segment of the z axis directly beneath the dipole. First, since a cosinusoidal distribution of current in the dipole was originally assumed, it might be expected that, as the distance of separation b becomes smaller and smaller, a plot of the relative amplitude A along the z axis and in the small

range under consideration should approach a cosine curve. That this is the case can be seen from Fig. 14 where a curve, represented by $\cos \beta_0 z$, is shown together with two of the z-axis curves of Fig. 10, namely, those for $b=0.02\lambda$ and $b=0.125\lambda$. The distance scale along the axis of abscissas has been expanded ten times in comparison with that on Fig. 10 in order to include only the range of present interest, namely, $0 \leqq z \leqq h=0.25\lambda$.

The behavior of the relative phase ϕ along the z axis in the same range as b becomes very small has been discussed previously in terms of an essentially infinite phase velocity. To repeat, the phenomenon in question is represented by the effectively horizontal portion of

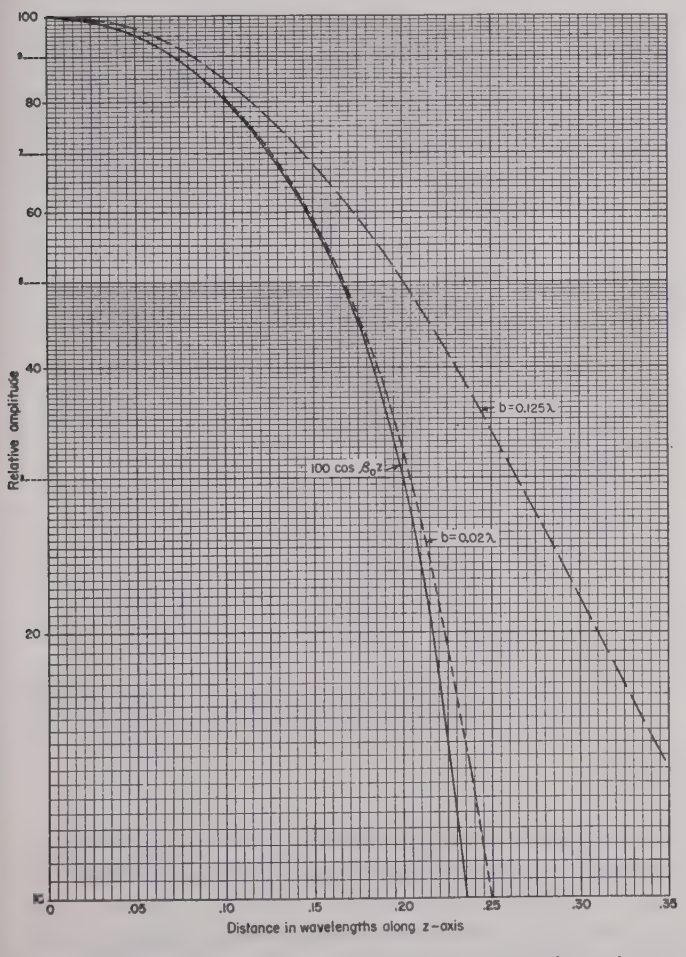

Fig. 14—The relative amplitudes of surface current density and magnetic field along the z axis for $b=0.02\lambda$ and $b=0.125\lambda$, as compared with a cosine curve.

the z-axis curves in Figs. 11 and 12 when b becomes small.

From a physical viewpoint such an effect is to be expected since it has been assumed that the relative phase of the current along the dipole is constant, and since as b approaches zero the boundary condition (12) or (13) implies that the current along the z axis in the range $-h \leqq z \leqq +h$ must be at all points oppositely directed to the current at corresponding points along the dipole.

Conclusion

In conclusion a few words regarding the initial assumptions are in order. These assumptions were: (a) the dipole is exactly one-half-wavelength long ($2h=\lambda/2$); (b) the distribution of current amplitude along the dipole is cosinusoidal with respect to its midpoint; (c) the relative phase of the current along the dipole is constant but not necessarily that of the driving voltage; and (d) the effect of mutual coupling between the dipole and the perfectly conducting plane does not invalidate these assumptions, even for very close spacings. Assumptions (b) and (c) are excellent approximations[4,5] if it is assumed that the radius a of the dipole and the distance d between the input terminals (Fig. 1) are both extremely small compared to the half-length. In fact, even in the case of a physically reasonable dipole, say $h=25a$, the distribution of current amplitude is cosinusoidal to within approximately ± 3 per cent, and the relative phase of the current along the dipole is constant to within approximately ± 3 degrees.

In order to discuss (d), let the infinite, perfectly conducting plane be replaced by an actual physical dipole satisfying the image characteristics. That is, consider two parallel half-wave dipoles separated a distance $2b$ and driven in phase opposition. For two coupled, parallel, half-wave dipoles, either or both of which may be driven, it has been shown[6] that when the separation distance $2b$ is not too small the input self-impedance of either dipole is not appreciably changed from the value it has for an isolated half-wave dipole; and, furthermore, that the mutual impedance computed on the basis of a first-order approximation to the correct current distribution differs negligibly from that computed on the basis of a cosinusoidal distribution (with respect to the midpoint). In addition, it has recently been shown[7] that in the event the spacing $2b$ becomes small there is a gradual transition to the transmission-line case. This evidence can be interpreted as meaning that, independent of the spacing, the current distribution as assumed under (b) and (c) above is a reasonably good approximation to the actual distribution along either dipole in the presence of the other; hence, that assumption (d) is justified.

[4] Ronold King and Charles W. Harrison, Jr., "The distribution of current along a symmetrical center-driven antenna," Proc. I.R.E., vol. 31, pp. 548–567; October, 1943.

[5] R. King and D. Middleton, "The cylindrical antenna; current and impedance," *Quart. Appl. Math.*, vol. III, pp. 302–335; January, 1946.

[6] Ronold King and Charles W. Harrison, Jr., "Mutual and self-impedance for coupled antennas," *Jour. Appl. Phys.*, vol. 15, pp. 481–495; June, 1944.

[7] C. T. Tai, "Theory of coupled antennas and its applications," Sc.D. Thesis, Graduate School of Engineering, Harvard University, 1946; Technical Report No. 12, Cruft Laboratory, Contract N5ori-76, T.O. 1.

Experimental Determination of Helical-Wave Properties*

C. C. CUTLER†, ASSOCIATE, I.R.E.

Summary—The properties of the wave propagated along a helix used in the traveling-wave amplifier are discussed. A description is given of measurements of field strength on the axis, field distribution around the helix, and the velocity of propagation. It is concluded that the actual field in the helix described is slightly weaker than would be predicted from the relations presented by J. R. Pierce for a hypothetical helical surface.

Introduction

RECENT PAPERS[1–3] have described a traveling-wave tube in which the circuit consists of a helix through which a beam of electrons is passed. Equations describing the electromagnetic wave on the helix have been developed for an idealized thin helical surface.[3] One might expect the field at a distance from a helix of finite wire size and pitch to be essentially of the form described for the idealized case, but the field would certainly be different in the vicinity of the wire. The quantity of interest in the traveling-wave tube, i.e., the longitudinal electric field for unit power propagated, might be smaller because of the increased field concentration near the wires, or greater because of the space occupied by the wires, within which there can be no field. Also, in using the equations there is a question as to what should be taken as the effective radius of the helix. Consequently, a program was undertaken to determine these factors experimentally.

Measurement of Wave Properties

The velocity of propagation on a copper helix of the size used in the 4000-Mc. traveling-wave amplifier was measured over a range of frequencies from 625 to 8220 Mc. by measuring the wavelength of the standing-wave pattern on a helix terminated by a metal plate.

In order to facilitate measurement of field strengths a scale model of the helix was made, scaling up by approximately a factor of seven, and field measurements were made at a frequency of 560 Mc. This gave a mean helix diameter of 3.38 centimeters, around which it was found possible to make measurements with electric and magnetic probes without greatly distorting the fields. The field configurations were measured using a carefully balanced dipole and a small loop antenna, such as are sketched in Fig. 1. Considerable difficulty was experienced in obtaining a balance in the dipole such that the currents on the coaxial transmission line connecting the probe did not affect the indication, but no such difficulty was experienced with the loop.

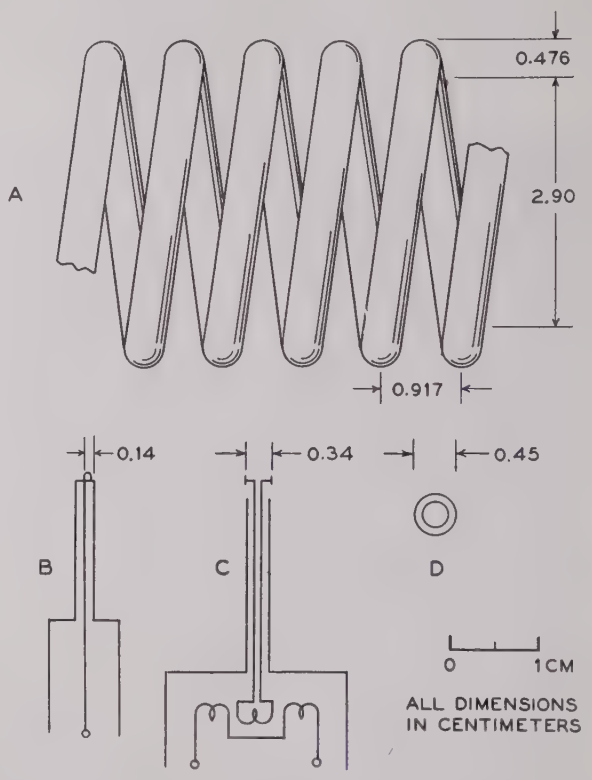

Fig. 1—Helix and probes for field measurement at 560 Mc. (a) Helix, (b) loop, (c) balanced dipole, and (d) neon tube.

To determine the absolute value of the field strength, a waveguide, coaxial transmission line, and a helix were connected in tandem, and the impedance of each carefully matched. The fields were then compared in the three systems with the dipole and loop probes, using a bolometer detector. In order to remove any doubt as to the effect of the coaxial line associated with the probes on the field itself, a tiny gas-discharge tube, about 5 mm. in diameter, was also used to measure the axial electric field.

It was found that the field required to initiate the gas discharge was rather inconsistent but that the field strength at extinction was consistent to within 5 per cent, which was sufficiently accurate for this purpose. The comparisons were made by mounting the tube at the position to be measured, monitoring the power level with a bolometer loosely coupled to the circuit, and varying the power level at the generator. For each obser-

* Decimal classification: R339.2×R271. Original manuscript received by the Institute, April 10, 1947; revised manuscript received, July 2, 1947. Presented, 1947 I.R.E. National Convention, March 4, 1947, New York, N. Y.

† Bell Telephone Laboratories, Inc., Murray Hill, N. J.

[1] R. Kompfner, "The traveling-wave tube as amplifier at microwaves," PROC. I.R.E., vol. 35, pp. 124–127; February, 1947.

[2] J. R. Pierce and L. M. Field, "Traveling-wave tubes," PROC. I.R.E., vol. 35, pp. 108–111; February, 1947.

[3] J. R. Pierce, "Theory of the beam-type traveling-wave tube," PROC. I.R.E., vol. 35, pp. 111–123; February, 1947.

vation, the oscillator level was raised to produce a discharge in the tube and then slowly lowered and the level recorded at the moment the discharge ceased.

The theoretical relation between electric or magnetic field and total transmitted power for the transmission systems used is given in Appendix B.

Discussion of Helical-Wave Properties

From the measurements and the equations in the appendix, the following properties of the wave on a helix may be deduced:

1. It was found that the electromagnetic field clings very closely to the helix. The energy is effectively trapped, or guided, by the circuit and there is no tendency of the helix to radiate; therefore, in many applications it is not necessary to shield the helix. Fig. 2 shows the distribution of the lines of force around the helix. The calculated and measured fields are compared in Fig. 3 and Table I. The form of the field is given satisfactorily by the equations for the cylinder except for variations near the wire. The indicated circumferential electric field is stronger than calculated, probably because of difficulty in obtaining a sufficiently well-balanced dipole to discriminate against other field components. The longitudinal electric field within the helix for a given transmitted power is somewhat weaker than calculated, as indicated in Table I.

It might be expected that the propagation would depart from theory at frequencies where the wavelength approaches the length of a circumference, because the physical helix would then radiate,[4,5] whereas the hypothetical surface used in the theory would not. This can be seen by considering the contribution of current elements in the circuit to the field at a distant point. In the helix the adjacent current elements are restricted to the wire, and if the circumference is equal to the wavelength they will be in phase and will contribute to give a finite field at a distance, whereas in the hypothetical surface the current elements may be taken as close as de-

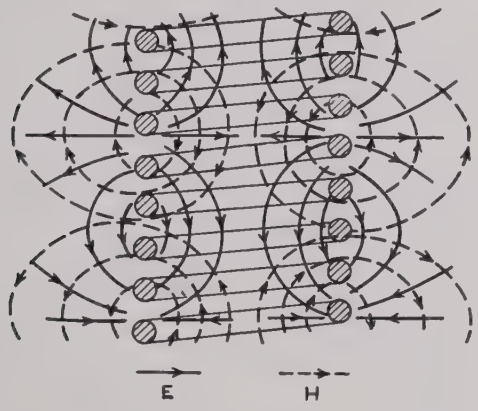

Fig. 2—Field configurations around a helix.

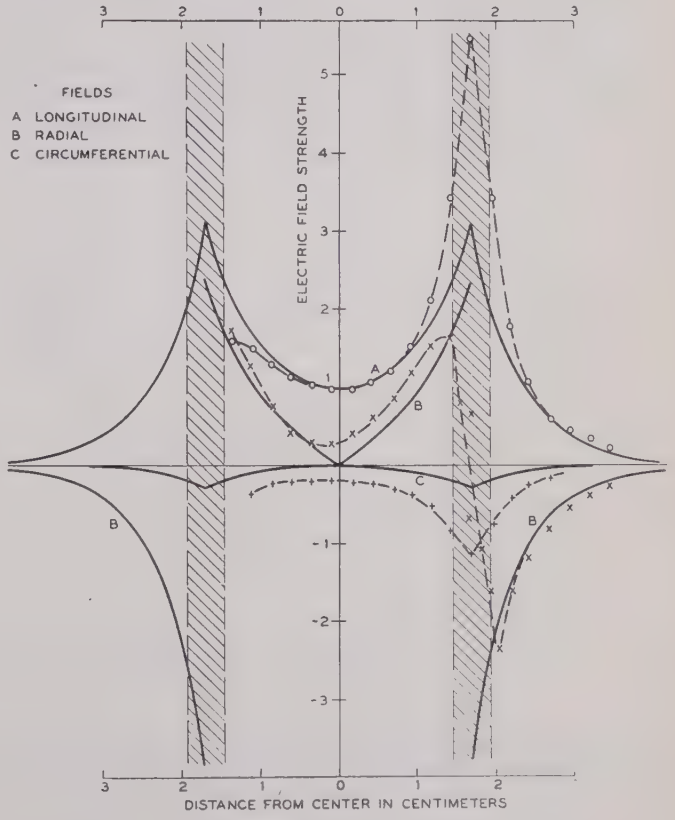

Fig. 3—Electric field strength around a helix. The solid lines are theoretical and the points are experimental. The probe was moved between turns, to the right, and directly opposite a turn of wire at the left.

TABLE I

Condition	Calculated Value	Measured Value	Difference	Probe
$\left[\frac{E_Z \text{ center of helix}}{E_Y \text{ 9 cm. from guide wall}} = 1\right]^2$	15.6 db	14 db	−1.6 db	Dipole
$\left[\frac{E_Z \text{ center of helix}}{E_Y \text{ center of guide}}\right]^2$	12.3 db	8.9 db	−3.4 db	Neon tube
$\left[\frac{H_Z \text{ center of helix}}{H_Z \text{ outer wall of guide}}\right]^2$	17.7 db	18 db	0.3 db	Loop
$\left[\frac{H_Z \text{ center of helix}}{H_\phi \text{ outer wall of coaxial}}\right]^2$	5.5 db	5.3 db	−0.2 db	Loop

Waveguide dimensions = 1.02 cm. × 38.1 cm.
Coaxial: Z_0 = 100 ohms, 2.54 cm. i.d. of outside conductor
Helix: Mean radius = 1.69 cm.
Wire diameter = 0.475 cm.

[4] H. A. Wheeler, "Helical antenna for circular polarization," Proc. I.R.E., vol. 35, pp. 1484–1489; December, 1947.
[5] J. D. Kraus, "Helical beam antenna," *Electronics*, vol. 20, pp. 109; April, 1947.

sired in any case, and the net contribution of a long circuit to a distant field is very small.

2. Within the helix, the fields are predominantly longitudinal. This is important because the longitudinal electric field is parallel to the electron stream and interacts with the electrons to give gain in the traveling-wave tube.

3. The radial and longitudinal fields tend toward equality at points distant from the helix. In fact, for waves propagating much slower than the velocity of light, the field at a distance outside the helix may be represented approximately by a circularly polarized wave traveling with the velocity of light in a helical path with the same pitch angle as the helix.

4. At high frequencies the wave progresses with a velocity such as might be explained approximately as that of a wave following the helix at the speed of light. Thus the axial velocity v is slower than the speed of light by approximately the ratio of the axial to the helical length of the circuit. Fig. 4 is essentially a plot of relative velocity against frequency, and was calculated from (13) using the mean radius of the helix for the radius of the equivalent cylinder. The measured velocity, indicated by the points, is in very good agreement with the theoretical curve over the greater part of the range shown. At relatively low frequencies, where the helix diameter is a small fraction of a wavelength, and the wave travels faster, the agreement with theory is not so good. It might also be expected that the helix properties would depart radically from the theory at very-high frequencies where the wavelength approaches a circumference and radiation takes place.

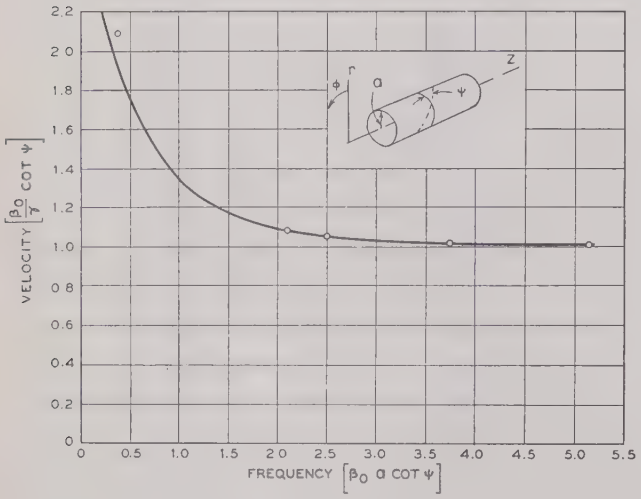

Fig. 4—Curve for propagation along a helically conducting cylinder which roughly shows the ration of the speed along the helical direction of the surface of the cylinder to the speed of light, versus a parameter proportional to frequency, radius, and pitch.

5. A wave reflected at a plane boundary tends to spiral in the wrong direction, and, if otherwise unconstrained, only a portion of the reflected energy follows the circuit while the remainder is radiated. The reflection properties are illustrated in Fig. 5, which shows the standing wave measured near the intersection of a helix and a plane conducting sheet, at 4000 Mc. The erratic nature of the curve near the end is caused by interference between the guided and the radiated wave. Farther from the termination the curve shows the attenuation of the wave to be 0.18 db per inch, and by extrapolation to the end indicates a loss of about 0.07 db at reflection.

The question might be raised as to whether the waves described are the only ones supportable by a helix. As a result of an extensive study over a wide range of frequencies, exciting conditions, and terminating conditions, no wave other than the one described and an essentially unguided free-space wave was detected. The latter wave may be reduced to a very small amplitude by appropriate launching and care in terminating the spiral waves, or by placing the helix inside a pipe too small to support other waveguide-type modes.

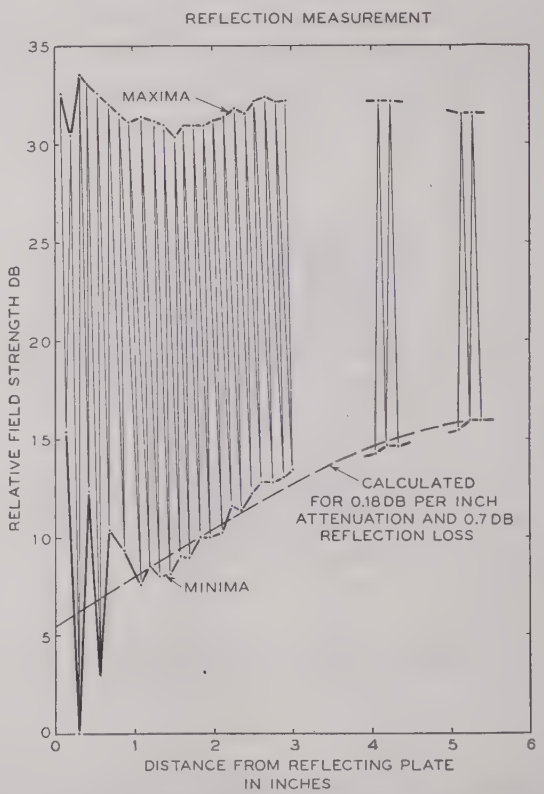

Fig. 5—Standing-wave pattern produced along a helix by intersection with a conducting plate.

Conclusion

These investigations indicate that the spiral-wave solution described gives reasonably accurate results in the case of an actual helix of the proportions used in the

traveling-wave amplifier, and that the axial electric field is slightly weaker than calculated.

The writer wishes to acknowledge his indebtedness to D. J. Brangaccio and R. S. Julian, who did much of the work described in this paper.

Appendix A

Equations for Wave Propagation on a Helix

Twelve equations are required to define completely the wave[3] guided by a hypothetical helical surface, i.e., a cylindrical surface conducting only in a helical direction making an angle Ψ with a circumference, and nonconducting in the helical direction normal to this. The equations are given here for reference.

Inside helix:

$$E_Z = BI_0(\gamma r)e^{j(\omega t-\beta z)} \tag{1}$$

$$E_r = jB\frac{\beta}{\gamma}I_1(\gamma r)e^{j(\omega t-\beta z)} \tag{2}$$

$$E_\phi = -B\frac{I_0(\gamma a)}{I_1(\gamma a)}\frac{1}{\cot\psi}I_1(\gamma r)e^{j(\omega t-\beta z)} \tag{3}$$

$$H_Z = -j\frac{B}{\eta}\frac{\gamma}{\beta_0}\frac{I_0(\gamma a)}{I_1(\gamma a)}\frac{1}{\cot\psi}I_0(\gamma r)e^{j(\omega t-\beta z)} \tag{4}$$

$$H_r = \frac{B}{\eta}\frac{\beta}{\beta_0}\frac{I_0(\gamma a)}{I_1(\gamma a)}\frac{1}{\cot\psi}I_1(\gamma r)e^{j(\omega t-\beta z)} \tag{5}$$

$$H_\phi = j\frac{B}{\eta}\frac{\beta_0}{\gamma}I_1(\gamma r)e^{j(\omega t-\beta z)}. \tag{6}$$

Outside helix:

$$E_Z = B\frac{I_0(\gamma a)}{K_0(\gamma a)}K_0(\gamma r)e^{j(\omega t-\beta z)} \tag{7}$$

$$E_r = -jB\frac{\beta}{\gamma}\frac{I_0(\gamma a)}{K_0(\gamma a)}K_1(\gamma r)e^{j(\omega t-\beta z)} \tag{8}$$

$$E_\phi = -B\frac{I_0(\gamma a)}{K_1(\gamma a)}\frac{1}{\cot\psi}K_1(\gamma r)e^{j(\omega t-\beta z)} \tag{9}$$

$$H_Z = j\frac{B}{\eta}\frac{\gamma}{\beta_0}\frac{I_0(\gamma a)}{K_1(\gamma a)}\frac{1}{\cot\psi}K_0(\gamma r)e^{j(\omega t-\beta z)} \tag{10}$$

$$H_r = \frac{B}{\eta}\frac{\beta}{\beta_0}\frac{I_0(\gamma a)}{K_1(\gamma a)}\frac{1}{\cot\psi}K_1(\gamma r)e^{j(\omega t-\beta z)} \tag{11}$$

$$H_\phi = -j\frac{B}{\eta}\frac{\beta_0}{\gamma}\frac{I_0(\gamma a)}{K_0(\gamma a)}K_1(\gamma r)e^{j(\omega t-\beta z)}. \tag{12}$$

Where I_0, K_0, I_1, and K_1 are modified Bessel functions $\eta=120\pi$ ohms, $\beta=\omega/v$, $\beta_0=\omega/c$, $\gamma^2=\beta^2-\beta_0^2$, a is the radius of the helix, v is the axial velocity, c is the velocity of light, and ω is the radian frequency.

The factor γ may be obtained from the circuit dimensions by the relation

$$(\gamma a)^2\frac{I_0(\gamma a)K_0(\gamma a)}{I_1(\gamma a)K_1(\gamma a)} = (\beta_0 a\cos\psi)^2. \tag{13}$$

Fig. 1 shows $\beta_0/\gamma\cot\Psi$ plotted against $\beta_0 a\cot\Psi$ for this expression. Making the approximation of a wave propagating slowly compared with the speed of light, so that β and γ are nearly equal, and β/β_0 is nearly equal to $\cot\Psi$, the equations may be simplified further.

Appendix B

Formulas Relating Fields to Transmitted Power

Associated with any transmitted wave, there is a certain transmitted power P. At any point in the field of such a wave the quantities E^2/P and H^2/P, where E and H are any components of the field, are properties only of the geometry of the field. They have dimension of ohm cm.$^{-2}$ and mho cm.$^{-2}$ if E and H are volts per centimeter and amperes per centimeter. These quantities have been evaluated for the transmission systems described in this paper in order to relate the fields in the transmission systems used.

Equations Relating Field and Power in the Transmission Systems Compared

Helical cylinders:[3]

$$\frac{E_Z^2}{P} = \frac{\gamma^4}{\beta\beta_0}F^3(\gamma a) \tag{14}$$

$$\frac{H_Z^2}{P} = \frac{\gamma^6}{\eta^2\beta\beta_0{}^3}\frac{I_0^2(\gamma a)}{I_1^2(\gamma a)}\frac{1}{\cot^2\psi}F^3(\gamma a), \tag{15}$$

where

$$F^3(\gamma a) = \frac{(\gamma a)^2}{240}\left[(I_1^2-I_0I_2)\left(1+\frac{I_0K_1}{I_1K_0}\right)+\left(\frac{I_0}{K_0}\right)^2(K_0K_2-K_1^2)\left(1+\frac{I_1K_0}{K_1I_0}\right)\right]. \tag{16}$$

Coaxial line, at radius r from axis of symmetry of line of characteristic impedance R ohms:

$$\frac{E_r^2}{P} = \frac{\eta^2}{2\pi^2}\frac{1}{r^2R} \tag{17}$$

$$\frac{H\phi^2}{P} = \frac{1}{2\pi^2}\frac{1}{r^2R}. \tag{18}$$

TE_{10} rectangular wave guide, cross section a and b with field measured at distance x from side of guide:

$$\frac{E_y^2}{P} = 4\eta\frac{\lambda g}{\lambda}\frac{1}{ab}\sin^2\frac{\pi x}{a} \tag{19}$$

$$\frac{H_z^2}{P} = \frac{\lambda\lambda g}{\eta a^2b}\cos^2\frac{\pi x}{a}\cdot\frac{H_z^2}{P} = \frac{4}{\eta}\frac{\lambda}{\lambda g}\frac{1}{ab}\sin^2\frac{\pi x}{a}. \tag{20}$$

A Tunable Vacuum-Contained Triode Oscillator for Pulse Service*

C. E. FAY†, SENIOR MEMBER, I.R.E., AND J. E. WOLFE‡, SENIOR MEMBER, I.R.E.

Summary—**A tunable push-pull triode oscillator is described in which the vacuum-tube components and the entire r.f. portion of the oscillator circuit are contained in an evacuated metallic envelope. A terminal is provided for coaxial output into a 50-ohm transmission line. The oscillator was developed for the frequency range of 390 to 435 Mc. and is tunable by mechanical means continuously through this range. Pulse power of above ½ megawatt is obtained with pulse voltages of 15 to 17 kilovolts applied.**

Introduction

THE PRODUCTION of high pulse power for radar purposes at frequencies below approximately 600 megacycles was a problem to which considerable of the war effort was devoted. The development of the multicavity magnetron[1] solved the problem of high pulse power very satisfactorily for frequencies higher than this value, but the size of the magnetron and its difficulties at lower frequencies became burdensome, especially when the necessary magnetic field was considered.

The use of conventional triodes in multitube circuits was an obvious expedient which was resorted to in early radar developments because tubes designed particularly for pulse service were not then available. It was found in such cases that circuit difficulties were paramount and that it was difficult to obtain reasonable efficiency at frequencies above about 200 megacycles.[2] Tubes designed for higher power were, of necessity, larger and hence more difficult to operate at high frequencies.

Since so much of the radio-frequency circuit was unavoidably contained within the tube, attention was given to improving the connections to the tube electrodes with the object of reducing the inductance and radio-frequency resistance of the leads. Several tubes have been described which incorporated these improvements.[3,4] An additional difficulty in obtaining high pulse power is sparkover in the oscillator circuit resulting from the high peak voltages encountered.

It seemed to the authors that the best answer to the problem lay in designing an oscillator in which both the tube electrodes and the rest of the oscillatory circuit were inside the vacuum-retaining envelope, as in the magnetrons. One tube employing these general principles has already been described.[5] The one about to be described here has some additional features which are believed to be of considerable advantage.

Design Features

The development of this tube, which is known as the 7C22, was undertaken by the Bell Telephone Laboratories, Inc., at the request of and under contract with the Bureau of Ships of the U. S. Navy. It has resulted in an oscillator in packaged form which is very rugged and easy to handle. The specifications called for peak pulse power of approximately ½ megawatt at a frequency of a little above 400 Mc. from an oscillator tunable over about a 7 per cent frequency range, the pulse length to be at least 5 microseconds and the duty cycle to be 0.001.

In a tube for high peak power it is advantageous to operate at as high a plate voltage as possible in order to keep cathode-emission requirements down. At the time of this development, pulse generators or modulators were available which would deliver up to 20-kv. pulses. It was therefore decided to design for a pulse plate voltage of 15 kv. to 20 kv. This then required that, with a push-pull oscillator, cathode emission of approximately 150 amperes per cathode must be provided. With other than oxide-coated cathodes, this amount of emission would require almost a prohibitive amount of heating power (more than 1.5 kw. per tube). Since oxide cathodes were by this time performing fairly satisfactorily in magnetrons and also in some pulse amplifier or modulator tubes, this type was chosen.

The structure is shown schematically in Fig. 1, and a section drawing is given in Fig. 2. Electrically, it is a push-pull Colpitts-type oscillator operating with "grounded anode." The outer metallic shell is the vacuum-retaining envelope and also the anode terminal. The two sets of vacuum-tube elements are disposed at opposite ends of the cylindrical shell. The grids are mounted on a metallic sleeve concentric with the outer shell, and the cathodes on a smaller sleeve concentric with the grid sleeve. One heater terminal is connected

* Decimal classification: R355.912×R537.121. Original manuscript received by the Institute, May 23, 1947. Presented, 1947 I.R.E. National Convention, March 4, 1947, New York, N. Y.

† Bell Telephone Laboratories, Inc., New York, N. Y.

‡ Formerly, Bell Telephone Laboratories, Inc.; now, Kansas State College, Manhattan, Kan.

[1] J. B. Fisk, H. D. Hagstrum, and P. L. Hartman, "The magnetron as a generator of centimeter waves," *Bell Sys. Tech. Jour.*, vol. 25, pp. 167–348; April, 1946.

[2] R. Colton, "Radar in the U. S. Army," PROC. I.R.E., vol. 33, pp. 740–750; November, 1945.

[3] R. R. Law, D. G. Burnside, R. P. Stone, and W. B. Whalley, "Development of pulse triodes and circuits to give one megawatt at 600 megacycles," *RCA Rev.*, vol. 7, pp. 253–264; June, 1946.

[4] J. J. Glauber, "Radar vacuum tube developments," *Elec. Commun.*, vol. 23, pp. 306–319; September, 1946.

[5] H. A. Zahl, J. E. Gorham, and G. F. Rouse, "A vacuum-contained push-pull triode transmitter," PROC. I.R.E., vol. 1, pp. 66–69; February, 1946.

to the cathode sleeve and the other is a rod inside the cathode sleeve and insulated therefrom by ceramic bushings. *The heaters are helices of tungsten wire which transfer heat to the cathodes by radiation.* The sleeves are supported from each other and from the outer shell by by means of ceramic insulators located at the center of the structure, which is at a r.f. voltage node.

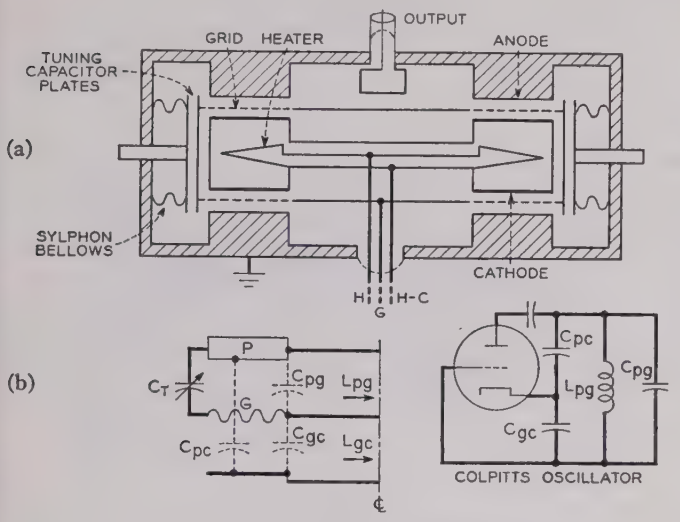

Fig. 1—(a) Schematic section of the 7C22 oscillator. (b) Equivalent circuit of the 7C22 oscillator compared to the conventional Colpitts circuit.

Tuning is accomplished by means of plates attached to sylphon bellows at each end of the structure which may be advanced and withdrawn by rotating a gear. The output is obtained from a coupling loop in the center of the grid-anode space which is connected to a concentric-line terminal. The cathode, heater, and grid terminals are at the center of the structure opposite the output terminal. The structure is cooled by means of air directed through the circular radiating fins appearing adjacent to the anode surfaces.

Mode of Operation

To consider the mode of operation of this device, the schematic shown in Fig. 1(b) represents half the tube broken at the center line. As stated previously, the basic circuit is the Colpitts oscillator, where, in this instance, the capacitances of the circuit are mainly the tube interelectrode capacitances. The short sections of transmission line L_{pg} and L_{gc} may be considered to be short-circuited by the center line, and, since these lines are physically short $[<(\lambda/4)]$, they may be considered as inductances. In the conventional Colpitts oscillator the frequency is given by

$$f = \frac{1}{2\pi\sqrt{L_{pg}\left(C_{pg} + \dfrac{C_{gc}C_{pc}}{C_{gc}+C_{pc}}\right)}}$$

where C_{pg} is the main capacitance component. The excitation ratio is C_{gc}/C_{pc}, which is the ratio of voltage at the plate to voltage at the grid with reference to the cathode. In the device shown here, C_{gc} must be considered as divided into two parts in parallel. One part resonates with L_{gc} at the operating frequency to provide effectively a $\lambda/4$ choke between cathode and ground as represented by the center line. The other part is the *effective* C_{gc} used in determining the excitation ratio and which appears in the expression for frequency.

Tuning is accomplished by varying C_{pg} effectively. This is done by advancing or withdrawing the capacitor plate attached to the sylphon bellows at the end of the structure. Actually, this capacitance has in series with it an amount of inductance resulting from the length of the circuit through the bellows and around the cavity to the anode. If this inductive reactance is kept low compared to the capacitive reactance, no difficulty is experienced, the only result being that a somewhat smaller variation of capacitance is required for a given tuning range compared to that required if no series inductance were present. Ordinarily, the Colpitts oscillator may be tuned by varying capacitance between grid and plate without affecting the excitation ratio, C_{pc}/C_{gc}. In this oscillator, however, this is not quite true, since more of the actual C_{gc} is required to resonate L_{gc} as the frequency is lowered, and hence less of C_{gc} is left to act in determining excitation. For the frequency range involved here, however, the effect is not serious, since the excitation ratio can vary considerably with very little effect on the output and efficiency, particularly where self-bias is employed.

In order to provide the required output at the desired plate voltage, it is necessary that the capacitance C_{pc} have a certain minimum value. The reason for this will be apparent from the following analysis:

In the Colpitts oscillator, the output electrodes of the tube (plate-cathode) are connected across the capacitance C_{pc}. The excitation is obtained from the voltage across the capacitance C_{gc} ((Fig. 1(b)). Since the circuit is resonant at the frequency of oscillation, in the absence of load resistance the voltage across C_{gc} will be just 180° out of phase with the voltage across C_{pc} if the cathode is taken as the reference point. The circulating current I_0 flowing through C_{pc} and C_{gc} will be given by $I_0 = E_p\omega C_{pc}$, where E_p is the alternating plate voltage and $\omega = 2\pi \times$ frequency of oscillation. If, however, a resistance is introduced into the circuit by loading, usually in the inductive portion, the current through C_{gc} will differ from that through C_{pc} by the fundamental component of plate current supplied by the vacuum-tube generator. Prince[6] has shown vector diagrams of these phase relationships. The phase of the voltage appearing across C_{gc} will differ from the 180° relationship with that across C_{pc} by an angle $\cot^{-1} R_0\omega C_{pc}$, where R_0 is the

[6] D. C. Prince, "Vacuum tubes as power oscillators," Proc. I.R.E., vol. 11, pp. 275–313, 405–435, 527–550; June, August, October, 1923.

equivalent load resistance which appears across the output terminals of the tube; e.g.,

$$R_0 = \frac{E_p^2}{\text{power output}}.$$

It was desired that this tube should operate into a 50-ohm coaxial output line with a standing-wave ratio as near unity as possible, and that as little tuning as possible should be required over the frequency range of

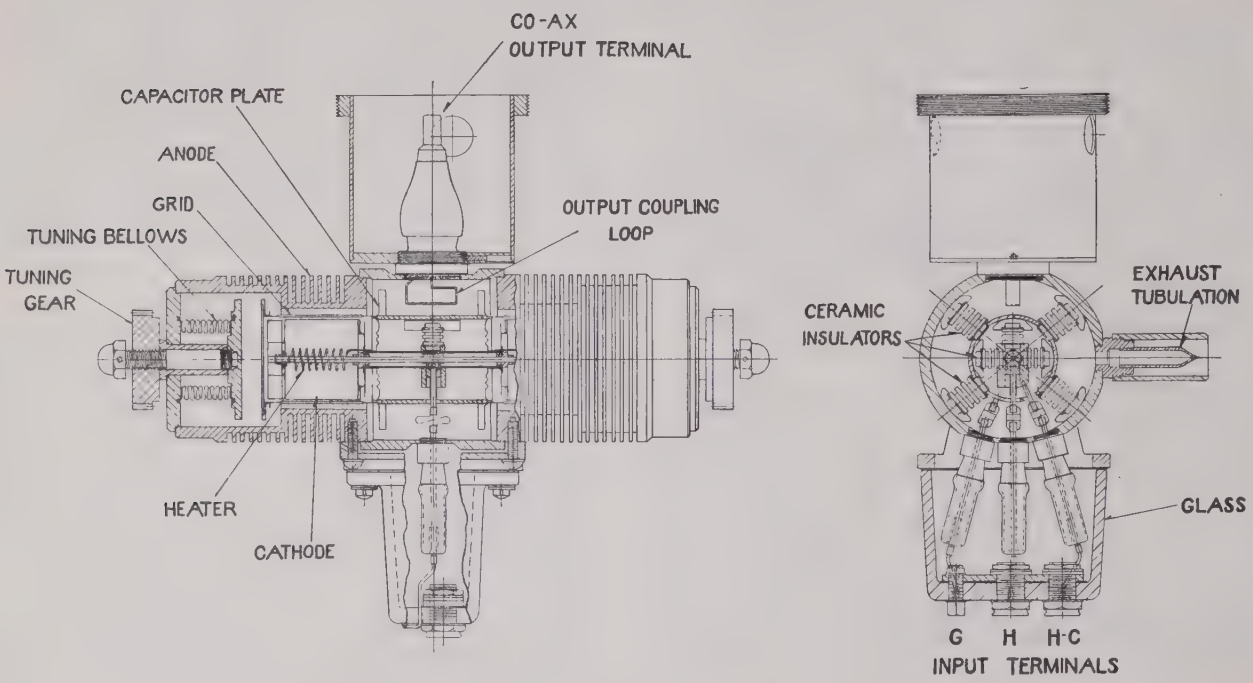

Fig. 2—Section drawing of the 7C22 oscillator.

In the case of the Colpitts oscillator, this departure from 180° phase relationship is in the direction to cause the exciting voltage to lead the plate voltage. This is of advantage in overcoming some of the effects of transit time in a high-frequency oscillator. In the present case, values of $R_0\omega C_p$ of about 5 seem to be the minimum permissible. This may be considered to be the apparent Q of the output circuit when viewed across C_{pc}. The actual Q of the circuit defined as

$$Q = \frac{2\pi \text{ energy stored}}{\text{energy lost/cycle}}$$

is always greater than this value because there are additional circuit elements storing energy (C_{gc}, C_{gp}, C_T). In the case of the 7C22 oscillator, the plate-cathode capacitance obtained by exposure of the cathode to anode through the grid was insufficient. Extra plate-cathode capacitance had to be provided in the form of a disk facing the edge of the anode. This disk was mounted from the cathode sleeve and extended as a spoked wheel through slots in the grid sleeve. Then, in order to provide the proper excitation ratio and also to tune the cathode line, additional grid-cathode capacitance in the form of a "hat" at the end of the cathode facing the grid-end disk was necessary. These details are shown in the section drawing in Fig. 2. They also act as heat shields at the ends of the cathode.

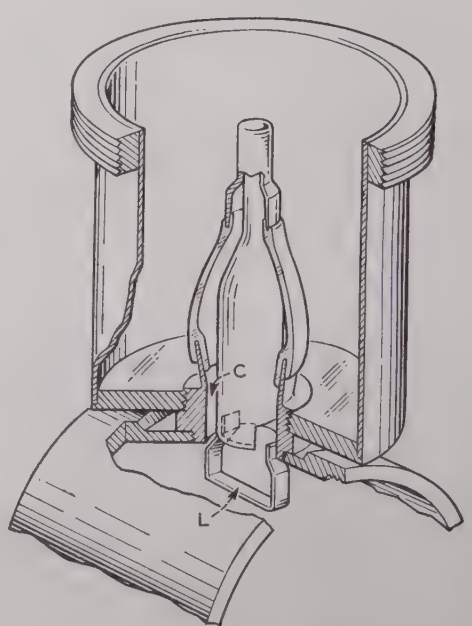

Fig. 3—Section drawing of the output terminal and coupling loop.

the tube. The output coupling loop and output terminal are shown in Fig. 3. The inductance of the loop is seen to be shunted by the capacitance between the center conductor and the shell of the lead. By suitably propor-

tioning this capacitance and inductance, it was found possible to obtain nearly full rated power at all frequencies within the tuning range of the tube when operating into a 50-ohm transmission line with a standing-wave ratio of unity.

Constructional Details

A photograph of the 7C22 is shown in Fig. 4, a cut-away model in Fig. 5, and an exploded view showing its parts in Fig. 6. The cathodes of the 7C22 oscillator have a coated area of approximately 40 square centimeters each. They are heated by radiation from a helical filament enclosed by each cathode. Ordinary oxide coating was used on a nickel base roughened to improve adherence.

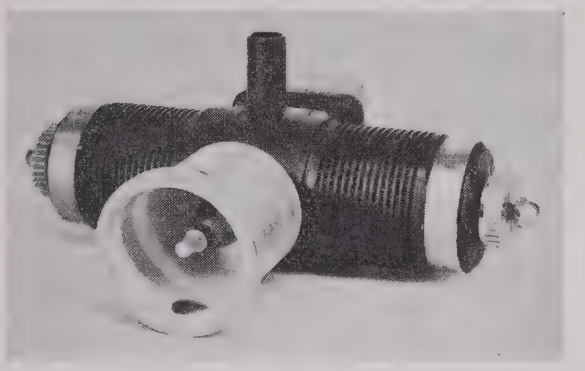

Fig. 4—Photograph of the 7C22 oscillator.

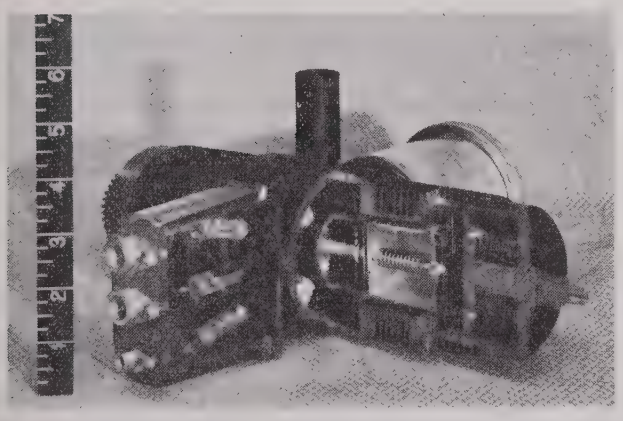

Fig. 5—Photograph of a cut-away model.

Fig. 6—Exploded view showing the component parts.

TABLE I

Cathodes:	
Equipotential oxide-coated	
Approximate emission per cathode	150 amperes
Cathode-heating time	3 minutes
Heater:	
Tungsten filaments	
Nominal heater voltage	9 volts
Nominal heater current	29.5 amperes
Amplification factor of triode elements	22
Capacitances:	
Approximate total direct capacitances measured at the terminals	
grid-anode	53 to 65 $\mu\mu$fd.
(depending on setting of tuning gears)	
grid-cathode	79 $\mu\mu$fd.
anode-cathode	23 $\mu\mu$fd.
Frequency range:	
Nominal, obtained by adjustment of tuning gears	390 to 435 Mc.

Maximum and Typical Operating Conditions
Plate-Pulsed

	Maximum Allowable	Typical Operation	
Plate pulse voltage*	18	16	kv.
Grid bias† (during pulse)	−3	−2	kv.
Average grid current	8	3	ma.
Average plate current	90	70	ma.
Peak plate current	80	63	amperes
Duty cycle (r.f. pulse length times repetition rate)	0.0012	0.001	
Pulse length‡	6	5	microseconds
Average plate dissipation	1000	600	watts
Average power output		550	watts
Peak power output		550	kw.
Peak power input	1400	1000	kw.
Peak efficiency		55	per cent

* Voltage from plate to cathode at the terminals of the tube.
† Obtained from combination of cathode resistor and grid resistor.
‡ The r.f. pulse length will usually be about 0.2 microsecond shorter than the plate pulse.

The grids are of novel construction, being formed from molybdenum sheets into which slots are punched. The slats remaining are then twisted 90° to the plane of the sheet. The sheet is then formed into cylindrical shape and welded, the slats running parallel to the axis. Diagonal stiffening wires are then welded to the outside surface of the formed grid. The entire grid is gold-plated to inhibit primary emission. This type of grid has several advantages at ultra-high frequencies. Longitudinal slats provide low inductance and low resistance to the heavy r.f. currents that must flow into the grid. Punched construction eliminates many welds and so provides better electrical and thermal conductivity. The slats, which are 0.008×0.025 inch in cross section, are weakest parallel to the surface of the grid cylinder, so that any tendency to buckle is in this direction rather than perpendicular to the grid surface where close clearances must be maintained. The normal clearance between cathode and grid is 0.050 inch. Between grid and anode it is 0.125 inch.

The grid connecting sleeve and the entire outer envelope including anodes is OFHC copper. The sylphon bellows are monel. All seals to glass are copper seals from the envelope and tungsten seals from lead wires except the output terminal, which is a copper-cup seal. A copper pinch-off exhaust tubulation is used.

Operation

The characteristics and ratings of the 7C22 tube are as shown in Table I.

A schematic of the typical circuit connection employed is shown in Fig. 7. A noninductive grid resistor of 200 to 400 ohms and a noninductive cathode resistor of 10 to 20 ohms are recommended.

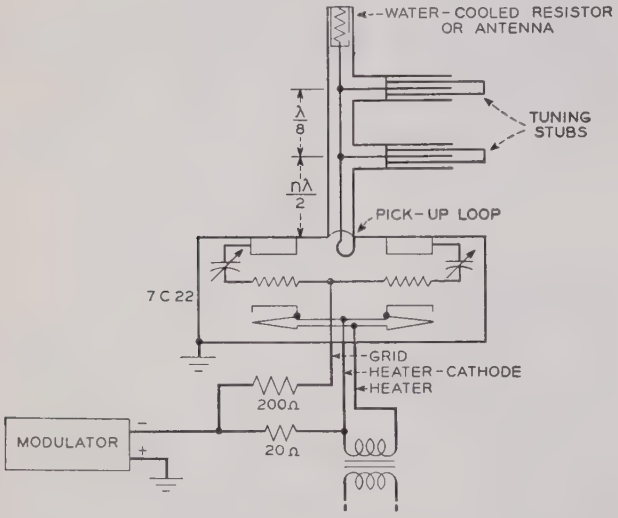

Fig. 7—Typical circuit for operation of the 7C22 oscillator.

The oscillator is normally adjusted at its low-frequency limit for balance, as indicated by a minimum amount of r.f. voltage on the input leads. The position of each tuning gear is marked at this point. Then, to increase frequency, each gear is rotated in a clockwise direction as viewed from its respective end of the tube. The tube may be inserted in a mounting rack designed to provide a ganged tuning control which rotates the gears simultaneously. Such a mounting is shown in Fig. 8.

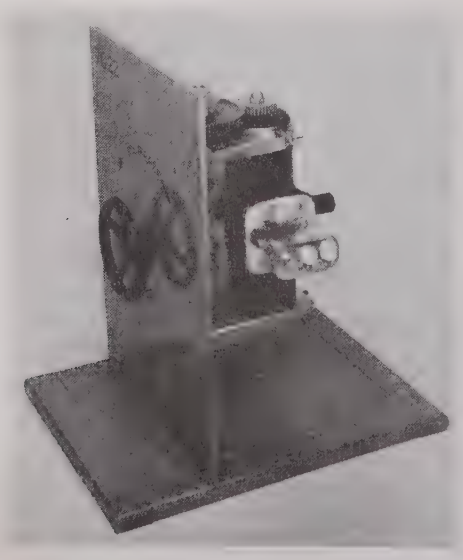

Fig. 8—A mounting rack for providing ganged tuning for the oscillator.

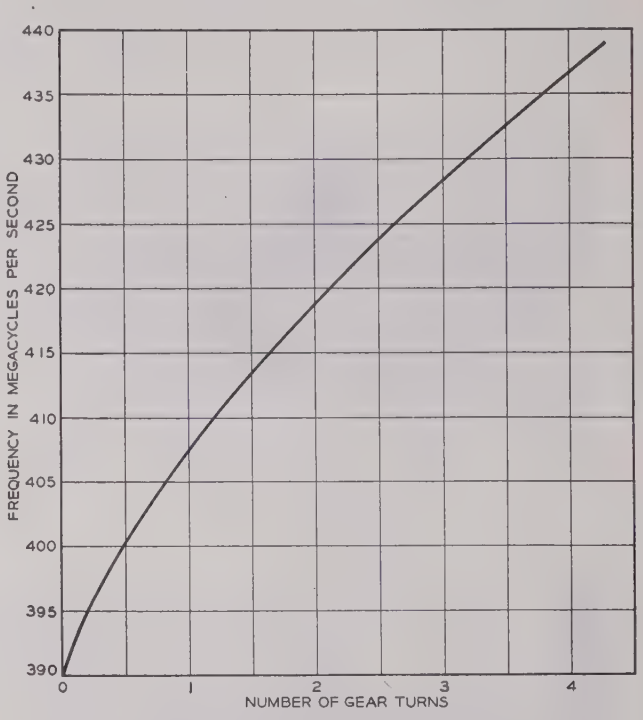

Fig. 9—Frequency range obtained by simultaneous rotation of tuning gears.

The efficiency of the 7C22 remains quite constant at about 55 per cent throughout its frequency range. If the load coupling is left unchanged, the output will be somewhat higher at the low-frequency end of the range because of the higher excitation prevailing there. The variation of frequency as a function of the turns of the tuning gears is shown in Fig. 9. An output-impedance diagram in the form devised by Rieke is shown in Fig. 10. This plot refers to the impedance of the load circuit as seen from the plane of the end of the output terminal of the 7C22. The impedances are given in terms of $Z_0 = 50$ ohms. It is seen from this diagram that, if a load of 50 ohms pure resistance is attached, approximately 90 per cent of the peak output will be obtained without need for tuning. Although this diagram applies for only one frequency in the range, the diagrams for other frequencies are very similar.

Since ruggedness was of prime importance, these tubes have been subjected to elaborate shock testing. Development models have withstood shocks of several hundred G's without breaking. A 50-G shock test was specified for the tube. The normal life of the 7C22 tube

as designed is in the vicinity of 500 hours. The end of life in practically all cases occurs when the active area

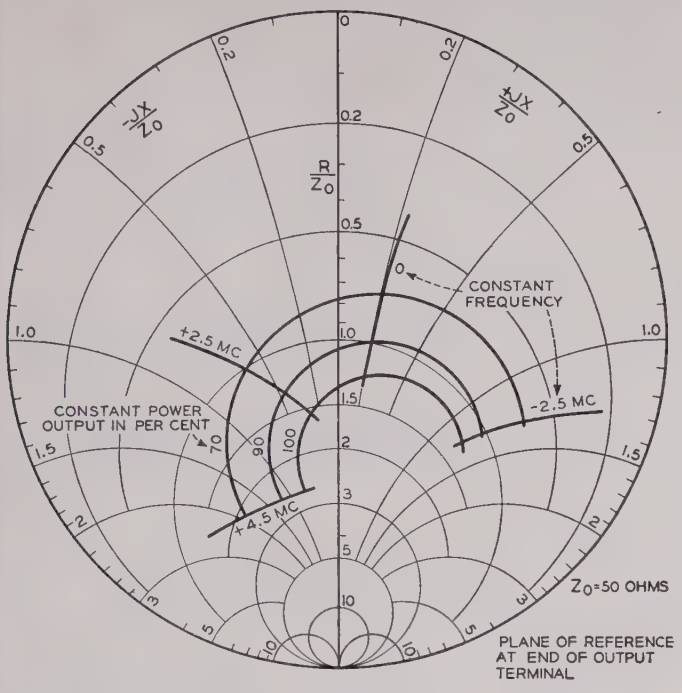

Fig. 10—Typical output-impedance diagram.

of the cathode has been so reduced by sparking that insufficient emission is available to provide the required output. In no case has grid emission been found to be a limiting factor in pulse service.

It was noted that the temperature of the cathodes increased during oscillation. This increase was about 20°C., the desired operating temperature being 800°C. to 820°C. Since this increase in temperature is produced by ohmic losses in the cathode and by electron back-bombardment of the cathode, which are r.f. losses, it is a factor in reducing the efficiency of the device.

It is expected that the life of these tubes can be greatly increased by applying knowledge gained in the development of nonsparking cathodes. At the end of the development a tube was made which used a cathode type found advantageous in magnetrons. The life of this tube was about 100 per cent longer than that of previous tubes tested. Extension of this oscillator design to higher and also to lower frequencies seems feasible. The use of relatively high pulse voltages postpones the limitations caused by transit time of electrons, but the sizes of the circuit and electrodes rapidly limit the power as the frequency is increased. At lower frequencies the main limitation would be the increasing length of the device and the resulting inconvenience of handling, plus the economic factor of having the circuit part of the expendable item.

Acknowledgment

As with any development produced by a large organization, many people made valuable contributions in this case. The authors wish, however, to acknowledge particularly the contribution of J. W. West in the mechanical design and assembly techniques which made this device successful.

Correspondence

Angular Frequency Shift*

In the paper by Ostlund, Vallarino, and Silver[1] there was described a frequency modulator using a reactance tube in the frequency-determining circuit of the master oscillator. The expression for the angular frequency change was given as

$$d\omega = -\frac{\omega_0}{2C}\Delta C.$$

This is based on the assumption that the actual change in angular frequency, $\Delta\omega$, is equal to $d\omega$; a condition that is only met when ΔC approaches zero. At values of ΔC other that zero there will be a discrepancy between the actual frequency shift and the computed value. The actual relation of angular relation of angular frequency shift $\Delta\omega$ and ΔC is

$$\Delta\omega = (\omega_0 + \Delta\omega) - \omega_0$$
$$= \frac{1}{\sqrt{L}\sqrt{C+\Delta C}} - \frac{1}{\sqrt{LC}}$$
$$= \frac{1}{\sqrt{L}}\left(\frac{1}{\sqrt{C+\Delta C}} - \frac{1}{\sqrt{C}}\right).$$

This shows that, contrary to the authors' statement, the frequency swing is not directly proportional to the change in injected capacitance. While the difference is negligible at small values of frequency swing, it may become large enough to constitute considerable distortion at higher modulation levels. Therefore it is necessary to select the other circuit parameters so that the nonlinearity is within the permissible limit of distortion, and not to work on the assumption that the circuit is sufficiently linear for all values of ΔC.

Sherman Rigby
WGHF (FM)
New York 16, N.Y.

* Received by the Institute, October 20, 1947.
[1] E. M. Ostlund, A. R. Vallarino, and Martin Silver, "Center-frequency stabilized modulation system," Proc. I.R.E., vol. 35, pp. 1144–1149; October-1947.

Discussion on

"Generalized Theory of Multitone Amplitude and Frequency Modulation"*

LAWRENCE J. GIACOLETTO

A. S. Gladwin:[1] The general formula (equation (32) in the paper) for the components of a frequency-modulated wave was first stated, without proof, by Carson and Fry,[2] and the first published proof appears to have been given by Cherry and Rivlin.[3] For calculating the amplitudes and phases of the side-frequency components, this formula is satisfactory when no linear relations exist between the modulating frequencies, but when such relations do exist, difficulties arise, as Mr. Giacoletto has pointed out, because a number (theoretically infinite) of the terms in the general formula have coincident frequencies. When the modulating signal contains more than a few components, the labor involved in calculating the spectrum by this method becomes very great. It would appear to be this consideration which has deterred the author from giving theoretical values for the spectra produced by square-wave and sawtooth-wave modulating signals.

When, however, the wave form of the modulating signal is sufficiently simple, e.g., rectangular or triangular, the spectrum may be obtained directly by Fourier analysis.

Let $f_m(t)$ denote the modulating signal which has a peak value of 1, and let $\Delta\omega$ be the peak frequency deviation of the modulated carrier in radians/second. Then a frequency-modulated wave can be written as

$$\cos\left\{\omega_c t + \Delta\omega \int f_m(t)dt\right\}$$

$$= R \exp j\left\{\omega_c t + \Delta\omega \int f_m(t)dt\right\}$$

$$= R \exp j\omega_c t \exp j\Delta\omega \int f_m(t)dt$$

where R denotes "the real part of."

Let $f_m(t)$ be periodic with a frequency ω_m radians/second. Then $\exp j\Delta\omega\int f_m(t)dt$ is also periodic with the same frequency, and may therefore be represented by the complex Fourier series

$$\sum_{n=-\infty}^{\infty} A_n \exp jn\omega_m t \tag{1}$$

in which the coefficients A_n are given by

$$A_n = \frac{1}{2\pi}\int_0^{2\pi} \exp\left(j\Delta\omega \int f_m(t)dt\right) \exp\left(-jn\omega_m t\right) d(\omega_m t)$$

$$= \frac{\omega_m}{2\pi}\int_0^{2\pi/\omega_m} \exp\left(j\Delta\omega \int f_m(t)dt - jn\omega_m t\right) dt. \tag{2}$$

The frequency-modulated wave is then

$$R \sum_{n=-\infty}^{\infty} A_n \exp j(\omega_c + n\omega_m)t. \tag{3}$$

The simplest example is that in which $f_m(t) = \cos \omega_m t$. Then

$$A_n = \frac{1}{2\pi}\int_0^{2\pi} \exp\left(j\frac{\Delta\omega}{\omega_m} \sin \omega_m t - jn\omega_m t\right) d(\omega_m t).$$

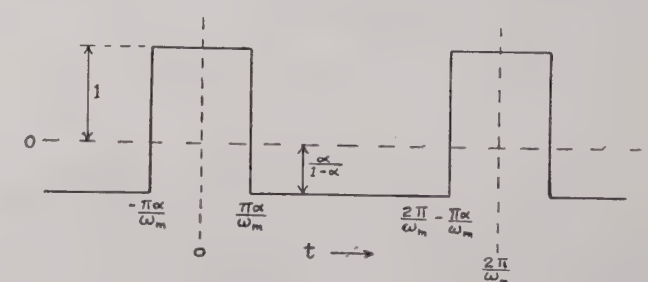

Fig. 1—Rectangular modulating wave.

This integral[4] defines the Bessel function of the first kind of order n and argument $\Delta\omega/\omega_m$

Hence $A_n = J_n(\Delta\omega/\omega_m)$, and the frequency-modulated wave is

$$\sum_{n=-\infty}^{\infty} J_n\left(\frac{\Delta\omega}{\omega_m}\right) \cos(\omega_c + n\omega_m)t.$$

The next simplest case is that for the rectangular modulating signal shown in Fig. 1.

* Proc. I.R.E., vol. 35, pp. 680–693; July, 1947.

[1] University of London, King's College, London, England.

[2] J. R. Carson and T. C. Fry, "Variable frequency electric circuit theory with application to the theory of frequency modulation," *Bell. Sys. Tech. Jour.*, vol. 16, p. 513; October, 1937.

[3] E. C. Cherry and R. S. Rivlin, "Non-linear distortion, with particular reference to the theory of frequency modulated waves," *Phil. Mag.*, ser. 7, vol. 32, p. 265; October, 1941.

[4] G. N. Watson, "Theory of Bessel Functions," p. 20. Cambridge, University Press, 1922.

From

$$t = 0 \text{ to } t = \pi\alpha/\omega_m,$$

$$f_m(t) = 1,$$

$$\text{and} \quad \int f_m(t)dt = t.$$

From

$$t = \pi\alpha/\omega_m \quad \text{to} \quad t = 2\pi/\omega_m - \pi\alpha/\omega_m,$$

$$f_m(t) = -\alpha/(1-\alpha)$$

and

$$\int f_m(t)dt = \frac{\alpha}{1-\alpha}\left(\frac{\pi}{\omega_m} - t\right).$$

From

$$t = 2\pi/\omega_m - \frac{\pi\alpha}{\omega_m} \quad \text{to} \quad t = 2\pi/\omega_m,$$

$$f_m(t) = 1,$$

and

$$\int f_m(t)dt = t - 2\pi/\omega_m.$$

Hence,

$$A_n = \frac{\omega_m}{2\pi}\int_0^{\pi\alpha/\omega_m} \exp j(\Delta\omega - n\omega_m)t\,dt$$

$$+\frac{\omega_m}{2\pi}\int_{\pi\alpha/\omega_m}^{2\pi/\omega_m - \pi\alpha/\omega_m} \exp j\left(\frac{\Delta\omega\alpha}{1-\alpha}\left(\frac{\pi}{\omega_m} - t\right) - n\omega_m t\right)dt$$

$$+\frac{\omega_m}{2\pi}\int_{2\pi/\omega_m - \pi\alpha/\omega_m}^{2\pi/\omega_m} \exp j\left(\Delta\omega\left(t - \frac{2\pi}{\omega_m}\right) - n\omega_m t\right)dt$$

The integrations are easily performed, and the sum of the results is

$$A_n = \frac{1}{\pi}\frac{\Delta\omega}{\omega_m}\cdot\frac{\sin\left\{\pi\alpha\left(\frac{\Delta\omega}{\omega_m} - n\right)\right\}}{\left(\frac{\Delta\omega}{\omega_m} - n\right)\left(\frac{\Delta\omega}{\omega_m}\alpha + n(1-\alpha)\right)}\cdot$$

The frequency-modulated wave is, therefore,

$$\frac{1}{\pi}\frac{\Delta\omega}{\omega_m}\sum_{n=-\infty}^{\infty}\frac{\sin\left\{\pi\alpha\left(\frac{\Delta\omega}{\omega_m} - n\right)\right\}}{\left(\frac{\Delta\omega}{\omega_m} - n\right)\left(\frac{\Delta\omega}{\omega_m}\alpha + n(1-\alpha)\right)}$$

$$\cdot\cos(\omega_c + n\omega_m)t. \quad (4)$$

This expression is indeterminate for values of $\Delta\omega$ equal to $n\omega_m$ (n positive) and $-n\omega_m(1-\alpha)/\alpha$ (n negative), but by finding the limits as $\Delta\omega$ approaches the critical values it is easy to show that when $\Delta\omega = n\omega_m$ the component of frequency $\omega_c + n\omega_m$ is $\alpha\cos(\omega_c + n\omega_m)t$ and when $\Delta\omega = -n\omega_m(1-\alpha)/\alpha$ the component of frequency $\omega_c + n\omega_m$ is $(-1)^n(1-\alpha)\cos(\omega_c + n\omega_m)t$.

Thus the components whose frequencies correspond to the maximum and minimum frequencies of the modulated carrier have amplitudes which depend only on the mark-space ratio of the modulating wave, and are independent of the frequency deviation and the modulating frequency.

For a square-wave modulating signal, $\alpha = \frac{1}{2}$ and (4) becomes

$$\frac{2}{\pi}\frac{\Delta\omega}{\omega_m}\sum_{n=-\infty}^{\infty}\frac{\sin\frac{\pi}{2}\left(\frac{\Delta\omega}{\omega_m} - n\right)}{\left(\frac{\Delta\omega}{\omega_m}\right)^2 - n^2}\cos(\omega_c + n\omega_m)t.$$

The spectrum produced by square-wave modulation was calculated by Van der Pol[5] many years ago with identical results.

A slightly more difficult example is that in which the modulating wave is triangular, as shown in Fig. 2.

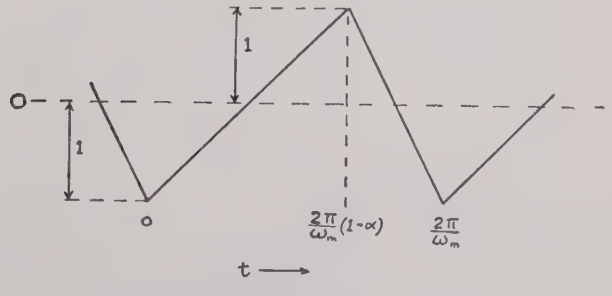

Fig. 2—Triangular modulating wave.

From

$$t = 0 \text{ to } t = \frac{2\pi}{\omega_m}(1-\alpha)$$

[5] Balth. van der Pol, "Frequency modulation," PROC. I.R.E., vol. 18, pp. 1194–1206; July, 1930.

$$f_m(t) = -1 + \frac{\omega_m t}{\pi(1-\alpha)}$$

and

$$\int f_m(t)dt = \frac{\pi}{3\omega_m}(1-2\alpha) - t + \frac{\omega_m t^2}{2\pi(1-\alpha)}.$$

From

$$t = \frac{2\pi}{\omega_m}(1-\alpha) \quad \text{to} \quad t = \frac{2\pi}{\omega_m}$$

$$f_m(t) = \frac{2-\alpha}{\alpha} - \frac{\omega_m t}{\pi\alpha}$$

and

$$\int f_m(t)dt = \frac{-\pi(6-7\alpha+2\alpha^2)}{3\omega_m\alpha} + \frac{2-\alpha}{\alpha}t - \frac{\omega_m t^2}{2\pi\alpha}.$$

The constants of integration have been chosen to make the integral continuous at $t=(2\pi/\omega_m)(1-\alpha)$, and also to make the mean value of the integral over the period equal to zero. Then, from (2),

$$A_n = \frac{\omega_m}{2\pi}\int_0^{2\pi(1-2)/\omega_m} \exp j\left\{\Delta\omega\left(\frac{\pi(1-2\alpha)}{3\omega_m} - t + \frac{\omega_m t^2}{2\pi(1-\alpha)}\right) - n\omega_m t\right\}dt$$
$$+ \frac{\omega_m}{2\pi}\int_{2\pi(1-2)/\omega_m}^{2\pi/\omega_m} \exp j\left\{\Delta\omega\left(\frac{-\pi(6-7\alpha+2\alpha^2)}{3\omega_m\alpha} + \frac{2-\alpha}{\alpha}t - \frac{\omega_m t^2}{2\pi\alpha}\right) - n\omega_m t\right\}dt.$$

If, in the first integral, the substitution

$$u = \left\{t - \pi(1-\alpha)\left(\frac{n}{\Delta\omega} + \frac{1}{\omega_m}\right)\right\}\left(\frac{\Delta\omega\omega_m}{\pi^2(1-\alpha)}\right)^{1/2}$$

is made, the integral can be written

$$\frac{1}{2}\left(\frac{\omega_m(1-\alpha)}{\Delta\omega}\right)^{1/2} \exp -j\pi\left\{n(1-\alpha) + \frac{1+\alpha}{6}\frac{\Delta\omega}{\omega_m} + \frac{n^2(1-\alpha)}{2}\frac{\omega_m}{\Delta\omega}\right\} \int_{-(\Delta\omega/\omega_m+n)(\omega_m(1-\alpha)/\Delta\omega)^{\frac{1}{2}}}^{(\Delta\omega/\omega_m-n)(\omega_m(1-\alpha)/\Delta\omega)^{\frac{1}{2}}} \exp(j\pi u^2/2)du. \quad (6)$$

The integral may be expressed in terms of Fresnel's integrals $C(x)$ and $S(x)$, which are defined as

$$C(x) = \int_0^x \cos\frac{\pi u^2}{2}du \qquad S(x) = \int_0^x \sin\frac{\pi u^2}{2}du.$$

In terms of these functions, (6) becomes

$$\frac{1}{2}\left(\frac{\omega_m(1-\alpha)}{\Delta\omega}\right)^{1/2}(\cos\theta_1 - j\sin\theta_1)(C(x_1)+C(x_2) + jS(x_1)+jS(x_2))$$

in which

$$\begin{cases} x_1 = \left(\dfrac{\Delta\omega}{\omega_m}+n\right)\left(\dfrac{\omega_m(1-\alpha)}{\Delta\omega}\right)^{1/2} \\ x_2 = \left(\dfrac{\Delta\omega}{\omega_m}-n\right)\left(\dfrac{\omega_m(1-\alpha)}{\Delta\omega}\right)^{1/2} \\ \theta_1 = \pi\left\{n(1-\alpha) + \dfrac{1+\alpha}{6}\dfrac{\Delta\omega}{\omega_m} + \dfrac{n^2(1-\alpha)}{2}\dfrac{\omega_m}{\Delta\omega}\right\}. \end{cases}$$

Similarly, the second integral in (5) can be expressed as

$$\frac{1}{2}\left(\frac{\omega_m\alpha}{\Delta\omega}\right)^{1/2}(\cos\theta_2 + j\sin\theta_2)(C(x_3)+C(x_4) - jS(x_3) - jS(x_4))$$

in which

$$\begin{cases} x_3 = \left(\dfrac{\Delta\omega}{\omega_m}+n\right)\left(\dfrac{\omega_m\alpha}{\Delta\omega}\right)^{1/2} \\ x_4 = \left(\dfrac{\Delta\omega}{\omega_m}-n\right)\left(\dfrac{\omega_m\alpha}{\Delta\omega}\right)^{1/2}. \\ \theta_2 = \pi\left\{n\alpha + \dfrac{2-\alpha}{6}\cdot\dfrac{\Delta\omega}{\omega_m} + \dfrac{n^2\alpha}{2}\dfrac{\omega_m}{\Delta\omega}\right\}. \end{cases}$$

Substituting the value of A_n found above into (2), the frequency-modulated wave is

$$\frac{1}{2}\sum_{n=-\infty}^{\infty}\left[\left(\frac{\omega_m(1-\alpha)}{\Delta\omega}\right)^{1/2}\{(C(x_1)+C(x_2))\cos\theta_1 + (S(x_1)+S(x_2))\sin\theta_1\} + \left(\frac{\omega_m\alpha}{\Delta\omega}\right)^{1/2}\{(C(x_3)+C(x_4))\cos\theta_2 + (S(x_3)+S(x_4))\sin\theta_2\}\right]\cos(\omega_c+n\omega_m)t$$
$$+\frac{1}{2}\sum_{n=-\infty}^{\infty}\left[\left(\frac{\omega_m(1-\alpha)}{\Delta\omega}\right)^{1/2}\{(C(x_1)+C(x_2))\sin\theta_1 - (S(x_1)+S(x_2))\cos\theta_1\} - \left(\frac{\omega_m\alpha}{\Delta\omega}\right)^{1/2}\{(C(x_3)+C(x_4))\sin\theta_2 - (S(x_3)+S(x_4))\cos\theta_2\}\right]\sin(\omega_c+n\omega_m)t. \quad (7)$$

The amplitudes and phases of the side-frequency components can be evaluated from this formula using

tables of the Fresnel integrals. For two special cases, namely, $\alpha=0$ and $\alpha=\frac{1}{2}$, the formula may be considerably simplified.

When $\alpha=0$, Fig. 2 becomes the sawtooth wave form investigated experimentally by Mr. Giacoletto. Equation (7) then reduces to

$$\frac{1}{2}\left(\frac{\omega_m}{\Delta\omega}\right)^{1/2}\sum_{n=-\infty}^{\infty}\{(C(x_1)+C(x_2))^2 + (S(x_1)+S(x_2))^2\}^{1/2}\cos\{(\omega_c+n\omega_m)t-\theta_1+\phi\}$$

where

$$\phi=\tan^{-1}\left\{\frac{S(x_2)+S(x_2)}{C(x_1)+C(x_2)}\right\}.$$

In the second case $\alpha=\frac{1}{2}$, and the modulating signal has then a symmetrical triangular wave form. Equation (7) reduces to

$$\left(\frac{\omega_m}{2\Delta\omega}\right)^{1/2}\sum_{n=-\infty}^{\infty}\{(C(x_1)+C(x_1))\cos\theta_1 + (S(x_1)+S(x_2))\sin\theta_1\}\cos(\omega_c+n\omega_m)t.$$

Although only rectangular-wave and triangular-wave modulating signals have been treated, it will be obvious that the spectrum produced by any modulating signal whose wave form is made up of straight lines only can be calculated by similar methods.

When the modulating signal is periodic but the wave form too complicated to allow of a simple analytical solution, the values of the coefficients A_n may be calculated from (2) by graphical or numerical integration, though for high-order side frequencies the labor is considerable.

If the modulating signal has K components and if $2K$ of the consecutive values of A_n have been found, it is possible to calculate the next value, and hence all the other values, by means of a recurrence formula. This formula is obtained as follows:

Let

$$f_m(t)=\sum_{k=1}^{K}\{a_k\cos k\omega_m t+b_k\sin k\omega_m t\}. \qquad (8)$$

From (2),

$$A_n=\frac{\omega_m}{2\pi}\int_0^{2\pi/\omega_m}\exp\left(j\Delta\omega\int f_m(t)dt\right)\exp(-jn\omega_m t)dt.$$

Integrating by parts,

$$A_n=\frac{\omega_m}{2\pi}\left.\frac{\exp j\left\{\Delta\omega\int f_m(t)dt-n\omega_m t\right\}}{-jn\omega_m}\right|_0^{2\pi/\omega_m} + \frac{\Delta\omega}{2n\pi}\int_0^{2\pi/\omega_m} f_m(t)\exp\left\{j\Delta\omega\int f_m(t)dt\right\}\exp(-jn\omega_m t)dt.$$

The first term is zero, and the second can be written by substituting for $f_m(t)$ and $\exp(j\Delta\omega\int f_m(t)dt$ according to (8) and (1):

$$A_n=\frac{\Delta\omega}{2n\pi}\int_0^{2\pi/\omega_m}\sum_{k=1}^{K}\{a_k\cos k\omega_m t+b_k\sin k\omega_m t\}\cdot\sum_{r=-\infty}^{\infty}A_r\exp jr\omega_m t\exp(-jn\omega_m t)dt.$$

(The subscripts in (1) have here been changed from n to r in order to avoid confusion with the particular value of n being considered.)

$$A_n=\frac{\Delta\omega}{4n\pi}\int_0^{2\pi/\omega_m}\sum_{k=1}^{K}\sum_{r=-\infty}^{\infty}\{A_r(a_k+jb_k)\exp j(r-n-k)\omega_m t + A_r(a_k-jb_k)\exp j(r-n+k)\omega_m t\}dt.$$

Only the terms for which $r-n-k=0$ or $r-n+k=0$ have a finite value, all others being equal to zero. Hence,

$$2n\frac{\omega_m}{\Delta\omega}A_n=\sum_{k=1}^{K}\{(a_k+jb_k)A_{n+k}+(a_k-jb_k)A_{n-k}\}.$$

This formula may be used to find the coefficient A_{n+k} in terms of the $2K$ preceding coefficients. Like all other devices for extrapolation, the range of this recurrence formula is limited by the accuracy of the primary data.

L. J. Giacoletto:[6] The material presented by Mr. Gladwin should be of value to anyone undertaking the calculation of frequency-modulation spectra. His method of obtaining sideband amplitude and phase can save a considerable amount of labor in those cases amenable to analytical solution. It should be pointed out, however, that in even relatively simple cases the analytic evaluation of the amplitudes of the Fourier series may be difficult. Thus, for a modulating signal composed of a fundamental and a single harmonic, the evaluation of the integral for the amplitudes of the Fourier series (equation (2) above) using known Bessel expansions merely leads to the same solution indicated by my expansion (equation (30) of the original paper). The summing of the resulting two-way series in this case and the extension of the solution for a modulating signal containing K harmonics would be a valuable contribution to frequency-modulation theory. Of course, the method of graphical or numerical integration indicated by Mr. Gladwin can be applied in any event.

[6] Radio Corporation of America, RCA Laboratories, Princeton N. J.

Contributors to the Proceedings of the I.R.E.

BEVERLY C. DUNN, JR.

❖

For a biography and photograph of C. C. CUTLER, see page 1328 of the November, 1947, issue of the PROCEEDINGS OF THE I.R.E.

❖

Beverly C. Dunn, Jr., (S'41–A'44) was born on November 16, 1917, in New York, N. Y. In 1940 he received the A.B. degree in mathematics, and in 1942, the M.A. degree in physics, from Harvard University. From 1942 through 1944 he was employed as a Teaching Fellow in the Officers Electronics Training Courses (Pre-Radar), Cruft Laboratory, Harvard University. His duties in this connection included laboratory instruction and lecturing on antennas and ultra-high-frequency circuits. During 1945 he worked as a research assistant in the antenna group at Central Communications Research Laboratory, which operated under contract between NDRC and Harvard University.

Since November, 1945, Mr. Dunn has divided his time between research in the field of electromagnetic radiation at Cruft Laboratory, the work being supported by the Navy and the Signal Corps, and graduate studies toward the Ph.D. degree in physics at Harvard. He is a member of Phi Beta Kappa, Sigma Xi, and the American Physical Society.

❖

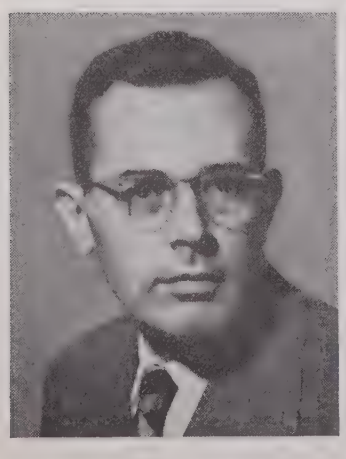

A. L. DURKEE

❖

Clifford E. Fay (A'26–SM'45) was born on December 2, 1903, at St. Louis, Mo. He received the B.S. degree in electrical engineering from Washington University in 1925, and the M.S. degree in electrical engineering and physics in 1927. Since 1927, he has been a member of the technical staff of the Bell Telephone Laboratories, Inc., where he has been engaged in the development of high-vacuum power tubes.

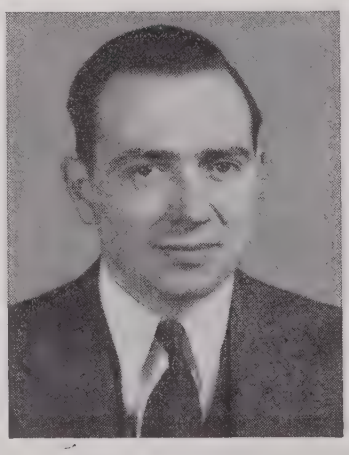

CLIFFORD E. FAY

❖

A. L. Durkee was born in Cambridge, Mass., on August 24, 1905. He was graduated from Harvard University in 1930 with the B.S. degree in engineering, and joined the department of development and research of the American Telephone and Telegraph Co. in July of that year. In 1934 he transferred to the Bell Telephone Laboratories, where his work has been largely on problems associated with the development of transoceanic and other radiotelephone systems. At present he is engaged in studies relating to microwave radio relaying.

RONOLD KING

Ronold King (A'30–SM'43) was born on September 19, 1905, at Williamstown, Mass. He received the B.A. degree in 1927 and the M.S. degree in 1929 from the University of Rochester, and the Ph.D. degree from the University of Wisconsin in 1932. He was an American-German exchange student at Munich from 1928 to 1929; a White Fellow in physics at Cornell University from 1929 to 1930; and a Fellow in electrical engineering at the University of Wisconsin from 1930 to 1932. He continued at Wisconsin as a research assistant from 1932 to 1934. From 1934 to 1936 he was an instructor in physics at Lafayette College, serving as an assistant professor in 1937.

During 1937 and 1938 Dr. King was a Guggenheim Fellow at Berlin. In 1938 he became instructor in physics and communication engineering at Harvard University, advancing to assistant professor in 1939, and

❖

JOHN F. MORRISON

RUBY PAYNE-SCOTT

❖

to associate professor in 1942. He was appointed Gordon MacKay professor of applied physics at Harvard University in 1946. Dr. King is a Fellow in the American Physical Society; American Association for the Advancement of Science; and American Academy of Arts and Sciences.

❖

J. F. Morrison (A'29–M'36–SM'43) was born at Buffalo, N. Y., on March 14, 1906. From 1923 to 1926 he was associated with the Federal Telephone and Telegraph Company, and during 1927, with the American Telephone and Telegraph Company. Mr. Morrison was vice-president and technical director of the Buffalo Broadcasting Corporation from 1927 to 1929. Since 1929 he has been a member of the technical staff of the Bell Telephone Laboratories, assigned to the radio development and research department.

❖

Paul I. Richards (A'45) was born at Orono, Maine, on February 8, 1923. Terminating his undergraduate work at Harvard University after his junior year, he entered the Radio Research Laboratory, Harvard University, where he held the position of research associate from June, 1943, to September, 1945. His work there concerned mainly the theory and design of distributed-constant filters and wide-band microwave receivers. In the fall of 1945, he entered the graduate school of Harvard University, obtaining the M.A. and Ph.D. degrees in physics in 1946 and 1947, respectively.

Dr. Richards is a member of Sigma Xi, Phi Beta Kappa, and the American Physical Society.

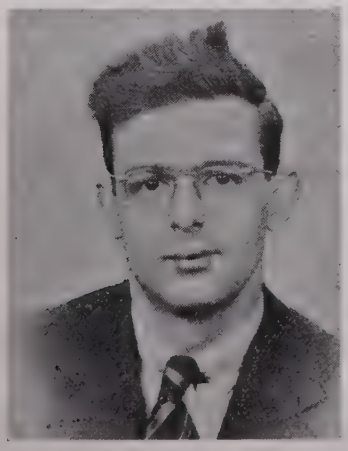

PAUL I. RICHARDS

❖

Ruby Payne-Scott was born in Grafton, N.S.W., Australia, on May 28, 1912. Obtaining the M.S. degree from Snyder University in 1936, she was associated with Amalgamated Wireless of Australasia from 1939 to 1941 as a radio engineer. Since 1941, she has been a member of the staff at the Radiophysics Laboratory of the Australian Council for Scientific and Industrial Research. At present she is engaged in carrying out research on radiation from the sun at meter wavelengths.

❖

GILBERT WILKES

Gilbert Wilkes was born in Denver, Colo., in 1900. He was educated abroad and received a mechanical engineering degree in Paris, France, after World War I, followed by a graduate degree. He returned to Paris after World War II to receive the degree of doctor of engineering from the Sorbonne.

In 1926 he joined the staff of W. S. Barstow and Company, and while there sponsored the design of several steam-power plants in the United States. In 1932 he took out professional licenses in Pennsylvania and New Jersey, and opened offices as a consulting engineer, specializing in steel-mill design. He joined the staff of the Applied Physics Laboratory of the Johns Hopkins University early in 1944, where he has been concerned more particularly with radiation.

Dr. Wilkes has been the originator of several thermodynamic, metallurgical, and radiation devices, and has published several papers on these subjects.

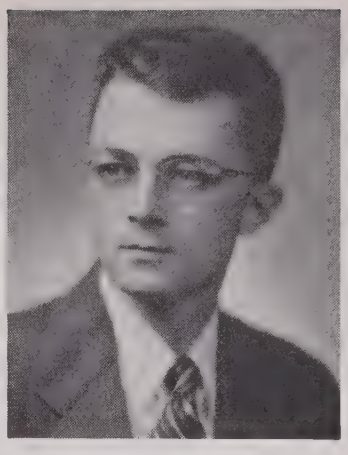

J. EDMOND WOLFE

J. Edmond Wolfe (S'40–A'41–SM'47) was born on February 21, 1917, at St. John, Kans. He received the B.S. degree in electrical engineering from Kansas State College in 1939, and the M.S. degree in 1940. From 1940 to 1941 he was an assistant in electrical engineering at the Massachusetts Institute of Technology. From 1941 to 1946, he was a member of the technical staff of the Bell Telephone Laboratories, Inc., engaged in the development of high-vacuum power tubes. In 1946, Mr. Wolfe joined the staff of the department of electrical engineering at Kansas State College, where he is now associate professor.

❖

E. L. Younker (S'42–A'45) was born in 1918 at Sidney, Ohio. He received the A.B. degree from Miami University, Ohio, in 1940, and the A.M. degree in physics from the University of Illinois in 1942. From 1942 to 1945 he was a staff member of the M.I.T. Radiation Laboratory. Since 1945 he has been employed as a member of the technical staff of the Bell Telephone Laboratories, at Whippany, N. J. Mr. Younker is a member of the American Physical Society.

E. L. YOUNKER

Institute News and Radio Notes

1948 I.R.E. National Convention News

BY PLANE and by train, by car and by boat, by subway and bus and pedal locomotion, thousands of radio engineers from every corner of North America and from a variety of global points of origin are now initiating plans to attend the 1948 National Convention of The Institute of Radio Engineers, to be held at the Hotel Commodore and Grand Central Palace in New York City, on March 22, 23, 24, and 25.

And wise are they who have begun such early planning. The hotel situation in New York remains acute, and reservations well in advance are advisable for those who seek desirable accommodations. Moreover, advance indications are that the same will apply to those who plan to attend technical sessions, the Radio Engineering Show, the annual banquet, president's luncheon, cocktail party—all of the recognized functions of an I.R.E. Convention, which this year promise to be more heavily attended than ever in the past.

As this is written, the technical papers program for the 1948 Convention has just been completed by Dr. Charles R. Burrows and his hard-working committee. Titles of papers scheduled and dates of presentation will be in the hands of members via a general mailing before these lines are read, and the complete program with summaries of all the papers will appear in the March issue of the PROCEEDINGS.

Ranging from a consideration of technical aspects of public telephone service on railroad trains, through practically every communications, navigation, industrial, and research topic, to health physics problems in atomic energy—the technical program covers the entire gamut of subjects of interest to workers in the radio and electronics and allied fields. Risking repetition, it is decidedly a program which no one in any way associated with those fields can afford to miss.

Further illustrative of the broad range of interests which will be catered to in this Convention is the following list of session titles:

Amplifiers
Antennas (two sessions; one dealing specifically with circular polarization)
Broadcasting and Recording
Circuits (two sessions; one dealing with active and the other with passive elements)
Components and Supersonics
Computers (two sessions; one covering systems and the other components)
Electronics (four sessions: Tube Design and Engineering, Industrial Applications and Electronic Circuits, Tube Manufacture, and New Forms of Tubes)
Frequency Modulation
Measurements (two sessions; one dealing specifically with v.h.f., u.h.f., and s.h.f. measurements)
Microwaves
Navigation Aids
Nuclear Studies
Propagation
Receivers
Superregeneration
Systems (two sessions)
Television
Transmission (lines and waveguides)

Special Technical Sessions Planned

Two high points of the technical program will be two special sessions; one devoted to "Advances Significant to Electronics," to be held on Wednesday Morning, March 24, and the other on "Nucleonics," scheduled for Tuesday evening, March 23. Both of these meetings will be symposia, with invited papers from outstanding authorities, and both will be held in the Grand Ballroom of the Commodore, with no conflicting parallel sessions.

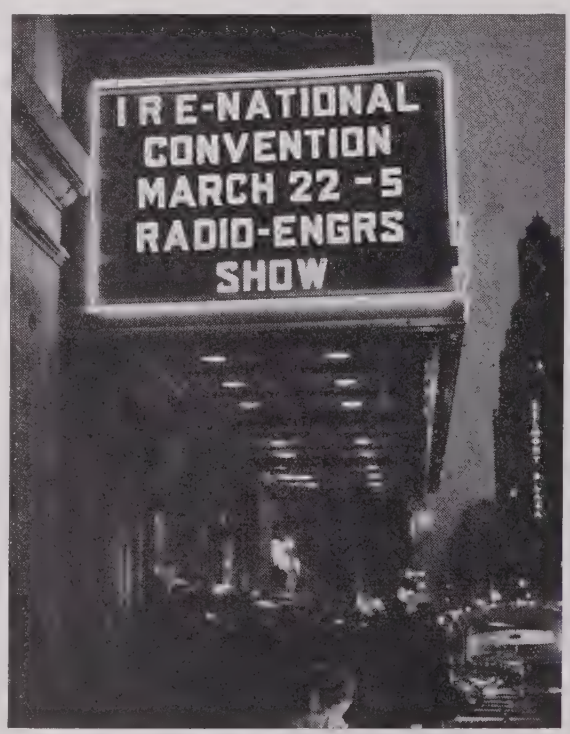

The "Nucleonics" symposium, sponsored by a Nuclear Science Symposium working group of the I.R.E. Nuclear Studies Committee, will be under the chairmanship of Dr. L. E. Hafstad, Executive Secretary, Research and Development Board.

The Wednesday morning meeting is expected by the Technical Program Committee to be "broadly stimulating to the electronic profession as a whole by conveying not only the important technical aspects, but also the broad implications of new scientific and technical advances." The Committee's announcement of the session continues: "The history of progress of special branches of science, and the engineering and industry erected upon them, show that they become increasingly complex as they are subjected to the searching light of concentrated inquiry. This complexity may ultimately become a barrier to their further development unless simplifying influences are introduced.

"These simplifications usually arise from the application of broad philosophical generalizations which make the science more readily intelligible. They remove the barriers to progress by lumping detailed and complex concepts or procedures into relatively simple but more generalized ideas and methods capable of widespread understanding and application. They may appear as generalized theories, methods, or procedures.

"These are the really significant steps in the progress of a science. Their early recognition and widespread promulgation keeps the science healthy, and ensures the rapid growth of the dependent engineering and industrial arts."

Both the technical program and the plans so far disclosed by exhibitors in the Radio Engineering Show amply fulfill the prophecy carried in these pages in the January issue that this will be the greatest and most worthwhile I.R.E. Convention ever held.

Plans for a most interesting program of Women's Activities are progressing, highlighted by a trip to the United Nations by chartered bus on Tuesday, March 23, and tickets to matinee performances of either "Antony and Cleopatra," or "High Button Shoes," now playing in New York. An all-day bus trip to West Point has been arranged for Thursday, March 25, with luncheon at the Thayer Hotel.

A Tea will be held at the I.R.E. Headquarters Building, 1 East 79 Street, on Tuesday afternoon, March 23.

Largest Radio Show on Record

As of January 15, 163 leading radio-and-electronic manufacturers have taken 244 exhibit units, totalling 27,109 net square feet of display in the Radio Engineering Show to be held in conjunction with the 1948 Convention. The first and second floors and half of the third floor of Grand Central Palace have been entirely reserved for these exhibits. Two large session halls will occupy the third floor to share with ballrooms at the Hotel Commodore in accommodating 28 sessions for the presentation of approximately 140 technical papers during the convention.

The space taken by exhibitors already exceeds that of the 1947 Radio Engineering Show by 25 per cent. The exhibits will be technical, showing the latest developments in transmitter equipment, components and assemblies, materials and instruments which are the engineering tools and materials of electronics and radio communication.

Sections

Chairman		Secretary
P. H. Herndon c/o Dept. in charge of Federal Communication 411 Federal Annex Atlanta, Ga.	ATLANTA February 20	M. S. Alexander 2289 Memorial Dr., S.E. Atlanta, Ga.
F. W. Fischer 714 Beechfield Ave. Baltimore 29, Md.	BALTIMORE	E. W. Chapin 2805 Shirley Ave. Baltimore 14, Md.
John Petkovsek 565 Walnut Beaumont, Texas	Beaumont—Port Arthur	C. E. Laughlin 1292 Liberty Beaumont, Texas
W. H. Radford Massachusetts Institute of Technology Cambridge, Mass.	BOSTON	A. G. Bousquet General Radio Co. 275 Massachusetts Ave. Cambridge 39, Mass.
A. T. Consentino San Martin 379 Buenos Aires, Argentina	BUENOS AIRES	N. C. Cutler San Martin 379 Buenos Aires, Argentina
R. G. Rowe 8237 Witkop Avenue Niagara Falls, N. Y.	BUFFALO-NIAGARA February 18	R. F. Blinzler 558 Crescent Ave. Buffalo 14, N. Y.
G. P. Hixenbaugh Radio Station WMT Cedar Rapida, Iowa	CEDAR RAPIDS	W. W. Farley 1920 Fourth Ave. S.E. Cedar Rapids, Iowa
Karl Kramer Jensen Radio Mfg. Co. 6601 S. Laramie St. Chicago 38, Ill.	CHICAGO February 20	D. G. Haines Hytron Radio and Electronics Corp. 4000 W. North Ave. Chicago 39, Ill.
J. F. Jordan Baldwin Piano Co. 1801 Gilbert Ave. Cincinnati, Ohio	CINCINNATI February 17	F. Wissel Crosley Corporation 1329 Arlington St. Cincinnati, Ohio
W. G. Hutton R.R. 3 Brecksville, Ohio	CLEVELAND February 19	H. D. Seielstad 1678 Chesterland Ave. Lakewood 7, Ohio
C. J. Emmons 158 E. Como Ave. Columbus 2, Ohio	COLUMBUS February 13	L. B. Lamp 846 Berkeley Rd. Columbus 5, Ohio
L. A. Reilly 989 Roosevelt Ave. Springfield, Mass.	CONNECTICUT VALLEY February 19	H. L. Krauss Dunham Laboratory Yale University New Haven, Conn.
Robert Broding 2921 Kingston Dallas, Texas	DALLAS-FT. WORTH	A. S. LeVelle 308 S. Akard St. Dallas 2, Texas
E. L. Adams Miami Valley Broadcasting Corp. Dayton 1, Ohio	DAYTON February 19	George Rappaport 132 E. Court Harshman Homes Dayton 3, Ohio
A. Friedenthal 5396 Oregon Detroit 4, Mich.	DETROIT February 20	N. C. Fisk 3005 W. Chicago Ave. Detroit 6, Mich.
N. J. Reitz Sylvania Electric Products, Inc. Emporium, Pa.	EMPORIUM	A. W. Peterson Sylvania Electric Products, Inc. Emporium, Pa.
F. M. Austin 3103 Amherst St. Houston, Texas	HOUSTON	C. V. Clarke, Jr. Box 907 Pasadena, Texas
R. E. McCormick 3466 Carrollton Ave. Indianapolis, Ind.	INDIANAPOLIS	M. G. Beier 3930 Guilford Ave. Indianapolis 5, Ind.
C. L. Omer Midwest Eng. Devel. Co. Inc. 3543 Broadway Kansas City 2, Mo.	KANSAS CITY	Mrs. G. L. Curtis 6003 El Monte Mission, Kansas
R. C. Dearle Dept. of Physics University of Western Ontario London, Ont., Canada	LONDON, ONTARIO	E. H. Tull 14 Erie Ave. London, Ont., Canada
Walter Kenworth 1427 Lafayette St. San Gabriel, Calif.	LOS ANGELES February 17	R. A. Monfort L. A. Times 202 W. First St. Los Angeles 12, Calif.
O. W. Towner Radio Station WHAS Third & Liberty Louisville, Ky.	LOUISVILLE	D. C. Summerford Radio Station WHAS Third & Liberty Louisville, Ky.
E. T. Sherwood Globe-Union Inc. Milwaukee 1, Wis.	MILWAUKEE	J. J. Kircher 2450 S. 35th St. Milwaukee 7, Wis.
R. R. Desaulniers Canadian Marconi Co. 211 St. Sacrement St. Montreal, P.Q., Canada	MONTREAL, QUEBEC February 25	R. P. Matthews Federal Electric Mfg. Co. 9600 St. Lawrence Blvd. Montreal 14, P.Q., Canada
J. E. Shepherd 111 Courtenay Rd. Hempstead, L. I., N. Y.	NEW YORK March 3	I. G. Easton General Radio Co. 90 West Street New York 6, N. Y.
L. R. Quarles University of Virginia Charlottesville, Va.	NORTH CAROLINA-VIRGINIA	J. T. Orth 4101 Fort Ave. Lynchburg, Va.
K. A. Mackinnon Box 542 Ottawa, Ont. Canada	OTTAWA, ONTARIO February 19	D. A. G. Waldock National Defense Headquarters New Army Building Ottawa, Ont., Canada
P. M. Craig 342 Hewitt Rd. Wyncote, Pa.	PHILADELPHIA March 4	J. T. Brothers Philco Radio and Television Tioga and C Sts. Philadelphia 34, Pa.
E. M. Williams Electrical Engineering Dept. Carnegie Institute of Tech. Pittsburgh 13, Pa.	PITTSBURGH March 8	E. W. Marlowe 560 S. Trenton Ave. Wilkinburgh PO Pittsburgh 21, Pa.
O. A. Steele 1506 S.W. Montgomery St. Portland 1, Ore.	PORTLAND	F. E. Miller 3122 S.E. 73 Ave. Portland 6, Ore.
N. W. Mather Dept. of Elec. Engineering Princeton University Princeton, N. J.	PRINCETON	A. E. Harrison Dept. of Elec. Engineering Princeton University Princeton, N. J.
A. E. Newlon Stromberg-Carlson Co. Rochester 3, N. Y.	ROCHESTER February 19	J. A. Rodgers Huntington Hills Rochester, N. Y.
E. S. Naschke 1073-57 St. Sacramento 16, Calif.	SACRAMENTO	
R. L. Coe Radio Station KSD Post Dispatch Bldg. St. Louis 1, Mo.	ST. LOUIS	N. J. Zehr Radio Station KWK Hotel Chase St. Louis 8, Mo.
Rawson Bennett U. S. Navy Electronics Laboratory San Diego 52, Calif.	SAN DIEGO March 2	C. N. Tirrell U. S. Navy Electronics Laboratory San Diego 52, Calif.
L. E. Reukema Elec. Eng. Department University of California Berkeley, Calif.	SAN FRANCISCO	W. R. Hewlett 395 Page Mill Rd. Palo Alto, Calif.
J. F. Johnson 2626 Second Ave. Seattle 1, Wash.	SEATTLE February 12	J. M. Patterson 7200—28 N. W. Seattle 7, Wash.
C. A. Priest 314 Hurlburt Rd. Syracuse, N. Y.	SYRACUSE	R. E. Moe General Electric Co. Syracuse, N. Y.
C. A. Norris J. R. Longstaffe Ltd. 11 King St., W. Toronto, Ont., Canada	TORONTO, ONTARIO	C. G. Lloyd 212 King St., W. Toronto, Ont., Canada
O. H. Schuck 4711 Dupont Ave. S. Minneapolis 9, Minn.	TWIN CITIES	B. E. Montgomery Engineering Department Northwest Airlines Saint Paul, Minn.
G. P. Adair 1833 "M" St. N.W. Washington, D. C.	WASHINGTON March 8	H. W. Wells Dept. of Terrestrial Magnetism Carnegie Inst. of Washington Washington, D. C.
J. C. Starks Box 307 Sunbury, Pa.	WILLIAMSPORT March 3	R. G. Petts Sylvania Electric Products, Inc. 1004 Cherry St. Montoursville, Pa.

SUBSECTIONS

Chairman		Secretary
P. C. Smith 179 Ida Avenue Akron, Ohio	Akron (Cleveland Subsection)	J. S. Hill 51 W. State St. Akron, Ohio
J. D. Schantz Farnsworth Television and Radio Company 3700 E. Pontiac St. Fort Wayne, Ind.	Fort Wayne (Chicago Subsection)	S. J. Harris Farnsworth Television and Radio Co. 3702 E. Pontiac Fort Wayne 1, Ind.
F. A. O. Banks 81 Troy St. Kitchener, Ont., Canada	Hamilton (Toronto Subsection)	E. Ruse 195 Ferguson Ave., S. Hamilton, Ont., Canada
A. M. Glover RCA Victor Div. Lancaster, Pa.	Lancaster (Philadelphia Subsection)	C. E. Burnett RCA Victor Div. Lancaster, Pa.
E. J. Ishister 115 Lee Rd. Garden City, L. I., N. Y.	Long Island (New York Subsection)	F. Q. Gemmill Sperry Gyroscope Great Neck, L. I., N. Y.
A. D. Emurian HDQRS. Signal Corps Engineering Lab. Bradley Beach, N. J.	Monmouth (New York Subsection)	Ralph Cole Watson Laboratories Red Bank, N. J.

Chairman		Secretary
J. B. Minter Box 1 Boonton, N. J.	Northern N. J. (New York Subsection)	A. W. Parker, Jr. 47 Cobb Rd. Mountain Lakes, N. J.
A. R. Kahn Electro-Voice, Inc. Buchanan, Mich.	South Bend (Chicago Subsection) February 19	A. M. Wiggins Electro-Voice, Inc. Buchanan, Mich.
W. M. Stringfellow Radio Station WSPD 136 Huron Street Toledo 4, Ohio	Toledo (Detroit Subsection)	M. W. Keck 2231 Oak Grove Place Toledo 12, Ohio
R. M. Wainwright Elec. Eng. Department University of Illinois Urbana, Illinois	Urbana (Chicago Subsection)	M. H. Crothers Elec. Eng. Department University of Illinois Urbana, Illinois
W. A. Cole 323 Broadway Ave. Winnipeg, Manit., Canada	Winnipeg (Toronto Subsection)	C. E. Trembley Canadian Marconi Co. Main Street Winnipeg, Manit., Canada

I.R.E. People

W. A. Marrison

Warren A. Marrison

The British Horological Institute's gold medal for 1947 has been awarded to Warren A. Marrison (A'28–SM'43), a member of the technical staff of the Bell Telephone Laboratories Inc., in recognition of pioneer researches in the development of the quartz crystal clock. The medal is the Institute's highest award. It was presented to Mr. Marrison by Sir Harold Spencer Jones, Astronomer Royal and president of the Institute, at its 89th annual general meeting in London on October 29, 1947.

Mr. Marrison was born in Kingston, Ontario, Canada, on May 21, 1896, and received the B.S. degree from Queens University, Kingston, in 1920, and the M.S. degree from Harvard the following year. During World War I he was a flying mechanic in the Royal Flying Corps. He has been associated with the Bell Laboratories since that time, working largely on problems of frequency standardization and time.

Albert R. Hodges

Albert R. Hodges (A'33–M'39–SM'43) joined Stromberg-Carlson's patent department toward the latter part of 1947. He will handle patent prosecution and related matters in the radio and electronic field.

Mr. Hodges was born in Ridgewood, N. J., and was educated at Hamilton College and Cornell University. Formerly he was a patent attorney with the Sperry Gyroscope Company, Inc., of Great Neck, N. Y., and with the Airborne Instruments Laboratory (Columbia University Division of War Research) at Mineola, N. Y. He has served in electrical engineering capacities for General Electric, Farnsworth Television and Radio, and for Ralph H. Langley, consulting engineer.

He is a member of the Admissions Committee and the Technical Committee on Radio Receivers of the I.R.E. His booklet on radio receivers, "Better Buymanship," published in 1939, was revised in 1947.

Albert R. Hodges

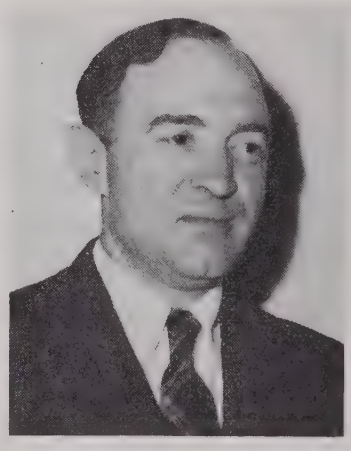

Charles E. Dean

Charles E. Dean

Charles E. Dean (A'29–M'36–SM'43), director of publications of the Hazeltine Electronics Corporation, Little Neck, L. I., was awarded a Certificate of Commendation by the United States Navy for his work and responsibility in the writing and production of the many thorough technical instruction books required for radio equipment designed by the firm.

The certificate awarded Mr. Dean was accompanied by a citation reading in part, "This award is made for your outstanding supervision and unremitting effort . . . . A standard of excellence of such a high degree was achieved that these books were considered exemplary as to content, format, arrangement and usefulness by both maintenance personnel and instructors in Naval radar schools. These books covered the entire field of radar identification equipment and its interconnection with search radar and beacon equipments."

JOHN M. CAGE

MAJOR GENERAL GEORGE L. VAN DEUSEN

On October 16, 1947, following a meeting of the Board of Directors of RCA Institutes, Inc., announcement was made of the election of Major General George L. Van Deusen (SM'46) as president and director of the Institutes.

General Van Deusen received the M.S. degree from Yale University and the B.S. degree from the United States Military Academy at West Point in 1909. During World War I he commanded the 105th Field Signal Battalion, 30th Division, in France and Belgium. From January, 1941, to January, 1945, he served successively as Commanding General, Signal Corps Replacement Center, Commandant, Eastern Signal Corps Schools, and Commanding General, Eastern Signal Corps Training Center at Fort Monmouth, N. J., and was awarded the Distinguished Service Medal. In January, 1945, he became Chief of the Engineering and Technical Service, Office of the Chief Signal Officer, Washington, D. C. General Van Deusen retired from the army with the permanent rank of Colonel on August 31, 1946.

RCA Institutes is a technical school devoted exclusively to instruction in radio and electrical communications and the associated electronic arts. It is stated to be the oldest school of its kind in America.

GEORGE L. VAN DEUSEN

JOHN M. CAGE

John M. Cage (M'41–SM'43) has recently joined the teaching staff of the School of Electrical Engineering, Purdue University, as professor of electrical engineering in charge of electronics. Formerly, he was manager of industrial electronics at the Raytheon Manufacturing Company, where he was in charge of engineering, sales and production of industrial equipment.

Professor Cage is a native of Texas. He received his bachelor's degree at Iowa State College in 1931, and was, for eight years, associated with the General Electric Company, working on electronic research and development. For five years he was on the faculty of the University of Colorado. He is a member of the American Institute of Electrical Engineers.

NEWELL ARROWSMITH ATWOOD

Commander Newell A. Atwood ('46) United States Navy, reported early in January to the New York Naval Shipyard in

N. A. ATWOOD

Brooklyn, New York, for duty as Electronics Officer, relieving Captain R. M. Huebl, United States Navy, who will remain as Industrial Engineering Officer.

Commander Atwood was born in Urbana, Ohio, on January 20, 1907, and received the A.B. degree from the University of Michigan in 1932, and the LL.B. degree from the George Washington University Law School. An active radio amateur since 1933, Commander Atwood has used station calls W8KOX and W3KTR. He was a member of the United States Naval Communication Reserve since 1933, and was appointed electronics engineering officer in 1946. During the war years he served with the Naval Research Laboratory, the Bureau of Ships, the Office of Naval Research, and the Norfolk Naval Shipyard. He was awarded the American Defense Medal, the American Theatre Medal, the World War II Victory Medal, the Naval Reserve Medal, and a Letter of Commendation from the Secretary of the Navy. He is a member of Delta Theta Phi Legal Fraternity and a registered patent attorney. From 1926 to 1927 he was connected with the research laboratories of the National Carbon Company, Cleveland, and from 1929 to 1936 he was on the faculty of the University of Michigan. He practiced patent law in Washington, D. C. from 1936 until he took up active navy duty in 1941.

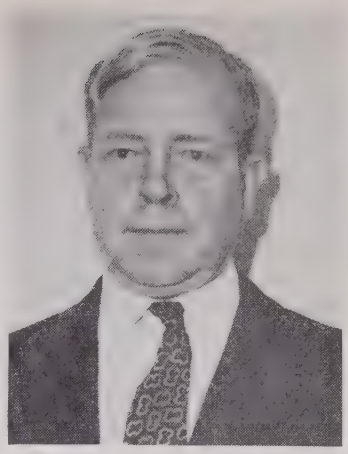

KNOX MCILWAIN

KNOX MCILWAIN

Knox McIlwain (A'31–M'40–SM'43), chief consulting engineer of the Hazeltine Electronics Corporation, Little Neck, L. I., was awarded a Certificate of Commendation by the United States Navy for his achievements during World War II. The certificate was accompanied by a citation reading, "This award is made for your outstanding supervision and great personal effort, as a Senior Department Head of the Hazeltine Electronics Corporation, in the design of test equipment which was of vital mportance to the efficient and effective operation of Naval radar identification equipment."

WILLIAM A. MACDONALD

William A. MacDonald (A'19–M'26–SM'43), president of the Hazeltine Electronics Corporation, New York City, was recently presented the President's Certificate of Merit for his distinguished services during World War II. The text of the certificate was as follows: "The President of the United States of America awards this Certificate of Merit to William A. MacDonald for outstanding fidelity and meritorious conduct in the aid of the war effort against the common enemies of the United States and its Allies in World War II." The certificate was accompanied by a letter of transmittal pointing out his outstanding services in the field of electronics which proved to be an invaluable contribution.

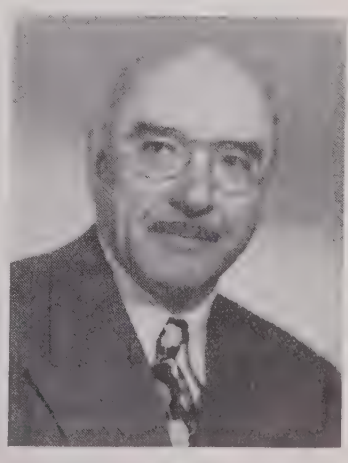

WM. A. MACDONALD

Board of Directors

December 10, 1947

Approval of Executive Committee Action of November 11, 1947. The Board of Directors, on recommendation of the Executive Committee, approved Executive Committee actions taken on this date (a copy of which had been mailed to the Board members): (1) That the Board adopt the recommendation of the Executive Committee that a Technical Committee on Audio and Video Techniques be established to cover the standardization of terminal equipment, and that the Constitution and Laws Committee be instructed to prepare the necessary By-law, and that Mr. Lack confer with the Chairmen of the Standards Committee and any other interested committees in determination of the scope of the committee. (Unanimously approved.) (2) That the Board adopt the recommendation of the Executive Committee that the appointment of Dr. F. B. Llewellyn as the I.R.E., Representative on the ASA Electrical Standards Committee be approved. (Unanimously approved.) (3) That the Board adopt the recommendation of the Executive Committee that the President be authorized to appoint one or more representatives of the I.R.E. on the RMA Spring Meeting Committee, which is handling the Syracuse Transmitter Meeting, and that the I.R.E. absorb, with the RMA the cost of this meeting over and above the income. (Unanimously approved.)

President Baker appointed V. M. Graham, Chairman, E. A. Laport, I.R.E. Representative, and announced M. R. Briggs as RMA Representative.

Student Branch. Mr. Lack moved that the Board approve the petitions for the formation of student branches at the following schools: University of Arkansas (I.R.E. Branch); Wayne University (I.R.E.-AIEE Branch).

Citation. President Baker stated that, since this was the last meeting of the Board of Directors for 1947, he wished to express his appreciation of the fine spirit of co-operation in which the Directors had acted throughout the year. He had greatly enjoyed his association with the Board. At this point, Mr. Pratt arose and suggested that all the Directors arise to express their approval of his motion that the Board recognize the commendable leadership of President W. R. G. Baker during the year 1947, particularly his success in making beneficial contacts with other groups and professional organizations, and for his activities in strengthening the fiscal position of the Institute. The Board arose and applauded.

Executive Committee

December 9, 1947

RMA of Canada. Both R. A. Hackbusch, and S. D. Brownlee, executive secretary of the RMA of Canada, have written Editor Goldsmith that the request of the I.R.E. for material from the Canadian RMA, for possible inclusion in the "Industrial Engineering Notes" in the PROCEEDINGS, has been favorably acted upon by the Board of Directors. The Institute has been placed on the mailing list for receipt of this material. The Editor has established the necessary routine in the Editorial Department to handle these items.

Schools of Recognized Standing. Mr. Lack moved that the President be authorized to appoint a committee to review schools which are not accredited in the Educational Directory, Part III, of the Office of Education of the Federal Security Agency, in the following two categories: (1) schools now making applications for student branches, or from whom individual student applications are being received; (2) schools which have been adopted by the Board in the past but which are not accredited in the Directory, and this committee to come up with a definite recommendation as to whether these schools should be retained, and also a ruling on all new schools. (Unanimously approved.)

I.R.E. Representatives on ASA Committees. Mr. Lack moved that the following be appointed as I.R.E. Representatives on ASA Committees: ASA Sectional Committee C-63, C. C. Chambers; ASA Sectional Committee C-42: A. B. Chamberlain.

"Methods of Testing the Sound and Video Sections of Television Receivers." Copies of "Methods of Testing the Sound and Video Sections of Television Receivers" were mailed to the Television Committee and Subcommittee members November 7. At a meeting of the Television Committee held in Rochester November 19 to review this material, a new task group was established under the Television Committee to expedite final drafting of these sections. This group is presently at work and plans to complete the final draft of revisions by the end of December. Mr. Lack stated that it is proposed that this standard will be published no later than May.

ASA Electrical Standards Committee. Mr. Lack moved that the executive committee recommend to the Board that the appointment of F. B. Llewellyn as the I.R.E. Representative on the ASA Electrical Standards Committee be approved. (Unanimously approved.)

Sections Committee Chairman. Mr. S. L. Bailey moved that Alois W. Graf be appointed chairman of the Sections Committee for 1948. (Unanimously approved.)

Admissions Committee Chairman. Mr. Henney moved that George T. Royden be appointed chairman of the Admissions Committee for 1948. (Unanimously approved.)

Public Relations Committee Chairman. Mr. Henney moved that Virgil M. Graham be appointed chairman of the Public Relations Committee for 1948. (Unanimously approved.)

Education Committee Chairman. Mr. Pratt moved that F. E. Terman be appointed chairman of the Education Committee for 1948. (Unanimously approved.)

Membership Committee Chairman. Mr. Henney moved that Beverly Dudley be appointed chairman of the Membership Committee for 1948. (Unanimously approved.)

President Baker stated, that since this was the last Executive Committee meeting of the year 1947, he wished to thank the Committee for their fine spirit of co-operation throughout the year and that he much enjoyed his association with the Committee. The same sentiment was expressed by the Committee to President Baker.

ANNUAL MEETING

The Annual Meeting of The Institute of Radio Engineers will be held on March 22, 1948, at 10:30 A.M. in the Grand Ballroom of the Hotel Commodore, New York City.

I.R.E. CINCINNATI CONFERENCE

The Cincinnati Section of the Institute of Radio Engineers is sponsoring its second annual Spring Technical Conference on Saturday, April 24, 1947, in Cincinnati, at the Engineering Society Headquarters Building. The Conference will feature television, and a number of prominent speakers are expected to present papers. Among other things there will be demonstrations of television receivers, and components.

VAGARIES OF CHANCE?

The Chairman of the Admissions Committee of The Institute, George T. Royden, has called attention to a remarkable coincidence, of a type unlikely to occur again for many years. It appears that C. H. Smith of Anchorage, Alaska, and W. N. Smith of Anchorage, Kentucky, were simultaneously admitted as Members of the I.R.E.! The Institute membership will welcome these gentlemen and will, it is believed, be impressed by the occasional strange vagaries of pure chance.

Industrial Engineering Notes

HIGH-SPEED LENS DEVELOPED

According to an Army announcement late in November, 1947, the fastest known high-speed all-refracting photographic lenses have been developed by Edward K. Kaprelian, chief of the Photographic Branch at the Squier Signal Laboratory, Fort Monmouth N. J. "The relative aperture system of the new lens can be made as large as $f/0.6$ approaching the theoretical maximum of $f/0.5$," according to the Signal Corps Engineering Laboratories, and they are used in making photographs under conditions of extremely low light level. It is said that they are particularly suitable for making motion pictures of x-ray fluorescent screens and of cathode-ray tube traces.

[1] The data on which these NOTES are based were selected, by permission, from "Industry Reports," issues of November 21, and 28, and December 5, and 12, 1947, published by the Radio Manufacturers' Association, whose helpful attitude in this matter is here gladly acknowledged.

Reports On German Developments

The universal condenser microphone, believed to be the first single-transducer unidirectional microphone to be made, and technical details on other German sound recording and reproducing equipment, are described in three reports released toward the latter part of November, 1947, by the Office of Technical Services. They are: PB-79584, German universal condenser microphone, 25 cents. PB-80572, filter design for communication systems; microfilm or photostat, $1.00. PB-69125, sound recording, reproducing and other electro-acoustic targets; microfilm, $1.00; photostat, $2.00. Four pamphlets were also issued by the OTS on German wartime telephone technology. The reports discuss coaxial cable and associated telephone and television systems, PB-1297; quadded toll cables, PB-1298; and rural telephone services and carrier telephone systems, PB-1299. All these reports and pamphlets may be purchased at the Office of Technical Services, Department of Commerce, Washington 25, D. C.

* * *

A report released toward the end of 1947 by the OTS describes the use of special ceramics in German communication equipment. Some of these are: titanium-dioxide thermistors, carbon-film fixed resistors on ceramic forms, and magnetic ceramic materials. The report, PB-1292, mimeographed, is priced at $1.00 and may also be obtained from OTS at the above address.

* * *

A new type of cathode-ray tube developed by a German inventor is capable of storing images over long periods of time. It is described in a report on sale by the OTS. The tube was developed with the idea of eliminating flicker in television pictures. Copies of the report (PB-78273) may be obtained by sending a check or money order for 75 cents, payable to the Treasurer of the United States, to the Office of Technical Services, Department of Commerce, Washington 25, D. C.

* * *

Another technical research report released by OTS describes new developments in high-current carbon lights. According to this report, the high-current carbon arc is of significant importance "to the future development of more powerful searchlights, better movie studio illumination, and improved motion picture projectors." Report (PB-81644) mimeographed, is priced at $5.75.

Study Of Solar Radio Noise

The National Bureau of Standards announced in December, 1947, that government scientists have initiated a project for the observation and analysis of radio noise generated by the sun, a companion project to cosmic radio noise studies already in progress. They will seek to determine the range of frequencies broadcast from the sun, received intensities, and correlation of solar noise with other solar, interstellar, and terrestrial phenomena. This investigation will be conducted at the Bureau's propagation laboratory at Sterling, Virginia.

Report on Army's Research Program

A summary of the Army's research and development program, both current and projected, including radio, radar, and electronic projects, was recently released by the Research and Development Division of the General Staff of the United States Army.

The 109-page booklet, entitled "War Department Research and Development Program Fiscal Year 1949," describes the Army's over-all projects for the 1949 fiscal year and briefly discusses anticipated 1950 operations.

Under current projects of applied research in the radio communications field, the Signal Corps referred to its contracts with educational institutions, commercial laboratories, and other government agencies. These include work on electron tubes; propagation studies in frequency ranges potentially suitable for radio relay equipment; research on stable filters, on detectors for f.m. sets, frequency stability and calibration accuracy in receivers, on circuits for improving the sensitivity characteristics of receivers, and on the power drain in receivers; work on antennas, and work on reduction of receiver radiation. Projects covering the development of equipment included a series of radio receivers; extremely lightweight and short-range miniature v.h.f. radio transmitter-receiver sets; man-pack, short-range v.h.f. radio sets; h.f. man-pack, longer-range radio sets adaptable for vehicular mounting; and a series of l.f., i.f., and h.f. devices for mobile use and adaptable for air transportation, and relay equipment.

The report said that the Signal Corps is continuing radar research on basic theories to obtain data for increasing range, for bettering resolution and accuracies, for widening the frequency bands over which equipments may operate, and to develop new methods of construction and utilizing equipment. The Signal Corps also is carrying out projects looking toward the development of improved radio direction finders and navigation devices to replace those now in service.

Television studies are underway to indicate the most advantageous utilization of television pictures with the smallest possible frequency band widths. The Signal Corps also is studying methods of developing television equipment for operation under extremely low light conditions.

The Air Forces is working on detection and tracking equipment, u.h.f. communications equipment, and navigation equipment, and is co-operating with the Signal Corps and Navy Department on projects involving tubes and parts.

The research document was issued under the signature of Colonel E. A. Routheau, Chief, Research Group.

Diathermy and Industrial Frequencies Changed

The Radio Administrative Conference held last summer at Atlantic City, N. J., resulted in the first international provision for use of frequencies by radio devices used for industrial, scientific, and medical purposes, the F.C.C. explained in announcing proposed changes in its rules governing these devices.

Under the proposed amended rules (Public Notice 14395), abandonment of the old frequencies will not be required until July 1, 1952. "However," the F.C.C. said, "it is expected that manufacturers of diathermy equipment who have already obtained type approval of equipment will wish to make the necessary minor changes in such equipment." The frequency band, the center frequency of channel, and the tolerance from the center frequency stipulated in the Atlantic City Radio Regulations are as follows:

Assigned Band, Kilocycles	Center Frequency of Channel, Kilocycles	Tolerance from Center Frequency, Kilocycles
13,553.22–13,566.78	13,560	± 6.78
26,957.28–27,282.72	27,120	±162.72
40,659.66–40,700.34	40,680	± 20.34

In general, the changes which apply to diathermy equipment also apply to industrial heating equipment, the F.C.C. pointed out.

F.C.C. Approves Telephone Recorders

On January 15, 1948, the F.C.C. put into effect an order approving the use of a recording device which reproduces telephone conversations. This is subject to an automatic tone warning that notifies all parties so engaged that their conversation is being recorded. The F.C.C. said that this device may be furnished or maintained by anyone, whether or not a telephone company, provided it meets certain characteristics.

Warning On Use Of Surplus Radar Equipment

A quickened interest in the use of radar equipment for training purposes in colleges and other educational institutions elicited some comments from the F.C.C. recently. The Commission pointed out the possibility of interference from radar transmitters to the regular radio services, and also the necessity for securing both station and operator licenses. The radar equipments in circulation, the F.C.C. further said, are war-born devices, and not necessarily engineered to operate on frequencies in accordance with the F.C.C. table of frequency allocations.

West Virginia University was the first educational institution to receive a grant from the Commission to use radar equipment for the purpose of training students in its theory and operation. This was issued at the end of November, 1947.

Second List Of Inventions Issued By OTS

Inventions for which the Government holds the right to file foreign patent applications, including more than forty electronic patents, were recently described in a second listing issued by the Office of Technical Services, United States Department of Commerce. These patents, which individual concerns registered abroad for the general benefit of American industry, were valid

only if registered before December 31, 1947. Government owned patents, the OTS said, are made available to American business and industry on a royalty free, non-exclusive licensing basis.

Commercial and College Laboratories Listed

The National Bureau of Standards has compiled a list of 220 commercial laboratories, with 30 branches or offices, and 189 college laboratories used for research and testing as well as instruction. The list is arranged both geographically and alphabetically. Miscellaneous Publication M187, entitled Directory of Commercial and College Laboratories, may be obtained from the Superintendent of Documents, Washington 25, D. C., at 30 cents per copy.

I.R.E. Annual Awards

The I.R.E.'s 1948 Medal of Honor has been awarded to L.C.F. Horle (A'14–M'23–F'25), chief engineer of the RMA Data Bureau, "for his contributions to the radio industry in standardization work, both in peace and war, particularly in the field of electron tubes, and for his guidance of a multiplicity of technical committees into effective action."

S. W. Seeley (M'40–SM'43–F'43) will receive the Morris Liebmann Memorial Prize, and W. H. Huggins (S'39–A'44) will receive the Browder J. Thompson Memorial Prize. These awards will be officially conferred upon the recipients at the 1948 I.R.E. National Convention in New York in March.

Mobile Radio Services Needs

From December 8 to 12, 1947, lengthy technical hearings involving twelve issues relating to the General Mobile Services furnished the six-member Federal Communications Commission with a voluminous record of testimony regarding two-way radio communication. The witnesses represented taxicab organizations, bus companies, telephone operating concerns, and three radio manufacturing companies.

The F.C.C. presented 16 exhibits including one showing a total of 617 land stations and 22,720 mobile units licensed in the General Mobile Service. Construction permits for another 607 land stations and 15,150 mobile transmitters have been issued, bringing the total authorizations to 1,224 land stations and 37,870 mobile stations. The F.C.C. has also received applications for 130 land stations and 2,810 mobile units.

Taxicab firms and bus companies are opposed to any allocation plan which requires "bulk" users in the mobile field to subscribe to a common-carrier service. They prefer a choice of service for large radio users and exclusive frequencies assigned to them. An over-all increase in the number of frequencies assigned to the General Mobile Services is desired.

Throughout the hearings Commission members indicated that they thought many of the troubles of the taxi concerns could be overcome by closer co-operation and co-ordination between the users of two-way mobile radio equipment.

Meeting Of Marine Services

The executive committee of the Radio Technical Commission for Marine Services held its regular monthly meeting on December 3, 1947, in the Old State Department Building.

Television Channel A Three-Cornered Battle

All six members of the F.C.C. attended the five-day hearing, November 17 to 21, presided over by Paul A. Walker, acting chairman. Television, f.m., and mobile interests are striving to protect or better their positions in the frequency spectrum. Thirty-six companies and organizations presented their claims.

F.m. interests termed television a "luxury service," and the spokesmen for both the Zenith Radio Corporation and the Stromberg-Carlson Company, J. E. Brown (A'24–M'28–SM'43), and Lee McCanne (A'36–SM'45), respectively, urged the F.C.C to return to the 44- to 50-Mc. band. Another of the two-score witnesses which represented the various interests believed that eventually television would absorb f.m. because of the added video interest. There were a few suggestions that television should be moved to the higher frequencies at once, but all witnesses were in substantial agreement that sharing of Television Channel No. 1 with the Mobile Services is detrimental to each service, and practically all agreed that the F.C.C. proposal concerning such interference had merits. However, there were a few strong hints and some direct statements addressed to the F.C.C. to the effect that various Government departments and agencies have been assigned more frequencies than are justified by their needs. These Government allocations are in reality the responsibility of the Interdepartmental Radio Advisory Commission, on which the F.C.C. has only one vote. Nevertheless, if the F.C.C. decides to abolish sharing of the proposed television channels, it is understood the Government will relinquish its frequencies in the remaining two television channels.

In general the television spokesmen conceded that twelve channels without the sharing requirement would be better than thirteen with that proviso, but that television needs additional frequencies for growth.

J. E. Brown said that the 88- to 108-Mc. allocation to f.m. is entirely inadequate, based "on engineering errors and failure to consider the facts involved." Addition of a second f.m. tuning band to a radio receiver, Mr. Brown stated, would not substantially raise its cost to the public. Lee McCanne, vice-president and general manager of Stromberg-Carlson, agreed in this. Zenith has sold about 40 per cent of the industry's total a.m.-f.m. table models. Stromberg-Carlson produced 11 per cent of the reported industry production, prewar and postwar, up to October 1, 1947, of 1,220,000 f.m.-a.m. receivers. Mr. McCanne testified that a recent survey of manufacturers showed a total of 635,000 sets capable of receiving the 44- to 50-Mc. band as compared to 585,000 sets capable of receiving the higher f.m. band only. Edwin H. Armstrong (A'14–F'27) and Everett L. Dillard (A'38), FM Association president, also urged that F.C.C. assign the lower band permanently to f.m. The FMA asked for this band for wide-area relay purposes only. As the representative of the Allen B. DuMont Laboratories, T. T. Goldsmith (Jr. A'38–SM'46) presented detailed technical exhibits showing results of tests revealing television interference from various other services and urged the F.C.C. to grant the video industry enough space for further expansion. F. J. Bingley (A'34–M'36–SM'43), of the Philco Corporation, emphasized the fact that "television, like standard broadcasting, is designed to reach the entire American public in their homes and to furnish them with a medium of hour-by-hour education and entertainment." He opposed the F.C.C. proposal and noted that more than twelve channels should be provided to meet, among other things, the problem of the television channels available to smaller communities. Daniel E. Noble (A'25–SM'44–F'47), of Motorola, Inc., presented evidence for RTPB Panel 13 which he described as representing the users of mobile equipment. He characterized the F.C.C. proposal as "inadequate," and suggested that Channel No. 1 be set aside for the exclusive use of the Mobile Services and that the 72- to 76-Mc. band and all unoccupied adjacent channel television bands be made available to mobile equipment users to the extent to which they may be used without interference to other services.

356 F.M. Stations On The Air End Of 1947

On December 11, 1947, F.C.C. records showed a total of 356 f.m. stations on the air. New stations are: Reading, Pa. (WEEU-FM); Meriden, Conn. (WMMV-FM); Waterloo, Iowa (KXEL-FM); Roanoke Rapids, N.C. (WCBT-FM); Shelby, N. C. (WOHS-FM); Shelbyville, Ind. (WSRK); Paterson, N. J. (WWDX); Winston-Salem, N. C. (WSJS-FM); Suffolk, Va. (WLPM-FM); Greenfield, Wisc. (WWCF); San Francisco, Calif. (KQW-FM); Chico, Calif. (KMPC-FM); Bellaire, Ohio (WTRF-FM); Albany, Ore. (KWIL-FM); Cleveland Heights, Ohio, (WSRS-FM); Roanoke, Va. (WSLS-FM); San Antonio, Tex. (KONO-FM); Port Huron, Mich. (WTTH-FM); Danbury, Conn. (WLAD-FM); Neenah, Wisc. (WNAM-FM); Poughkeepsie, N. Y. (WVA); Portland, Me. (WGAN-FM), and Roanoke, Va. (WROV-FM).

Three conditional grants for new f.m. stations, and one construction permit for a commercial television station, were issued in November, 1947. They were for Houston, Tex., Burlington, N. C., and Harding College, Memphis, Tenn. The television station is to be erected at Harding College.

Excise Collections Show Increased Sales

October sales of radio sets, phonographs, and component parts, reached a new high of $5,513,134.48, in October, 1947. This, as shown by the collection of excise taxes by the United States Bureau of Internal Reve-

nue, was an increase of almost 2 million dollars over the September, 1947, sales which amounted to $3,623,929.13, and more than a half-million dollars above the October, 1946 sales, amounting to $4,996,204.00.

Tube Sales Show Increase

According to an RMA tabulation, sales of radio receiving tubes in October, 1947, totalled 20,343,796, an increase of 3,958,249 over September's. Cumulative sales from January to October, 1947, inclusive, were 165,884,528.

Set Output Estimated at Seventeen Million in 1948

A new publication of the Department of Commerce, which is designed to furnish a monthly summary of business information to the trade publications and associations, estimated recently that radio receiving set production in 1948 is expected "to approximate the 1947 volume of about 17 million units."

"Any loss in the production of standard a.m. sets," the article stated, "is expected to be offset by a gain in a.m.-f.m. and television sets. Total production of sets equipped to receive f.m. will probably be several million as a result of increased broadcasting coverage. The Department estimated that television receivers produced in 1948 would total around 750,000 and that by the end of this year nearly 1 million sets will be in use.

Radio-Appliance Sales at New High

The October sales figure of $193,000,000 was up 12 per cent over September and 25 per cent over October, 1946. Sales for the year through October were up 47 per cent over the corresponding 1946 period. Sales of appliance and specialty wholesalers totalled $16,306,000, a 60 per cent increase over October, 1946, and 19 per cent over September of this year. Sales for 1947 through October were up 67 per cent over the same 1946 period.

Set Shipments Over 100 Thousand

More than 100,000 receiving sets were exported during October, 1947, according to the United States Department of Commerce. Foreign shipments of radio equipment in October totalled 4,866,265 units valued at $9,014,503, compared with 5,468,689 valued at $8,075,631 in September. Receiving sets exported numbered 107,779 valued at $4,142,437, against 97,768 valued at $3,514,942 in September.

October Radio, Television Output Breaks All Industry Records

Radio set production, including television and f.m.-a.m. receivers, broke all industry records in October, an RMA tabulation of weekly Haskins & Sells reports for the five weeks ending October 31 revealed. For the first time in the industry's history more than 2,000,000 radio and television receivers were manufactured by RMA member-companies, in one month. October's record output covered five working weeks, September 29 through October 31, but the average weekly output was well above that for the past ten months.

F.m.-a.m. sets produced in October numbered 151,244 and were well above the production of any other month this year. Television receivers manufactured also reached a new high of 23,693, although the September reported figure of 32,719 was higher due to the inclusion of 16,991 sets produced earlier but not reported. Total radio and television set production by RMA manufacturers numbered 2,002,303 in October and brought the 1947 ten-month total to 14,364,218. F.m.-a.m. sets for the ten months totalled 830,106, while television receivers for the same period numbered 125,081. The television set production in October represented an increase of 110 per cent over the average output for the previous nine months.

October f.m.-a.m. sets included 49,319 table models, 555 converters and tuners, 656 consoles, and 100,714 radio-phonograph consoles. Television receivers included 13,503 radio table models, 10,181 consoles and radio-phonograph combinations, and 9 converters.

Sales to manufacturers were 85.84 per cent of sales in October, 1946, as compared with the September percentage of 97.7 per cent. Sales to jobbers were 88.99 per cent of those during the corresponding month last year and about equal to the September percentage of 88.78.

RMA Activities

Toward the latter part of November, 1947, L. C. F. Horle A'14–M'23–F'25), chief engineer of the RMA Data Bureau, was reappointed for a three-year period as RMA representative on the Standards Council of the American Standards Association. Virgil M. Graham, associate director of the RMA engineering department, was named alternate.

* * *

RMA members received copies of the RMA Trade Directory and Membership List at the close of 1947. The directory also lists division members and includes the recently adopted and recommended warranties for radio parts manufacturers, and the standard warranty for set manufacturers. It lists all committees.

* * *

RMA director Walter Evans, of Baltimore, Md., has been appointed a director of JETBC, representing the National Electrical Manufacturers Association, according to information received from NEMA. Mr. Evans succeeds A. C. Streamer, who has retired from NEMA activities.

* * *

L. C. F. Horle, chief engineer of the RMA engineering department, recently informed the Atomic Energy Commission, the Navy Department, and the Army-Navy Electronic and Electrical Standards Agency that the RMA Data Bureau, on the basis of requests of the armed services, is now prepared "to operate in the field of electron tube type designation in its special application to counter tubes." Provisions now exist for making available to all makers of counter tubes the type designation assignment facilities of the Data Bureau.

RMA-I.R.E. Committee Meeting In Chicago

During the annual RMA mid-winter conference in Chicago there was a joint meeting of the Executive Committee and Section Chairmen of the RMA Transmitter Division. S. P. Taylor, of New York, presided as chairman at the January 21 meeting. On the same day the Executive Committee of the Amplifier and Sound Equipment Division held a meeting under the chairmanship of Fred D. Wilson, of Chicago.

RMA-I.R.E. Rochester Fall Meetings

New developments in the radio and electronic field were under discussion at the RMA-I.R.E. Rochester Fall Meeting. Members of the RMA engineering department, members of the I.R.E., and some members of the Canadian RMA attended the three-day sessions which took place at the Sheraton Hotel from November 17 through 19, under the chairmanship of Virgil M. Graham (A'24–M'27–F'35).

Fred S. Barton (F'35), director of Communications Development for the British Ministry of Supply and formerly director of radio engineering for the British Air Commission in Washington, was awarded the annual citation of the Rochester Fall Meeting "in recognition of his great accomplishments in bringing about many firm and lasting friendships in the radio engineering profession in the United States, Canada, and England through his unfailing good humor, kindliness, and understanding of the other fellow's point of view." Speaking on the status of the radio industry in the United Kingdom, Mr. Barton said that about 25 per cent of the industry's output is now being exported. He exhibited an automatically manufactured type of receiver which has recently gone into production in England.

E. Finley Carter (A'23–F'36), vice-president in charge of engineering of Sylvania Electric Products, Inc., spoke on "Engineering Responsibilities in Today's Economy." He urged engineers to assume a greater responsibility for the applications, as well as the developments, of their engineering skill.

A plea for more simple designs in radio receivers to enable the maintenance man to make repairs more easily was made by A. C. W. Saunders (M'47) of the Saunders Radio and Electronic School.

RMA Meetings

The following RMA engineering meetings were held:

December 2—Committee on Amplifiers
December 2—Committee on Speakers
December 2—Executive Committee
December 3—Committee on Microphones
December 3—Subcommittee on Antennas
December 5—Task Group B
December 10—Subcommittee on Point-to-Point Communication
December 16—Subcommittee on 12-Inch Bulb Standardization
January 9—Subcommittee on Tube Sockets

Books

Elementary Nuclear Theory, by H. A. Bethe

Published (1947) by John Wiley & Sons, Inc., 440 Fourth Avenue, New York 16, N. Y. 121 pages+6-page index+17-page appendix+vi pages. 17 figures. 5½×8½ inches. Price, $2.50.

This slender volume is a set of notes on a series of twenty lectures given by Prof. H. A. Bethe to engineers and scientists of the General Electric Company, covering selected topics in the modern theory of nuclear forces from an empirical point of view. Because of the condensed lecture-note style, the book contains far more meat than its 121 pages of text would imply offhand.

The first section covers the descriptive theory of nuclei. After a brief review of basic facts about nuclei and our knowledge of their size, beta disintegration, nuclear spin and statistics, and the neutrino are described. The main portion of the book is devoted to the quantitative theory of nuclear forces. In this part the deuteron is treated at some length since it enjoys in nuclear theories much the same position that the hydrogen atom holds in atomic theory. The topics covered include the physical properties of the proton, neutron, and deuteron, the ground state of the deuteron, scattering of neutrons by free and bound protons, interaction of the deuteron with radiation, proton-proton scattering, noncentral forces, and saturation of nuclear forces. The meson theory of nuclear forces is given only a very brief treatment, since it is not yet in a form that permits useful predictions. In the third section of the book beta disintegration and the compound nucleus are discussed. A seventeen-page table of nuclear species is given as an appendix.

In selecting his topics Professor Bethe has tried to emphasize the fundamental aspects of the theory; therefore, discussion is centered on the simplest nuclei, and topics such as fission and the theory of complicated nuclei are omitted. The theory of alpha radioactivity is also omitted, since it can be found in many of the standard texts on quantum mechanics.

The book will be of greatest value to those whose knowledge of nuclear physics was acquired some years ago and who wish to bring themselves up to date on the modern theory. For this purpose it has no rival. In addition to some acquaintance with nuclear physics, a familiarity with the concepts and methods of quantum mechanics is assumed. Professor Bethe's lectures are clear, well-organized, and very much to the point, and the note-takers, Melvin Lax, Conrad Longmire, and Arthur S. Wightman, are to be congratulated on an excellent job.

J. B. H. Kuper
Brookhaven National Laboratory
Upton, L. I., N. Y.

Principles and Practice of Electrical Engineering, by Alexander Gray (Revised by G. A. Wallace)

Published (1947) by McGraw-Hill Book Company, Inc., 330 West 42 Street, New York 18, N. Y. 551 pages+8-page index +xv. 487 illustrations. 6×9 inches. Price, $4.50.

This is the sixth edition of a work which first appeared in 1914; the fourth revision prepared since the death of Professor Gray in 1921.

The book was written for college students, specializing in branches other than electrical engineering, who desire a working knowledge of the principles and practice of the subject, but who have only a limited time at their disposal. Subsequent editions of the book have held to this object, seeking only to keep the subject matter up to date. In the present edition the m.k.s. system of units is introduced in addition to the use of c.g.s. units, the material on three-phase systems and the transformer have been extended, and new subjects have been included, as, for example, the amplidyne, fluorescent lamps, and vacuum tubes.

The treatment throughout is clear, concise, and interesting, with the employment of a minimum of mathematics. Particularly well done are the chapters on batteries, direct-current machinery, and control of apparatus, alternating-current machinery, and transmission. In the chapters on vacuum tubes are sketched their characteristic curves and their fundamental functions as rectifiers, amplifiers, and oscillators, but no claim is made of a detailed treatment. The emphasis of the book is on power circuits, power apparatus, and low-frequency transmission lines.

The book is copiously illustrated, the pictures of apparatus well chosen for clarifying the treatment in the text. Practical problems and test questions accompany each chapter and a short list of laboratory experiments. The book should be useful for students in general with moderate mathematical equipment. The calculus is used only sparingly.

Frederick W. Grover
Union College
Schenectady, N. Y.

Sunspots in Action, by Harlan True Stetson

Published (1947) by The Ronald Press Company, 15 East 26 St., New York 10, N. Y. 227 pages + 7-page bibliography+ 6-page table+7-page index+iv; foreword by Sir Edward V. Appleton. Price, $3.50.

Few books on the subject of radio, whether technical or nontechnical, give more than a cursory treatment of sunspots. Dr. Stetson, who is himself a radio engineer as well as a distinguished astronomer and a physicist, has helped to fill in this gap over a number of years in several of his books. The latest, "Sunspots in Action," extends his previous discussions and collects into a highly informative and thoroughly readable form a wealth of information covering various aspects of sunspot phenomena. The book brings together what is known about sunspots, including relevant information crossing several fields of science that bear upon the relation of the earth to its cosmic environment.

This volume is written for the intelligent layman and not for the expert, although the expert will find it to be most entertaining reading. Technical language has been held to a minimum, but this is not an indictment against the book from the point of view of the professional radio engineer. The volume contains much information which will prove useful and interesting to the most technical man.

"Sunspots in Action" is not limited to the effects of sunspots on radio communication. Dr. Stetson treats with this phase of sunspot phenomena in some detail but only as a part of a much broader approach. Throughout the book, emphasis is placed on the various effects of cosmic phenomena on the earth's atmosphere and the terrestial consequences thereof.

The first few chapters deal with the sun, its source of energy, and its radiation. The effects of this radiation and the changes brought about by the appearance of sunspots is then covered. Sunspots themselves are discussed and various methods of predicting their appearance are surveyed. The effects of the other planets on the existence of sunspots and on the earth's atmosphere are brought into the discussion, together with material concerning the northern lights, solar eclipses, cosmic effects, and the earth's magnetism.

In addition to the chapters on sunspots and radio communication and prediction, Dr. Stetson outlines evidence available relating to effects of sunspots on the earth's atmosphere as an ultimate source of weather, on life cycles in plants and animals, and on the possible correlation of sunspots with economic trends. Some of the more plausible hypotheses in these various fields are critically examined.

This book is well worth reading not only for the broader picture of the universe which it presents but also because sunspots may well be proven to have an even more pronounced and direct effect on human life than is definitely known today.

George M. K. Baker
RCA Laboratories Division
Radio Corporation of America
Princeton, N. J.

Patent Notes for Engineers

Published (1947) by the Radio Corporation of America, Princeton, N. J. 146 pages +14-page index+vi pages. 37 figures. 6×9 inches. Price, $2.50.

This is the first volume in the new engineering book series published by the RCA Review Department of RCA Laboratories Division. While published primarily for the use of RCA divisions and subsidiary companies, the information contained in the volume is of interest to all scientists, engineers, and attorneys concerned with patent matters.

One half of the book is given to the treatment of invention; invention in the popular sense and in the statutory sense, the nature of invention, and invention as a practical matter. Numerous illustrations and examples help to clarify and explain this important subject under each heading and subheading.

The remainder of the book presents a perspective of patent prosecution, records of invention, interferences, and ownership and use of patents. Sufficient treatment of each subject is given for a general understanding by the reader without becoming unduly involved in technicalities or the detailed intricacies of these patent matters.

The introduction states that these notes represent a serious effort to bridge the technical gap between engineers, research workers and inventors generally, and their patent attorneys. This small volume is indeed a step in the right direction, narrowing the gap.

No mention is made of patent approval infringement, and such other matters frequently encountered by the engineer and those concerned with production, all of which necessitate co-operation with patent counsel in behalf of the employers' interests. This omission, however, does not detract from the value of the present work, which has such a complete table of contents and index as to assure the use of the book as a frequent reference manual.

Alois W. Graf
Patent Lawyer
120 S. LaSalle Street, Chicago 3, Ill.

Men and Volts at War, by John A. Miller

Published (1947) by Whittlesey House, 330 West 42 Street, New York 18, N. Y. 245 pages+10-page appendix+16-page index+xi pages, 255 illustrations. 6×9 inches. Price, $3.75.

When the axis powers launched the all-out emprise known as World War II, German plans were based largely upon conducting a mechanical war. When the United States joined the Allies opposing the axis, the outcome of the struggle was not long in doubt, because a mechanical war was, in the vernacular, "up our alley." Once American industry was converted to war production, the public was aware of the extent and speed of production largely through announcements of "E" awards to particular manufacturing plants or departments for excellence, or continued excellence, in production of war materials. This book deals with the war production efforts of one American manufacturing company which received a total of seventy-six "E" and "M" awards from the Government: The General Electric Company.

The book deals with research and production contributions made by this company and its subsidiaries to practically all arms of the services, and the author has done an excellent job of presenting in clear and readable text the nature of these contributions and their applications in the war theaters. If there are omissions in the text these are exclusive systems and devices produced by other manufacturers. As an authentic record of what was accomplished by industry during the war period, and what could be accomplished again should the need arise, this book should prove of direct interest to engineers, teachers, officers of the armed services, and the public in general. In the pages of this comprehensive work the reader may, perhaps for the first time, learn the manufacturing and application facts about instrumentalities which were war secrets (not written about) during the war years, such as: magnetic-mine defense, degaussing measurements, the bazooka, power trains for the Soviet drive to Berlin, radiolocation in the Battle of Britain, radar countermeasures, radio for combat communication, uranium and atomic energy, and hundreds of other war developments for offense and defense in war operations. These are well organized in twenty readable chapters.

Donald McNicol
Consulting Engineer
25 Beaver St., New York, N. Y.

Tables of Integrals and Other Mathematical Data (revised edition), by Herbert Bristol Dwight

Published (1947) by The Macmillan Company, 60 Fifth Avenue, New York, N. Y. 207 pages+2-page index+37-page appendix+viii pages. 10 figures. 5×8 inches. Price, $2.50.

This compact little volume contains many numerical tables of functions. These include algebraic, trigonometric, logarithmic exponential, elliptic, hyperbolic, and Bessel functions. A well-organized table of integrals is accompanied by useful algebraic relations and many series often encountered in engineering physics. A usable index adds to the utility of the book.

George H. Brown
RCA Laboratories
Princeton, New Jersey

Electronics and Their Application in Industry and Research, edited by Bernard Lovell

Published (1947) by Harper & Brothers, 49 East 33 Street, New York 16, N. Y. 176 pages+13-page index+xi pages. 18 illustrations. 5½×8¼ inches. Price, $3.00.

This book is the work of about a dozen authors, each one in general contributing a chapter. The editor provided an excellent introduction, particularly the section on electronics and the Second World War.

In his introduction the editor states that he purposely has excluded subjects already dealt with in many other texts and has aimed to include chiefly examples of important advances in the science which have occurred during the past few years. Thus conventional radio engineering aspects are omitted, but such subjects as infrared photocells, the betatron, servomechanisms, and new applications in medicine and physiology are covered in considerable detail.

The book may be likened to a group of well-prepared papers presented at a meeting of a technical society. It is thus not a textbook, but should be of considerable value to engineers in the field of industrial electronics interested in new developments in England.

W. C. White
General Electric Co.
Schenectady, N. Y.

Omission in "Television—III"

Two sheets listing original publication data for the summaries contained in the appendix of Volume III of "Television," edited by Alfred N. Goldsmith, Arthur F. Van Dyck, Robert S. Burnap, Edward T. Dickey, and George M. K. Baker, have been issued by the publishers. These may be pasted in the volume, thus eliminating the omission. They are obtainable by request at the Radio Corporation of America, RCA Laboratories Division, Princeton, N. J.

Notice

The new I.R.E. television standard, "Standards on Television: Methods of Testing Television Transmitters—1947," is now available. The price is $0.75 per copy, including postage to any country.

Orders may be sent to The Institute of Radio Engineers, Inc., 1 East 79 Street, New York 21, N. Y., with remittance and address to which copies are to be sent.

Calendar of

Coming Events

I.R.E. National Convention
March 22-25, 1948

Cincinnati Spring Meeting
April 24, 1948

Syracuse RMA-I.R.E. Spring Meeting
April 26-28, 1948

Chicago I.R.E. Conference
April 17, 1948

New England Radio Engineering Meeting
May 22, 1948

1948 West Coast Convention of the I.R.E.
September 30–October 2, 1948

THE NATIONAL PHYSICAL LABORATORY, TEDDINGTON, MIDDLESEX, ENGLAND

Aerial view of the main part of the Laboratory.

J. W. McRae

Member of the Board of Editors

J. W. McRae (A'37–F'47) was born on October 25, 1910, in Vancouver, British Columbia. He received the B.S. degree in electrical engineering from the University of British Columbia in 1933, the M.S. degree in 1934 from California Institute of Technology, and the Ph.D. degree from the same institution in 1937. Earlier in the same year, he had joined the Bell Telephone Laboratories, where he engaged in research on transoceanic radio transmitters. His next assignment was in the field of microwave research, which led naturally to work on military projects, including a special microwave oscillator for the National Defense Research Committee and early association with several microwave radar projects.

Early in 1942 he accepted a commission as major in the United States Army Signal Corps and was assigned to the Office of the Chief Signal Officer in Washington, D. C. He remained in Washington for more than two years, engaged in co-ordinating development programs for airborne radar equipment and for radar countermeasures devices. He later received the Legion of Merit for his work on these programs. In June of 1944 he was transferred to the Headquarters of the Signal Corps Engineering Laboratories at Bradley Beach, N. J., as chief of the engineering staff. Some time after this he became deputy director of the Engineering Division and attained the rank of colonel before returning to civilian life at the end of 1945. Once again associated with the Bell Telephone Laboratories, he was appointed director of Radio Projects and Television Research in June of 1946, which made him responsible for work on the New York-to-Boston radio relay project as well as for research on television. With the addition of responsibility for electron-dynamics research in February, 1947, he became director of electronic and television research. He received Honorable Mention for 1943 in the Eta Kappa Nu awards for outstanding young electrical engineers. This was presented to him on January 26, 1948, at the AIEE Winter General Meeting in Pittsburgh, Pa.

Dr. McRae has been a member of the Board of Editors of the Institute since 1946, and was a member of the 1947 I.R.E. Convention Committee. He is now vice-chairman of the New York Section and a member of the Program Committee of the Technical Societies Council of New York. He is also a member of the AIEE and Sigma Xi.

Developments in Radio Sky-Wave Propagation Research and Applications During the War*

J. H. DELLINGER†, FELLOW, I.R.E., AND NEWBERN SMITH†, SENIOR MEMBER, I.R.E.

Summary—**This paper discusses the work done by the Interservice Radio Propagation Laboratory during World War II. The circumstances leading to the establishment of IRPL are described and the problems which are faced are stated. The measures taken in the solutions of these problems are outlined, and some of the results are presented. Specific services performed by IRPL during the war for the armed forces and commercial companies are recounted.**

THE INFLUENCE of the ionized layers of the earth's upper atmosphere, the ionosphere, on radio wave propagation has been recognized ever since the experiments of Breit and Tuve and of Appleton proved its existence. Because of the scarcity of adequate ionospheric data, however, and because relatively few radio men realized its importance, the use of ionospheric data in radio communications before the war was relatively small.

The important part played by radio during the war brought to light the necessity for having adequate radio propagation information. No matter how good the equipment was at the transmitting and receiving ends, satisfactory communication could not be had unless the waves were propagated with sufficient strength to be receivable. Variations in propagation conditions proved to be several orders of magnitude greater than variations in transmitter power or receiver sensitivity. Furthermore, the extreme crowding of the radio-frequency spectrum made necessary full utilization of all available frequencies, and an appropriate selection of frequencies could be made only with the help of radio propagation data. Also, security considerations dictated that the frequencies used should be the best for use and the least likely to be intercepted by the enemy. The design of equipment, especially of antenna systems, was found to depend critically upon a knowledge of radio propagation conditions. In addition, other applications of radio, such as radar and direction finding, involved considerations of propagation regarding range, accuracy, and receivable intensities.

With the widespread use of radio communication by the armed forces, especially in parts of the world where but little experience had been had, the need for improved radio propagation information became apparent early in the war. An aircraft disaster in the European Theater led to the establishment of the British Inter-Services Ionosphere Bureau (ISIB) in 1941, and the exigencies of air force operation in the Southwest Pacific resulted in the formation of the Australian Radio Propagation Committee (ARPC), both instituted to furnish radio propagation data and predictions to their respective armies, navies, and air forces. Correspondingly, in 1942, the Interservice Radio Propagation Laboratory (IRPL) was established in the National Bureau of Standards by order of the U. S Joint Chiefs of Staff, acting through the Wave Propagation Committee of the U. S. Joint Communications Board, with the functions of (1) centralizing data on radio propagation and related effects, from all available sources, (2) keeping continuous world-wide records of ionosphere characteristics and related solar, geophysical and cosmic data, and (3) preparing the resulting information and furnishing it to the armed forces. This involved maintaining ionospheric observatories, centralizing data from these and other ionospheric observatories operated by other agencies and other countries, performing experimental and research work as necessary to supplement existing sources of data, preparing predictions and forecasts of radio propagation conditions for all parts of the world, issuing charts, tables, handbooks, and bulletins for immediate dissemination to the armed forces, maintaining a "special problem" consulting service to give immediate answers to urgent military problems, and co-operating in this work with other agencies of the United Nations.

The groundwork for the prediction of radio propagation conditions and ranges of useful frequencies had been laid by the previous ionosphere researches of the National Bureau of Standards, some of the results of which were published in the PROCEEDINGS OF THE I.R.E. from 1937 to 1940, under the title, "Characteristics of the Ionosphere at Washington, D. C." During 1941 to 1943, at the request of the National Defense Research Committee, the National Bureau of Standards made a study of the correlation of direction-finder errors with ionospheric conditions, and prepared a "radio transmission handbook" to permit usable frequency calculations.

In meeting the requirement of predicting useful frequencies over any paths anywhere in the world, the IRPL was confronted by five major problems: (1) the obtaining of adequate ionospheric data on a world-wide basis, (2) the development of methods for calculating maximum usable frequency over long paths, (3) the development of methods for calculating sky-wave field intensities, (4) the determination of minimum required field intensities, and (5) the development of methods for forecasting ionosphere storms.

* Decimal classification: R112.41×R113.65. Original manuscript received by the Institute, January 15, 1947; revised manuscript received, May 2, 1947. Presented, 1946 Winter Technical Meeting, New York, N. Y., January 26, 1946.

† Interservice Radio Propagation Laboratory, National Bureau of Standards, Washington, D. C.

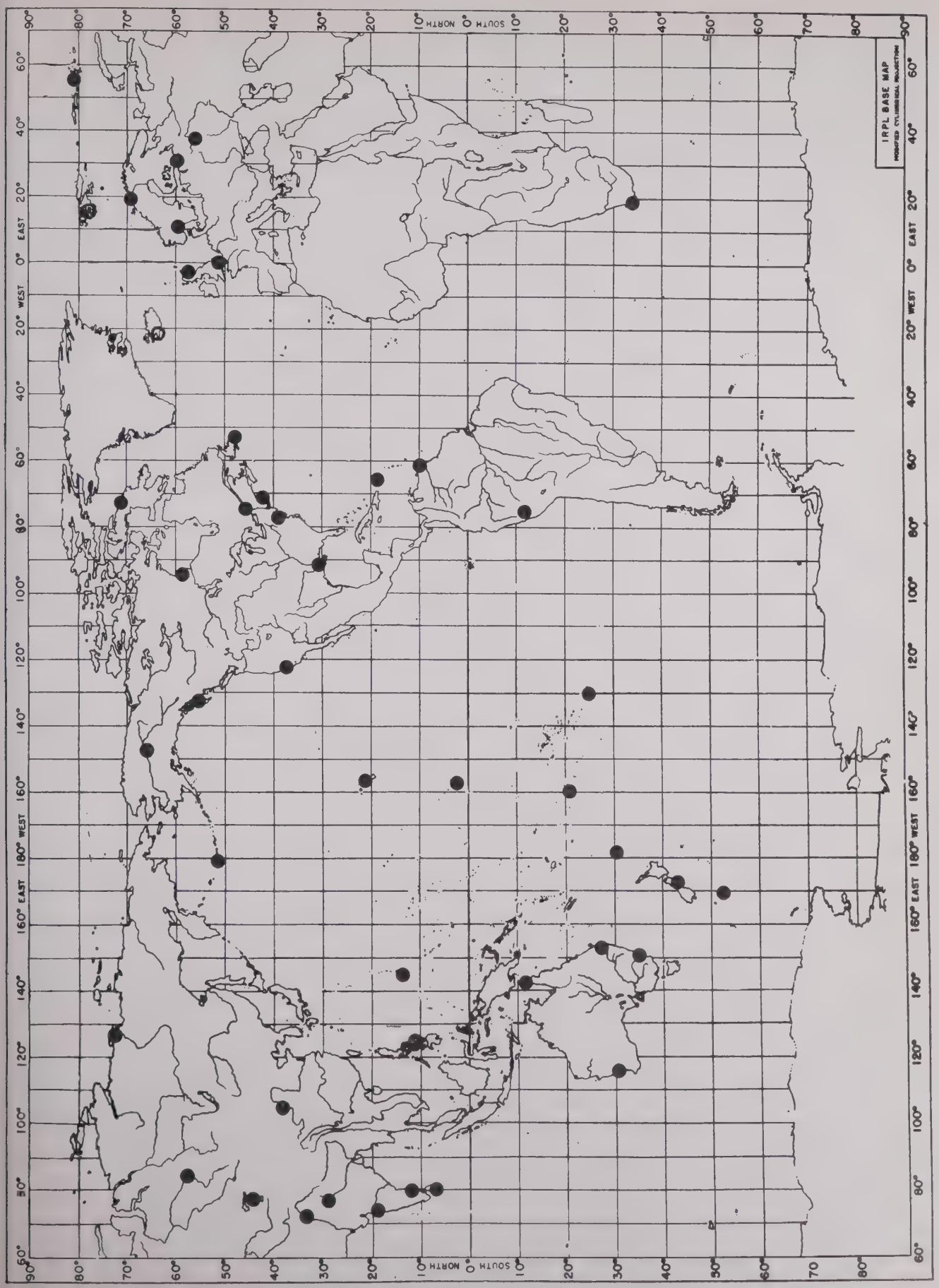

Fig. 1—Active ionospheric stations reporting data to IRPL in 1945.

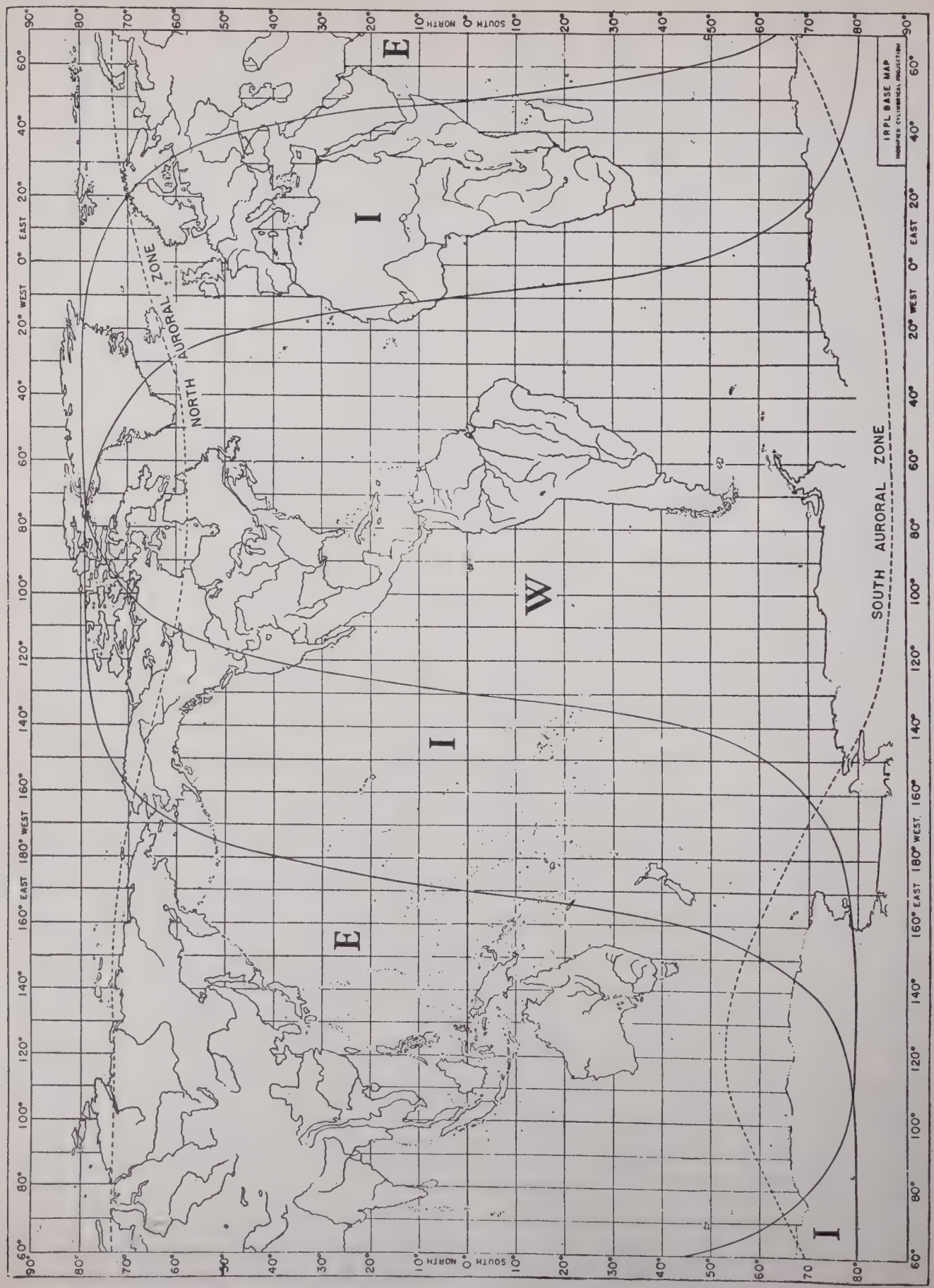

Fig. 2—World map showing zones covered by predicted charts.

At the outset, the IRPL was faced with the necessity of obtaining sufficient ionospheric data to permit predictions to be made anywhere in the world. At that time ionospheric observations were being made only at six locations in the world: Washington, D. C.; Slough, England; Huancayo, Peru; Watheroo and Sydney, Australia; and Christchurch, New Zealand. Regular data were available to the IRPL only from the first, third, and fourth of these. Immediate steps were taken to expand the world-wide coverage, with the cooperation of the Carnegie Institution of Washington; the United States Army and Navy; the Canadian Navy and Air Force; the British Admiralty, ISIB, the National Physical Laboratory and the British Broadcasting Corporation; the Australian organization, the ARPC; and the U.S.S.R., with the result that by the end of the war 44 stations were regularly reporting ionospheric observations, as shown in Fig. 1. This network of stations, together with analysis of radio traffic data from a number of communications networks, permitted the continual improvement of world charts of predicted ionosphere characteristics, from the small beginnings in 1941, based on only three stations, to the comprehensive charts now published monthly in the IRPL-D series reports. The knowledge gained from the greatly expanded world-wide ionospheric coverage permitted a much improved delineation of the regular variations of the ionosphere with latitude and local time, so that, for example, the hitherto seemingly anomalous behavior of northern and southern hemisphere stations fell into a consistent world picture.

In the course of their work it became necessary to place radio propagation predictions on a regular, world-wide basis, such that the great mass of data could be handled expeditiously and practical predictions issued regularly.

In order to use the data which were being received from all over the world for prediction purposes, it was necessary not only to understand their geographic, diurnal, and seasonal variations, but also to determine their relationship to relative sunspot numbers. A simple correlation of values of ionosphere characteristics with relative sunspot numbers had been previously found, but during the war trends of the variation of these characteristics with sunspot number were determined for the locations on earth of many of the ionosphere stations. A technique of prediction of ionosphere characteristics at any location, using standard statistical methods, was evolved, involving an estimate of the relative sunspot number for the month of prediction. A nomographic method for doing this type of prediction rapidly was later developed.

As another consequence of the improved world-wide coverage, the so-called "longitude effect" was discovered and put into operational use in 1943. This was the discovery that ionosphere characteristics were not, as previously supposed, the same, at the same local time, for stations at about the same latitude but different longitudes. Instead, they depended to a great extent on the geomagnetic latitudes of the station. Thus the station at Delhi, India, showed quite different characteristics from those observed at Baton Rouge, La.

Following this discovery, the world was divided, for practical operational purposes, into the three zones shown in the map of Fig. 2. In each zone the characteristics are independent of longitude, to a good enough practical approximation.

The second problem faced by the IRPL was the development of a simple rapid method of obtaining the maximum usable frequency (m.u.f.) over any paths in any part of the world. The groundwork for this was laid in 1936 when the "transmission curve" method of scaling ionospheric records was devised, leading to factors which could be applied to critical-frequency data to obtain m.u.f. values. These factors were satisfactory for distances up to 2500 miles, but for greater distances the method of multiple hops proved clumsy and, indeed, quite inadequate in the light of observed radio propagation data.

Consequently, the empirical "two-control point" method was devised (independently at the IRPL and ISIB) for paths longer than 2500 miles, whereby the m.u.f. over such a path is limited by the lower of the 2500-mile m.u.f. at two control points, 1250 miles from each station along the great-circle path connecting the two stations. This procedure gave much better results. As the volume of data increased, it became more and more apparent that normal F_2- or E-layer propagation was completely inadequate to account for a considerable part of the observed transmissions, particularly at times when E_s (sporadic E) was present. Consequently an extended analysis of E_s occurrence was made, and sufficient regularity was found to make E_s predictions possible, subject to the much wider day-to-day variability than in the case of the normal layers. Considerable further improvement in m.u.f. calculations was then made by including the effects of "sporadic-E" (E_s) propagation, also on a two-control-point basis.

World charts were prepared giving predictions of maximum usable frequencies, three months in advance. These, are continued in the monthly publication now issued through the Government Printing Office.

The urgent need for knowing distance ranges and lowest useful high frequency (l.u.h.f.) led to the next major problem undertaken by the IRPL—the calculation of sky-wave field intensities. To meet this, the field-intensity-recording program, begun by the National Bureau of Standards early in the last decade, was greatly expanded by installation of recorders at the new United States ionospheric stations. Fig. 3 shows a sample automatic field-intensity record. At the same time, theoretical studies of ionospheric absorption at oblique and vertical incidence were undertaken, in an attempt to obtain a simplified solution to the problem as rapid in operation as the method of calculating m.u.f.

An "equivalence theorem," similar to that used in

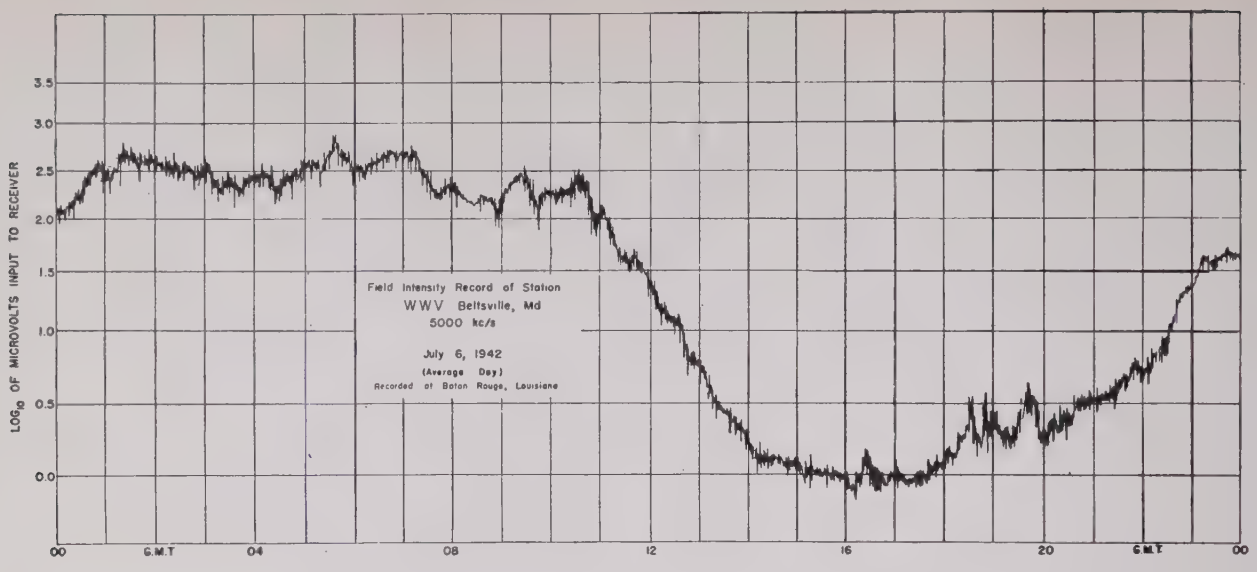

Fig. 3—Continuous automatic record of received radio field intensities.

calculating m.u.f., was used, employing the observed field-intensity data to supply numerical values to the many uncertain factors in the equation. It was found that the diurnal variation of ionospheric absorption varied to a good approximation, on the average, linearly with the cosine of the zenith angle of the sun, a fact which simplified greatly the integration of ionospheric absorption over a given transmission path; the absorption could then be determined as a function of frequency, distance, and average solar zenith angle over the path.

The determination of sky-wave field intensity did not of itself give the whole story, however, unless information also could be available as to the minimum fields required for radio communication. Thus, the fourth major problem confronting the IRPL was the determination of minimum field intensities necessary to overcome atmospheric radio noise, which was the principal type of noise encountered at sky-wave frequencies. This is still the subject about which least is known in the field of sky-wave communication. Some fragmentary measurements were available, and a beginning on the problem had been made at the ISIB in England. All available data on atmospheric radio noise and required fields were collected, as well as data on thunderstorms, which are the source of atmospheric noise. The result of the analysis was to divide the world into zones corresponding to different grades of noise intensity, taking into account both the generation and the propagation of the noise. Fig. 4 shows one such chart, for November through March. The principal noise-generating centers are in the East Indies, Central and South America, and Africa, with secondary centers in the tropical oceans—the "doldrum belts." For each noise grade, a set of curves of required intensities was constructed, similar to the one shown in Fig. 5. These were for good 95 per cent intelligible radiotelephone communications, and empirical factors were deduced for other types of service; for example, manual c.w. telegraphy required only 1/7 as great intensities, while four-tone single-side-band six-channel radio teletype might required only 1/14 as great intensities. Much of this work was done with the close collaboration and assistance of the Radio Propagation Unit of the Office of the Chief Signal Officer of the U. S. Army.

For convenience in use, the required field graphs were plotted on nomograms involving frequency and absorption index, so that the l.u.h.f. could be read off directly.

The fifth major problem of the IRPL was the forecasting of ionosphere storms—those abnormalities often associated with geomagnetic storms—which disrupt radio communications, especially in the Arctic. The military importance of the North Atlantic, which reaches into the auroral zone, or zone of maximum disturbance, made it indeed urgent to know when communications were likely to be interrupted. The urgency is apparent when it is realized that aircraft depended largely on radio aids for navigation over the North Atlantic.

Therefore a program was undertaken, in collaboration with the Department of Terrestrial Magnetism, Carnegie Institution of Washington, to study the relations between ionosphere storms and the sun, whose radiations produce the storms. Improved observational techniques, like the Harvard University coronagraph, a device for photographing the extremely active solar corona, contributed to the study. As a result of the analysis, a weekly forecast was issued, which proved to be of some value to the armed services. The world was divided into zones of varying ionospheric disturbance, as shown in Fig. 6, and forecasts were made for each zone.

A different approach, however, led to a considerably

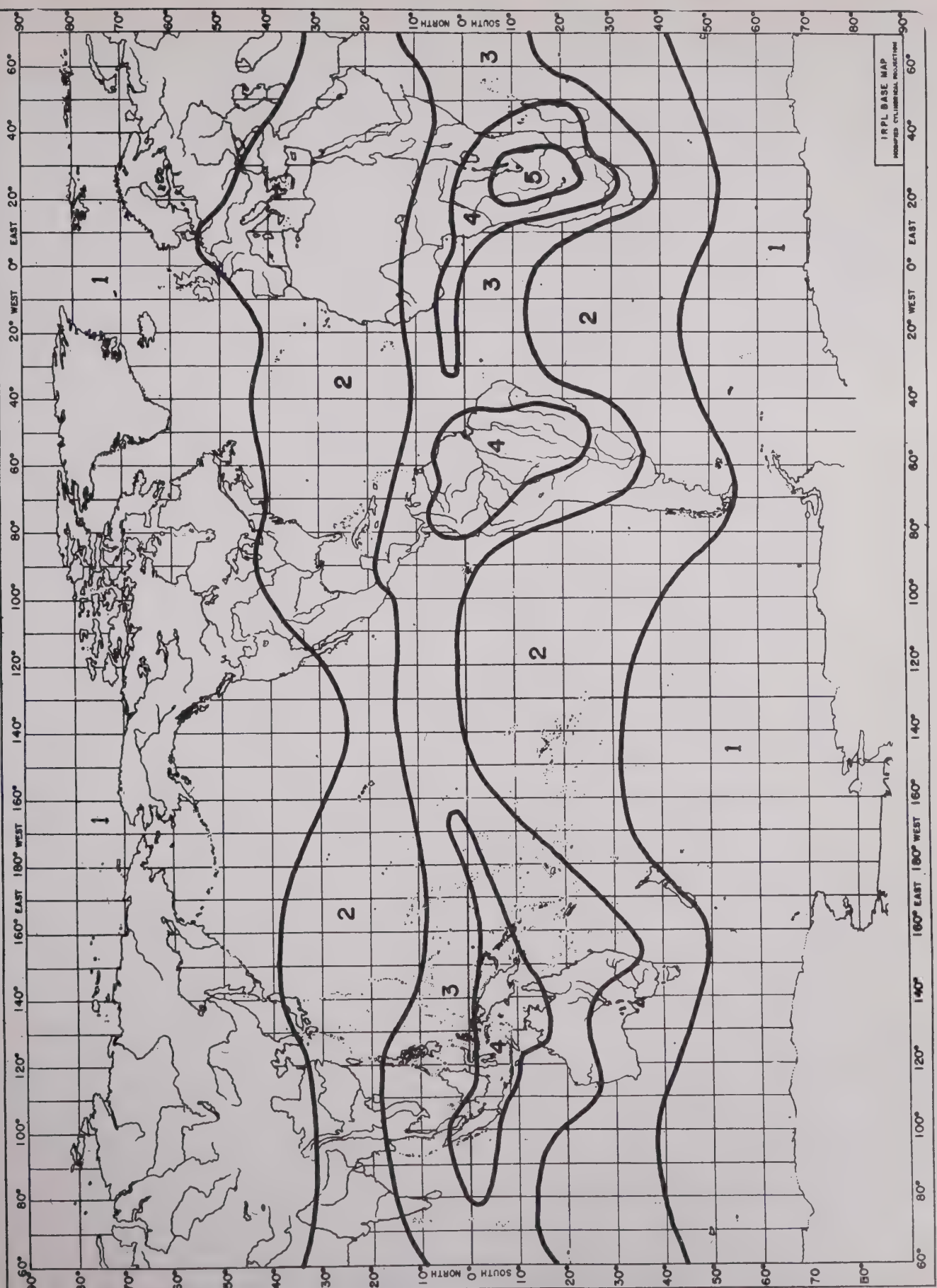

Fig. 4—Map showing atmospheric radio noise zones (November through March).

more accurate service of forecasting disturbances a shorter time in advance. In this, studies of the behavior of radio-d.f. bearings over the North Atlantic path showed that it was possible to issue warnings of radio disturbance a few hours to a half day or more in advance. Consequently a short-time warning service was

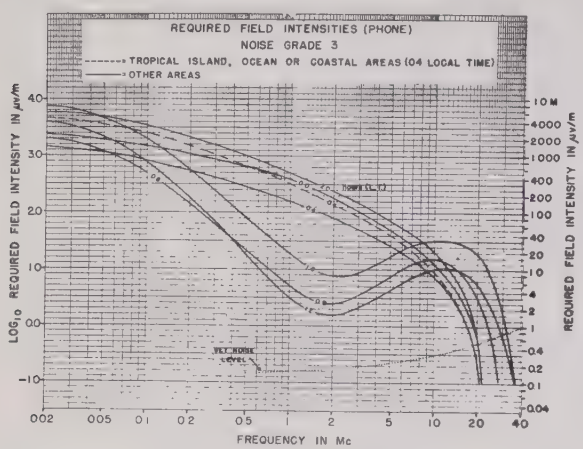

Fig. 5—Minimum field intensities required for satisfactory radiotelephone communications in the presence of atmospheric radio noise (noise grade 3).

inaugurated whereby such warnings were telephoned and telegraphed daily to interested agencies. With the lifting of wartime restrictions, this warning service is now being broadcast regularly over WWV, the National Bureau of Standards station at Beltsville, Md., at 20 and 50 minutes past each hour. A group of N's or W's is transmitted, the former meaning "no warning" (quiet conditions expected) and the latter "warning" (disturbed conditions over the North Atlantic expected or in progress).

During the war the IRPL performed many specific services for the armed forces and commercial companies doing war work, involving consultation and advice, on their special problems involving radio wave propagation. Types of problems included the determination of best usable frequencies for specified services, such as point-to-point, short-distance tactical operations, plane-to-ground, high-frequency broadcast, the prediction of ground-wave and sky-wave distance ranges under different conditions, advice as to types of antennas and lowest required radiated power for specified purposes, and frequency allocation. As the techniques promulgated by IRPL became more widely disseminated, many types of problems, especially those in frequency allocation, were eventually solved by the Army and Navy groups in which they originated.

In January, 1944, a two-weeks training course in radio wave propagation was given by IRPL. It was for officers who were to be taught the principles of radio wave propagation and methods of problem solution and then assigned to overseas communication groups, where they could put on a scientific basis the assignment of radio operating frequencies in the field. Others were then to be sent to training units within the United States to organize courses in which additional officers could be instructed in this work. The student body consisted of two groups, the first group consisting of eleven Army Air Forces officers, four officers from the Signal Corps, and three Navy officers, and the second group consisting of fifteen enlisted men and one officer from the Signal Corps, who formed the nucleus of the Radio Propagation Unit of the Signal Corps. The course comprised twenty-five lectures by scientists and others working directly in radio wave propagation, interspersed with problem sessions in which the students were coached in the solution of practical radio wave propagation problems.

As a further aid in determining the proper usage of radio frequencies, three handbooks were issued. The first handbook, "Radio Transmission Handbook—Frequencies 1000 to 30,000 kc.," was issued in January, 1942, giving the basic principles of radio sky-wave propagation, and such computational procedures as were extant at that time, together with preliminary versions of prediction charts and predictions for the winter. A supplement to this handbook was issued June 1, 1942, which gave summer predictions.

On November 15, 1943, the "IRPL Radio Propagation Handbook, Part 1" was issued. This handbook, issued as an IRPL publication, and also as an Army training manual (TM 11-499) and a Navy publication (DNC-13), gave a descriptive discussion of the behavior of the ionosphere and of the theory behind maximum usable frequencies and lowest useful high frequencies. Prediction charts of maximum usable frequencies and absorption constants were given. Techniques for the determination of m.u.f. and l.u.b.f. over any path at any time were given to the extent that they had been developed at the time. It is impossible to express fully the valuable aid and support received by the IRPL from other agencies. Close and continuous liaison was maintained with the Department of Naval Communications (CNO) and the Radio Propagation Unit of the Army Signal Corps (SPSOL); valuable assistance and suggestions were interchanged with personnel in those departments working with IRPL in the solution of basic problems and applications. Close co-operation was maintained with other branches of the Army and Navy having need of radio propagation data, including the Army Security Agency, the Army Air Forces, other branches of the Signal Corps, the Navy Bureau of Ships, Bureau of Aeronautics, Coast Guard, and other branches of Naval Operations.

Acknowledgment is made to the Department of Terrestrial Magnetism, Carnegie Institution of Washington, for its extremely valuable assistance in operating ionosphere stations and collecting much of the geophysical and solar data upon which the services of the IRPL were based, and to the untiring work of its staff in cooperating in the entire radio propagation program. Acknowledgment is also wholeheartedly given to the full co-operation, from the very beginning, of the radio prop-

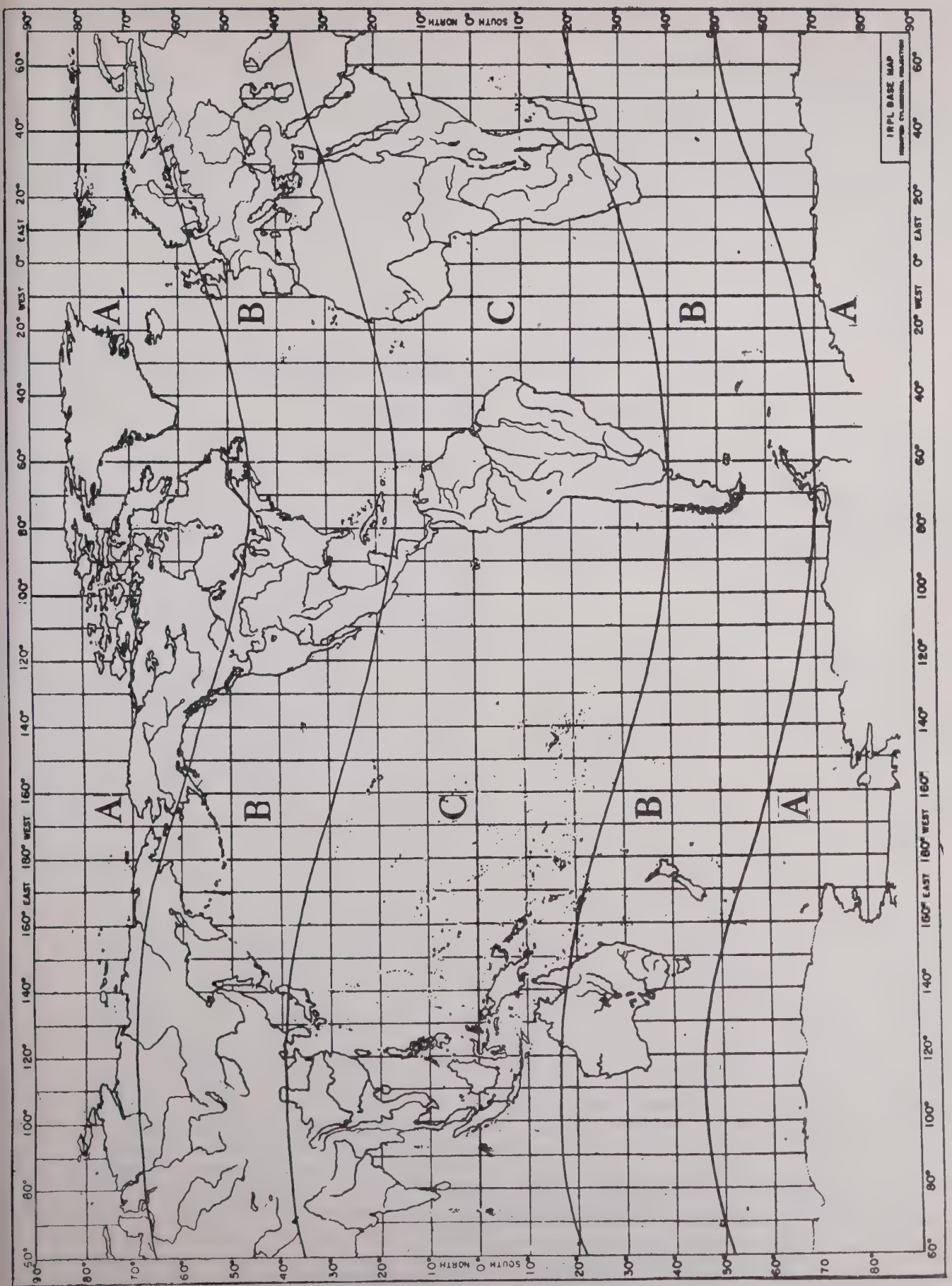

Fig. 6—World map showing zones of different degrees of ionospheric disturbance.

agation organizations of other countries—Canada, Great Britain, Australia, and New Zealand—without which no world-wide radio propagation program would have been possible.

Many commercial organizations and other agencies gave valuable assistance to the work of the IRPL. An analysis of radio traffic data was regularly provided by United States communication companies, such as RCA Communications, Mackay, Press Wireless, and A. T. & T., from Army and Navy networks, and from other Government agencies such as the C.A.A. and the F.C.C.; this analysis assisted greatly in predicting and checking predictions of usable frequencies, and in correcting and corroborating theoretical processes of analysis.

With the conversion to the postwar era, the work of the IRPL is carried on and extended by the Central Radio Propagation Laboratory of the National Bureau of Standards. Particular emphasis is laid on research in radio propagation at all frequencies.

Alternating-Current Measurements of Magnetic Properties*

HORATIO W. LAMSON†, FELLOW, I.R.E.

Summary—**Herein is presented a critical analysis of various procedures for determining the permeability and core loss of ferromagnetic materials, together with a discussion of the limitations under which such observations are made and the interpretations which should be applied to the data obtained.**

Introduction

IT IS THE purpose of this paper to discuss various methods for the a.c. measurement of the magnetic properties of a specimen of ferromagnetic material and, it is hoped, to clarify certain phases of these techniques about which some misunderstanding has existed. The system of magnetic nomenclature and definitions recently adopted by the American Society for Testing Materials[1] will be used.

Magnetic Condition of the Specimen

It is a well-known, but sometimes ignored, fact that all ferromagnetic materials exhibit the phenomenon of hysteresis and have, in effect, a "memory," so that any present (instantaneous) condition is more or less influenced by past events. To obtain significant and reproducible data it is first essential to erase all memory of previous conditions. This preliminary demagnetization may be accomplished by subjecting the specimen to a substantial a.c. magnetization which is then gradually reduced to zero. Thereafter, any applied a.c. magnetization must be removed by a gradual reduction to zero, rather than by interrupting the circuit at some arbitrary time in the cycle.

If any subsequent magnetization is then due to a symmetrically alternating current (having no d.c. component), the specimen will be in a symmetrically cyclically magnetized (SCM) condition, wherein the mean values of both induction and magnetizing force are zero. For either polarity of magnetization, the *peak* values of each of these parameters will be equal, and are designated as their *normal* values.

In addition to hysteresis, it is less generally known that some materials exhibit a definite *magnetization lag*. If, having acquired in them a stabilized variation in B and H, a change is made in the amplitude of the cyclic variation of H, some time (representing a considerable number of cycles) may elapse before a completely stabilized variation and a new maximum value of induction is attained. This magnetization lag appears to be more pronounced for a given increase than for a corresponding decrease in magnetizing force, doubtless due to the effect of retentivity.

When measuring a specimen at different values of cyclic H, it would thus appear desirable to start with the maximum contemplated value and successively reduce this parameter. For incremental measurements, however, the biasing component of H must be increased progressively from an initially demagnetized condition to avoid any retentivity in the biasing H.

It should be remembered that the magnetic properties of some materials may, to a certain degree, be modified by mechanical strains in punching operations on flat laminations, or in the rolling of flat stock into toroidal cores. Subsequent metallurgical treatment may then be necessary to restore the natural magnetic condition of the material. The author is of the opinion, however, that a limited amount of easy and careful shearing may not disturb the specimen as much as is sometimes anticipated (see Appendix E).

* Decimal classification: R282.3. Original manuscript received by the Institute, March 11, 1947; revised manuscript received, July 10, 1947. Presented, Rochester Fall Meeting, November 11, 1946, Rochester, N. Y.

† General Radio Company, Cambridge, Mass.

[1] A.S.T.M. Specification A127-44T, 1944 Book for Metals, pp. 1437–1443.

Interpretation of an Iron-Cored Inductor

A simple iron-cored inductor consists physically of a ferromagnetic core circumscribed N times by a single conductive winding. This inductor possesses two types of impedance: a reactive component corresponding to energy storage without loss, and a resistive component representing eddy current, hysteresis, and ohmic heat losses. The core is assumed to be homogeneous and to have a uniform cross section A and a mean length λ for the flux path (c.g.s. units), so that the core reluctance is given by

$$\mathcal{R} = \frac{\lambda}{\mu A}. \tag{1}$$

With this geometric symmetry, the specimen will be subjected to the same values of induction and magnetizing force at all points. This paper deals with the basic concepts of magnetic measurements, thereby assuming that any leakage flux is negligible and that all the flux traverses an iron path and links completely any winding on the inductor.

The specimen core may be constructed of rectilinear strips overlapping at their extremities to form an Epstein square; it may have a shell-type configuration, or it may be toroidal in shape and assembled by stacking annular laminations, by rolling flat stock spiral-wise, or by molding iron-dust mixtures. The author also has used rectangular strips of the specimen material forming a diameter across annular laminations, the latter having sufficiently high permeability and increased cross section to offer negligible reluctance.[2]

It is a natural and long-established practice to visualize the total impedance Z of this inductor as the rectilinear sum of its inductive reactance ωL_s and its equivalent series resistance R_s accounting for all losses (see Fig. 1). The parameter L_s is the equivalent series

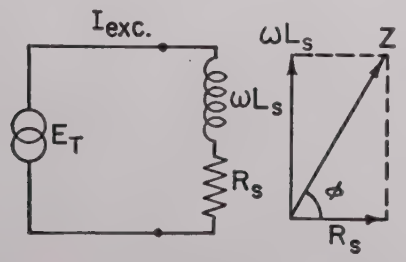

Fig. 1—Series representation of an inductor.

inductance and ϕ is the phase angle of the inductor having a dissipation factor D. Then the vector impedance value becomes

$$Z = R_s + j\omega L_s \tag{2}$$

while

$$D \equiv \cot \phi = \frac{R_s}{\omega L_s}. \tag{3}$$

While this representation is mathematically permissible, it does not correspond to certain empirically determined facts concerning the electromagnetic behavior of the inductor.

Consider Fig. 1, which implicitly stipulates that the application of an external a.c. terminal voltage E_T produces an exciting current I_{exc} which, circumscribing the core N times, creates a magnetomotive force which, in turn, produces the flux therein. If i is the instantaneous value of the exciting current, the instantaneous value of the magnetomotive force is frequently considered to be given by

$$F = 0.4\pi N i, \tag{4}$$

and to be in phase with i. The instantaneous value Φ of the flux in the core will be the ratio of F to the core reluctance. Stipulating that the production of flux by a magnetomotive force is an instantaneous phenomenon, it would apparently follow that *the flux is in phase with the exciting current* (see Fig. 2).

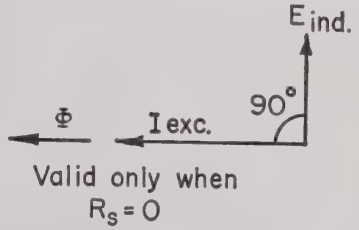

Fig. 2—Phases in an inductor with no loss.

Another basic law of physics states that the instantaneous voltage induced in a circuit e_{ind} is proportional to the rate of change of the flux linking this circuit.

$$e_{ind} = -\frac{N}{10^8}\frac{d\Phi}{dt}. \tag{5}$$

If the flux is varying sinusoidally,

$$\Phi = \Phi_{max} \sin \omega t, \tag{6}$$

whence

$$e_{ind} = -\frac{\omega N \Phi_{max}}{10^8} \cos \omega t. \tag{7}$$

Comparing (6) and (7), it follows that *the induced voltage and the flux are in quadrature*, e_{ind} lagging Φ by an angle $\pi/2$. Fig. 2 shows these phase relationships at the arbitrary instant when e_{ind} has a maximum positive value.

Correlation of the italicized statements in the two preceding paragraphs leads to the *erroneous* conclusion that the induced voltage lags the exciting current by $\pi/2$. By applying a secondary winding to the inductor it

[2] Horatio W. Lamson, "A method of measuring the magnetic properties of small samples of transformer laminations," Proc. I.R.E., vol. 28, pp. 541–548; December, 1942.

can be demonstrated that the induced voltage lags the exciting current by an angle $\pi/2$ plus the hysteretic angle β. Consequently, the flux is *not* in phase with the full exciting current, but lags I_{exc} by the angle β. These correct phase relationships are indicated in Fig. 3, which

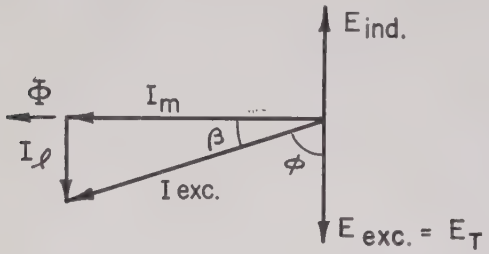

Fig. 3—Phases in an inductor with core loss, but no copper loss.

assumes zero copper loss in the inductor winding. In this case, the exciting voltage (always equal in magnitude and opposite in phase to the induced voltage) is the applied terminal voltage and, hence, leads I_{exc} by the phase angle ϕ. This makes β the complement of ϕ in Fig. 3.

Since the production of flux, per se, represents a storage of energy with no dissipation (disregarding radiation), and since flux must be in phase with that current which produces it, it follows that the exciting current must be the vector sum of two quadrature components; namely, the true magnetizing current I_m in phase with the flux, and the loss current I_l which, when squared and multiplied into the proper resistance, gives the power dissipation in the core of the inductor.

The magnetizing current, from which the magnetomotive force and flux may be calculated, is thus but a portion of the exciting current and is given by

$$I_m = I_{exc} \cos \beta. \tag{8}$$

Likewise, if copper loss can be neglected,

$$I_m = I_{exc} \sin \phi. \tag{9}$$

It is apparent that the magnetizing current must be produced by an exciting voltage E_{exc} equal and opposite to E_{ind}, and hence leading I_m by $\pi/2$. The voltage E_l producing the loss current must be in phase with that current. Consequently, both I_l and E_l must be coincident in phase with the exciting voltage.

Parallel Concept Neglecting Copper Loss

These current and voltage relationships are quite incompatible with the series representation of the impedance components of an inductor (Fig. 1). However, if it is considered that E_l and E_{exc} are not only coincident but also equal in magnitude, and hence may be the *same* voltage, the representation of the inductor by parallel admittance or impedance components agrees with the known facts (see Fig. 4). The purely reactive path, involving flux energy storage, I_m in quadrature with E_{exc}, consists of the equivalent parallel inductance L_p and carries the magnetizing current; while the purely resistive path, involving core losses, I_l in phase with E_{exc}, consists of the equivalent parallel resistance R_p and carries the loss current. The impedance of this inductor has a vectorial value:

$$Z = \frac{R_p \omega L_p (\omega L_p + jR_p)}{R_p^2 + \omega^2 L_p^2}. \tag{10}$$

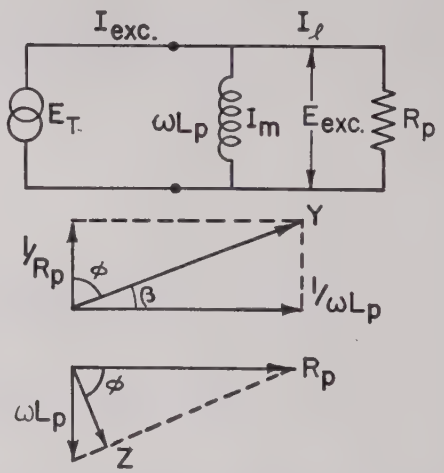

Fig. 4—Parallel representation of an inductor with core loss, but no copper loss.

Intercomparison between the impedance values of an inductor evaluated from its series and its parallel components establishes the well-known relationships:

$$L_p = L_s/\sin^2 \phi = L_s(1 + \cot^2 \phi) = L_s(1 + D^2) \tag{11}$$

$$R_p = R_s/\cos^2 \phi = R_s(1 + \tan^2 \phi) = R_s(1 + Q^2) \tag{12}$$

$$D \equiv \cot \phi = \frac{1}{Q} = \frac{R_s}{\omega L_s} = \frac{\omega L_p}{R_p}. \tag{13}$$

Parallel Concept with Copper Loss

When representing the inductor by Fig. 4, the parallel resistance R_p *should* correspond, strictly, only to *magnetic* losses due to hysteresis and eddy currents. Any *ohmic* losses (copper losses) must be represented by an additional series resistance R_c which carries the full exciting current (see Fig. 5). The purely reactive impedance $\omega L'$ is in parallel with the resistance R', which accounts for the magnetic losses. The vector impedance of this network takes the more elaborate form:

$$Z = \frac{R_c R'^2 + \omega^2 L'^2 (R_c + R') + j\omega L' R'^2}{R'^2 + \omega^2 L'^2}, \tag{14}$$

involving both R' and L' in its real and imaginary components, but R_c only in its real component. From (2) and (14),

$$L' = L_s[1 + (D - D_c)^2] \tag{15}$$

$$R' = (R_s - R_c)\left[1 + \frac{1}{(D - D_c)^2}\right]$$

$$= \omega L_s\left[D - D_c + \frac{1}{D - D_c}\right] \tag{16}$$

where the "copper-loss" dissipation factor D_c is defined as

$$D_c \equiv \frac{R_c}{\omega L_s} \cdot \tag{17}$$

As long as skin effect in the inductor winding is negligible, R_c may be considered to be the d.c. resistance of the winding. Note that both L' and R' differ from the L_p and R_p values of Fig. 4.

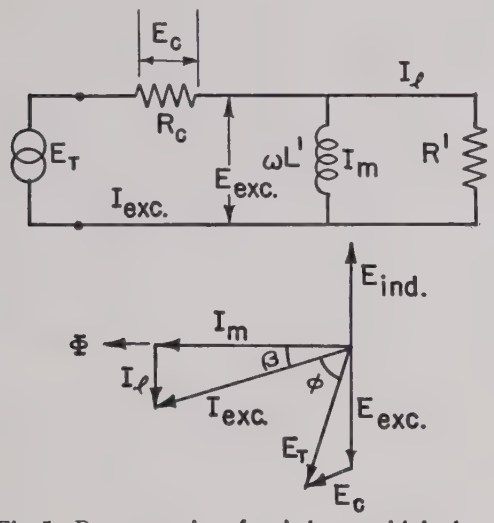

Fig. 5—Representation of an inductor with both core and copper losses.

The inclusion of copper losses gives rise to a small copper-loss voltage drop E_c in phase with the exciting current, so that the terminal voltage E_T exceeds the exciting voltage and β is less than the complement of ϕ. Whenever D_c is not a negligible component of D, the magnetizing current must be evaluated by (8), or by

$$I_m = \frac{I_{exc}}{\sqrt{1 + (D - D_c)^2}} \cdot \tag{18}$$

The loss current will be

$$I_l = I_{exc} \sin \beta = \frac{I_{exc}(D - D_c)}{\sqrt{1 + (D - D_c)^2}} \cdot \tag{19}$$

Finally, from the geometry of Fig. 5, the exciting voltage may be computed in terms of the terminal voltage:

$$E_{exc} = \frac{E_T \sin \phi}{\cos \beta} = E_T \sqrt{\frac{1 + (D - D_c)^2}{1 + D^2}} \cdot \tag{20}$$

Evaluation of Normal Permeability

Normal permeability, hereinafter symbolized as μ, is defined as the ratio of the normal, or peak, value of the induction (flux density) B to the corresponding normal (peak) value of the magnetizing force H, when the magnetic material is in a symmetrically cyclically magnetized (SCM) condition.

$$\mu \equiv \frac{B}{H} \cdot \tag{21}$$

To measure normal permeability, which, as will be shown later, is the most significant of the several "a.c. permeabilities," the normal magnetizing force may be evaluated in terms of the peak magnetizing current, represented by the symbol $\hat{I}_m$, regardless of the wave form of this current.

$$H = \frac{0.4\pi N \hat{I}_m}{\lambda} \cdot \tag{22}$$

Note that the true *magnetizing* current, rather than the exciting current, is involved here. If the flux has a cyclic variation which is symmetrical but not necessarily sinusoidal, the normal induction can then be evaluated in terms of the half-period average or the effective (r.m.s.) values of the exciting voltage by the following equation:

$$B = \frac{10^8 E_{exc}\,(\text{av.})}{4NAf} = \frac{10^8 E_{exc}\,(\text{r.m.s.})}{4(ff)NAf} \cdot \tag{23}$$

The third member of (23) is derived from the second member by defining the form factor (ff) of a cyclic variation as the ratio of its effective to its half-period average value.

The normal permeability for any symmetrical variation (SCM condition) is then:

$$\mu = \frac{10^8 \lambda E_{exc}\,(\text{av.})}{1.6\pi N^2 A f \hat{I}_m} \cdot \tag{24}$$

Normal Permeability With Sinusoidal Parameters

On the hypotheses that H and B are varying in a sinusoidal manner, the form factor of all cyclic parameters becomes $\pi/2\sqrt{2} = 1.11072\ldots$. The normal induction can be evaluated in terms of the peak or the r.m.s. value of the exciting voltage:

$$B = \frac{10^8 E_{exc}\sqrt{2}}{\omega NA} = \frac{10^8 \hat{E}_{exc}}{\omega NA} \cdot \tag{25}$$

Then the normal permeability becomes

$$\mu = \frac{10^8 \lambda E_{exc}}{0.4\pi N^2 A \omega I_m} = \frac{10^8 \lambda L'}{0.4\pi N^2 A}, \tag{26}$$

since, by definition, the parallel reactance $\omega L'$ equals the ratio E_{exc}/I_m.

Thus normal permeability, for any specified normal induction or normal magnetizing force, may be evaluated in terms of the geometry of the core and a measured value of the *parallel* inductance L'. It should be recalled that most inductance-measuring bridges yield directly the equivalent *series* inductance (Maxwell, Owen, Hay). Using (15), the normal permeability evaluated in terms of the *series* inductance becomes

$$\mu = \frac{10^8 \lambda L_s [1 + (D - D_c)^2]}{0.4\pi N^2 A}, \tag{27}$$

and demands a knowledge of the dissipation factors of the inductor.

The substantial error which may be introduced by omitting the factor $[1+(D-D_c)^2]$ in (27) and evaluating normal μ directly in terms of L_s, using the concepts of Fig. 1, is demonstrated in Appendix A. The effect of neglecting copper loss and assuming that D_c is negligible at lower frequencies is demonstrated in Appendix B.

If copper loss may be neglected, so that Fig. 4 is valid, it can be demonstrated[3] that normal permeability may be computed in terms of the reactive power P_q, measured in vars, which is taken by the inductor, together with the frequency f, the core volume V (cubic centimeters), and either the normal induction or the normal magnetizing force:

$$\mu = \frac{B^2 fV}{0.4 \times 10^8 P_q} = \frac{0.4 \times 10^8 P_q}{H^2 fV}. \qquad (28)$$

Effects of Harmonic Distortion

Due to the nonlinear character of the d.c. magnetization curve and the phenomenon of magnetic saturation, an inherent distortion exists in the core material, so that, with a generator developing, per se, a pure sinusoidal voltage, the cyclic variations of H and/or B will contain odd-harmonic components. Furthermore, the relative distortion in either parameter will be a function of the series resistance of the circuit.

Assuming no copper losses in the winding, if the inductor could be connected directly across the terminals of a resistanceless sinusoidal generator, the exciting voltage applied across the inductance L_p (Fig. 4) would be sinusoidal. The induced voltage and the flux variation would then have to be sinusoidal and harmonic distortion would exist in the magnetizing current and in H. Total lack of flux distortion would demand an impossible circuit of zero series resistance. On the other hand, if the series resistance of the circuit is made very large compared with the reactance of the inductor, the generator would be working into an essentially resistive load, so that both the exciting and magnetizing currents, and hence H, would be practically sinusoidal. Distortion would then exist in both the induced voltage and the cyclic variation of flux.

The existence of flux distortion may, in many cases, be demonstrated by examination of the terminal voltage of the inductor with a cathode-ray oscillograph or, more precisely, with a harmonic analyzer. It is not universally recognized, however, that, if the resistance of the sinusoidal generator is low, an examination of the terminal voltage of the inductor may not show the existing flux distortion which is introduced by the internal copper-loss resistance R_c (Fig. 5). An infallible procedure for observing true flux distortion would be the examination of the open-circuit voltage induced in a secondary winding on the inductor core. An approximate evaluation of the distortion existing in H may be obtained by analyzing the exciting current, i.e., the voltage drop across a resistor in series with the inductor. To maintain the initial conditions, this resistance must be negligible compared to the reactance of the inductor, unless it is purposely made large to ensure a small distortion in H.

External circuit resistance thus increases flux distortion while reducing the distortion of magnetizing force. The presence of a nominal amount of circuit resistance gives harmonic distortion of *both* B and H, and yields somewhat ambiguous data which are a function of the measuring circuit external to the inductor. It would be desirable to have *one* of these parameters as free from distortion as possible. The question thus arises, should a.c. magnetic measurements be standardized at sinusoidal B or at sinusoidal H? The answer is somewhat determined by the method of measurement and the contemplated use of the specimen material. An empirical comparison between sinusoidal B and sinusoidal H measurements is given in Appendix A.

In the various *meter* methods of measurement the circuit resistance, using a low-resistance generator such as a 60-cycle power line, may be kept small, thus permitting a good approximation to sinusoidal B *if copper losses are small.*

Whenever the generator has a significant amount of resistance, and in most *bridge* methods of measurement which insert an appreciable amount of resistance into the circuit between the generator and the inductor, sinusoidal B is impossible. It would then appear desirable to go the whole distance and to standardize on conditions yielding sinusoidal H. This was done in a magnetic test set developed by the author[2] by inserting considerable resistance in series between the generator and the bridge, with a corresponding increase in the e.m.f. of the generator to obtain a specific normal H. Sinusoidal currents are thus ensured. If a selective null-balance detector, responsive to the *fundamental* component of the voltage induced in the inductor, is then employed, the conditions for bridge balance will correspond to sinusoidal values of both H and B. This will permit normal μ, referred to the fundamental components, to be evaluated in terms of the measured inductance by (27).

Regardless of any distortion in H, its normal value may be computed in terms of the peak value of the magnetizing current by the use of (22). When using nonselective measuring instruments it should be noted that, if appreciable distortion exists in the flux, (23) rather than (25) must be used for evaluating normal induction.

Normal μ Determined From the A. C. Hysteresis Loop

It is common practice to plot the a. c. hysteresis loop of a magnetic specimen by using as ordinates values of B obtained from the induced voltage, and as abscissae values of a pseudo-H computed from the *exciting* cur-

[3] An analysis first brought to the author's attention in an unpublished memorandum from S. L. Burgwin to J. P. Barton, dated February, 1942.

rent. This technique will be illustrated by some 60-cycle data taken at a small induction by Burgwin[3] upon an Epstein inductor having a Hipernik core and using a d. c. voltmeter together with a synchronous commutator to obtain values of B and H at successive phases around the loop.

The pseudo-H values measured by using a low-resistance, air-core mutual inductor in series with the specimen inductor were closely sinusoidal. Core losses are nonexistent in this mutual inductor, so that its value of R' becomes infinite and its hysteretic angle is zero. Consequently, the entire exciting current is producing flux, and the open-circuit secondary voltage may be calibrated in terms of the exciting current. It should be emphasized, however, that whenever such a mutual inductor is used, the current values obtained must be corrected by (8) before evaluating the normal magnetizing force in the specimen inductor from (22).

The B data (exciting voltage) were given a small correction to obtain the fundamental sinusoidal component which was given by

$$B = 682 \sin \omega t + 693 \cos \omega t. \tag{29}$$

The hysteretic angle was, therefore,

$$\beta = \cot^{-1}\left(\frac{682}{693}\right) = 45°28', \tag{30}$$

and the normal induction

$$B = \frac{682}{\cos \beta} = \frac{693}{\sin \beta} = 972 \text{ gausses.} \tag{31}$$

In Fig. 6, loop A is a duplication of Burgwin's data showing a semiloop corresponding to positive values of induction. Burgwin also gave the d. c. hysteresis loop C

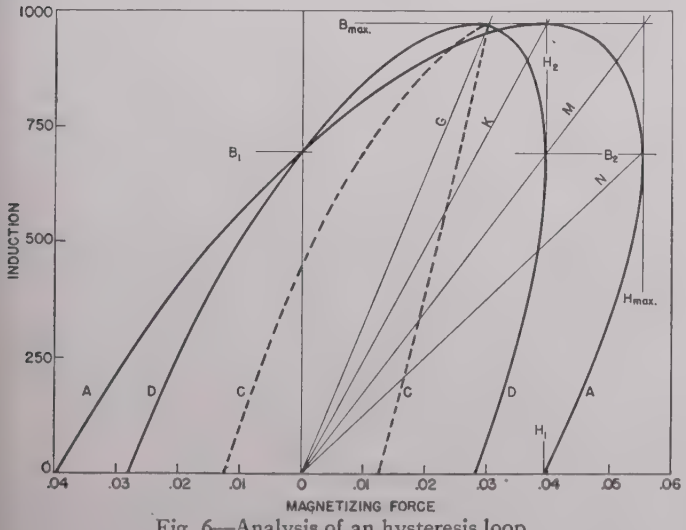

Fig. 6—Analysis of an hysteresis loop.

for the same specimen carried to the same maximum induction value. For loop C the abscissa values are, of course, true d. c. values of H. For loop A, however, the abscissae give pseudo-H values calculated in terms of *exciting* current. This loop shows six significant values as follows:

$H_{max} = 0.0550$ oersteds, maximum value of pseudo-H

$H_1 = 0.0392$ oersteds, pseudo-H corresponding to $B = 0$

$H_2 = 0.0386$ oersteds, pseudo-H corresponding to B_{max}

$B_{max} = 972$ gausses, maximum value of B, i.e., normal B

$B_1 = 693$ gausses, induction corresponding to pseudo-$H = 0$

$B_2 = 682$ gausses, induction corresponding to H_{max}.

Time sequence around this loop is counterclockwise and, since both components are sinusoidal, it can be shown that

$$\sin \beta = \frac{H_1}{H_{max}} = \frac{B_1}{B_{max}} \tag{32}$$

$$\cos \beta = \frac{H_2}{H_{max}} = \frac{B_2}{B_{max}} \tag{33}$$

$$\tan \beta = \frac{H_1}{H_2} = \frac{B_1}{B_2}. \tag{34}$$

The maximum H for the loop C is seen to be 0.0300 gausses; consequently, the d. c. permeability of the specimen has a value of 32,400, given by the slope of the radius G in gausses per oersted. Three different a. c. permeabilities may be defined from loop A.

The slope of the radius K gives

$$\mu_K \equiv B_{max}/H_2 = 25,200. \tag{35}$$

The slope of the line M gives

$$\mu_M \equiv B_{max}/H_{max} = 17,670. \tag{36}$$

The line M is not the major axis of the ellipse unless B_{max} and H_{max} are scaled to be equal distances on the diagram.

The slope of the radius N gives

$$\mu_N \equiv B_2/H_{max} = 12,395. \tag{37}$$

These permeabilities have the relation

$$\mu_{d.c.} > \mu_K > \mu_M > \mu_N, \tag{38}$$

and it can be shown from the above equations that μ_M is the geometric mean of μ_K and μ_N.[4]

The loop A encloses an area proportional to the total core loss because it is evaluated in terms of exciting current, which leads the flux and the true magnetizing current by the angle β.

If, for each induction value, the phase of the corresponding pseudo-H value is retarded by the angle β, the loop A degenerates into the line M, enclosing no

[4] This relation was pointed out by S. L. Burgwin.

area. Line M has the same H_{max} value as loop A, but has been made coincident in time with B_{max} (normal B). However, the magnitude of H_{max} is determined by the exciting current, so that, to determine the true path of B versus H variation, the abscissa value of each point on line M must be reduced by cos β (compare (8)). The true path is, therefore, line K, so that H_2 is the true normal H for the given normal B, and μ_K (slope of line K) is, in fact, the normal permeability of the specimen.

This same result may be achieved by first reducing the abscissa of each point of loop A by cos β, giving loop D. Then when, for each B value of loop D, the corresponding H value is retarded by the angle β, this loop degenerates into the line of operation K which encloses no area, since the loss component of the exciting current has been removed.

Assuming a negligible value of copper loss, the significance of μ_N may be seen by taking the ratio of (35) to (37) and substituting from (33) to obtain

$$\mu_N = \mu_K \cos^2 \beta = \mu_K \sin^2 \phi. \tag{39}$$

The normal permeability μ_K has been shown in (24) to be computable directly from the parallel inductance L'. Likewise, from (11) and (15), μ_N may be considered to be the permeability computed directly from the series inductance omitting the factor $[1+(D-D_c)^2]$ in (27).

The only significance which can be attached to the μ_M value is its definition (36) as the ratio of the normal induction to the maximum value of pseudo-H evaluated in terms of the full exciting current. It follows that a second evaluation of μ_M is given by

$$\mu_M = \mu_K \cos \beta = \frac{B_2}{H_2}. \tag{40}$$

It is apparent that the normal H_2 required to produce the dynamic cycle of induction exceeds the maximum static value of H required to produce the same maximum induction (total flux) in the d. c. loop C. It may be considered that the shielding effect of eddy currents in the core reduces the actual interior induction, so that to produce a given total flux more magnetizing current would be required. The departure of normal μ below $\mu_{d.c.}$, or, graphically, the angle between lines G and K, would thus increase with the frequency and the lamination thickness of a given material. Data supporting this hypothesis[5] will be found in Appendix B.

The foregoing data show close agreement between the values H_1 and H_2 and again between B_1 and B_2. This is only because, for loop A, the hysteretic angle was close to 45°. In Fig. 7 a pseudo-H loop has been constructed for the same normal B, but having increased core loss, resulting in the angle β becoming 55°. The significant values for this loop, which degenerates into the same line K when corrected for phase displacement and into terms of magnetizing current, are as follows:

$H_{max} = 0.0672$ oersteds
$H_1 = 0.0551$ oersteds
$H_2 = 0.0386$ oersteds, as before (normal H)
$B_{max} = 972$ gausses, as before (normal B)
$B_1 = 796$ gausses
$B_2 = 558$ gausses.

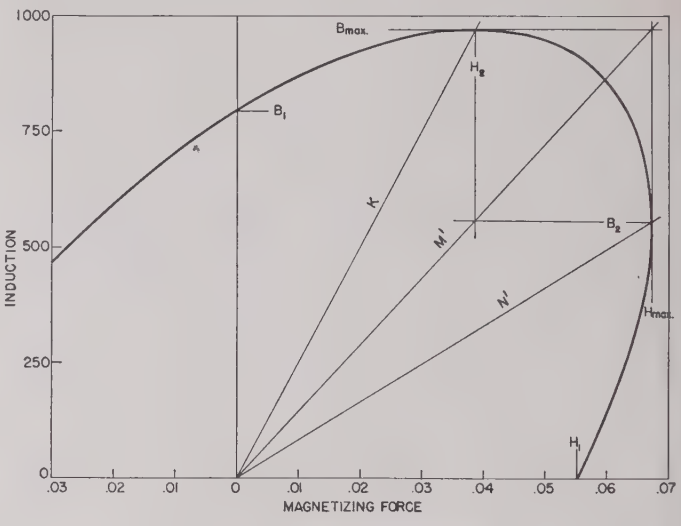

Fig. 7—Hysteresis loop with larger β.

These data yield:

$\mu_K = 25{,}200$, as before (normal μ)
$\mu_M = 14{,}460$
$\mu_N = 8{,}290$.

Note that, here, μ_N (series inductance) is less than one-third of μ_K (parallel inductance).

For any of these sinusoidal pseudo-H loops, normal permeability may be evaluated from (33). A precise value of H_2 is difficult to observe, since the loop is horizontal at its summit. It will be useful to note that, from the geometry of any of these sinusoidal loops, the radius K bisects each horizontal chord of the loop, while the radius N bisects each vertical chord of the loop. The radius K (normal μ) may thus be located more accurately as the bisector of the horizontal chord having an ordinate value B_1, and the radius N as the bisector of the vertical chord having the abscissa value H_1.

It should be noted that, had harmonic distortion existed in H and/or B, correcting the observed loop for phase displacement and true H magnitude would have degenerated it into a curved line, in reality the initial d.c. magnetization curve displaced horizontally by eddy-current shielding. The slope of the straight line K drawn to its extremity would then determine normal μ.

Measurement of Core Loss

The core-loss power P_c jointly due to hysteresis and eddy-current losses may be measured in various ways. Using a wattmeter reading P and an r.m.s. ammeter to measure the exciting current,

$$P_c = P - I_{exc}^2 R_s. \tag{41}$$

[5] Suggested by R. F. Field.

The copper-loss correction term in (41) may be avoided if the voltage coil of the wattmeter, together with an r.m.s. voltmeter reading E, are connected in parallel to constitute a resistive load r across a secondary winding on the inductor. The wattmeter will respond to the product of the in-phase parameters E_{exc}, and the currents through the resistances R' and r, so that

$$P_c = \gamma\left(P - \frac{E^2}{r}\right) \tag{42}$$

where γ is the reciprocal of the turns ratio.

In bridge measurements the r.m.s. values of the exciting current or the terminal voltage may be obtained by using (16), (19), and (20):

$$P_c = I_l^2 R' = I_{exc}^2 \omega L_s (D - D_c) = I_{exc}^2 (R_s - R_c) \tag{43}$$

$$P_c = \frac{E_{exc}^2}{R'} = \frac{E_T^2}{\omega L_s}\left(\frac{D - D_c}{1 + D^2}\right), \tag{44}$$

or, in terms of the apparent power,

$$P_c = E_T I_{exc}\left(\frac{D - D_c}{\sqrt{1 + D^2}}\right) = E_T I_{exc} \cos \phi - I_{exc}^2 R_c. \tag{45}$$

Equations (44) and (45) stipulate sinusoidal flux. However, it will be demonstrated in Appendix D that, in the presence of flux distortion, the use of a tuned voltmeter to measure E_T or E_{exc} (across a secondary winding) will give P_c values from (44) which check those obtained from (43).

Composition of Core Loss

When the specimen material is in a SCM condition, the existing core loss P_c is composed of two additive components: hysteresis power P_h, and eddy-current power P_e. By means of the following analysis[6] it is possible to separate the measured core loss into these two components, provided that the total dissipation factor D and the copper-loss dissipation factor D_c are known.

The hysteresis power is directly proportional to the frequency and is given by

$$P_h = \eta V f B^{\epsilon} \times 10^{-7}, \tag{46}$$

which involves the coefficient η and the Steinmetz exponent ϵ, both of which are not too well known and by no means constant functions of the normal induction.

The eddy-current power is directly proportional to the square of the frequency and is given by

$$P_e = \frac{\pi^2 f^2 B^2 \delta^2 V}{6 \times 10^{16} \rho} \tag{47}$$

where δ is the lamination thickness, and ρ is the resistivity of the specimen material (c.g.s. units).

In Fig. 5 consider the resistor R' to be replaced by two parallel components R_h and R_e which, if divided into E_{exc}^2, would yield, respectively, the values P_h and P_e. The hysteresis and eddy-current dissipation factors may be defined as

$$D_h \equiv \frac{\omega L'}{R_h} = 2^{(1+\epsilon/2)} \eta \mu B^{(\epsilon-2)} \tag{48}$$

$$D_e \equiv \frac{\omega L'}{R_e} = \frac{2\pi^2 \delta^2 \mu f}{3\rho \times 10^9}. \tag{49}$$

The following relation is shown to exist[6]:

$$D = D_c + D_h + D_e. \tag{50}$$

If these values are plotted versus frequency on log-log paper and no eddy-current shielding (constant inductance) is assumed, D_h will be a horizontal line; D_c will be a straight line with a negative unity slope, assuming a constant R_c value; and D_e will be a straight line having a positive unity slope. The total D will be a hyperbolic curve asymptotic to D_c and D_e and having a vertical axis. Thus, D will have a minimum value at that frequency which makes D_c equal to D_e and will be the reciprocal of the familiar Q versus frequency curve. D_c thus predominates at low frequencies and D_e at high frequencies.

Without trying to compute D_h, D_e may be evaluated from (49). Then, using (50), the ratio

$$\frac{D_e}{D_e + D_h} = \frac{D_e}{D - D_c} = \frac{P_e}{P_e + P_h} \tag{51}$$

will give the fractional part of the total core loss P_e which is due to eddy currents. Consequently,

$$P_e = \frac{D_e P_c}{D - D_c} \tag{52}$$

and, finally,

$$P_h = P_c - P_e. \tag{53}$$

Empirical data illustrating this procedure are given in Appendix C.

A.S.T.M. Testing Methods

The A.S.T.M. has compiled a useful series of standardized testing procedures for the measurement of μ and P_c[7] which embody the principles that have been discussed. Lack of space prevents a further detailed analysis of these procedures herein. The reader should remember that their validity depends upon certain limitations; namely, (1) that H must be evaluated in terms of true magnetizing current; (2) that a bridge-measured μ must be computed in terms of L'; and (3) that, if flux distortion exists, B must be obtained from (21) rather than from (23). It will be shown in Appendix D, however, that in the presence of flux distortion, values of μ determined by (25) and, independently, by (19) will agree within observational errors, provided that instruments tuned to the fundamental frequency are used.

[6] P. K. McElroy and R. F. Field, "How good is an iron-cored coil?" *Gen. Rad. Exp.*, vol. 16, pp. 1–12; March, 1942.

[7] A.S.T.M. Specification A34-44, 1944 Book for Metals, pp. 679–704.

Acknowledgment

The author wishes to thank S. L. Burgwin of the Westinghouse Electric Corporation for permission to use his valuable hysteresis-loop data. He is also indebted to his colleague, R. F. Field, for many helpful suggestions in the preparation of this paper.

APPENDIX A

Sinusoidal H versus Sinusoidal B Error in Using Fig. 1

The following appendices give data taken upon a 25-cm. Epstein square loaded with 29-gauge Wheeling VII 72 silicon steel. Measurements were made with an Owen bridge using a harmonic analyzer as a null detector. This instrument also served as a tuned voltmeter for current and voltage measurements. Unless otherwise noted, the bridge was excited at a frequency of 60 cycles.

In order to ascertain the differences existing between measurements made under conditions of sinusoidal H and, again, under conditions of sinusoidal B, the data depicted in Figs. 8 and 9 were obtained. The tuned voltmeter permitted normal B values to be evaluated from (25), while normal H was obtained from (22) and normal μ values were computed from (27).

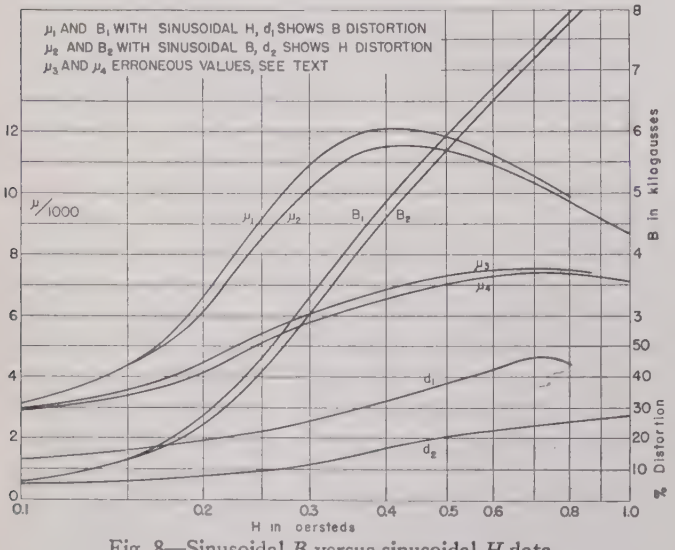

Fig. 8—Sinusoidal B versus sinusoidal H data.

In the first run the generator resistance was made sufficiently high (20 kilohms) to ensure sinusoidal H. In Fig. 8 the curves μ_1, B_1, and d_1 show the variations of μ, B, and the simultaneous percentage distortion in B versus normal H. In the second run the generator resistance was essentially a 10-ohm bridge arm, resulting in closely sinusoidal B conditions, and yielded the corresponding curves μ_2, B_2, and d_2, the latter giving the simultaneous distortion in H.

Fig. 9 shows the core-loss values P_1 (sinusoidal H) and P_2 (sinusoidal B) computed from either (43) or (44).

From the foregoing data it will be seen that the distinction between sinusoidal H and sinusoidal B measurements was not measurable below an H of 0.15; that it was most pronounced in the region of μ_{max}, and finally became less significant at higher induction values. Maximum differences of about 8 per cent in μ and B and about 5 per cent in P_e were observed.

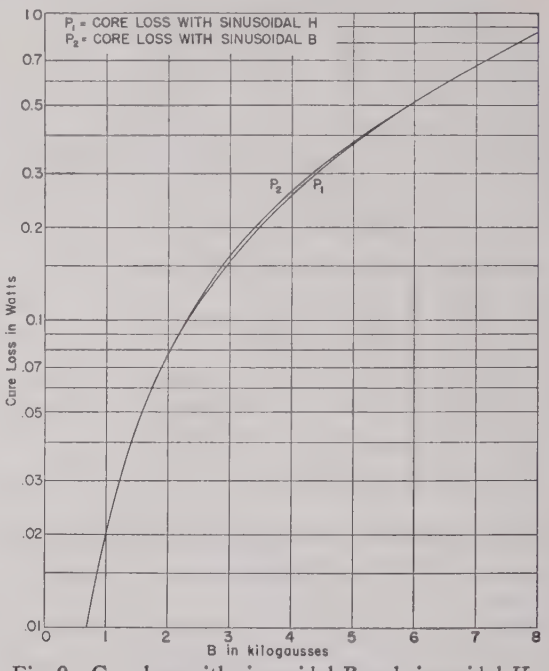

Fig. 9—Core loss with sinusoidal B and sinusoidal H.

The inductor had a dissipation factor which varied between 0.4 and 0.8. Accordingly, if the *erroneous* assumptions of Fig. 1 are used and the permeability is computed directly in terms of series inductance and the geometry of the Epstein square, while a pseudo-H is evaluated in terms of the full exciting current, the curves μ_3 (sinusoidal H) and μ_4 (sinusoidal B) in Fig. 8 are obtained. The substantial departure between these curves and those depicting the true values μ_1 and μ_2 is apparent.

APPENDIX B

Data Supporting the Hypothesis of Eddy-Current Shielding; Effect of Copper Loss

The following typical data (Table I) taken from the U. S. Steel Technical Bulletin No. 2 for their Motor Grade ($2\frac{1}{2}$ per cent silicon) show the decrease in normal μ with increasing sheet thickness for specific values of normal H.

TABLE I

Gauge	$H=0.4$	$H=1.05$	$H=4.0$
29	2750	6100	3000
26	2200	5780	2890
24	2100	5400	2810

To investigate the effect of frequency variation, the author made the Owen-bridge determinations of normal μ upon the 25-cm. Epstein, while maintaining a con-

stant total flux corresponding to an average normal induction of 100 gausses shown in Table II.

TABLE II

Frequency (c.p.s.)	Normal μ		Core Loss	
	A	B	A	B
33⅓	1571	1556	0.165	0.145
50	1555	1545	0.242	0.215
75	1537	1531	0.368	0.350
100	1525	1520	0.498	0.477
150	1509	1505	0.784	0.763
200	1499	1495	1.112	1.090
250	1492	1489	1.45	1.43
300	1486	1484	1.84	1.82
400	1479	1477	2.67	2.67

In columns A the values of μ and core loss (evaluated in milliwatts) were computed assuming copper loss negligible (Fig. 4); in columns B the true values are given taking the copper loss into account (Fig. 5). The discrepancy is seen to be appreciable at the lower frequency values when D_c becomes a substantial part of D.

The two foregoing tabulations demonstrate the shielding effect of eddy currents which causes normal μ to become less than the d. c. permeability as either the lamination thickness or the frequency is increased.

APPENDIX C

An Analysis of Core Loss into P_h and P_e

Using the data given in Appendix B and equations (17) and (49) through (53), together with the measured data $R_c = 1.81$ ohms, $\delta = 0.0384$ cm., and $\rho = 66.7 \times 10^{-6}$ ohm-cm., the following data were computed as shown in Table III.

TABLE III

f (c.p.s.)	P_e mw.	P_h (mw.)	P_e/f^2	P_h/f	P_e/P_c	P_h/P_e
33.3	0.006	0.139	54×10^{-7}	417×10^{-5}	0.043	0.96
50	0.014	0.201	56	402	0.063	0.94
63.5	0.022	0.264	55	418	0.078	0.92
75	0.032	0.318	57	424	0.091	0.91
100	0.056	0.421	56	421	0.117	0.88
150	0.126	0.637	56	425	0.165	0.83
200	0.225	0.865	56	423	0.206	0.79
250	0.350	1.08	56	432	0.244	0.76
300	0.50	1.32	56	440	0.276	0.72
400	0.89	1.78	56	445	0.335	0.66

At the frequency of 63.5 c.p.s. the D_c and D_e values were closely identical, while D had its minimum value.

The constancy of the two ratios P_e/f^2 and P_h/f attests the validity of this analysis and of (50), even though the theoretically linear graphs of D_c, D_h, and D_e may have small curvatures due to the slow variation of inductance with frequency.

APPENDIX D

Intercomparison of Methods

To compare the methods of measuring permeability and core loss using tuned and untuned voltmeters in the presence of B and H distortion, the Owen-bridge data were taken upon the Epstein square as shown in Table IV. Values of normal μ were then computed from (27) and values of R' from (16). Simultaneous values of I_{exc} were obtained with a voltmeter across a 100-ohm resistive arm of the bridge carrying I_{exc}, whence the magnetizing current was computed from (18) and normal H from (22). Simultaneous values of E_{exc} were obtained from the voltage induced in the secondary winding and the turns ratio, whence normal B was computed from (25).

Each of these two voltage measurements was made with two different instruments, a tuned voltmeter (harmonic analyzer) tuned to the fundamental frequency, and an untuned vacuum-tube voltmeter. A harmonic analysis of I_{exc} (H) and of E_{exc}(B) was likewise made. From the data a second (independent) value of normal permeability μ_A was computed as the B/H ratio obtained with the tuned voltmeter, and a third value μ_B as the B/H ratio obtained with the untuned voltmeter. Using the tuned voltmeter readings, core-loss power was evaluated in two independent ways, P_1 from (43) and P_2 from (44).

TABLE IV

H	Per Cent Distortion		μ	$\frac{\mu}{\mu_A}$	$\frac{\mu}{\mu_B}$	$\frac{P_1}{P_2}$
	in H	in B				
2.37	10.2	37.5	5,410	0.980	1.482	0.973
1.74	7.2	34.7	6,690	0.974	1.373	0.909
1.323	5.7	29.6	7,990	0.977	1.305	0.929
1.000	4.5	26.5	9,320	0.977	1.212	0.967
0.756	3.9	24.0	10,800	1.008	1.156	1.043
0.576	3.2	19.7	11,890	1.045	1.090	1.096
0.431	2.57	16.8	12,210	1.002	1.038	1.007
0.341	2.32	12.7	11,630	1.008	1.010	1.012
0.272	1.98	9.4	9,570	1.040	1.009	1.075
0.203	2.04	6.0	6,190	0.995	0.988	0.988
0.149	2.38	5.1	4,210	1.024	0.990	1.060
Average				0.999		1.005

Recalling that the accuracy of the μ_A, μ_B, P_1, and P_2 values depends upon the precision of voltmeter readings, the close equality between the two independent values μ and μ_A and between P_1 and P_2 is evident. The value of μ_B (B/H ratio obtained with an untuned voltmeter) progressively diminishes from the true μ value as the distortion in B increases, demonstrating that (25) is valid only for sinusoidal components and that, with flux distortion, (23) must be used.

APPENDIX E

Effect of Shearing on Normal μ and Core Loss

The 3-cm. strips were then removed from the Epstein square and each sliced longitudinally to give three strips each one cm. wide. Each of two pieces was thus subjected to a shearing strain along one of its edges, while the third piece was subjected to shearing strains along both of its edges. The same iron was then replaced in the

Epstein square and a duplicate test run was made. By interpolation, the percentage changes in normal μ and core loss for specific values of H, and again for specific values of B, were determined as shown in Table V.

TABLE V

H (oersteds)	Original μ	Per Cent Change in μ	Original P_c (watts)	Per Cent Change in P_c
0.20	6,050	+ 0.7	—	—
0.30	10,580	− 1.7	0.175	0.0
0.40	12,070	− 3.3	0.355	− 2.8
0.50	12,150	− 4.3	0.52	− 6.8
0.75	10,700	− 5.1	0.87	−11.5
1.00	9,320	− 4.9	1.13	− 8.9
1.50	7,370	− 4.2	1.57	− 8.3
2.00	6,120	− 3.4	1.96	− 8.2
2.50	5,170	− 2.9	2.33	− 8.2
B (kilogausses)				
1	5,400	+ 1.3		
2	8,270	+ 0.8		
3	10,530	− 1.0		
4	11,760	− 1.9		
5	12,160	− 3.2	0.280	0.0
6	12,130	− 5.0	0.53	+ 0.9
8	10,860	− 9.8	0.86	+ 2.3
10	8,850	−15.0	1.23	+ 7.3
12	6,620	−21.6	1.78	+14.0
14	4,250	−31.7	2.72	+21.7

The effect of shearing strains is seen to be: a reduction in μ (except at low induction), a reduction in core loss for specific values of H, and an increase in core loss for specific values of B. For specific values of H a maximum fractional change in both μ and P_c occurs at an H value which is somewhat in excess of that corresponding to μ_{max}. For specific values of B, the effect of shearing upon μ and P_c increases progressively with rising values of induction.

APPENDIX F

The author has used with success a method of measuring μ which involves a direct determination of the angles ϕ or β by means of a cathode-ray oscilloscope (see Fig. 10). A suitable resistance R is placed in series with the specimen inductor and shunted by a peak-reading voltmeter, so that the ratio $\hat{E}_R/R$ gives the value of the exciting current. The adjustable high-resistance voltage divider P draws no appreciable current through R. The source generator E_g through a transformer feeds a phase-shifting network consisting of two equal fixed capacitors C and two equal adjustable resistors r. With low input and high output impedances, the output voltage of this network is essentially constant and has a phase displacement α from the input voltage given by

$$\tan \alpha = \frac{2r\omega C}{1 - r^2\omega^2C^2}. \tag{54}$$

Joint adjustment of the two r resistors thus varies the phase of the reference voltage E_{ref} (output of the amplifier A_1) which is applied to the horizontal deflectors of the c.r.o. By means of the switch B-H either the voltage drop across R or a suitable portion of the terminal voltage may be applied through the amplifier A_2 to the vertical deflectors.

If copper loss may be considered negligible, the exciting voltage may be taken to be the terminal voltage read on the high-impedance voltmeter E_T. The operating procedure is as follows: With the switch open, adjust the gain of the amplifier A_1 to give an appropriate length

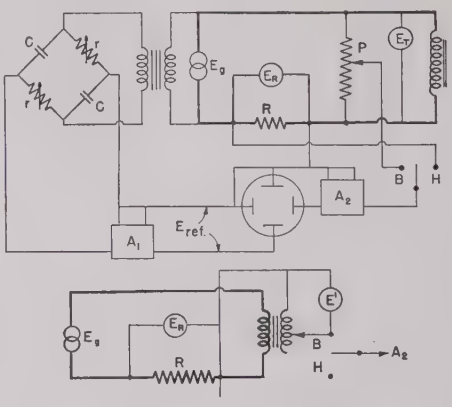

Fig. 10 —Measurement of μ by determining the angles ϕ or β.

of the vertical sweep on the screen. Close the switch to the H position and adjust the phase network to reduce the elliptical pattern on the screen into a line with, say, a positive slope. The phase of the reference voltage E_{ref} having a relative displacement α_H has thus been matched to the phase of the exciting current. The most accurate determination of this matching may be made if the slope of the line is made approximately 45° by an appropriate gain adjustment of the amplifier A_2. Any distortion in H will introduce curvature into the line, in which case the center portion should be closed. Leaving the amplifier A_2 unchanged, throw the switch to the B position and readjust the phase network to provide a new relative displacement α_B which will match the phase of E_{ref} with the terminal voltage of the inductor, resulting in a line with a positive slope which may be approximated to 45° by adjustment of the potentiometer P. The phase angle ϕ of the inductor will then be the algebraic difference between the two relative displacements α_H and α_B.

Normal magnetizing force may then be computed by substituting (9) into (22). For measurements with sinusoidal B (small R values), the voltmeter E_T must read peak values. Substituting E_T for E_{exc} in (25) gives the normal induction, whence the normal permeability becomes

$$\mu = \frac{10^8 \lambda R}{0.4\pi N^2 A\omega \sin \phi}\left(\frac{\hat{E}_T}{\hat{E}_R}\right). \tag{55}$$

For measurements with sinusoidal H (large R values) the voltmeter E_T must read average values and normal induction obtained from (28). In this case normal permeability is given by:

$$\mu = \frac{10^8 \lambda R}{0.8N^2 A\omega \sin \phi}\left(\frac{E_T\,(\text{av.})}{\hat{E}_R}\right). \tag{56}$$

Copper losses could be taken into account in this method by substituting the factor $\cos\beta$ for $\sin\phi$ in (55) and (56) and substituting (8) into (22). The angle β can be measured by connecting the B contact of the switch across an appropriate number of secondary turns on the inductor. The observed displacement α_B' would then be the angle between E_{ref} and the induced voltage. It follows that the algebraic difference between the two relative displacements α_H and α_B' will be the angle between E_{ind} and I_{exc}, and hence will equal β plus $\pi/2$. The voltmeter reading E_T would be replaced by E' across the secondary winding, as indicated in the lower portion of Fig. 10, so that its peak or its average reading divided by the turns ratio would give the exciting voltages to replace the corresponding terminal voltages in (55) or (56).

APPENDIX G

Units of Magnetic Measurement

There are currently three systems of magnetic units in use. Since some confusion exists in the interpretation of these systems and the relationships between them, the following summary was considered desirable.

The A.S.T.M. specifications embody the nonrationalized c.g.s. electromagnetic system of units (used in this paper) in which magnetomotive force F, measured in gilberts, is given by 0.4π times the ampere-turns circumscribing the flux path, and the unit of reluctance $\mathcal{R}$, sometimes called the "magnetic ohm," is the reluctance across a centimeter cube of free space. Magnetic flux Φ, measured in maxwells or "lines," is then the ratio $F/\mathcal{R}$. In a symmetrical and homogeneous flux path the magnetizing force H, measured in oersteds, is the ratio F/λ; while the induction B, measured in gausses, is the ratio Φ/A. In this system permeability μ is the ratio B/H evaluated in gausses per oersted, and has a value of unity in free space.

In the practical nonrationalized m.k.s. electromagnetic system, F is measured in pragilberts and given by 4π times the ampere-turns, so that a pragilbert is in reality a decigilbert. The unnamed unit of reluctance may be defined as 10^{-9} magnetic ohms. Flux is measured in webers, one weber being 10^8 maxwells. H is measured in praoersteds (pragilberts per meter), so that a praoersted is a millioersted. B is measured in a unit (webers per square meter) which equals 10 kilogausses. Hence, in this system the permeability of free space has a value of 10^{-7}.

In the rationalized m.k.s. electromagnetic system F is measured directly in ampere-turns, while the units of Φ and B remain the same as in the nonrationalized m.k.s. system. Consequently, the rationalized m.k.s. units of F, $\mathcal{R}$, and H are each larger than the corresponding nonrationalized m.k.s. units by the factor 4π and the permeability of free space becomes $4\pi\times10^{-7}$. The conversion tables shown in Table VI may be used.

TABLE VI

I. *Converting c.g.s. into nonrationalized m.k.s. values*

To convert	*into*	*multiply by*
F in gilberts	F in pragilberts	10
$\mathcal{R}$ in magnetic ohms	$\mathcal{R}$ in m.k.s. (N-R) units	10^9
Φ in maxwells	Φ in webers	10^{-8}
H in oersteds	H in praoersteds	10^3
B in gausses	B in webers/square meter	10^{-4}
μ c.g.s.	μ m.k.s. (N-R)	10^{-7}

II. *Converting c.g.s. into rationalized m.k.s. values*

To convert	*into*	*multiply by*
F in gilberts	F in ampere-turns	$10/4\pi$
$\mathcal{R}$ in magnetic ohms	$\mathcal{R}$ in m.k.s.-R units	$10^9/4\pi$
Φ in maxwells	Φ in webers	10^{-8}
H in oersteds	H in ampere-turns/meter	$10^3/4\pi$
B in gausses	B in webers/square meter	10^{-4}
μ c.g.s.	μ m.k.s.-R	$4\pi\times10^{-7}$

III. *Converting nonrationalized m.k.s. into rationalized m.k.s. values*

To convert	*into*	*divide by*
F in pragilberts	F in ampere-turns	4π
$\mathcal{R}$ in m.k.s. (N-R)	$\mathcal{R}$ in m.k.s.-R units	4π
Φ in webers	Φ in webers	1
H in praoersteds	H in ampere-turns/meter	4π
B in webers/square meter	B in webers/square meter	1
μ m.k.s. (N-R)	μ m.k.s.-R	$1/4\pi$

The Degenerative Positive-Bias Multivibrator*

SIDNEY BERTRAM†, SENIOR MEMBER, I.R.E.

***Summary*—The operation of a multivibrator with positive grid supply and cathode degeneration is described. It is shown that, for suitable circuit parameters, the frequency of the multivibrator is very nearly a linear function of the applied grid voltage. Since the grid voltage can be controlled with relatively simple auxiliary circuits, the positive-bias multivibrator becomes a useful variable-frequency source.**

* Decimal classification: R146.2×R357.21. Original manuscript received by the Institute, June 27, 1946; revised manuscript received, June 25, 1947.

† Ohio State University, Columbus, Ohio.

THE MULTIVIBRATOR is well known and much has been written about its operation. However, the extremely useful characteristics of multivibrators operating with positive grid return are not well known. Bartelink[1] has indicated that the frequency of a multivibrator varies approximately linearly with the grid-bias voltage. The purpose of this paper is to

[1] E. H. B. Bartelink, "A wide-band square-wave generator," *A.I.E.E. Trans.*, vol. 60, pp. 371–376; June, 1941. Supplement to *Elec. Eng.*, transactions section.

describe the operation of a multivibrator operating with positive grid return and cathode degeneration, and to show that it is possible to choose the circuit constants so as to make the grid-voltage versus frequency relationship extremely linear over a frequency range of well over an octave. This inherent linearity should make the multivibrator adaptable to a wide variety of applications.

The multivibrator shown in Fig. 1 consists of a two-stage resistance-coupled amplifier with the output coupled back to the input so that the circuit is regenerative. The mode of operation is easily seen.

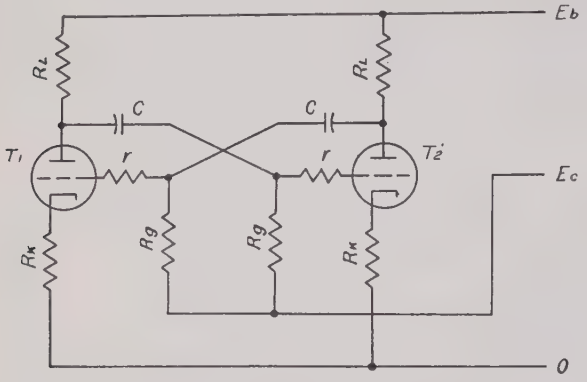

Fig. 1—The positive-bias multivibrator.

Suppose the multivibrator has just been turned on and is not yet oscillating. Any disturbance during the warm-up period would then be amplified regeneratively until it started the oscillation. Thus, if the plate current of tube T_2 is momentarily increased, it would start the following chain of reactions: (a) the plate voltage of T_2 would decrease; (b) the grid of T_1 would become more negative; (c) the plate current of T_1 would decrease, allowing the plate voltage to increase; (d) the grid of T_2 would become more positive; and (e) the plate current of T_2 would increase, adding to the original change that started the reaction.

If the over-all gain around the loop is greater than unity, the system is unstable; in this case the reaction will progress at a rapid rate until tube T_1 is cut off, so that its plate is at substantially the voltage of the supply, while T_2 has its grid positive with respect to its cathode and considerable drop across its plate load (time A in Fig. 2). The voltage on the grid of T_1 now rises as the coupling capacitor charges, approaching the voltage of the grid supply E_c asymptotically. When the grid of T_1 nears the cutoff voltage, T_1 starts to conduct (B in Fig. 2), so that its plate becomes increasingly negative. This reduces the voltage on the grid of T_2, causing its plate to become increasingly positive and thus accelerating the already rising voltage on the grid of T_1. When T_1 becomes sufficiently conducting to make the combined gain of T_1, T_2 greater than unity, the circuit "flips over"; i.e., the two tubes change places, the grid of T_1 becoming positive with respect to its cathode while the grid of T_2 is driven below the cutoff voltage. The operation is then repeated, the grid of T_2 rising exponentially until T_2 becomes conducting, when a second flip-over occurs, etc.

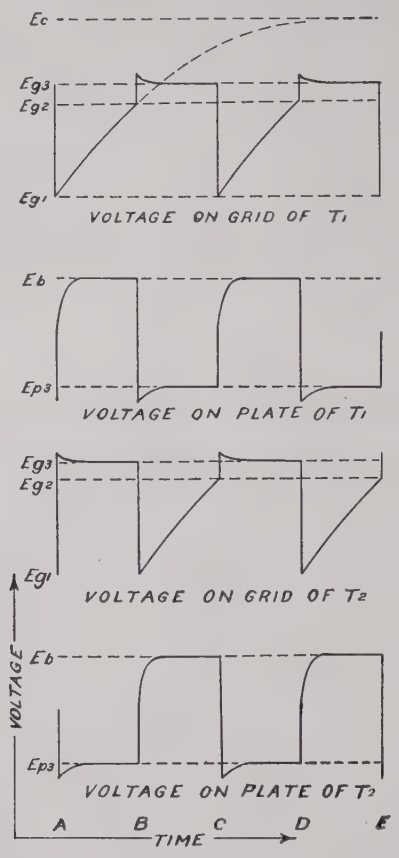

Fig. 2—Multivibrator wave shapes.

The above analysis has neglected the small but observable effect of grid current on the operation of a multivibrator. When the multivibrator flips over, the grid of the tube, becoming conducting, goes positive with respect to its cathode. This prevents the plate voltage of the opposite tube from immediately reaching the plate-supply voltage (being restrained by the grid current). As the coupling capacitor charges, the grid voltage of the conducting tube decreases, allowing its plate voltage to increase; this change in plate voltage is carried over to the grid of the nonconducting tube, modifying the rate of rise of its grid voltage. In a multivibrator it is important that R_g be large compared to R_L (grid-circuit time constant large compared to plate-circuit time constant), so that the grid current will decrease to a low value, compared to its maximum value immediately following a flip-over, before the next flip-over occurs; otherwise, the grid current will affect the stability of the multivibrator. Another factor that affects the multivibrator operation is the input capacitance of the tubes, which reduces the signal to the grids; this is particularly true at high frequencies where the coupling capacitance is small.

The period of the multivibrator is dependent upon the amplitude of the oscillations, the resistance-capacitance combination in the grid circuit, and the voltage to which the grids are returned. The half-period is very nearly the time necessary for the grid to change from its highly negative voltage following the flip-over to the cutoff voltage. The period will be increased by (a) increasing the amplitude of oscillations by increasing the plate load resistance or decreasing the cathode resistance; (b) increasing either the resistance or capacitance in the grid circuit, thus decreasing the rate at which the capacitor charges; and (c) decreasing the grid-return voltage E_c, thus decreasing the rate at which the capacitor charges.

The voltage versus frequency relationship of a multivibrator is fairly linear (except at very low or very high grid-supply voltages) for any circuit values. The relationship has an inflection point, and it is possible to choose the circuit parameters so that the point of inflection is at the center of the desired operating range of E_c. In designing a multivibrator, it is convenient to adjust the cathode resistance R_k to obtain the desired linearity; the grid-circuit parameters (R_g, C) can then be adjusted to give the desired operating range.[2] When

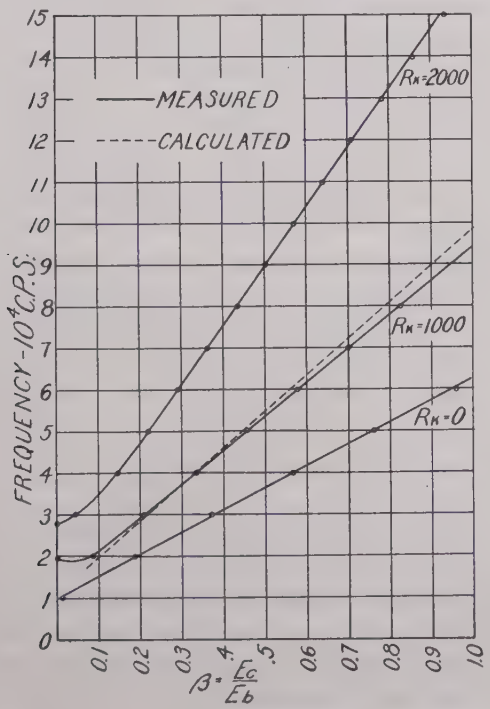

Fig. 3—Voltage versus frequency relationship of the multivibrator using two 6J5 tubes, with $R_L = 5000$ ohms, $R_g = 270{,}000$ ohms, $C = 100$ $\mu\mu fd.$, and $E_b = 250$ volts, for different values of R_K.

this adjustment is properly made it is found that the grid-voltage versus frequency relationship is quite linear. Thus, in Fig. 3 the curve is slightly concave downwards for $R_k = 0$, very linear for $R_k = 1000$ ohms, and concave up for $R_k = 2000$ ohms. It is not possible to show the degree of linearity obtainable on the curve.

[2] The resistors r are often necessary to suppress parasitic oscillations in the grid circuit (200 ohms is sufficient).

In making the measurements, the frequency was set at harmonics of a low-frequency standard (5000 c.p.s.) by varying the grid-return voltage, and the voltage then read on a three-decade potentiometer. A change in β from 0.3 to 0.7 resulted in a change in frequency from 37 to 70 kilocycles with a departure from linearity of less than ± 200 c.p.s. It is particularly significant that this linear operation is essentially independent of the tubes used, so long as their characteristics fall within normal limits. Thus, once a suitable set of values is obtained, the results can be duplicated with only ordinary care in choosing the elements.

Since the grid return is a high-impedance circuit, the voltage can be varied dynamically, if desired, using low-power circuits. Here the high degree of linearity obtainable makes the positive-bias multivibrator very useful as a frequency-modulated source.

Appendix

The frequency of a multivibrator can be approximated in terms of the constants of Figs. 1 and 2. When a grid is rising exponentially from its maximum negative value (taken at time $t=0$), its instantaneous voltage can be expressed as

$$e_g = [E_c - (E_c - E_{g1})\epsilon^{-t/R_g C_s}]$$

where $C_s = C + C_{in}$ is the effective capacitance in the discharge circuit. The circuit will flip over when e_g reaches the cutoff value $E_{g2} = -(E_b/\mu)$; the value of t for this cutoff condition is the half-period of the multivibrator, and thus determines the frequency. The voltage E_{g1} is found as follows[3]:

$$E_{g1} = E_{g2} - (E_b - E_{p2})\left(\frac{C}{C + C_{in}'}\right)$$

where

$$E_{g2} = \frac{R_K E_b}{R_p + R_L + R_K}$$

and

$$(E_b - E_{p2}) = \frac{R_L E_b}{R_p + R_L + R_K}.$$

The frequency of a multivibrator can now be written

$$f = \frac{1}{2R_g C_s \log_\epsilon \dfrac{\mu(\beta - \gamma)}{\mu\beta + 1}} \qquad (1)$$

where

$$\beta = \frac{E_c}{E_b} \quad \text{and} \quad \gamma = \frac{E_{g1}}{E_b}.$$

[3] In calculating C_s, the input capacitance is $C_{in} = C_{gk} + C_{gp} + C_s$, the plate voltage being constant in the discharge period. In calculating E_{g1} the voltage transferred from the plate to the other grid is reduced by the input capacitance; for this condition, $C_{in'} \approx C_{gk} + 2C_{gp} + C_s$, because the plate voltage moves positively about the same amount that the grid moves negatively.

In deriving the frequency equation, the following simplifying approximations have been made. It is assumed that, before a flip-over occurs, an equilibrium condition is reached in which the grid of the conducting tube is at the same voltage as its cathode; the plate current is then determined by the intersection of the load line for the combined plate and cathode loads with the zero-bias plate current. The effective amplification factor is determined by the grid voltage at the effective cutoff point—the point where the over-all gain is just unity. Actually, a very good approximation is obtained if the values for μ and R_p given in the tube manuals are used.

The frequency equation (1) is cumbersome and not readily interpreted. It can be transformed as follows: Let β_0 be the center of the operating range of β and x the deviation from the center, i.e., $\beta=\beta_0+x$; then, if the additional substitutions $a=1/\beta_0-\gamma$ and $b=\mu/1+\mu\beta_0$ are made, (1) becomes

$$f=\frac{1}{2R_gC_e\left[\log_\epsilon\frac{b}{a}+\log_\epsilon\left(\frac{1+ax}{1+bx}\right)\right]}. \tag{2}$$

It is expedient at this point to expand the second logarithmic expression (involving x) in a power series; thus

$$\begin{aligned}\log_\epsilon\left(\frac{1+ax}{1+bx}\right)&=(a-b)x-\left(\frac{a^2-b^2}{2}\right)x^2\\&\quad+\left(\frac{a^3-b^3}{3}\right)x^3-\left(\frac{a^4-b^4}{4}\right)x^4\\&\quad+\cdots\\&=(a-b)x\left[1-\left(\frac{a+b}{2}\right)x\right.\\&\quad+\left(\frac{a^2+ab+b^2}{3}\right)x^2\\&\quad\left.-\left(\frac{a^3+a^2b+ab^2+b^3}{4}\right)x^3+\cdots\right].\end{aligned}$$

If a is not too different from b, then

$$\frac{a^2+ab+b^2}{3}\approx\left(\frac{a+b}{2}\right)^2,$$

and, in general,

$$\frac{a^n+a^{n-1}b+a^{n-2}b^2+\cdots+b^n}{n+1}\approx\left(\frac{a+b}{2}\right)^n.$$

Thus, the above series is approximated by the new series[4]

$$\begin{aligned}\log_\epsilon\left(\frac{1+ax}{1+bx}\right)&\approx(a-b)x\left[1-\left(\frac{a+b}{2}\right)x\right.\\&\quad+\left(\frac{a+b}{2}\right)^2x^2-\left(\frac{a+b}{2}\right)^3x^3\\&\quad\left.+\cdots\right]\\&\approx\frac{(a-b)x}{1+\left(\frac{a+b}{2}\right)x}.\end{aligned}\tag{3}$$

In terms of this approximation the frequency equation becomes

$$f\approx\frac{1+\left(\frac{a+b}{2}\right)x}{2R_gC_e\left\{\log_\epsilon\frac{b}{a}+x\left[\left(\frac{a+b}{2}\right)\log_\epsilon\frac{b}{a}+(a-b)\right]\right\}}. \tag{4}$$

It is possible to adjust the circuit parameters so that the coefficient of x in the denominator vanishes. Thus, if $(a+b/2)\log_\epsilon b/a=b-a$, the denominator is constant and the frequency becomes a linear function of the grid-return voltage $\beta=E_c/E_b$. Under these conditions the frequency equation takes the simplified form

$$f\approx\left[\frac{1-\left(\frac{a+b}{2}\right)\beta_0}{2R_gC_e\log_\epsilon\frac{b}{a}}\right]+\left[\frac{a+b}{4R_gC_e\log_\epsilon\frac{b}{a}}\right]\beta \tag{5}$$

R_g = grid-return resistance
$C_e=C+C_{in}$ = effective circuit capacitance
$\beta_0=E_{c_0}/E_b$ = design-center grid-return voltage
$\beta=E_c/E_b$ = grid-return voltage
$a=1/\beta_0-\gamma$, $b=\mu/1+\mu\beta_0$, and

$$\gamma=\frac{R_K-R_L\left(\frac{C}{C+C_{in}'}\right)}{R_p+R_L+R_K}.$$

For a multivibrator employing two 6J5 tubes, with $R_L=5000$ ohms, $R_K=1000$ ohms, $R_g=270{,}000$ ohms, and $C=100$ $\mu\mu$fd. (also, from tube manuals, $R_p=7700$ ohms, $\mu=20$, and, including 5 $\mu\mu$fd. of stray capacitance, $C_{in}'=22$ $\mu\mu$fd.), (5) reduces to

$$f\approx(11+88\beta)\times10^3 \text{ c.p.s.} \tag{6}$$

where β_0 has been taken at $\beta=0.5$.

The three experimental curves of Fig. 3 illustrate the effect of varying the cathode degeneration. With zero resistance the frequency characteristic is very slightly concave downwards; with 1000 ohms the characteristic is extremely linear over a range of about two octaves. With larger values of cathode resistance the frequency characteristic is concave upwards. The dotted line is the straight-line frequency variation of (6).

[4] There is no error in the constant or linear terms of the approximating series. In the case of the 6J5 multivibrator used as an example, $a=1.38$ and $b=1.82$; for these values the error in the lower-order terms are: second degree, 0.6 per cent; third degree, 2.0 per cent; fourth degree, 3.6 per cent; and fifth degree, 6.3 per cent.

A Variable-Radio-Frequency-Follower System*

R. F. WILD†, ASSOCIATE, I.R.E.

Summary—This paper deals with a new follow-up or servo system for amplification of mechanical forces and remote positioning. The system described makes use of variable radio frequencies representative of the respective positions of system leader and follower. Two parallel-resonant circuits are provided, one of which is the frequency-determining circuit of an oscillator, while the other is the balance-frequency-determining circuit of a balanced-frequency discriminator. One of the circuits can be tuned by the leader, while the other is tuned by the follower; or, one of the circuits can be tuned by both leader and follower. System balance is reached when both circuits are tuned to the same frequency. Of the possible variety of system modifications, four significant types are described with their particular applications. The system provides for low-frequency keying of the radio-frequency signal before application to the frequency discriminator, in order to obtain a low-frequency-discriminator output signal of one phase or opposite phase, depending upon the direction of system unbalance. For system balance no discriminator output signal is produced. The low-frequency signal is used to control a two-phase induction motor driving the follower.

System design considerations and performance data are given. Wide-band frequency-discriminator tuning is discussed with respect to constant system sensitivity. Experimental and production models are described.

IN THE PAST few years much development work has been done in the field of follow-up or servo systems for use either solely for amplification of mechanical forces or for remote positioning and metering. The multitude of different systems, their requirements and applications, and their limitations, is too great for even a brief discussion in this paper. It may be sufficient to say that all of these systems include a circuit arrangement which can be unbalanced by a leader movement to produce an unbalance or error signal, which is amplified and used to control a power device or motor to move a follower to restore the balance of the circuit arrangement.

Depending upon the circuit arrangement, the unbalance signal usually consists of a d.c. signal of variable amplitude and polarity or a low-frequency a.c. signal of variable amplitude and phase. Some systems are applicable to wire transmission only, while some are applicable to wireless transmission.

The present system makes use of variable radio frequencies representative of the respective positions of leader and follower. For remote transmission, particularly, the use of a variable frequency has the advantage that the frequency of a transmitted signal of single frequency is not affected by changes in the characteristics of the transmission path, and therefore eliminates the need for transmission of an additional reference signal.

* Decimal classification: R570×621.375.104. Original manuscript received by the Institute, April 30, 1947. Presented, 1947 I.R.E. National Convention, March 5, 1947.

† Formerly, Brown Instrument Company, Philadelphia, Pa.; now, E. I. DuPont de Nemours and Company, Inc., Wilmington, Del.

Furthermore, a system of this type can easily be designed for a multiplicity of receivers, any of which can be switched on and off without affecting the operation of the operating receivers.

Basically, the system comprises two separate tuned circuits which are tuned to the same frequency when the system is balanced. There are two species of this system. In the first, the balance frequency remains constant, and the detuning of one of the tuned circuits causes a follow-up action to restore its tuning to the original balance frequency. In the second species, a detuning of one of the tuned circuits is followed by a corresponding detuning of the second circuit. When both circuits are tuned to the same frequency the system is balanced. Obviously, in this species there exists a range of balance frequencies.

Fig. 1 shows four types of the system, all including a radio-frequency oscillator *O*, a keying stage *K*, a frequency discriminator *D*, a voltage amplifier *V.A.*, a phase-sensitive power amplifier *P.A.*, and a two-phase induction motor *M*. Keying is effected in phase and synchronism with the power amplifier and motor-energizing voltage.

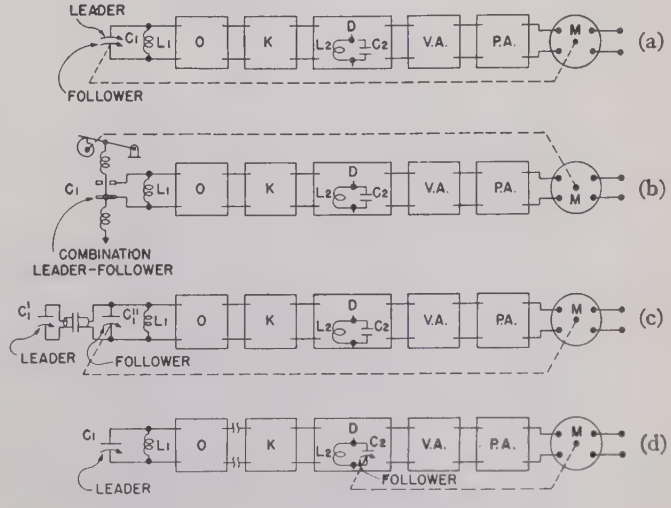

Fig. 1—System types.

Types (a), (b), and (c) operate at a fixed balance frequency determined by the fixed discriminator tuning. Types (a) and (b) are for amplification of mechanical forces alone, while type (c) can be used for short-distance remote transmission.

In type (d), both oscillator and discriminator are tuned, and the balance frequency varies over a relatively wide range. This system is unlimited in distance and can be used for wire and wireless transmission.

In types (b), (c), and (d), the follower movement can be made to be practically any desired function of the leader movement, depending on the shape of the cam of type (b) and the shape of the capacitor plates of types (c) and (d). Inductive tuning can be used in place of capacitive tuning and has been used in types (b) and (d).

It may be noted that in the first three types the feedback loop extends around the entire system between motor and oscillator. In type (d), the feedback loop extends around a portion of the system only, between motor and discriminator.

Fig. 2 shows the discriminator characteristics typical of a conventional discriminator, such as used in frequency-modulation receivers and for automatic frequency control.

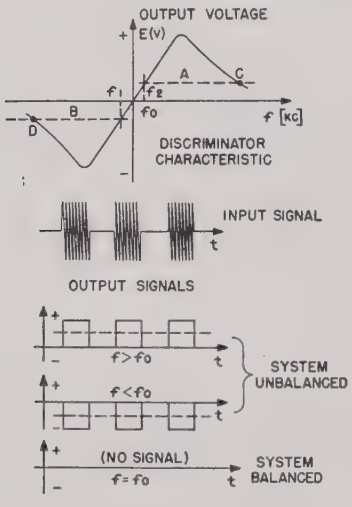

Fig. 2—Discriminator characteristic and discriminator signals.

Such a discriminator delivers no output signal in the absence of an input signal as well as for an input signal of the frequency to which the discriminator is tuned. This is the system balance frequency f_0, at which no discriminator output signal is desired. For keyed radio-frequency signals of frequencies above and below f_0, a series of positive or negative pulses is obtained, containing a keying-frequency signal component of one phase or the other depending upon the direction of system unbalance.

Lines A and B indicate the discriminator output signal magnitudes at which the limiting action of the subsequent voltage amplifier takes place. Therefore, the shape of the discriminator characteristic above A and below B is of no consequence to the operation of the system.

A free choice of operating frequencies is governed by the following factors: The percentage change of frequency over the operating range should be as great as feasible in order to minimize the effects of frequency drifts. Such drifts can be caused by changes in temperature, relative humidity, and the like, and by supply-line variations.

The tuning elements should be of small physical size, and for remote positioning systems their total variation should be large as compared with their manufacturing tolerances.

The most-preferred compromise between these requirements was found to be a range of operating frequencies between 350 and 500 kc.

Fig. 3 shows a schematic circuit diagram of a torque amplifier and a typical damping system for step excursions. The torque amplifier proper is of the system type (a), and operates on a fixed balance frequency of 450 kc.

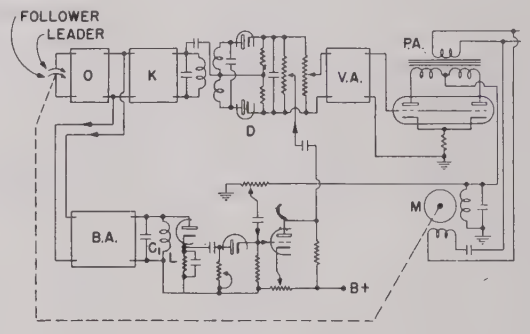

Fig. 3—Schematic of torque amplifier with damping system.

Leader and follower are parts of the same oscillator-tuning capacitor, the leader consisting of a small vane between two follower plates. The frequency excursion from the balance position to total vane and plate engagement and disengagement was about 50 kc. in an experimental model. Maximum and minimum capacitances were 48 and 17 $\mu\mu$fd., respectively. Full motor torque and maximum follower speed was obtained for a leader movement of $\frac{1}{3}$ degree rotation, or 0.1 per cent of maximum rotation. This vane movement corresponds to a capacitance change of less than 0.1 $\mu\mu$fd., and produces a discriminator output signal of 2 volts peak to peak. The maximum permissible leader speed for the model, excluding the damping circuit, was 1 revolution in 7.4 seconds.

For higher speeds a damping circuit is provided including a buffer amplifier ($B.A.$) with a third resonant circuit tuned to the balance frequency. The magnitude of the signal across this circuit changes rapidly in the vicinity of system balance. This signal is rectified and differentiated to produce positive pulses on balance approach and negative pulses on departure from balance. The positive pulses are selected and used to actuate a control tube to inject a reverse-phase voltage into the system. This voltage is derived from the motor and is proportional to motor speed. With this arrangement, sudden braking of the motor is accomplished just

before balance is reached. Upon motor-speed reduction the feedback voltage diminishes and the gain of the control tube is reduced as the positive pulse decays until the negative-feedback damping circuit is inactivated when system balance is reached.

Fig. 4 shows a schematic circuit of a remote transmission system of the system type (d). The oscillator is tuned by the leader, while the discriminator secondary

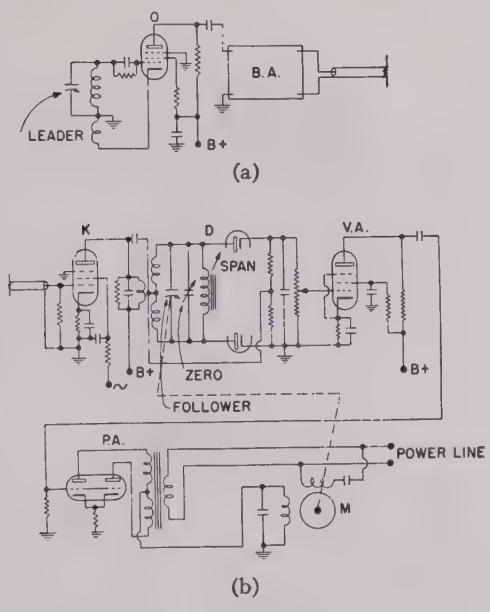

Fig. 4—Schematic of remote positioning system: (a) transmitter, and (b) receiver.

circuit is tuned by the follower. System balance is reached when both circuits are tuned to the same frequency. Keying is accomplished by applying a power-line-frequency voltage of, say, 60 cycles to the screen grid of the keyed amplifier. A trimmer capacitor in the discriminator secondary circuit is provided for zero adjustment, while a variable-inductance coil is provided for span adjustment. If leader and follower capacitors have straight-line-capacitance characteristics, zero adjustment is possible without changing span, while a span adjustment requires zero readjustment.

Fig. 5 illustrates the problem of obtaining constant sensitivity; that is, a constant discriminator output signal per unit-leader movement over the entire span, for straight-line-capacitance leader and follower capacitors for linear transmission. For such capacitors the frequency variation per unit-capacitance change is not linear, but varies as the cube of the ratio of the particular operating frequency to the maximum operating frequency, as shown by curve β. Also, the discriminator sensitivity—that is, the output signal per kilocycle frequency deviation—changes over the range of operating frequencies because of the fixed tuning of its primary circuit, and causes, therefore, the amplitude variation of its primary voltage as illustrated by curve γ. Fortunately, these two effects can be opposed, and by proper tuning and loading of the discriminator primary

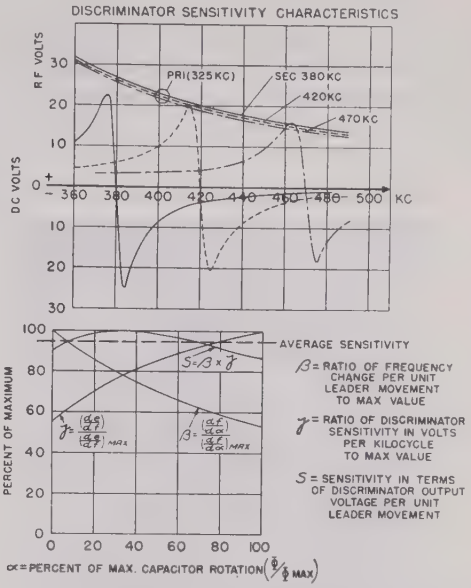

Fig. 5—Discriminator characteristics for wide-band operation and system-sensitivity characteristics.

this curve can be so shaped that the system sensitivity $S=\beta\times\gamma$, and the discriminator output voltage per unit-leader movement can be made sufficiently constant over the operating range, as shown by curve S. In a

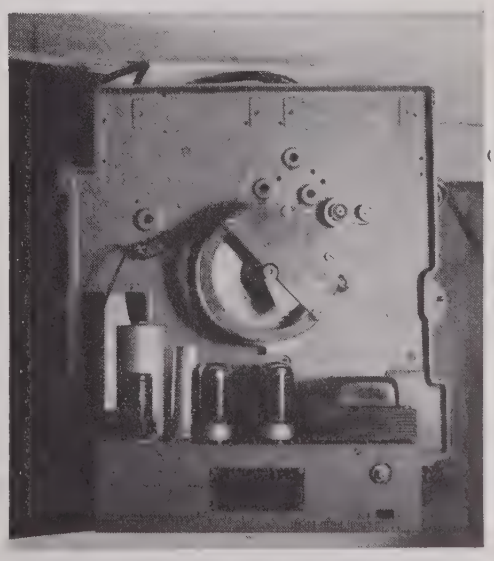

Fig. 6—Model of torque amplifier (type (a)).

particular case, the discriminator primary was tuned to 325 kc. and loaded with a resistance of 7500 ohms, for an operating range from 370 to 460 kc.

Fig. 6 shows a model of a torque amplifier (of type (a)

of Fig. 1) with a leader vane and two associated semicircular plates driven by the motor pinion, visible to the left. This model uses the circuit substantially as shown in Fig. 3, and the design and performance data given in connection with that figure pertain to this model.

Fig. 7 shows a model including a rate-of-flow meter with a force amplifier of system type (b), and an integrating flow meter with a torque amplifier of system type (a). The circuits in both cases are substantially as shown in Fig. 3.

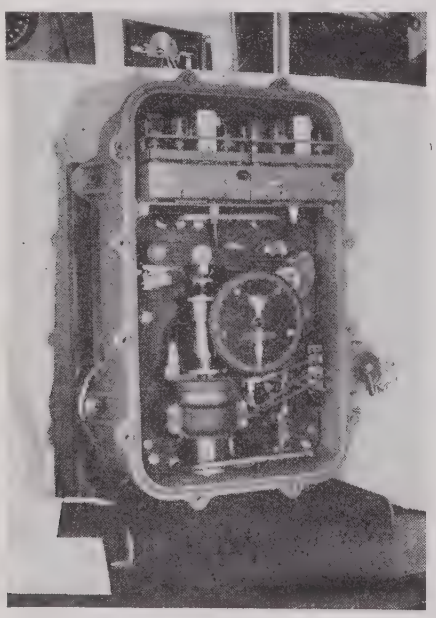

Fig. 7—Model with force amplifier (type (b)) and torque amplifier (type (a))

The rate-of-flow meter comprises a differential-bellows arrangement with the movable capacitor plate rigidly attached to the bellows diaphragm. This plate is also attached by means of a spring to a cam-operated lever, so that the movable plate is always returned to the same relative position with respect to the fixed capacitor plate by increasing or decreasing the spring tension. By this action, the bellows diaphragm is also always returned to the same position, thus reducing bellows travel to a minimum in order to eliminate hysteresis effects. The cam is provided for extracting the square-root relation between the rate-of-flow and the differential-bellows pressure. The pointer is coupled to the cam, so that the angular cam position is indicated on the scale.

The integrating flow meter comprises a constant-speed turntable and a radially movable friction wheel contacting the turntable at a radius depending upon the rate-of-flow. Since such an arrangement should not be mechanically loaded, the friction wheel shaft is provided with a leader vane, which is followed by a motor-driven follower plate, forming a capacitor in co-operation with the leader vane. The number of follower revoluations is counted to indicate flow.

The electronic equipment for the rate-of-flow and flow meters is seen at the top of the case.

Fig. 8 and 9 show the transmitter and receiver, respectively, of a remote plotting system, in which movements of the transmitter writing stylus are faithfully followed by the receiver recording pen. This system is of type (d) of Fig. 1, and uses two circuits, substantially as shown in Fig. 4, for the two co-ordinates.

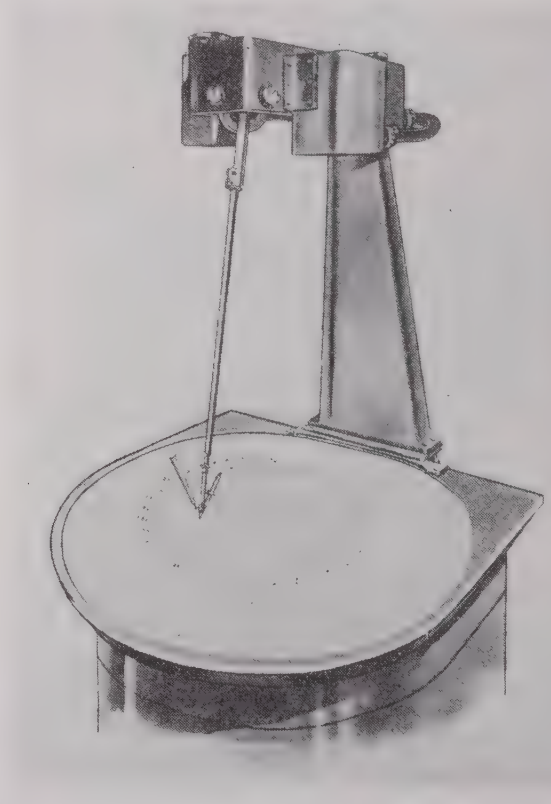

Fig. 8—Remote-plotting-system transmitter.

Fig. 8 shows the stylus arm with the writing stylus. The writing stylus is equipped with a pressure contact for actuation of the recorder pen at the receiver. This arm is mounted in gimbal joints and is coupled to the rotors of two capacitors by way of correction cams, provided to extract the tangent relations between the position of the stylus point and the angle of the stylus arm. The transmitter head includes the gimbal joints, correction cams, oscillator-tuning capacitors, and associated oscillators. The oscillators are keyed alternately, so that only a single channel is required for transmitting both co-ordinate-system signals.

Fig. 9 shows a receiver with the door open. This door, equipped with a window 18×18 inches, carries the transparent chart paper, on the back of which pen recordings are made. This feature eliminates the obstruction of the record by the pen and its supporting and actuating mechanism.

To the right, the follower capacitors and their drive motors are visible. The pen carriage is supported by the cross bars, guided and driven by the drive motors by way of a rack-and-pinion arrangement and cable drive. The pen carriage also carries the pen-actuating relay, energized whenever the pressure contact at the transmitter stylus is closed.

The two receiver-amplifier units are alternately keyed in phase and synchronism with the transmitter oscillator keying, so that only corresponding transmitter oscillators and receiver amplifiers are operated at any time.

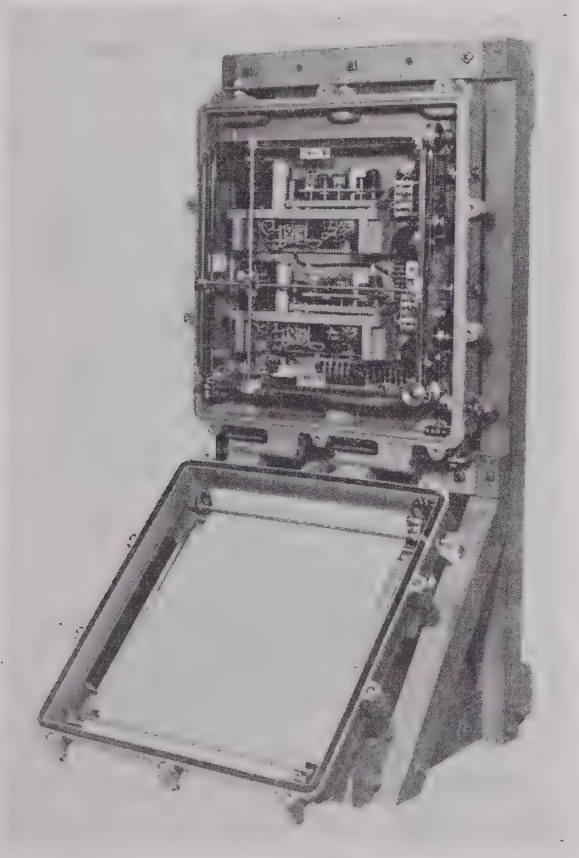

Fig. 9—Remote-plotting-system receiver.

This system is connected as a wired radio system and operates over a frequency range of 370 to 460 kc. with a pen speed of 12 inches per second. A typical warm-up drift, for which the system is not compensated, is about 0.2 per cent of full-scale travel. Pen movements due to temperature and supply-voltage changes are inconsequential. The system accuracy, including all tolerances, was found to be about 0.3 per cent, on the average, while the repeatability was about 0.03 per cent or better.

In a typical system one to six receivers are selectively or simultaneously connected to one transmitter. Failure of one receiver does not affect the operation of the other connected receivers.

Apparatus of the remote positioning type has been used successfully for production checking of coil inductances with the aid of high- and low-limit coils. Small tolerances can be spread over a large-scale portion for ease of reading and accurate checking. Another possible application of this system is the constant-frequency regulation of oscillators, such as the oscillator of a frequency-modulation transmitter.

The broad idea of using the frequency of a signal for remote transmission of the variation of a condition is not new, and various other systems based on this idea have been proposed. In concluding this paper, a brief comparison of the present system with others is presented.

Systems have been suggested in which an unkeyed radio-frequency signal is applied to a discriminator, to which a low-frequency keying voltage is also applied. In order to maintain a usable wave shape of the discriminator output signal for efficient motor drive, the applied keying voltage must be considerably greater than the applied radio-frequency signal. This makes for low discriminator sensitivity and makes the system highly susceptible to slight discriminator unbalances. This is a disadvantage which is not present in the new system.

In another system a steady low-frequency component due to the discriminator keying voltage is present even for system balance, and considerably reduces the efficiency of the amplifier between discriminator and motor.

Certain proposed audio-frequency systems use frequency indicators as output devices. Since these arrangements have very low-torque output, they are not, per se, suited for remote power positioning.

Some proposed systems use a radio-frequency or superaudible signal, the frequency of which is varied over a narrow range and then heterodyned to produce a variable audio frequency. In such systems any error due to undesired frequency drift is extremely serious, because the system error is determined by the ratio of frequency error to the operating-frequency range, which, in other words, is simply the noise-to-signal ratio. Consequently, the narrower the range, the greater the system error caused by deviations from the desired frequency.

To safeguard against such errors and to ensure a high degree of stability, a relatively wide frequency range was chosen in the new system.

For narrow-band transmission of the signals of the new system, by wire or wireless, it is feasible to narrow the frequency band by frequency division before direct transmission or modulation on a carrier, and to expand the frequency band after reception by frequency multiplication. In this way, the high quality of performance can be retained in spite of narrow-band transmission.

New Techniques in Glass-to-Metal Sealing*

JOSEPH A. PASK†

Summary—The new techniques in glass-to-metal sealing described in the paper include accurate and controlled oxidation of the metal, and the powder-glassing method of making seals. The accompanying experimental data refer to Kovar, since most of the laboratory work has been on glass-to-Kovar seals.

Data are presented for Kovar oxidized at a number of controlled temperatures and varying times. Excellent adherence of glass to Kovar is obtained with a weight gain of about 0.0003 to 0.0007 grams per square centimeter regardless of temperature of oxidation. With preoxidation, any tendency for peeling or flaking shows up readily on cooling to room temperature. This condition is undesirable, since it indicates subsequent poor glass-to-metal adherence

The powder-glassing method of making seals consists of grinding the glass, suspending the powdered glass in a suitable liquid, applying it to the prepared metal, and fusing to form a thin glass layer. The glass tube or bulb is subsequently joined to this layer as a glass-to-glass seal. Several examples of applications are given, one of them pertaining to multisection blanks employing butt seals.

Hypotheses on the function of H_2 baking of Kovar, the adherence of glass to Kovar, and the nature of the oxidation process of Kovar are presented.

Introduction

IN MAKING glass-to-metal seals the usual technique consists of cleaning the metal, oxidizing it the proper amount in order to develop a strong, vacuum-tight seal, and sealing the glass to the metal while it is still hot. Consequently, in seals made on the glass lathe, success is entirely dependent upon the skill and judgment of the operator. This is especially true on large and intricate seals. He must decide whether he is oxidizing sufficiently and, also, whether a firmly adhering oxide layer has been obtained.

The development of the powder-glassing method at the Research Department of the Westinghouse Lamp division enables the making of seals on a controlled basis. The new techniques in glass-to-metal sealing to be described include accurate and controlled oxidation of the metal, and the application of the glass in a powdered state that is fused to form a thin glass layer to which the glass tube or bulb is subsequently joined as a glass-to-glass seal.

Oxidation of Metal

Since most of the laboratory work has been on glass-to-Kovar seals, references to specific data will be on Kovar, an iron-nickel-cobalt alloy developed at Westinghouse.

Prior to oxidation the Kovar is baked in a wet hydrogen atmosphere at 1100°C. for 15 to 30 minutes, in order to eliminate possible bubbling at the glass-metal interface during sealing.

Experiments on oxidation were carried out in an electrically heated oven at controlled temperatures and varying times. Curves for weight gain per unit area versus time were thus obtained for a number of constant temperatures, as shown in Fig. 1. A range of values is indicated, since such variations occurred with changes in H_2 baking, cleanliness of pieces, standing prior to oxidation, etc.

The excellent adherence of the glass to Kovar is obtained with a weight gain of about 0.0003 to 0.0007 grams per square centimeter regardless of temperature of oxidation, i.e., approximately 17 minutes at 800°C., 3 minutes at 900°C., 1 minute at 1000°C., or $\frac{1}{4}$ minute at 1100°C.

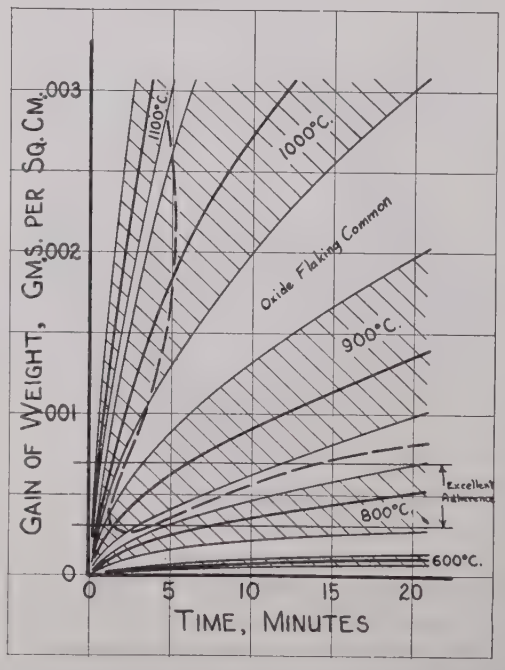

Fig. 1—Oxidation of Kovar. Time-rate curves are shown. Area inside V-shaped dotted curve indicates conditions under which greatest tendency for oxide flaking exists.

If the piece is underoxidized, the strength of the seal is poor but it is still vacuum tight. If it is overoxidized, the strength is good but the seal may be a leaker because the glass is unable to penetrate the oxide layer completely, thus leaving a continuous porous path through which gases can seep into the tube.

* Decimal classification: R720. Original manuscript received by the Institute, January 16, 1947; revised manuscript received, August 21, 1947. Presented, 1947 I.R.E. National Convention, March 4, 1947, New York, N. Y.

† Westinghouse Electric Corporation, Bloomfield, N. J.

With the preoxidation of Kovar any tendency for peeling or flaking shows up on cooling to room temperature. Statistical recording has shown that this tendency exists more strongly under certain conditions of temperature and time, as indicated in Fig. 1 by the area inside the V-shaped dotted line. Flaking is emphasized by improper or lack of H_2 baking, dirty Kovar, and other factors.

Pieces with flaking or peeling oxide layers should be eliminated immediately, since poor oxide adherence also results in poor glass adherence. Such a tendency may be missed with the usual glassing technique, wherein the glass is sealed to the oxidized metal while the latter is still hot.

Powder-Glassing Method of Making Seals

Grinding of glass, in any form, to pass through a 200-mesh sieve constitutes the first step in the preparation of the glass for use in the powder-glassing method of making seals. A porcelain-ball mill is used to avoid contamination by iron. The composition of the ground glass is the same as normally used for sealing to a given metal; for instance, Corning 7052 or 704 for Kovar.

The powdered glass is suspended in a suitable liquid such as water or alcohol. With alcohol, which has been used most extensively at Westinghouse, a few drops of $LiNO_3$ solution or NH_4OH keep the glass particles from settling out into a hard mass, thus enabling the suspension to be easily dispersed after standing. The best ratio of liquid to solid is determined by careful experimentation.

The powdered-glass suspension is then applied to the oxidized Kovar surface by spraying. The pressure of the spray is controlled by the viscosity of the suspension and the shape of the piece. Pressures ranging from 10 to 40 pounds have been employed.

If the powdered glass is to be applied by dipping or slushing, the suspension is adjusted to the proper viscosity and mobility to obtain the necessary thickness of coating. In either case, the glass is restricted to the desired areas by proper masking prior to application, or by brushing afterwards.

The dried powdered-glass coating is then fused in an electrically heated oven. 7052 and 704 glasses produce a smooth coating by firing at 1000°C. for 6 minutes. The powdered glass can also be fused by fires or by induction heating of the metal. Kovar-glass seals are fired in air, since the rate of oxidation of the Kovar is slow in relation to the rate of fusion of the glass. For seals with copper, however, if oxidation during fusion is undesirable, the firing would have to be carried out in a neutral atmosphere, since the rate of oxidation of the metal is faster than the rate of fusion of the glass. The fired pieces are removed from the heat and allowed to cool in air without any annealing. These powder-glassed parts are now ready for tube assembly and can be stored indefinitely.

The thickness of the fused-glass coating is not critical but has ranged mostly from 4 to 6 mils. The thinner coatings are generally preferred, since there is less tendency for pulling away from edges. Considerable amounts of bubbles, seen with low-power magnification, are present. However, these can be ignored, since no detrimental effects have been noticed because of their presence.

Afterwards, the sealing of the tube or bulb to the powder-glassed parts becomes simply a glass-to-glass seal. Nothing is gained in temperature, since just as much heat and "working" are necessary to make the glass-to-glass seal. The advantage lies in the fact that the seals are now protected and extended heating will not affect them, allowing the operator to work on the seals without any time limitations, which is very important in some cases.

Hypotheses

Hydrogen Baking

Wet-hydrogen baking, for instance, in the time allotted should remove any carbon in the surface of the Kovar at either 900 or 1100°C., but the temperature also controls the grain size of the Kovar, as shown in Fig. 2. Variations in time also alter the grain size, but not as effectively. The whole temperature range is used in baking but the large-grain-size structure is desirable,

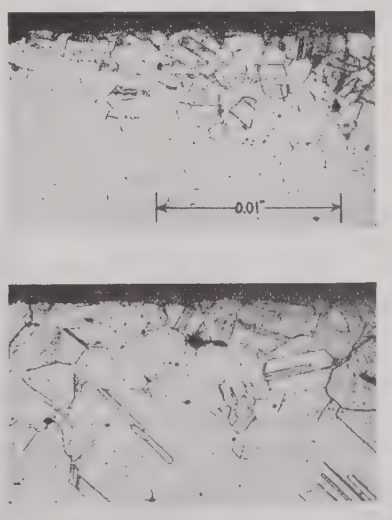

Fig. 2—Effect of wet-hydrogen baking at several temperatures on grain size of Kovar. Magnification, 85×.

since the oxide, and the glass in turn, then have been found on an average to adhere more firmly to the metal surface.

Adherence

The adherence of glass to metal can be attributed to both ionic bonds and physical roughness of the metal. The ionic bond is the oxygen bond resulting in an affinity between the metal and glass, manifested as wetting of the former by the latter. Firing in air without any noticeable preoxidation is sufficient to cause this wetting action. Some adherence because of this wetting alone is evidenced by glassing untreated polished Kovar, but this adherence is weak.

The desirable function of oxidation is to roughen the metal surface by action on the grains, as well as along grain boundaries. The degree of roughness is related to the severity of oxidation, and hence the need for a minimum thickness of oxide to develop the adherence strength of the glass. The maximum thickness of this type of oxide is restricted by the ability of the molten glass to penetrate, but not necessarily dissolve completely, the oxide layer at sealing temperature, primarily because of vacuum-tightness considerations. Final adherence strength is thus realized because of the mechanical clinging of the glass or oxide to the roughened metal surface. A good finished seal, however, does not have nor does it need a continuous oxide layer at the interface.

The preference for large grain texture is due to the resulting decrease of grain boundaries. Oxide ridges are formed at boundaries because the volume of oxide is greater than the volume of a corresponding amount of metal, and more metal surface is available there for oxidation. These ridges are not as completely penetrated by the glass as the oxide on the grain surface, with a subsequent loss of some strength, since the glass develops its chief mechanical adherence by direct contact with the roughened metal surface.

Oxidations

Photomicrographs of cross sections of two Kovar-to-glass seals are shown in Fig. 3, in which the Kovar had been preoxidized at 1000°C. for 1 minute to produce the normal amount of oxidation, and also for 10 minutes.

An observation of considerable interest is the presence of a new metallic layer in the surface of the Kovar, with an average thickness of about 10 microns in the normal seal. X-ray studies of the layer indicate the same structure as that for the alloy Kovar but with a condensed crystal lattice because of less iron. In turn, X-ray examinations and chemical analyses of the oxide layer indicate that it is primarily Fe_3O_4. Therefore, in the oxidation of Kovar, iron diffuses preferentially, forming an oxide layer composed primarily of iron oxide and a new alloy layer at the surface consisting mostly of nickel and cobalt.

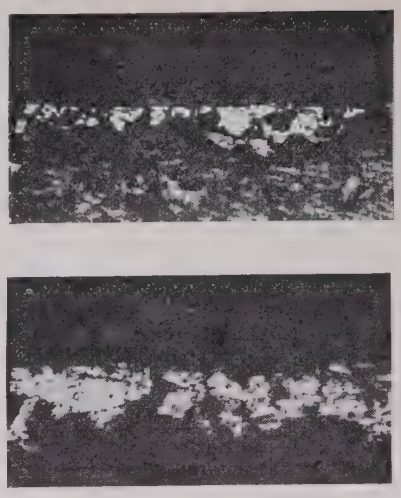

Fig. 3—Photomicrographs of cross sections of Kovar-to-glass seals showing presence of new alloy layer at Kovar surface. Magnification, 350×.

Applications

The use of the powder-glassing techniques can be referred to several specific examples. Part of the liquid air trap in the mass spectrometer consists of a special Kovar cylinder brazed to a heavy copper tube. Glass-to-metal seals are required on each end of the part. Prior to the use of the new methods, usual sealing techniques resulted in a shrinkage of about 40 per cent. The powdered-glass method allowed the making of successful seals with no shrinkage. Fig. 4 shows the powder-glassed portions of the cylinder to which subsequent seals were made.

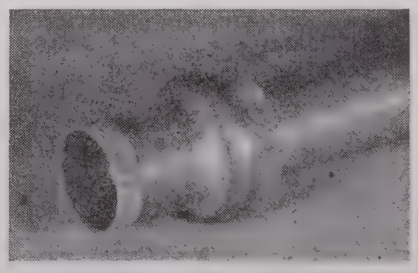

Fig. 4—Part of the liquid air trap in the mass spectrometer, showing the fused thin glass coating applied to the Kovar part. Magnification about 1/3×.

Similar experiences prevailed in the making of multisection blanks employing butt seals. Such butt seals were normally found impossible to make on a glass lathe, since the opposite side of a Kovar ring was oxidizing while the glass blower was making a seal. By first powder-glassing the rings on both sides this difficulty was eliminated, since the glass coating protected the seal interface during subsequent heat applications. Consequently, good multisection butt seals with controlled oxidation resulted, and such blanks became pos-

sible as shown in Fig. 5. The steps in the glassing of the Kovar rings are also indicated.

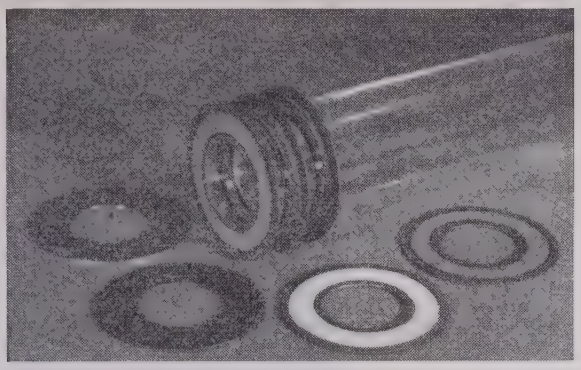

Fig. 5—Multisection blank employing butt seals. The following steps in the powder-glassing of the Kovar rings are shown: cleaning, oxidizing, spraying of powdered-glass suspension, and fusing of coating to form thin layer (on both sides). Magnification, 1/3×.

Conclusion

Although the techniques which have been described have been specifically referred to the use of Kovar, they can also be applied to other sealing metals. The processing steps are simple, but the introduction and development of new types of equipment are necessary for plant production.

The broad advantages of the techniques described are the resultant possibilities of making glass-to-metal seals on a controlled basis, developing mass-production methods, improving glass-blowers' efficiency, producing intricate seals that previously have been too difficult or too costly, and indefinite storing of powder-glassed parts without any special precautions. Lastly, the method of powder-glassing is a valuable research tool, since assembly of intricate designs now becomes possible.

Contributors to Waves and Electrons Section

Sidney Bertram (A'36–SM'47) was born at Winnipeg, Canada, on July 7, 1913. He attended the Los Angeles City College from 1930 to 1933. From 1934 to 1936 he was an instructor at the Radio Institute of California, leaving to enter the California Institute of Technology where he received the B.S. degree in engineering in 1938. Later Mr. Bertram was employed as a research engineer by the International Geophysics Company. In 1939 he entered the Ohio State University, receiving the Master's degree in electrical engineering in 1941. From 1941 to 1942 he was engaged in war research under the O.S.U. Research Foundation. In 1942 he joined the staff of the University of California, Division of War Research, where he was engaged in the development of underwater-sound-ranging equipment. In 1945 Mr. Bertram joined the staff of the Physical Research Unit of the Boeing Aircraft Company and in 1946 he returned to the Ohio State University as an assistant professor in electrical engineering. He is a member of Sigma Xi, Tau Beta Pi, and Eta Kappa Nu.

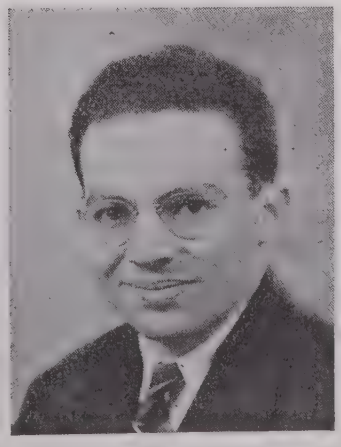

Sidney Bertram

❖

J. H. Dellinger (F'23) was born on July 3, 1886, at Cleveland, Ohio. He attended Western Reserve University from 1903 to 1907, received the A.B. degree from George Washington University in 1908, the Ph.D. degree from Princeton University in 1913, and the D.Sc. degree from George Washington University in 1932.

Dr. Dellinger has been on the staff of the National Bureau of Standards as physicist since 1907, and from 1928 to 1929 was chief engineer of the Federal Radio Commission, on loan from the Bureau. He has been a representative of the United States Government at numerous international radio conferences since 1921, and of the Department of Commerce on the Interdepartment Radio Advisory Committee since 1922.

Dr. Dellinger was vice-president of The Institute of Radio Engineers in 1924, and president in 1925. He has been vice-president of the International Scientific Radio Union since 1934, and chairman of the Radio Technical Commission for Aeronautics since 1941.

Contributors to Waves and Electrons Section

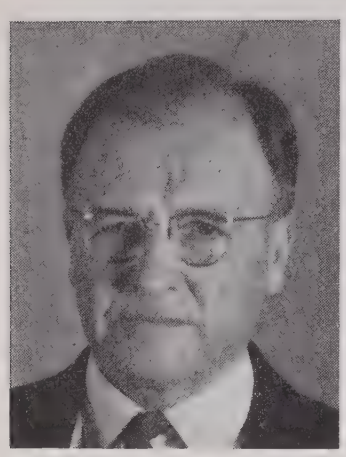

J. H. DELLINGER

❖

Horatio Wellington Lamson (A'15–M'27–F'33) was born on January 2, 1893, at Somerville, Mass. He received the S.B. degree in physics in 1915 from Massachusetts Institute of Technology, and the A.M. degree in physics in 1917 from Harvard University.

Mr. Lamson was a member of the United States Naval Reserve Force during World War I and assistant to G. W. Pierce in the development of antisubmarine devices. Subsequently he became a physicist in the United States Navy Department. Since 1921 he has been a research engineer with the General Radio Company.

Mr. Lamson is a Fellow of the Acoustical Society of America and a member of the American Institute of Electrical Engineers.

❖

Joseph A. Pask was born on February 14, 1913, in Chicago, Ill. He received the B.S. degree from the University of Illinois in 1934, the M.S. degree from the University of Washington in 1935, and the Ph.D. degree from the University of Illinois in 1941.

Dr. Pask served as an instructor in ceramic engineering at the University of Illinois from 1938 to 1941. He then became assistant professor and head of the department of ceramic engineering at the University of Washington until 1943, when he joined the Westinghouse Electric Corporation. At present he is section research engineer in charge of the ceramic section in the research department at Bloomfield, N. J.

Dr. Pask is a member of the American Ceramic Society, the Institute of Ceramic Engineers, the Society of Glass Technology, the Society of Experimental Stress Analysis, Sigma Xi, and Keramos.

H. W. LAMSON

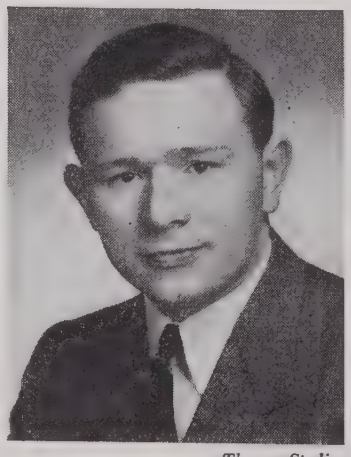

Thomas Studios

JOSEPH A. PASK

❖

Newbern Smith (A'41–SM'46) was born on January 21, 1909, at Philadelphia, Pa. He was graduated from the University of Pennsylvania, Moore School of Electrical Engineering, with the degrees of B.S. in 1930 and M.S. in 1931, in electrical engineering; and of Ph.D. in physics in 1935.

Since 1935 Dr. Smith has been a physicist at the National Bureau of Standards. During the war he was Assistant Chief of the Interservice Radio Propagation Laboratory which was set up by the U. S. Joint Chiefs of Staff to meet Army-Navy needs for radio propagation information. He has participated in several international radio propagation conferences.

❖

R. F. Wild (A'37) was born in New York, N. Y., on August 27, 1910. He received the M.S. degree in communications engineering from the Berlin Institute of Technology in 1935, and then joined the research group of Farnsworth Television, Inc., at Philadelphia, Pa. He remained there until 1939 when the company was reorganized under the name of Farnsworth Television and Radio Corporation and moved to Fort Wayne, Ind. He was connected with the new organization in the capacity of research consultant and patent engineer until the end of 1941, and then joined the patent department of Zenith Radio Corporation, Chicago.

Since the latter part of 1942, Mr. Wild has been senior electronic research engineer for the Brown Instrument Company of Philadelphia. In this capacity he has supervised the design and development of special electronic equipment to be used with precision measuring instruments. He is now employed in the applied physics section of the experimental station, E. I. DePont de Nemours and Company, Inc., Wilmington, Del.

NEWBERN SMITH

❖

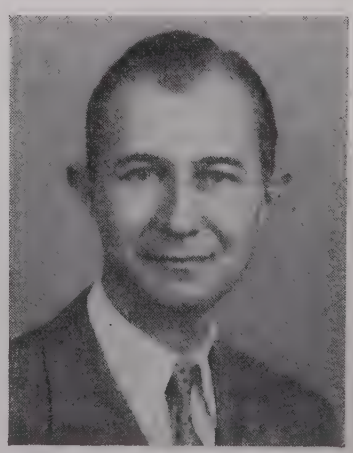

R. F. WILD

Abstracts and References

Prepared by the National Physical Laboratory, Teddington, England, Published by Arrangement with the Department of Scientific and Industrial Research, England, and *Wireless Engineer*, London, England

NOTE: The Institute of Radio Engineers does not have available copies of the publications mentioned in these pages, nor does it have reprints of the articles abstracted. Correspondence regarding these articles and requests for their procurement should be addressed to the individual publications and not to the I.R.E.

The number in heavy type at the upper left of each Abstract is its Universal Decimal Classification number and is not to be confused with the Decimal Classification used by the United States National Bureau of Standards. The number in heavy type at the top right is the serial number of the Abstract.

The Annual Index to these Abstracts and References, covering those published from January, 1947, through December, 1947, may be obtained for 2s. 8d., postage included from the *Wireless Engineer*, Dorset House, Stamford St., London S. E., England

ACOUSTICS AND AUDIO FREQUENCIES

534.143:518.4 1

Magnetostriction Resonant Frequencies—R. C. Coile. (*Electronics*, vol. 20, p. 130; September, 1947.) An abac giving the natural vibrating frequencies of an oscillator when the rod length and material are known.

534.213+534.844 2

Mean Free Path of Sound in an Auditorium—A. E. Bate and M. E. Pillow. (*Proc. Phys. Soc.* (London), vol. 59, pp. 535–541; July 1, 1947.) A brief review of the subject, with proofs that the mean free path of sound in an enclosure is equal to 4 (Volume versus Surface Area) for rectangular, spherical, and cylindrical rooms of any dimensions.

534.321.9 3

Absorption of Supersonic Waves in Liquids—S. B. Gurevich. (*Compt. Rend. Acad. Sci.* (U.R.S.S.), vol. 40, no. 1, pp. 17–20; 1947. In Russian.) Formulas derived by Stokes (1) and Mandelstam and Leontovich (2) are discussed and a more general formula (7) is proposed.

534.321.9:546.212 4

A Pulse Method for the Measurement of Ultrasonic Absorption in Liquids: Results for Water—J. M. M. Pinkerton. (*Nature* (London), vol. 160, pp. 128–129; July 26, 1947.) Measurements were made at frequencies between 7.37 and 66.1 Mc. using a quartz crystal as a transceiver. The pulse recurrence frequency was 250 c.p.s. and the pulse length variable from 2 to 40 microseconds. The values obtained for the amplitude absorption coefficient α are higher than those given by the theory of Stokes.

534.442.1:621.317.757 5

Electronic Indicator for Low Audio Frequencies—A. E. Hastings. (PROC. I.R.E., vol. 35, pp. 821–827; August, 1947.) For analysing a periodic complex wave form. The components within the frequency band 1 c.p.s. to 1 kc. are displayed on four parallel linear scales traced on a c.r.t. Only a rough measurement of amplitudes of the frequency components was desired, but the frequency scales can be set up, without frequency calibration and within an accuracy of 3 per cent from design equations developed in this paper. The performance and limitations of the instrument are described.

534.62 6

A New Sound-Absorbing Device of High Efficiency and the Construction of a Sound-Damped Room—E. Meyer, G. Buchmann, and A. Schoch. (*Akus. Zeit.*, vol. 5, pp. 352–364; December, 1940.) Measurements of the absorption by cones of various shapes led to the use of cones of 1 meter overall length for the lining of a sound-absorbing chamber. The cones were constructed by hand from slagwool, with a bitumen binder, and had a parallel section 15 centimeters long, the mouth being 15 by 15 centimeters. About 32,000 of these cones were used, fixed to the walls and roof by hooks and pins, and with points inwards, giving a clear space of 14 meters by 9 meters by 7 meters. Results of tests carried out in the completed room are shown graphically and discussed.

534.756 7

Investigations on the Theory of Hearing—H. Jung. (*Akus. Zeit.*, vol. 5, pp. 268–283; September, 1940.) Mathematical treatment of the propagation of sound in an elastic tube filled with a viscous incompressible fluid is used to draw conclusions as to the hydrodynamic processes which take place in the ear. The results are in agreement with the phenomena occurring in an electrical network analogous to the elastic tube and are compatible with the resonance theory of hearing.

534.756.1 8

Transient Reception and the Degree of Resonance of the Human Ear—R. J. Pumphrey and T. Gold. (*Nature* (London), vol. 160, pp. 124–125; July 26, 1947.) Experiments have been conducted which support the Helmholtz theory of pitch discrimination based on high-Q resonators of the cochlea. Q values of 200 to 350 at 10 kc falling to about 50 at 1 kc were obtained.

534.851:621.395.66 9

Experimental Volume Expander and Scratch Suppressor—McProud. (*See* 46.)

534.86:534.322.1 10

Frequency Range Preference for Speech and Music—H. F. Olson. (*Electronics*, vol. 20, pp. 80–81; August, 1947.) Tests with live performers heard through a removable acoustic low-pass filter cutting off at 5 kc., showed that 69 per cent of the listeners preferred the full acoustic range, in contrast to accepted results on reproduced programs. Reasons are suggested. See also 3007 of 1947 (Webster and McPeak) and 3765 of January.

534.86:534.322.1 11

Psycho-Acoustical Aspects of Listener Preference Tests—C. J. LeBel. (*Audio Eng.*, vol. 31, pp. 9–12, 48; August 1, 1947.) A detailed and critical analysis of various attempts to discover whether listeners prefer reproduction systems to have a full or a restricted a.f. range. The economic aspects of possible improvements in the quality of reproduction are also considered. See also 3765 of January (Olson) and 10 above.

534.861.1/.2 12

Microphone Placement for Studio Liveness—(*Tele-Tech*, vol. 6, pp. 44–45, 103; July, 1947.)

621.395.623.7 13

Loudspeaker Damping—F. Langford-Smith, G. N. Patchett, P. J. Walker, C. J. Mitchell, and E. J. James. (*Wireless World*, vol. 53, pp. 309 and 343–344; August and September, 1947.) The electromagnetic damping of a loudspeaker is limited by the equivalent series impedance of the loudspeaker itself, but at resonant points, the efficiency considerably exceeds its mean value, and the equivalent impedance is thus reduced.

621.395.623.8 14

The Distribution of Acoustic Power—L. Chrétien. (*T.S.F. Pour Tous*, vol. 23, pp. 158–160 and 180–182; July, August, and September, 1947.) Practical circuits for feeding a number of similar or different loudspeakers. See also 2317 and 3770 of January.

621.395.623.8 15

U.N. Broadcast and Public-Address Systems—A. W. Schneider. (*Audio Eng.*, vol. 31, pp. 26–29, 44; August 1, 1947.) A description, with illustrations and block diagrams, of the public-address and broadcasting facilities in the United Nations conference room and General Assembly auditorium, New York.

621.395.625.2 16

On the Linear and Nonlinear Distortions of Sound Disk Apparatus—G. Guttwein. (*Akus. Zeit.*, vol. 5, pp. 330–349; December, 1940.) A comprehensive experimental investigation of the dependence of distortion on recording processes, disk material, and reproducing methods.

621.395.625.2 17

The Design of a High-Fidelity Disc Recording Equipment—H. Davies. (*Jour. I.E.E.* (London), part III, vol. 94, pp. 296–300; Discussion, pp. 275–295; July, 1947.) Section

1: Comparison of disk recording with alternative systems, and discussion of standardization of disk and groove dimensions, cutting, and turntable speeds, the magnitudes of stylus amplitudes, velocities, and accelerations, the use of radius compensation, and the choice of the optimum recording characteristic. Section 2: Discussion of turntable drive, design and mounting of the cutter head, methods of making cue marks and of removing swarf while recording, and of obtaining radius compensation. Section 3: Description of a high-fidelity disk-recording equipment developed for the B.B.C., and of its performance.

621.395.625.2:621.395.667 18
Bass Compensation—J. Ellis. (*Wireless World*, vol. 53, pp. 319–320; September, 1947.) For bass compensation with disk records, the amplification must be inversely proportional to frequency below about 250 c.p.s. This is achieved by making the negative feedback proportional to the frequency.

621.395.625.3 19
Frequency Response of Magnetic Recording—O. Kornei. (*Electronics*, vol. 20, pp. 124–128; August, 1947.) The effects on frequency response of the thickness of the magnetic recording medium, the depth of penetration of magnetization into the medium, and the size of the recording head and gap are discussed.

621.395.625.3 20
Design of Magnetic Tape Recorders—R. H. Ranger. (*Tele-Tech*, vol. 6, pp. 56–57, 100; August, 1947.) Discussion of German war-time development of magnetic tape recording, and American post-war improvements.

621.396.645.029.3:621.396.665 21
Automatic Gain Control and Limiting Amplifier—Jurek and Guenther. (*See* 69.)

AERIALS AND TRANSMISSION LINES

621.392.029.64 22
$TM_{0,1}$ Mode in Circular Wave Guides with Two Coaxial Dielectrics—S. Frankel. (*Jour. Appl. Phys.*, vol. 18, pp. 650–655; July, 1947.) "Field components for a transverse magnetic wave in a wave guide with two coaxial dielectrics are computed. A typical example is given to show the calculation of guide dimensions to reduce phase velocity to a preassigned value."

621.392.029.64 23
Properties of Ridge Wave Guide—S. B. Cohn. (PROC. I.R.E., vol. 35, pp. 783–788; August, 1947.) Equations and curves, checked experimentally, giving cutoff frequency and impedance are presented for rectangular waveguides having a rectangular ridge projecting inward from one or both wide sides. The guide has a lower cutoff frequency and impedance and greater higher-mode separation than a plain rectangular waveguide of the same width and height. A number of applications are suggested.

621.396.67 24
The Influence of the Width of the Gap upon the Theory of Antennas—L. Infeld. (*Quart. Appl. Math.*, vol. 5, pp. 113–132; July, 1947.) A mathematical paper concerned with the effect of the gap across which the voltage is applied. As in the work of Stratton and Chu (1888 of 1941) the Dirac function is used to derive the driving point admittance of a spherical aerial; a concluding section deals with the spheroidal aerial. The finite width of the gap is taken into account in both cases. The alternative approach used by the earlier workers, in which the gap width is initially allowed to tend to zero—thus resulting in an infinite driving point admittance—is critically examined.

621.396.67 25
Effect of Feed on Pattern of Wire Antennas—D. C. Cleckner. (*Electronics*, vol. 20, pp. 103–105; August, 1947.) Measured polar diagrams for straight wires of lengths between one-half λ and 3λ are given, showing how the feed point affects the number, orientation, and magnitude of the lobes.

621.396.67 26
A Tentative Investigation of a Complex System of Tower Radiators for Radio Broadcasting—B. V. Braude, I. M. Rushchuk, and M. M. Pruzhanski. (*Radiotekhnika* (Moscow), vol. 2, pp. 22–33; July and August, 1947. In Russian.) In designing a radiating system having four self-supporting towers at the corners of a square, and intended for both directional and nondirectional broadcasting, experiments were conducted with a model using brass lattice towers 250 centimeters high, erected on a ground system of galvanized iron sheets. The radiators were fed through single conductor feeders from two u.s.w. oscillators covering a wavelength range from 3 to 9 meters. Measurements were made of the input impedance of the radiators, of the phase velocity of e.m. waves along them, and of the directivity coefficient of the system for various operating conditions. Experimental curves so obtained are shown and the conclusions reached regarding the operation of the proposed system are enumerated.

621.396.67:517.512.2 27
Fourier Transforms in Aerial Theory: Part 3—Operations with Fourier Transforms—Ramsay. (*See* 155.)

621.396.67:621.396.621 28
Is a Big Aerial Worth While?—M. G. Scroggie. (*Wireless World*, vol. 53, pp. 314–318; September, 1947.) Discussion showing the many advantages of a good outdoor aerial.

621.396.67:621.397.5 29
Television Aerials—F. R. W. Strafford and J. N. Pateman. (*Wireless World*, vol. 53, p. 344; September, 1947.) Comment on 3799 of January (Besk and Beebe).

621.396.67:621.397.5 30
Performance Characteristics of the WABD TV Antenna System—G. E. Hamilton. (*Communications*, vol. 27, pp. 16–18, 43; July, 1947.) The advantages of the 3-bay superturnstile batwing aerial system used are discussed. The performance specifications are listed and compared with actual results. An earlier article on the installation and testing of this system was noted in 3432 of 1947 (Deneke).

621.396.67.029.64 31
Radiators for Centimeter Waves—(*Tele-Tech*, vol. 6, pp. 55–56; July, 1947.) Summary of 1622 of 1947 (Gutton). U.D.C. of 1622 should read as above.

621.396.67.029.64:621.317.79 32
Microwave Antenna Beam Evaluator—H. LeCaine and M. Katchky. (*Electronics*, vol. 20, pp. 116–120; August, 1947.) Apparatus for automatic tracing of polar diagrams of microwave aerials to an accuracy within 1 per cent. Square law detectors are used at the transmitter, whose aerial is rotated, and at the fixed receiver. A self-balancing system using motor-driven ganged potentiometers gives the traced diagram a linear scale and eliminates errors due to varying transmitting power and external interference.

621.396.674 33
Calculation of the Current for Frame Receiving Aerials—J. Müller-Strobel and J. Patry. (*Schweiz. Arch. Angew. Wiss. Tech.*, vol. 13, pp. 193–202; July, 1947.) An approximate solution for circular frame aerials of N turns is based on the theory of Hallén, assuming that the wire radius is small compared with the coil radius and that the coil radius is small compared with the wavelength of the incoming radio waves.

621.396.674 34
Note on Circular Loop Antennas with Non-Uniform Current Distribution—G. Glinski. (*Jour. Appl. Phys.*, vol. 18, pp. 638–644; July, 1947.) The radiation patterns, power gain, and radiation resistance are calculated for a closed loop of perimeter $\leqq \frac{1}{2}\lambda$ with a hyperbolic-cosine current distribution. The effective attenuation constant of the equivalent transmission line is deduced from the radiated power. The theory agrees closely with experiment.

621.396.69 35
Antenna Tower Design—R. G. Peters. (*Communications*, vol. 27, pp. 28–29; July, 1947.)

CIRCUITS AND CIRCUIT ELEMENTS

518.5 36
Electronic Computing Circuits of the ENIAC—Burks. (*See* 158.)

518.5:612.318 37
Use of Magnetic Amplifiers in Computing Circuits—Beyer. (*See* 159.)

621.314.23:621.396.69 38
Practical Transformer Design and Construction: Parts 2 and 3—C. Roeschke. (*Radio News*, pp. 58–59, 137 and 60, 124; July and August, 1947.) The design of filter chokes, anode modulation transformers, and audio output transformers. Part 1: 3038 of 1947.

621.316.722.1:621.385.38 39
Shunt Tube Control for Thyratron Rectifiers—J. A. Potter. (*Bell Lab. Rec.*, vol. 25, pp. 273–276; July, 1947.) The inherent delay of thyratron rectifiers in eliminating brief, steep-fronted voltage variations by changes of grid bias is overcome by connecting the anode circuit of a tube across the load. The grid bias of this tube is controlled by a regulating circuit so that small current changes pass through the tube without flowing through the thyratron, which reacts only to the average load.

621.316.8:621.317.33 40
Method for Determining the Time-Constant of Resistors at Low Frequency—Ney. (*See* 166.)

621.318.323.2:538.213 41
Auxiliary Magnetization—*Elec. Times*, vol. 112, pp. 211–212; August 21, 1947.) Summary of article in the June and July 1947 issue of *Brown Boveri Rev.* Methods are given for calculating the effective permeability of current transformer cores using a.c. auxiliary magnetization.

621.319.4 42
Significance of Watt-Second Ratings of D.C. Capacitors—J. D. Stacy. (*Communications*, vol. 27, pp. 24–25; 41; August, 1947.) When the life and the high-temperature performance of capacitors are to be considered, watt-second rating gives a better criterion than voltage and capacitance rating.

621.392:003.62 43
Shorthand Circuit Symbols—B. G. (*QST*, vol. 31, pp. 46–47; August, 1947.) Comment on 2030 of 1947 (Keen).

621.392:518.5 44
Machine Computing of Networks—Dunstan. (*See* 160.)

621.392.1 45
Transformers—Obvious and Otherwise—"Cathode Ray." (*Wireless World*, vol. 53, pp. 388–390; October, 1947.) An elementary explanation of the way in which various tuned

and untuned coupling networks do, in fact, act as transformers, as was stated in the article abstracted in 2919 of 1947 (Moxon).

621.395.66:534.851 46

Experimental Volume Expander and Scratch Suppressor—C. G. McProud. (*Audio Eng.*, vol. 31, pp. 13–15; 41; August 1, 1947.) A number of familiar circuits are combined into one unit. Block and circuit diagrams are given and component values stated. The unit is preceded by a 2-stage preamplifier.

621.396.611.3 47

Variation of an RC Parallel-T Null Network—H. S. McGaughan. (*Tele-Tech*, vol. 6, pp. 48–51, 95; August, 1947.) "When used in the negative feedback loop of an amplifier, this network produces either a frequency-selective amplifier or an oscillator, depending on the choice of circuit parameters. An unasymmetrical null network is shown which provides greater selectivity than is possible with the conventional network under the same conditions of amplification." See also 1464 of 1946 (Hastings).

621.396.611.4:518.4 48

Charts for Resonant Frequencies of Cavities—R. N. Bracewell. (Proc. I.R.E., vol. 35, pp. 830–841; August, 1947.) Six abacs are given which may be used for designing cylindrical resonant cavities whose cross sections are circles, concentric circles, squares, or rectangles. The equations involved, the method of use, and the special advantages of each abac are described, together with the method of construction. The effects of small deformations or of wavelength changes are considered.

621.396.615 49

RC Oscillator Control—B. J. Solley. (*Wireless World*, vol. 53, pp. 321–322; September, 1947.) A network is described, by which the frequency of a *RC* oscillator may be adjusted over a wide range, using a single potentiometer control. A frequency range of 4 to 1 may be obtained with only 1 db variation in amplitude, and a range of 25 to 1 if greater amplitude variation is permissible.

621.396.615.029.3 50

A Wide Range Audio Oscillator—F. W. Dawe. (*Electronic Eng.* (London), vol. 19, pp. 246–248; August, 1947.) An *RC* amplifier backcoupled through a frequency discriminating network of the Wien bridge type. Frequency range is 20 to 20,000 c.p.s., covered in three bands.

621.396.615.029.5/.63 51

Wide-Range Sweeping Oscillator—Engineering Staff, Kay Electric Co. (*Electronics*, vol. 20, pp. 112–115; August, 1947.) A 50-kc. to 500-Mc. beat-frequency oscillator with sawtooth frequency modulation variable up to 40 Mc. Two 3-centimeter klystron oscillators are used, one being varied in frequency by a panel control of cavity resonator shape and modulated in frequency by variation of the repeller electrode potential. The two klystron frequencies are measured by a precision absorption wavemeter, the difference giving the beat frequency.

621.396.615.14 52

U.S.W. Oscillators—E. P. Korchagina (*Radiotekhnika* (Moscow), vol. 2, pp. 34–43; July and August, 1947. In Russian.) The effects of interelectrode capacitances and of the inductance of the leads on the operation of the oscillators are investigated theoretically. Suitable oscillating circuits are discussed and design methods indicated.

621.396.615.14 53

High Power U.S.W. Valve Oscillators—A. M. Kugushev and D. I. Karpovski. (*Radiotekhnika* (Moscow), vol. 2, pp. 48–54; July and August, 1947. In Russian.) The use of transmission lines with distributed constants as tuning elements for high-power demountable tubes is considered and experiments are described with such tubes operating on wavelengths from 2 to 3.5 meters and with outputs from 8 to 60 kw.

621.396.615.142.2:621.392.029.64:
621.396.619.11 54

Ultra High Frequency Modulation on Wave-Guides—H. Gutton and J. A. Ortusi. (*Jour. Brit. I. R. E.*, vol. 7, pp. 205–210; October, 1947. Discussion, pp. 210–211.) A description of a method of modulating a master klystron oscillator combined with a v.m. amplifier tube. The energy produced is fed to the radiator by a waveguide across which is connected a magnetron working in a cutoff condition and such that variations of anode voltage vary its impedance. By means of a transformer between the magnetron and the guide, the impedance across the guide can be made to vary from zero to infinity, thus enabling 100 per cent modulation to be obtained.

Application to a 100-watt television transmitter for a wavelength of 21.5 centimeters and up to 20 Mc. modulation frequency is described briefly.

For a fuller account see *Onde élect.*, vol. 27, pp. 307–312; August and September, 1947.

621.396.615.18 55

Cathode-Coupled Half-Shot Multivibrator R. K. F. Scal. (*Electronics*, vol. 20, pp. 150, 158; September, 1947.) Describes a double-triode common-cathode *RC* trigger circuit with two stable states operated alternately by successive negative pulses applied across the cathode-bias resistor; the output from either anode, therefore, occurs at half the repetition frequency of the initiating pulses, and is square-wave in form. Successive frequency division may be obtained by connecting units in tandem with differentiating *RC* coupling circuits.

621.396.619.23+621.396.645 56

A 120-Watt Modulator and Speech Amplifier—C. V. Chambers. (*QST*, vol. 31, pp. 13–18; August, 1947.) A compact 3-stage amplifier-modulator, using Type 807 tubes in class AB2 and having a restricted a.f. response. Full circuit and construction details are given.

621.396.621+621.396.69 57

British Printed and Sprayed Circuits—(*See* 238.)

621.396.621 58

Theory and Practice of Cathodyne Dephasing—S. Bertrand. (*T.S.F. Pour. Tous*, vol. 23, pp. 166–169; July and August, 1947.) A qualitative and quantitative treatment, with experimental verification of the theory.

621.396.622.71 59

Ratio Detector for F.M. Signals—(*See* 248.)

621.396.645 60

Amplifier with Variable Bandwidth—F. Juster. (*Toute la Radio*, vol. 14, pp. 258–260; September, 1947.) A design giving (a) very large bandwith with low sensitivity, (b) medium bandwith with medium sensitivity, or (c) small bandwidth with high sensitivity. The changes are effected by varying the anode resistance of each tube.

621.396.645 61

Harmonic-Amplifier Design—R. H. Brown. (Proc. I.R.E., vol. 35, pp. 771–777; August, 1947.) Two methods are presented for calculating the ideal performance of harmonic-amplifier stages as used in frequency multiplication. The first gives approximate results while the second, a graphical method, is exact. Performance may be adversely affected by degenerative effects introduced by the grid-anode capacitance and by inductance in the cathode circuit common to both grid and anode circuits. Circuit arrangements for overcoming these degenerative effects are discussed theoretically and applications are indicated.

621.396.645:518.3 62

Square Wave Response—A. J. Baracket. (*Electronics*, vol. 20, p. 130; August, 1947.) Abac giving the degree of tilting of a square wave by an *RC* coupling circuit.

621.396.645:518.4 63

Gain Chart for Cathode Followers—G. Houck. (*Tele-Tech*, vol. 6, pp. 54–55; August, 1947.)

621.396.645:621.317.755 64

Wide Band Oscilloscope Amplifier—C. E. Hallmark and R. D. Brooks. (*Tele-Tech*, vol. 6, pp. 38–39, August, 1947.) "Balanced push-pull direct-coupled stages provide characteristics necessary for square wave analysis and television applications." Net bandwidth is 15 Mc.

621.396.645:621.317.755 65

Direct-Coupled Oscillograph Amplifier—D. R. Christian. (*Elec. Eng.*, vol. 66, p. 927; September, 1947.) Summary of A.I.E.E. Dayton paper. A stabilized amplifier for use with a magnetic-pen motor recorder. General requirements, circuit details, and applications are discussed.

621.396.645:621.385.029.63/.64 66

On Two Designs for V.H.F. Electronic Amplifiers with Travelling-Wave Valves—J. P. Voge. (*Compt. Rend. Acad. Sci.* (Paris), vol. 223, pp. 1117–1119; December 23, 1946.) Ramo has considered small oscillations of the form $F(r)e^{j(\omega t-\gamma z+n\theta)}$, with symmetry of order n about the axis of a cylindrical electron beam (4352 of 1939). A formula is here deduced for the power flow through a section of the beam when it is surrounded by an infinitely long cylindrical metal sheath and there is an intense axial field. This formula shows the existence of successive bunchings and debunchings, and a theoretically infinite amplification for a certain length. The energy, being kinetic, should be picked up inductively.

Formulas are also derived for the case where the beam is surrounded by a matched, lossless transmission line, with which the beam has a continuous exchange of energy. The gain is found to be independent of ω and proportional to the square root of the charge per unit length.

621.396.645.029.3 67

Multi-Purpose Audio Amplifier—M. P. Johnson. (*Audio Eng.*, vol. 31, pp. 20–23, 39; August 1, 1947.) "Combines high gain, unusually high fidelity, and an expander-compressor circuit. It can be easily built from readily obtainable components." Full circuit and constructional details are given.

621.396.645.029.3:621.396.61 68

Level-Governing Audio Amplifier—(*Tele-Tech*, vol. 6, pp. 67–69, 96; August, 1947.) Design of a program-operated amplifier which will automatically minimize overmodulation of the radio transmitter. A control circuit reduces amplifier gain when the input exceeds a predetermined value. See also 1189 of 1942 (Black and Norman).

621.396.645.029.3:621.396.665 69

Automatic Gain Control and Limiting Amplifier—W. M. Jurek and J. H. Guenther. (*Electronics*, vol. 20, pp. 94–97; September, 1947.) Describes in detail an audio program amplifier, installed between the studio audio apparatus and the transmitter, for maintaining a high peak modulation depth without danger of over-

loading and with minimum reduction of dynamic range. For another account see *Communications*, vol. 27, pp. 18, 37; August, 1947.

621.396.645.029.62 70

Four-Tetrode F.M. Power Amplifier—V. Zeluff. (*Electronics*, vol. 20, pp. 132, 134; August, 1947.) A 10-kw. amplifier having four tetrodes arranged in a square. Four rods leading vertically from the anodes to a shorting plate form a 4-wire $\lambda/4$ line with adajcent wires fed in antiphase. This system gives a small external field. The aerial coupling system is described.

621.396.662.2.076.2:621.396.621 71

Permeability Tuning of Broadcast Receivers—L. O. Vladimir. (*Electronics*, vol. 20, pp. 94–99; August, 1947.) An analysis of the series-loop and transformer-coupled loop aerial circuits and a comparison with the capacitance-tuned high-impedance circuit. Coil-winding data for obtaining the correct pitch for oscillator tracking are given.

621.396.662.212.029.58:621.315.212 72

A Plug-In Type Resonant Line Tank Coil—H. C. Sherrod. (*CQ*, vol. 3, pp. 19–21; June, 1947.) For use at 28 Mc. in a high-level, a.m. R/T transmitter. A $\lambda/4$ resonant line is used to increase the output tank-circuit efficiency.

621.396.662.3+621.314.6 73

Analysis of Full-Wave Rectifier and Capacitive-Input Filter—D. L. Waidelich. (*Electronics*, vol. 20, pp. 120–123; September, 1947.) The effects of finite filter inductance were determined by means of the author's steady-state operational calculus (1276 of 1946). Data concerning flow angles, output voltage, ripple, and peak tube currents enable the circuit to be designed for any load and frequency.

621.396.621.004.67 74

Most-Often-Needed 1947 Radio Diagrams and Servicing Information [Book Review]—Beitman. (*See* 256.)

GENERAL PHYSICS

53.081 75

Magnetic Units—"Cathode Ray." (*Wireless World*, vol. 53, pp. 339–342; September, 1947.) The c.g.s. and the m.k.s. systems are discussed and the great advantages of the latter emphasized. See also 1392 and 2383 of 1947 (Dorgelo and Schouten).

540.145.6 76

On the Frequency and Phase Velocity of Monochromatic Plane Waves in Wave Mechanics—L. de Broglie. (*Compt. Rend. Acad. Sci.* (Paris), vol. 225, pp. 361–363; August 25, 1947.) In wave mechanics, a plane monochromatic wave Ψ is characterized by the four quantities: frequency ν, wavelength λ, phase velocity V and group velocity U, of which only λ and U are directly measurable. Some authors have concluded that, for Ψ waves, ν and V are at least partially indeterminate. It is shown here that this is not the case and formulas are derived which give directly the values of ν and V corresponding to a value of λ. From these formulas, the classical expressions for ν and V are deduced.

521.53:519.24 77

Fluctuations in Quasi-Sinusoidal Physical Quantities—A. Blanc-Lapierre and P. Lapostolle. (*Jour. Phys. Radium*, vol. 7, pp. 153–164; June, 1946.) Reprint. A study of various mechanisms from the statistical point of view, taking account of amplitude and phase stability and particularly of the spectral distribution of energy. The mechanisms considered are: (a) pendulum with little damping excited by external shocks evenly distributed, nearly evenly distributed or completely irregular; (b) pendulum with little damping, self-maintained by shocks whose amplitude and time of application fluctuate about the normal values (i.e., equal shocks when the pendulum passes the equilibrium position); (c) alternator with slight speed fluctuations.

537.212:621.392.029.064 78

The Electrostatic Field of a Point Charge Inside a Cylinder, in Connection with Wave Guide Theory—C. J. Bouwkamp and N. G. de Bruijn. (*Jour. Appl. Phys.*, vol. 18, pp. 562–577; June, 1947.) A theoretical paper in which the case of an axial point charge is considered in detail. Three methods of approach are used; from the point of view of wave propagation inside the cylinder, stress is laid on the third method in which the potential is developed in terms of discrete normal solutions of the potential equation. This enables the distant fields to be calculated from the behavior close to the exciting source; as an illustration, the theory is applied to the propagation of sound waves from a vibrating point source.

621.317.33.011.5.029.64:[546.212+546.212.02 79

On the Dielectric Properties of Ordinary Water, Heavy Water and of Ionic Solutions at High Frequencies—D. M. Ritson, J. B. Hasted and C. H. Collie. (*Compt. Rend. Acad. Sci.* (Paris), vol. 225, pp. 285–287; August 4, 1947.) Measurements of the real and imaginary parts of the dielectric constant were made for water between 0°C and 75°C, and for heavy water between 5°C and 40°C, at wavelengths of 10, 3 and 1.25 centimeters. Application of Debye's equations gives values within 1 per cent of the optical constants. The critical wavelength decreases with rise of temperature and is in agreement with Onsager's theory. Results for various solutions are discussed.

537.228.1 80

Deflection of a Piezoelectric Rod.—A. A. Kharkevich. (*Zh. Tekh. Fiz.*, vol. 13, nos. 7 and 8, pp. 423–430; 1943.) In Russian. The vibration of a rod consisting of two parallel layers of Rochelle salt is investigated mathematically for different operating conditions.

537.291+538.691 81

The Principles of a General Theory of the Focusing Action of Static Electric and Magnetic Fields—G. A. Grünberg. (*Zh. Tekh. Fiz.*, vol. 13, nos. 7 and 8, pp. 361–368; 1943. In Russian.. A general method is proposed for determining the fields necessary for obtaining an electron or ion beam of a given form. The number of possible trajectories of particles in a beam is established for different types of field. Particular attention is paid to the focusing of narrow beams.

537.291 82

Electron Reflectors with a Quadratic Axial Potential Distribution—J. M. Lafferty. (Proc. I.R.E., vol. 35, pp. 778–783; August, 1947.) A theoretical paper. The electrons are injected into a retarding field through a central aperture in one of the two electrodes between which the field is established. The permissible angle of divergence or convergence which an incident electron may have and yet be focused back through the aperture is examined. The transit time for axial electrons is computed. Possible electrode shapes to set up the desired field distribution are discussed.

537.311.2 83

Ohm's Law—T. Carter. (*Elec. Rev.* (London), vol. 141, pp. 167–168; August 1, 1947.) A discussion based on Ohm's original treatise, "The Galvanic Circuit, Mathematically Treated." See also 1063 and 2393 of 1947.

537.311.3 84

Electronic Conductivity of Non-Metallic Materials—E. J. W. Verwey. (*Philips Tech. Rev.*, vol. 9, no. 2, pp. 46–53; 1947.) The simultaneous occurrence of electronic conductivity, photoelectrical phenomena, light absorption, and deviation from stoichiometric composition in certain semiconducting materials indicates possible causes of these phenomena.

537.311.3:536.48 85

Measurement of the Resistance of PbS near Absolute Zero—Yu. A. Dunaev. (*Compt. Rend. Acad. Sci.* (U.R.S.S.), vol. 40, no. 1, pp. 21–23; 1947. In Russian.) The conclusions of an experimental investigation are: (a) PbS is not a semiconductor in the usual sense of the word; (b) the hole and electron types of PbS behave identically at low temperatures; (c) no superconductivity effects have been observed.

537.311.33:621.314.634 86

Effect of Bending on Selenium Rectifier Disks—P. Selényi and N. Székely. (*Nature* (London), vol. 160, p. 197; August 9, 1947.) Bending a Se rectifier disk causes a temporary increase of the current flowing through it in both directions. The effect is greatest for the reverse current; it is explained by dissociation of the impurity centers, combined with plastic relaxation effects.

537.311.33:621.396.622.6 87

Application of the Theory of Conduction in Semiconductors to Crystal Detectors—M. Leblanc. (*Bull. Soc. Franç. Élec.*, vol. 7, pp. 445–452; August, 1947.) The modifications of the structure of the crystal lattice brought about by the presence of small quantities of impurities can explain the rectification properties of certain semiconductors. The latent image in photography, the properties of oxide cathodes, and probably the phenomena of fluorescence, may be explained similarly. See also 1468 of 1947.

537.533:539.23 88

An Investigation of Auto-Electron Emission from Thin Dielectric Films—D. V. Zernov, M. I. Elinson, and N. M. Levin. (*Bull. Acad. Sci.* (U.R.S.S.), Classe Sci. Tech., no. 3, pp. 166–181; 1944. In Russian.)

537.533.8 89

Present State of Knowledge of Secondary Electron Emission from Solids—P. Palluel. (*Ann. Radioélec.*, vol. 2, pp. 199–213; July, 1947.) The important part played by secondary emission effects in tubes is reviewed briefly and a detailed discussion is given of the principal laws, and of the composition and fundamental mechanism of the secondary radiation. The emissive properties of the alkaline earth and alkali metals, metallic compounds, complex layers, oxide cathodes, and alloys of high output are examined in detail, numerous curves being given.

538.569.4.029.64:546.171.1 90

The Hyperfine Structure of the Ammonia Inversion Spectrum in an Electric Field—J. M. Jauch. (*Phys. Rev.*, vol. 72, p. 535; September 15, 1947.) Summary of Amer. Phys. Soc. paper.

GEOPHYSICAL AND EXTRATERRESTRIAL PHENOMENA

523.53:551.510.535 91

Evaporation of Meteors—T. L. Eckersley. (*Nature* (London), vol. 160, p. 91; July 19, 1947.) Discussion of certain radar photographs in *Nature* and *The Times*. It is suggested that scatter clouds can be produced by the evaporation of small meteors, and that meteors below a certain size will evaporate. The photographs probably show scatter clouds rather than meteors large enough to be visible. There is a close analogy between the scattering of radio waves from scatter clouds and that of α-particles from heavy molecules, leading to Rutherford's fourth power law. It is the small clouds, the invisible evaporating meteors, which scatter effectively.

523.53:551.510.535 92
Radio Reflexions from Meteoric Ionization—J. S. Hey. (*Nature* (London), vol. 160, pp. 74-76; July 19, 1947.) Notes on a discussion at a Physical Society meeting on January 31, 1947, of recent researches by radio and radar methods into ionospheric ionization by meteors. See also 93 below.

523.53:551.510.535 93
Meteors, Comets, and Meteoric Ionization—A. C. B. Lovell. (*Nature* (London), vol. 160, pp. 76–78; July 19, 1947.) Notes on a conference held at Manchester University under the auspices of the Physical Society. See also 92 above.

523.7 94
The Sun a Regular Variable Star—C. G. Abbot. (*Science*, vol. 105, p. 632; June 20, 1947.) Summary of National Academy of Sciences' paper. The solar constant of radiation for the years 1924 to 1944 has a regular periodicity of 6.6456 days. Statistical studies show fluctuations of temperature of identical average period and average range 5°F.

523.72+523.854]:621.396.822 95
Emission of Radio-Waves by the Galaxy and the Sun—J. S. Shklovsky. (*Nature* (London), vol. 159, pp. 752–753; May 31, 1947.) Henney's and Keenan's theory of long-wave radio emission (*Astrophys. Jour.*, vol. 91, pp. 625 ff.; 1940) is extended to take account of the absorption due to free electrons. In order to correlate the theory with observations on the emission from the sun, it is necessary to assume that the electron temperature of the outer corona is about 3500°.

The occasional intense solar emission in the range 7 to 30 meters may be due to excitation of the corona plasma by the flow of charged corpuscles through the corona with a velocity greater than that of sound. This would give a magnetic storm about one day after the anomalous radio emission.

523.72:621.396.822.029.62 96
Relation between the Intensity of Solar Radiation on 175 Mc/s and 80 Mc/s—M. Ryle and D. D. Vonberg. (*Nature* (London), vol. 160, pp. 157–159; August 2, 1947.) Simultaneous observations at the two frequencies were made between December, 1946 and April, 1947, by the technique described in 89 of 1947. Short-lived bursts having an intensity up to five times the mean value and lasting from 1 to 20 seconds occur at both frequencies but at uncorrelated times; bursts having intensities 20 to 100 times the mean value can persist for many minutes and are usually observed on both frequencies. The day-to-day variation of intensity on the two frequencies is also investigated. See also 3508 of 1947 (Appleton and Hey).

523.74 97
A Short-Lived Solar Phenomenon in High Latitude—A. D. Thackeray. (*Nature* (London), vol. 160, pp. 439–440; September 27, 1947.) An intensely dark absorption flocculus was observed in the region with heliographic coordinates 6°W, 61°S from 09h. 46 m. GMT onwards on June 19, 1947. It appears to be similar to the dark flocculi in regions surrounding sunspots and flares, and there is evidence that it was associated with increased radio noise on 175 Mc.

523.745 98
Information on Solar Activity by Radio—(*Nature* (London), vol. 160, p. 293; August 30, 1947.) The daily sunspot (relative) numbers given by the Swiss Federal Observatory, Zurich are broadcast monthly in the short-wave service of the Swiss Broadcasting Corporation. Dates, times, wavelengths, and languages of the transmissions are detailed.

523.746.5 99
On the Forecasting of Sunspots—M. Mayot (*Compt. Rend. Acad. Sci.* (Paris), vol. 224, pp. 1699–1701; June 16, 1947.) A method making use of 1884 to 1946 data to derive formulas giving the probable Wolf-Wolfer numbers for each month for one and two years in advance. The numbers for 1948 approximate to those of Gleissberg (1830 of 1946 and back references) and of Waldmeier (2560 of 1946).

523.854:538.12]:537.591 100
On the Magnetic Field of the Milky Way and Its Effect on Cosmic Radiation—M. S. Vallarta. (*Phys. Rev.*, vol. 72, p. 519; September 15, 1947.) Comment on 3891 of 1947 (Babcock). "So long as the condition of weak magnetic coupling among the stars of a galaxy still obtains, stellar dipole moments are still oriented at random and the resultant field of the galaxy almost vanishes."

537.591 101
On the Production Process of Mesons—V. F. Weisskopf. (*Phys. Rev.*, vol. 72, p. 510; September 15, 1947.)

537.591:523.75 102
Solar Effects in Cosmic Rays—S. E. Forbush. (*Science*, vol. 105, p. 634; June 20, 1947.) Summary of National Academy of Sciences' paper. Magnetograms from several magnetic observatories indicate that three sudden increases in cosmic-ray intensity during the past ten years cannot be ascribed to changes in the earth's magnetic field. Arguments are propounded suggesting that changing magnetic fields associated with a sunspot or solar flare may act as magnetic accelerators for charged particles.

538.712 103
Forecasting the Diurnal Variation of the Magnetic Declination—J. Coulomb. (*Compt. Rend. Acad. Sci.* (Paris), vol. 224, pp. 1727–1728; June 16, 1947.) A method making use of past records and the Wolf-Wolfer numbers to derive a simple formula.

550.38 104
Frenkel's Views on the Origin of Terrestrial Magnetism—L. B. Slichter and E. C. Bullard. (*Nature* (London), vol. 160, p. 157; August 2, 1947.) Comment on 2896 of 1946. A paper entitled "Magnetic Field of Sunspots" by T. G. Cowling (*Mon. Not. R. Astr. Soc.*, pp. 39–48; November, 1933) contains a theorem which appears to invalidate Frenkel's theory.

551.510.535 105
On the Sporadic F_2 Layer of the Ionosphere—Ya. L. Al'pert. (*Compt. Rend. Acad. Sci.* (U.R.S.S.), vol. 55, no. 1, pp. 25–26; 1947. In Russian.) As a result of recent ionsophere investigations, it is suggested that the three- and four-tailed characteristics of ionosphere reflection records (Figs. 1 and 2) are due to double refraction of the ray taking place in the main F_2 layer and in semitransparent sporadic ionized clouds appearing in this layer.

551.510.535:525.624 106
Atmospheric Tides in the Ionosphere: Part 2—Lunar Tidal Variations in the F Region near the Magnetic Equator—D. F. Martyn. (*Proc. Roy. Soc. A*, vol. 190, pp. 273–288; July 8, 1947.) Examination of the data for the heights and critical frequencies of the F regions over three years at Huancayo, Peru, shows the existence of semidiurnal tides in all quantities except f_1^0. The lunar variation in the F_2 region depends on solar time in both phase and amplitude and at certain epochs attains very large amplitudes, up to 60 kilometers for h_2^{max} and 28 per cent for f_2^0.

The theory of these variations given in part I of this paper (2421 of 1947) is extended.

551.510.535:621.396.11 107
The Ionospherc—J. H. Dellinger. (*Sci. Mon.*, vol. 65, pp. 115–126; August, 1947.) A general survey of ionosphere characteristics such as layer height, ionization density, energy absorption, and radio noise, and their significance. World-wide observations have extended knowledge of these phenomena, thus allowing reliable predictions to be made of radio propagation conditions.

551.510.535:621.396.11 108
A Frequency Prediction Service for Southern Africa—Hewitt, Hewitt, and Wadley. (*See* 229.)

551.524.4 109
The Daily Course of Temperature in the Troposphere—E. S. Seleznyova. (*Bull. Acad. Sci.* (U.R.S.S.), *sér. géogr. géophys.*, vol. 9, no. 2, pp. 82–88; 1945. In Russian with English summary.) The daily oscillations of temperature in the lower layers of the troposphere appear to be influenced by the earth's surface, and their amplitude decreases with increasing height. In the middle and upper troposphere, an independent diurnal variation occurs, determined by physical properties of the atmosphere.

551.594.221 110
Lightning Research in Switzerland—K. Berger. (*Weather* (London), vol. 2, pp. 231–238; August, 1947.) A description of the technique and equipment employed at Monte San Salvatore, together with an analysis of the 25 oscillograms of lightning strokes obtained during the period 1943 to 1946. See also 2269 of 1939 (McEachron).

LOCATION AND AIDS TO NAVIGATION

621.396(99) 111
Electronics in the Antarctic—Bailey. (*See* 259.)

621.396.932 112
International Recommendations for Marine Electronic Aids—(*Electronics*, vol. 20, pp. 144, 244 and 144, 145; July and August, 1947.) Abstract of the report of the 1947 International Meeting on Marine Radio Aids to Navigation. Performance standards are laid down for radio equipment and radar for position-fixing within range of suitable fixed targets, either natural or artificial. Compulsory fitting of radar and frequency standardization is not yet contemplated. Development of a reliable overall performance monitor and of devices for better identification of shore features and small ships is recommended. Medium-frequency d.f. services, though not fully satisfying standard requirements, should be continued. Decca services should be expanded, and for long range, standard loran should be adopted. Medium-range aids should have priority over long-range, but marine requirements should be considered when setting up long-range aircraft aids. For short-range communication, 2-way 150-Mc. R/T is recommended. Main components of equipment should be standardized.

621.396.933 113
Radio Navigational Aids—W. J. O'Brien. (*Jour. Brit. I.R.E.*, vol. 7, pp. 215–246; October, 1947. Discussion, pp. 247–248.) A general discussion, with particular reference to the Decca system.

621.396.933:621.396.96 114
Radar System for Airport Traffic and Navigation Control: Part 1—F. J. Kitty. (*Tele-Tech*, vol. 6, pp. 40–44, 104; August, 1947.) Description of a fixed ground radar system, based on the war-time Navy G.C.A., for airport surveillance, height finding, traffic control, and instrument approach under all conditions of visibility. The height-finder, azimuth, and eleva-

tion systems operate at frequencies near 9000 Mc., and the search system at 2900 Mc. Two-way communication with aircraft is provided in the 2 to 9 Mc. and 100 to 156 Mc. bands.

621.396.933:621.396.96 115
Airborne Radar—(*S.A.E. J.*, vol. 55, pp. 27–31; August, 1947.) Based on a paper entitled "American Airlines' Evaluation of Airborne Radar," read before the S.A.E. Mid-Continent Section. The APS-10 radar, with the aerial modified to give a pencil beam, provides a simple and effective method of collision prevention under blind-flying conditions. A number of photographs are given of actual PPI displays obtained during flight tests.

621.396.96:621.318.572 116
Video Switching and Distribution System—R. D. Chipp. (*Tele-Tech*, vol. 6, pp. 50–54, 111; July, 1947.) Naval equipment for plan-position indications to remote repeaters.

621.396.96:621.396.619.23:778 117
Photographing Pulse Wave Shapes of Radar Modulators—Marks. (*See* 288.)

621.396.96 118
Radar Engineering [Book Review]—D. G. Fink. McGraw-Hill, London, 644 pp., 35s. (*Wireless World*, vol. 53, p. 345; September, 1947.) "A presentation of the underlying principles and commonly-used techniques, illustrated by some typical examples."

MATERIALS AND SUBSIDIARY TECHNIQUES

533.5:621.3.032.53 119
The Effect of Heat Treatment in Different Atmospheres on the Stress in Tungsten-to-Glass Seals—M. Manners. (*Jour. Soc. Glass Tech.*, vol. 30, pp. 217–238; August to October, 1946.) A study of the relations between the heating time and temperature, in air or in hydrogen, and the longitudinal stress at the glass-metal boundary of single-wire "oxide" or "oxide-free" seals.

533.5:621.3.032.53 120
Metal-Ceramic Vacuum Seals—N. T. Williams. (*Rev. Sci. Instr.*, vol. 18, pp. 394–397; June, 1947.) A complete account of processes using AlSiMag 243 (2460 of 1947). Mixtures of Mo and carbonyl-iron powders are fired on to the ceramic at 1400°C in a H.N atmosphere and to the surface thus obtained a Ni powder is sintered to provide a base for brazing. An alloy of 50 per cent Fe, 50 per cent Ni is used for outside seals and an alloy of 42 per cent Ni, 5½ per cent Cr, 52½ per cent Fe for inside seals.

533.5:621.3.032.53 121
Ceramic-Metal Seals—M. Kuhner. (*Le Vide* (Paris), 11 pp., January, 1947; Reprint.) Discusses the advantages of using ceramics instead of glass in the construction of u.h.f. tubes and describes processes for direct ceramic-metal seals without a glass intermediate.

533.5:621.315.616 122
The Vacuum Properties of Some Synthetic Dielectrics—B. G. Hogg. (*Phys. Rev.*, vol. 72, p. 522; September 15, 1947.) Summary of Amer. Phys. Soc. paper. An investigation to determine the suitability of some new dielectrics for use in the vacuum system of a mass spectrograph.

535.37:621.386 123
Microsecond Measurement of the Phosphorescence of X-Ray Fluorescent Screens—F. Marshall. (*Jour. Appl. Phys.*, vol. 18, pp. 512–518; June, 1947.) The build-up and decay of light emitted by fluorescent materials when irradiated by X-ray pulses was displayed on a c.r.o.

537.228.1 124
Electromechanical Properties of Rochelle Salt at the Lower Curie Point—R. M. Lichtenstein. (*Phys. Rev.*, vol. 72, pp. 492–501; September 15, 1947.) The electromechanical constants calculated from measurements of the electrical characteristics near the lower Curie point agree with those determined for the upper Curie point. This fact furnishes an explanation of the existence of two Curie points for Rochelle salt.

537.228.1:546.431.823 125
Single Crystals of Barium Titanate—B. T. Matthias, R. G. Breckenridge, and D. W. Beaumont. (*Phys. Rev.*, vol. 72, p. 532; September 15, 1947.) Summary of Amer. Phys. Soc. paper. Perfect single crystals of up to 5 mm. were obtained by a cooling process not lasting longer than 8 hours. They were found to be strongly piezoelectric. "The dielectric behavior points to a new, third kind of ferro-electrics in addition to Rochelle salt and the dihydrogen phosphates."

537.228.1:546.431.823 126
Barium Titanate Crystals—H. F. Kay and R. G. Rhodes. (*Nature* (London), vol. 160, pp. 126–127; July 26, 1947.) Crystals with linear dimensions up to 2 mm. have been produced. They are piezoelectric at room temperatures and consist of individuals of tetragonal symmetry twinned about the 101 and 011 planes. Above 120°C there is a transition to cubic symmetry. See also 127 below.

537.228.1:546.431.823:621.315.612.4.011.5 127
Dielectric Properties of Single Crystals of Barium Titanate—J. K. Hulm. (*Nature* (London), vol. 160, pp. 127–128; July 26, 1947.) At 18°C, the permanent polarization characteristic is estimated at about 16 microcoulombs per centimeter². Curves showing maximum polarization as a function of temperature for various field strengths indicate a Curie temperature of about 124°C. See also 126 above.

537.311.33 128
The Physics of Electronic Semiconductors—G. L. Pearson. (*Elec. Eng.*, vol. 66, pp. 638–642; July, 1947.) Long summary of A.I.E.E. paper. A short review of present knowledge with an elementary account of the band theory of solids, and the classification of the various semiconductors. This theory explains the magnitude of the conductivity and its temperature coefficient, and also certain anomalies in sign of the Hall and thermoelectric effects. See also the work of A. H. Wilson (1932 Abstracts, *Wireless Eng.*, p. 108).

537.311.33:621.396.622.6 129
Application of the Theory of Conduction in Semiconductors to Crystal Detectors—Leblanc. (*See* 87.)

537.32+538.632]:546.24 130
The Electrical Behavior of Vacuum Evaporated Tellurium—W. Scanlon and K. Lark-Horovitz. (*Phys. Rev.*, vol. 72, p. 530; September 15, 1947.) Summary of Amer. Phys. Soc. paper. Anomalies in the Hall effect and thermoelectric power of Te heated in air are absent when it is heated in a high vacuum.

538.221/.222 131
Relaxation Effects in Paramagnetic and Ferromagnetic Resonance—C. Kittel. (*Phys. Rev.*, vol. 72, p. 529; September 15, 1947.) Summary of Amer. Phys. Soc. paper. A theoretical discussion. The effects of anisotropy and exchange interactions on the condition $\omega=\gamma(BH)^{1/2}$ for feromagnetic resonance are considered. See also *ibid.*, February 15, 1947, vol. 71, p. 270, and 747; 1947 (Griffiths).

538.221+669.018.5 132
Magnetic Alloys of High Permeability—(*Engineer* (London), vol. 184, pp. 78–79; July 25, 1947.) A review of the development of such materials, and an account of the properties of Supermalloy, extracted from Boothby's and Bozorth's paper (2802 of 1947).

538.221+669.018.5 133
The Production of Small Permanent Magnets—(*Engineer* (London), vol. 184, p. 40; July 11, 1947.) A note on the use and properties of a new pressed powder material of high coercive force called "Caslox," manufactured by the Plessey Co. The material consists of a mixture of Fe-Co oxides with a plastic binder.

538.221 134
Variation of the Coercive Field as a Function of the Density of Compressed Ferromagnetic Powders—L. Weil. (*Compt. Rend. Acad. Sci.* (Paris), vol. 225, pp. 229–230; July 28, 1947.) Experimental verification, for powders of Fe and of Fe-Co with 30 per cent Co, that the coercive field of compressed powders diminishes as the density increases, according to the formula $H_c=k(d-d_0)/d_0$, where k is a characteristic constant of the powder at infinite dilution, d the density of the solid metal and d_0 the mass of the ferromagnetic material per centimeter³ in the compressed powder. See also 3151 and 3152 of 1947 (Néel). *Note.* In the text of the article it would appear that the definitions of d and d_0 should be interchanged.

538.221 135
Gyromagnetic Resonance in Ferrites—J. L. Snoek. (*Nature* (London), vol. 160, p. 90; July 19, 1947.) A note on the experimental behavior of magnetic ferrites of great homogeneity as a function of frequency. The rapid decrease of μ_0 at high frequencies is probably due to gyromagnetic resonance around directions prescribed by the internal fields.

538.221:621.317.41.029.63/.64 136
High-Frequency Permeability of Ferromagnetic Materials—G. Eichholz and G. F. Hodsman. (*Nature* (London), vol. 160, pp. 302–303; August 30, 1947.) A description of the technique used and the results obtained in the frequency band 2 300 to 3 400 Mc.

The permeability is deduced from measurement of the difference in attenuation constant of a coaxial transmission line when the inner conductor, made of the ferromagnetic material under test, is replaced by a nonmagnetic material of the same dimensions.

Materials tested comprise Fe with low carbon content and steel (0.50 to 0.55 per cent carbon); in both cases hard-drawn and white annealed specimens were used. Commercial Ni was also examined. See also 3923 of January (Johnson, Rado, and Maloof) and back references.

538.221:669.14–122.2:621.318.32 137
Cold-Worked Electrical Low Loss Steels—(*Elec. Times*, vol. 112, pp. 177–181; August 14, 1947.) A description of the processing of silicon steel strip "Crystalloy" for minimum hysteresis loss. The steel is alternately cold-rolled in a Steckel mill and annealed, thus orienting the crystals with their edges parallel; the magnetic field must be applied parallel to the edges for minimum hysteresis loss. Typical curves and methods of testing are given.

546.289:538.56 138
Spontaneous Electrical Oscillations in Germanium Crystals—S. Benzer. (*Phys. Rev.*, vol. 72, p. 531; September 15, 1947.) Summary of Amer. Phys. Soc. paper.

546.289:621.315.59:536.48 139
Resistivity and Hall Constant of Germanium Samples at Low Temperatures—I. Estermann, A. Foner, and J. A. Randall. (*Phys. Rev.*, vol. 72, p. 530; September 15, 1947.) Summary of Amer. Phys. Soc. paper.

546.289:621.315.59:536.48 140
Theory of Low Temperature Semiconductor Resistivity—V. A. Johnson and K. Lark-Horovitz. (*Phys. Rev.*, vol. 72, p. 531; September 15, 1947.) Summary of Amer. Phys. Soc. paper. The resistivity of Ge semiconductor has been calculated, using classical statistics above and Permi statistics below the degeneracy temperature. The results are in close agreement with observations.

546.841-3:621.385.2.032.216 141
Thermionic Properties of Thoria—D. A. Wright. (*Nature* (London), vol. 160, pp. 129–130; July, 26, 1947.) A coating of thoria 0.1 mm. thick was sprayed on to a Ta strip and incorporated in a diode. A saturated emission of 2.5 A per centimeter² was obtained under d.c. conditions at 1900°K. 10 A per centimeter² under d.c. conditions and 30 A per centimeter² under pulsed conditions were obtained at 2100°K without flashover. A thoria cathode was also made in tubular form by extrusion and sintering. The emission fell rapidly on continuous operation and the cathode was sentitive to thermal shock.

549.514.51:548.24 142
Artificial Electrical Twinning in Quartz Crystals—J. J. Vormer. (Proc. I.R.E., vol. 35, pp. 789–790; August, 1947.) For another account see 1463 of 1947.

549.514.51:621.396.611.21 143
FT-241A Frequency Control [Quartz Crystal] Unit—I. E. Fair. (*Bell Lab. Rec.*, vol. 25, pp. 295–298; August, 1947.) Construction of a unit for 200 to 1 040 kc. using CT- or DT-cut quartz plates, which are much smaller than AT-cut plates for a given frequency. Vibration in face shear and not thickness shear is used and a technique is developed for mounting the plates on small wires soldered at the nodal points.

549.514.51:621.396.611.21:621.386.001.8 144
A Method for the Determination of Crystal Cuts by Applying the Reflection of X-Rays from a Known Lattice Plane—V. Petržílka and J. Beneš. (*Phil. Mag.*, vol. 37, pp. 399–410; June, 1946.) The method uses a Seemann electron diffraction spectrograph. The required information is derived from measurements on a single photograph.

621.315.612:537.523.3 145
High Altitude Flashover and Corona Correction on Small Ceramic Bushings—W. W. Pendleton. (*Elec. Eng.*, vol. 66, p. 925; September, 1947.) Summary of A.I.E.E. Dayton paper. Improvement of corona and flashover voltages was obtained by the use of semiconducting coatings. A sensitive oscilloscope method detects disturbances at voltage gradients where the ionization-by-collision process begins. These gradients are calculated from graphical maps of the dielectric fields associated with the bushings. A method is given for correlating flashover data with bushing size and shape.

621.315.612:621.319.4 146
Fabrication of Thin Ceramic Sheets for Capacitors—G. N. Howatt, R. G. Breckenridge and J. M. Brownlow. (*Jour. Amer. Ceram. Soc.*, vol. 30, pp. 237–242; August 1, 1947.) Description of their manufacture and use as capacitor dielectrics. For TiO_2 sheets, graphs are given showing the relation of breakdown strength to thickness and temperature for a.c. and d.c. voltages. The dielectric properties of TiO_2 and of various titanates are tabulated.

621.315.616:546.287 147
Test of Silicones for Shipboard Use—H. P. Walker. (*Elec. Eng.*, vol. 66, pp. 647–649; July, 1947.) Consideration of their possible uses as insulating varnishes, resins for laminated and moulded thermosetting materials, resins for high-temperature paints, bearing lubricants, and rubber for gaskets.

621.315.616.7 148
Structural Features of GR-S Rubber—W. G. Straitiff. (*Bell. Lab. Rec.*, vol. 25, pp. 299–303; August, 1947.)

621.317.37+621.3.011.5]:621.396.611.4 149
Resonant Cavities for Dielectric Measurements—Works. (*See* 173.)

621.775.7 150
Powder Metallurgy—(*Engineer* (London), vol. 184, pp. 52–53, 72–73, 106–108, 119–121, 152–154, and 165–168; July 18 and August 22, 1947.) A report of the discussion at the Institution of Civil Engineers on a symposium of 28 papers on various aspects of powder metallurgy, including magnetic powders and products.

621.775.7 151
Modern Powder Metallurgy—H. W. Greenwood. (*Engineering* (London), vol. 163, p. 492; June 13, 1947.) A general survey. Hitherto progress has been somewhat empirical. Planned investigation and fundamental research are now required.

669 152
New Metals for Old—E. V. Appleton. (*Beama Jour.*, vol. 54, pp. 256–259; July, 1947.) Summary of the Edward Williams lecture to the Institute of British Foundrymen on recent metallurgical research and its relation to the electrical engineering industry. Increased tensile strength of overhead conductors, losses in magnetic substances, and improvements in magnetic hardness are discussed. Details are given of alloys having a high resistance to creep deformation under stress at high temperatures. Brief summary in *Nature* (London), vol. 160, pp. 308–309; August 30, 1947.

MATHEMATICS

501(05) 153
The Quarterly Journal of Mechanics and Applied Mathematics—(*Nature* (London), vol. 160, p. 427; September 27, 1947.) A new periodical beginning publication in April, 1948.

517.512.2:518.4 154
Graphical Methods for Evaluating Fourier Integrals—W. J. Cunningham. (*Jour. Appl. Phys.*, vol. 18, pp. 656–664; July, 1947.) Three methods are described, all involving an analysis of the function considered into the sum of simpler functions whose transforms are known. The methods are useful where an analytic solution is too complicated or the data take the form of curves obtained experimentally.

517.512.2:621.396.67 155
Fourier Transforms in Aerial Theory: Part 3—Operations with Fourier Transforms—J. F. Ramsay. (*Marconi Rev.*, vol. 10, pp. 41–58; April to June, 1947.) Continuation of 3561 of 1947. Discussion of elementary operations with Fourier transforms, namely: (a) change of sign of the independent variable, (b) interchange of function, (c) identity of function; self-reciprocal transforms, (d) the Gaussian and Rayleigh transforms, (e) even and odd functions, (f) real and imaginary parts; complex conjugates, (g) the displacement theorem, (h) multiplication by a constant, (i) change of scale, (j) addition and subtraction, (k) differentiation of transforms and (l) the transform of a product.

517.93+531 156
Introduction to Non-Linear Mechanics: Parts 1–4—N. Minorsky. (*United States Navy; David W. Taylor Model Basin, Reports* 534, 546, 558, and 564.) These reports review the progress up to approximately 1940 in obtaining solutions to many kinds of nonlinear differential equations. Numerous examples are given, many of which are of an electrical nature. Much of the work is a presentation of material which has hitherto existed only in Russian books and papers. Part 1 is concerned with solutions by topological methods of qualitative integration, while part 2 gives an outline of the three principal analytical methods of Poincaré, van der Pol, and Kryloff-Bogoliuboff. In part 3 there is a discussion of the complicated phenomena of nonlinear resonance, with its numerous ramifications, such as internal and external subharmonic resonance, entrainment of frequency, and parametric excitation. Finally, part 4 contains a review of the developments of Mandelstam, Chaikin, and Lochakow in the theory of relaxation oscillations for large values of the parameter μ which appears in the basic quasi-linear equation

$$\ddot{x}+x=\mu F(x, \dot{x})$$

All analytical approaches to a solution of this equation assume that μ is very small, whereas for oscillations such as those conforming to van der Pol's differential equation, μ is large.

518.5 157
Electrical Analogue Computing: Part 3—Functional Transformation—D. J. Mynall. (*Electronic Eng.* (London), vol. 19, pp. 259–262; August, 1947.) Electromechanical and electronic devices are described for causing one quantity to vary as a predetermined function of another. The system is similar to that used for multiplication, but some of the potentiometers or variable resistors involved are nonlinear. Parts 1 and 2: 3563 of 1947.

518.5 158
Electronic Computing Circuits of the ENIAC—A. W. Burks. (Proc. I.R.E., vol. 35, pp. 756–767; August, 1947.) "The design principles that were followed in order to insure reliable operation of the electronic computer are presented, and the basic types of computing circuits are analyzed. . . . The Eniac performs the operations of addition, subtraction, multiplication, division, square-rooting, and the looking up of function values automatically. The units which perform these operations, the units which take numerical data into and out of the machine, and those which control the over-all operation are described. The technique of combining the basic electronic circuits to perform these functions is illustrated by three typical computing circuits: the addition circuit, a programming circuit, and the multiplication circuit." See also 2481 of 1947 (Wilkes) and 3952 of January (Hartree).

518.5:621.318 159
Use of Magnetic Amplifiers in Computing Circuits—R. T. Beyer. (*Phys. Rev.*, vol. 72, p. 522; September 15, 1947.) Summary of Amer. Phys. Soc. paper. These amplifiers have been used for the algebraic addition of small direct currents to an accuracy of ± 0.1 per cent of the maximum sum and also for the differentiation of slowly varying voltages. The circuits have low input impedance, high stability, and the input levels of the currents can be independent of each other and of the output level.

518.5:621.392 160
Machine Computing of Networks—L. A. Dunstan. (*Elec. Eng.*, vol. 66, pp. 901–906; September, 1947.) The data and conditions of a standardized power distribution network problem are stated in the form of a master diagram, and the results are obtained by the use of punched-card accounting machines. A comparison is made of this method with the network analyzer method.

51:621.3 161
Modern Electrical Engineering Mathematics:[Book Review]—S. A. Stigant. Hutchinson's Scientific and Technical Publications, London, 1947, 372 pp., 31s. 6d. (*Beama Jour.*, vol. 54, pp. 242–243; July, 1947.) " . . . a milestone in the application of modern mathematical methods to the solution of problems in complicated electrical networks."

51(083.5) 162

The Mathematical Tables Project [Book Notice]—National Bureau of Standards. Columbia University Press, New York. (*Jour. Appl. Phys.*, vol. 18, p. 687; July, 1947.) A list of 20 sets of tables published up to 1947 is given. These include powers, exponential and circular functions, probability functions, Bessel functions, Lagrangian interpolation coefficients, etc. See also 3339 of 1946 (Fletcher, Miller, and Rosenhead).

MEASUREMENTS AND TEST GEAR

621.317.2:621.396.621.001.4 163

Chassis Testing on a Quantity Basis—A. H. Beattie. (*Murphy News*, vol. 22, pp. 188–191; August, 1947.) The equipment consists of a central transmitter unit incorporating 24 individual crystal-controlled oscillators, which provide suitable signals for all chassis testing. Each oscillator is enclosed in an aluminum screening box. The test points are fed through matched lines. Each test point is provided with a buffer amplifier fitted with continuously variable output control, giving complete flexibility and permitting the use of low signal levels in the feeders.

621.317.311 164

A Method for the Measurement of Small Direct Currents—E. J. Harris. (*Electronic Eng.* (London), vol. 19, pp. 249–250; August, 1947.) The small e.m.f. to be measured is interrupted at 50 c.p.s. and applied, in opposition to a variable known e.m.f., to the primary of a transformer. The secondary rings with an amplitude increasing with the difference between the known and unknown e.m.fs. The damped oscillations are amplified and applied to an oscilloscope which is used as a null detector.

621.317.32:537.533.73 165

Measurement of Peak High Voltages by Electron Diffraction—J. J. Trillat and J. Barraud. (*Rev. Gén. Élec.*, vol. 56, pp. 310–314; July, 1947.) A method similar to that previously given for d.c. voltages (791 of 1947). The use of powdered magnesia or ZnO eliminates certain measurement errors. A peak voltage of 45 kv. can be measured to within about ±500 volts.

621.317.33:621.316.8 166

Method for Determining the Time Constant of Resistors at Low Frequency—G. Ney. (*Compt. Rend. Acad. Sci* (Paris), vol. 225, pp. 227–228; July 28, 1947.) A semisubstitution method, using a Schering bridge, gives the self-inductance and the distributed capacitance of a resistor and hence its time constant. Measurements on numerous metallized resistors show that the distributed capacitance is practically negligible and Ohm's law is followed up to frequencies of many hundreds of kc. Measurements on resistors of 1 to 100,000 ohms show, in general, errors in determining the time constant of the order of 10^{-9} seconds.

621.317.332 167

Conductivity of Metallic Surfaces at Microwave Frequencies—E. Maxwell. (*Jour. Appl. Phys.*, vol. 18, pp. 629–638; July, 1947.) Two methods of measurement which have been used at λ 1.25 centimeters are described. The first involves the measurement of the standing-wave ratio, and hence the transmission loss, in a shorted waveguide; the second involves the measurement of the Q of a resonant cavity. The results for a number of metals are given. Deviations from d.c. conductivity are ascribed to surface roughness.

621.317.335 168

A Capacitance Test Bridge—J. M. Heinrich (*Radio News*, vol. 38, pp. 42–43, 150; August, 1947.) A direct reading instrument for capacitances between 1 pF and 100 μF.

621.317.335 169

Connection Errors in Capacitance Measurements—R. F. Field. (*Gen. Rad. Exper.*, vol. 21, pp. 1–4; May, 1947.) Stray capacitance errors are largely eliminated by use of a wire of small diameter for connection to the high potential terminal, the wire being curved so as to increase its average distance from earthy conductors. Correction of the residual error is applied by observing the effect of varying the initial separation of the end of the wire and the terminal.

621.317.361+621.317.761 170

Royal Observatory Standard Frequency Transmissions—(*R.S.G.B. Bull.*, vol. 23, p. 24; August, 1947.) Brief details are given of the 2-Mc. standard frequency transmissions from Abinger. The accuracy is better than 1 in 10^7.

621.317.361+621.317.761 171

WWV Standard Frequency Broadcasts—W. W. George. (*F M and Telev.*, vol. 7, pp. 25–27, 44; June, 1947.) Details of the various transmissions, with photographs of some of the equipment.

621.317.37+621.3.011.5]:621.365.92 172

Dielectric Loss at High Frequency—J. B. Whitehead. (*Elec. Eng.*, vol. 66, pp. 907–911; September, 1947.) A calorimetric substitution method of measuring the dielectric properties of a material whose temperature may be changing at a rate of the order of 50°F. per min. For another account see *Science*, vol. 105, p. 637; June 20, 1947.

621.317.37+621.3.011.5]:621.396.611.4 173

Resonant Cavities for Dielectric Measurements—C. N. Works. (*Jour. Appl. Phys.*, vol. 18, pp. 605–612; July, 1947.) The susceptance variation method of measuring dielectric constant and dissipation factor, widely used in the frequency range 10 kc. to 100 Mc. is extended to frequencies up to 1000 Mc. Fixed and variable length re-entrant resonant cavities are described; the specimens are in the form of small disks. Design principles are discussed and formulas given for calculating the required dielectric properties. Good agreement is found with values measured by other methods. Some results for typical dielectrics are shown graphically.

621.317.382.029.63 174

A Coaxial Load for Ultra-High-Frequency Calorimeter Wattmeters—W. R. Rambo. (Proc. I.R.E., vol. 35, pp. 827–829; August, 1947.) Design considerations and description of a broad-band water load for operation in the frequency band 1000 to 3000 Mc. at input levels within the range 5 to 150 watts. Dimensions are 9 inches long by three-eighths inch in diameter. See also 2172 of 1947 (Shaw and Kircher).

621.317.41 175

A Method of Measuring Magnetic Permeability for Weak Fields and a Wide Range of Frequencies—I. Épelboïm. (*Compt. Rend. Acad. Sci.* (Paris), vol. 225, pp. 535–537; September 29, 1947.) An account of the method used at the Sorbonne and at the Laboratoire National de Radioélectricité. The demountable coil previously described (797 of 1947) can be used for frequencies up to 12 Mc. in the most favorable case. A new coil extends the range to 25 Mc. and two others now under construction should enable mesaurements to be made to 100 Mc. Preliminary results are quoted for powdered-iron cores of low μ and relatively large cross section and for permalloy strip.

621.317.41 176

A Permeameter for Magnetic Measurements on High Permeability Material—W. J. Carr, Jr. (*Phys. Rev.*, vol. 72, p. 530; September 15, 1947.) Summary of Amer. Phys. Soc. paper. The magnetic force is measured by placing a small winding with a high permeability core very close to the surface of the test specimen. The core is energized with a.c. above the knee of its magnetization curve and the second harmonic of the voltage is a measure of the field in the specimen.

621.317.42:621.317.755 177

A Cathode-Ray B-H Tracer—J. Zamsky. (*Elec. Eng.*, vol. 66, pp. 678–680; July, 1947.) Two coils are used to pickup voltages from the test sample in a magnetic circuit and apply them by means of an electronic circuit to the vertical (flux density B) and the horizontal (magnetic intensity H) sets of deflecting plates of the c.r. tube. The B coil encloses the sample, the H coil is inside it. The magnetic properties are deduced from photographs of the c.r. traces. See also 2247 of 1946 (Long and McMullen).

621.317.43 178

Apparatus for Measuring Power Loss in Small Ferromagnetic Samples Subject to an Alternating Magnetic Field—K. H. Stewart. (*Jour. Sci. Instr.*, vol. 24, pp. 159–162; June, 1947.) For samples about 15 centimeters by 1 centimeter by 0.03 centimeter. Includes a B_{max} meter and a wattmeter in which the a.c. quantities to be measured are balanced against d.c. quantities, thus allowing all readings to be made on d.c. meters.

621.317.7 179

Electrical and Acoustical Instruments shown at the Physical Society's Exhibition [1947]—T. B. Rymer. (*Jour. Sci. Instr.*, vol. 24, pp. 148–151; June, 1947.) An account of a few of the exhibits, including the following:—(a) A spectrum analyzer for the output of a klystron, using a cavity resonator whose piston is vibrated by a loudspeaker unit, causing the resonance frequency to vary harmonically. The output from the wavemeter is applied to the y-plates of a c.r.o. whose x-plates are fed from the a.c. source operating the loudspeaker. (b) A complete test set for radar installations. (c) A standard frequency generator capable of producing substantially pure frequencies of any integral number of kc. from 2 kc. to 10 Mc. with an accuracy of 3 parts in 10^7. (d) Counting and pulse circuits. (e) Moving-coil meters, including a d.c. instrument of 100,000 ohms per volt resistance. (f) A supersonic flaw detector. (g) An electroencephalograph with an 8-pen recorder. (h) Magnetic variometers with sensitivity which can be adjusted from 10^{-4} gauss per division upwards, the usual value being 3×10^{-4} gauss per division. See also 3581 of 1947 and back references.

621.317.733 180

A Wide-Frequency-Range Capacitance Bridge—R. F. Field and I. G. Easton. (*Gen. Rad. Exper.*, vol. 21, pp. 1–7; April, 1947.) The RCA capacitance bridge Type 716-C is a Schering bridge circuit adapted for capacitance measurements up to 1000 pF over the frequency range 30 c.p.s. to 300 kc., and up to 1 μF at 1 kc.

621.317.733 181

A V.H.F. Bridge for Impedance Measurements between 20–140 Mc/s.—R. A. Soderman. (*Communications*, vol. 27, pp. 26–27; August, 1947.) Summary of New England Radio Engineering meeting paper. For measurements on lumped-parameter circuits, or on distributed-parameter circuits using coaxial transmission lines. A modified Schering bridge circuit is used, whereby both the resistive and the reactive components of the unknown impedance are measured in terms of incremental capacitances.

621.317.733 182

The Maxwell Bridge at Low Frequencies—V. A. Brown and B. P. Ramsay. (*Phys. Rev.*, vol. 72, p. 528; September 15, 1947.) Summary of Amer. Phys. Soc. paper. The bridge has been used to measure inductance and a.c. resistance

at periods of 1 to 200 seconds. Application to inductances of several hundred henries, with solid ferromagnetic cores, is mentioned.

621.317.738.029.5 183

R.F. Inductance Meter—H. A. Wheeler. (*Electronics*, vol. 20, pp. 105–107; September, 1947.) Two r.f. oscillators, one with the unknown inductance in series and the other with a variable capacitance in parallel, are tuned to zero beat. Direct-reading accuracy is within 1 per cent from 1 microhenry to 100 millihenrys.

621.317.755:621.396.621.001.4 184

Qualities and Defects of Alignment by the Oscilloscope—J. Bernhardt. (*Toute la Radio*, vol. 14, pp. 237–240; September, 1947.) A discussion of the various possible sources of error in lining up the h.f. and i.f. stages in receivers by means of a c.r.o., including the oscillograph itself and its associated amplifier, the detector, and amplifier stages of the receiver and the generator. The errors are found to be considerable only in extreme cases.

621.317.757:534.442.1 185

Electronic Indicator for Low Audio Frequencies—Hastings. (*See* 5.)

621.317.763 186

Wavemeter of High Accuracy—R. Aschen. (*T.S.F. Pour Tous*, 1947. vol. 23, p. 150; July to August, 1947.) The instrument uses a tuned circuit with unscreened interchangeable coils to give different ranges. This circuit is connected through small capacitors to the cathode and grid of a magic-eye tuning indicator mounted for anode detection. Damping of the tuned circuit is thus suppressed, which accounts for the sensitivity. Heater and anode voltages for the indicator are provided by a transformer without rectification. Over-all size is 13 centimeters by 6 centimeters by 9 centimeters.

621.317.784 187

A Milliwattmeter for Power Measurements in the Super Frequency Band of 8700–10,000 Mc/s.—W. Rosenberg. (*Jour. Sci. Instr.*, vol. 24, pp. 155–158; June, 1947.) For waveguide measurements for powers from 7 microwatts to 7 milliwatts. The power-sensitive element is a thermistor bead. A substitution method is used in which d.c. power and r.f. power are assumed equivalent. Since mean power is measured, the meter can be used for either c.w. or pulse transmissions. Estimated accuracy is 6 per cent.

621.317.789:621.385.1.032.22 188

A Calorimetric Method for Direct Measurement of Plate Dissipation—R. T. Squier. (*Elec. Eng.*, vol. 66, p. 927; September, 1947.) Summary of A.I.E.E. Dayton paper. The discriminator section of an amplifier circuit is considered and the difficulties encountered in determining anode dissipation are analyzed. The construction and operation of the calorimeter used to overcome these difficulties is described.

621.317.79:621.3.015.33 189

Pulse Rise and Decay Time Measurement—A. Easton. (*Electronics*, vol. 20, pp. 180–190; September, 1947.) The various parameters to be measured (rise, fall, overshot, etc.), are discussed briefly. A method of measurement in which the pulse is applied to the x-plates and a synchronized sinusoidal timing wave is applied to the y-plates of a c.r. tube is described. A differentiating circuit, operated by the pulse, blanks out the return trace. High accelerating voltages must be used to ensure that the time of rise or fall of the pulse occupies most of the tube face. See also 1599 of 1946.

621.317.79:621.396.611.21 190

Quartz Beat-Frequency Oscillator—A. V. J. Martin. (*Toute la Radio*, vol. 14, pp. 253–256; September, 1947.) Full circuit details and lay-out of an instrument using in the fixed-frequency oscillator, crystals of frequencies 2000, 2002, 2004, 2006, and 2008 kc., any one of which may be selected. The variable-frequency oscillator also uses a quartz crystal, whose frequency is varied between 999 and 1000 kc. by altering the crystal air-gap. Frequency doubling gives a range from 1998 to 2000 kc., so that, when combined with the fixed-frequency oscillations, the range from 0 to 10,000 c.p.s. is covered in 5 steps. Distortion is low and stability excellent.

621.317.79:621.396.813 191

Distortion Meter—R. Besson. (*Toute la Radio*, vol. 14, pp. 242–244; September, 1947.) Circuit details and lay-out of an instrument comprising supply unit, amplifier, tube voltmeter, and a simple type of T-filter using a single inductance with a number of capacitors selected by a switch.

621.317.79/621.397.62.001.4 192

Visual Alignment of Television Receivers—M. H. Kronenberg. (*Radio News*, vol. 38, pp. 64–65, 122; August, 1947.) Method of using an f.m. signal generator, in conjunction with an auxiliary c.r. tube for aligning the various stages.

621.317.791 193

Design and Construction of a Universal Meter—A. V. Howland. (*R.S.G.B. Bull.*, vol. 23, pp. 22–24; August, 1947.) The circuit diagram and component values are given for a universal meter to measure a.c. and d.c. voltage, d.c. current, and resistance, using a 0–1-milliampere moving coil meter and a 1-milliampere bridge-connected instrument rectifier. A buzzer is incorporated for continuity testing.

621.317.794 194

Construction and Characteristics of Evaporated Nickel Bolometers—B. H. Billings, E. E. Barr, and W. L. Hyde. (*Rev. Sci. Instr.*, vol. 18, pp. 429–435; June, 1947.) The bolometers described are approximately 200 Å thick and are evaporated on to a nitrocellulose pellicle about 1000 Å thick, which is supported on a glass base with a sand-blasted groove below the bolometer strip. A typical bolometer has a time constant of 0.004 second and a threshold of 3.3 by 10^{-8} watts for radiation modulated at 30 c.p.s., the bandwidth being 100 c.p.s.

OTHER APPLICATIONS OF RADIO AND ELECTRONICS

531.775:621.317.361 195

Measuring Speed with WWV—J. C. Coe. (*Electronics*, vol. 20, pp. 90–93; August, 1947.) The a.f. output of a variable-reluctance tachometer generating 2000 c.p.s. at 30,000 r.p.m. is compared with the output of a variable-frequency oscillator, which is calibrated by means of harmonics of the standard 440-c.p.s. signal broadcast by station WWV.

539.16.08 196

On the Rise of the Wire-Potential in Counters—S. A. Korff. (*Phys. Rev.*, vol. 72, pp. 477–481; September 15, 1947.) An analysis of the factors which determine the rate of change of wire-potential. Experimental work in support of the theoretical predictions is quoted.

551.508.1:621.396.9 197

The Kew Radio Sonde—E. G. Dymond. (*Proc. Phys. Soc.*, vol. 59, pp. 645–666; July 1, 1947.) A radio transmitter of frequency 26 to 30 Mc. is modulated by an audio oscillator whose frequency is controlled in turn by temperature, pressure, and humidity units. The modulation thus gives the values of these three quantities in the neighborhood of the balloon carrying the transmitter. A detailed description is given of the apparatus, and its accuracy is discussed. See also 4263 of 1938 (Thomas).

621.318 198

Applications of Magnetic Amplifiers—W. E. Greene. (*Electronics*, vol. 20, pp. 124–128; September, 1947.) The magnetic amplifier, essentially a saturated core reactor in which the current in an auxiliary winding controls that in the main winding by varying the permeability of the high-μ core, was first used in 1916. It was superseded by the electronic amplifier until the Germans, employing high-μ cores and *Se* rectifiers, used it for servomechanism amplifiers during the war. The mechanical strength and low ohmic losses make the amplifier suitable for many post-war applications. Research is proceeding to overcome the slowness of response at very low frequencies, an inherent fault, and to produce better core materials. By using feedback, power gains of 10^4 have already been obtained.

621.319.339.027.3 199

The Imperial College High-Voltage Generator—W. B. Mann and L. G. Grimmet. (*Proc. Phys. Soc.*, vol. 59, pp. 699–730; July 1, 1947.) "The design and construction of two pressure-insulated electrostatic generators similar to those of Van de Graaff and Trump are described briefly. Voltage tests with one of the generators with mixtures of nitrogen and freon under pressure have shown it to be capable of producing voltages in excess of two million."

621.319.43:621.317.79:[531.718.4+531.787.9 200

A Variable Capacitor for Measurements of Pressure and Mechanical Displacements; A Theoretical Analysis and Its Experimental Evaluation—J. C. Lilly, V. Legallaris, and R. Cherry. (*Jour. Appl. Phys.*, vol. 18, pp. 613–628; July, 1947.) The capacitor consists of a fixed plane electrode and a parallel diaphragm, which is clamped at the edges. Small displacements, volume changes, or pressure differences, acting upon the diaphragm, are deduced by electrical measurement of the resulting change in capacitance.

621.365.5.001.8+621.365.92.001.8 201

Practical Applications of H.F. Induction and Dielectric Heating—M. J. A. (*Toute la Radio*, vol. 14, pp. 233–236; September, 1947.) A discussion of the frequencies and the various types of equipment suitable for particular purposes.

621.365.92[621.317.37+621.3.011.5 202

Dielectric Loss at High Frequency—Whitehead. (*See* 172.)

621.38:629.13.054 203

Precision Balancing at Mass-Production Speed—S. Bousky. (*Electronics*, vol. 20, pp. 98–104; September, 1947.) The periphery of a gyro rotor is stamped with a series of numbers; unbalance at any point is indicated when a stroboscopic lamp illuminates the corresponding number. Full constructional details and operational procedure are given. A rotor can be balanced to within 5×10^{-6} oz-inches in 2 minutes.

621.38/.39].001.8:629.13 204

Electronics and Aeronautical Research—(*Engineering* (London), vol. 164, p. 91; July 25, 1947.) An account of equipment on view at an exhibition arranged by the Instrumentation Department, R. A. E., Farnborough, including various types of acceleration and pressure pickups, multichannel recording equipment, 4-way c.r. equipment, 600-way static strain recording equipment, transmitting and statistical accelerometers, and an electronic torque-meter. See also *Engineer* (London), vol. 184, pp. 85, 87; July 25, 1947.

621.383.001.8:551.591:535.247.4 205

Visibility Measurements by Transmissometer—C. A. Douglas. (*Electronics*, vol. 20, pp. 106–109; August, 1947.) The intensity of light incident on a phototube up to 4000 ft. away from a fixed 350,000-cp source is recorded continuously, using pulse technique.

621.384 206

An Electron Accelerator with an Air-Cored Field—R. D. Hill. (*Nature* (London), vol. 159, pp. 774–775; June 7, 1947.) The electric field, produced by a pulsed 25-centimeter magnetron, having recurrence frequency 100 per second pulse width 1 microsecond, and peak power 200 killowatts, is fed to dees by a Lecher wire system. The dees are 2 centimeters deep, have a radius of 5 centimeters and contain a tungsten filament and a target. The focusing static field is 425 gauss and the dynamic field 300 gauss at the peak of a sinusoidal 250-kc. oscillation. Absorption curves show that the inclusion of a dynamic field results in an increased X-ray yield of harder radiation.

621.384:621.396.611.4 207

Experiments in Multiple-Gap Linear Acceleration of Electrons—W. D. Allen and J. L. Symonds. (*Proc. Phys. Soc.*, vol. 59, pp. 622–629; July 1, 1947.) Design and construction details of a 3-stage cavity for the acceleration of electrons up to 0.85 Mev. The cavity is fed with power from a 500-kw. magnetron operating at λ 10 centimeters.

621.384.6 208

The Acceleration of Charged Particles to Very High Energies—M. L. Oliphant, J. S. Gooden, and G. S. Hide. (*Proc. Phys. Soc.*, vol. 59, pp. 666–677; July 1, 1947.) A synchrotron is being built at Birmingham University to accelerate protons to 1000 Mev. The advantages of the technique and the design of the magnet and its excitation are described in detail. Electron energies up to 300 to 400 Mev. are possible, higher energies being prevented by radiation loss. For proton energies above 10^{10} e.v., the cost of this method would be prohibitive. For theory see 209 below.

621.384.6 209

Theory of the Proton Synchrotron—J. S. Gooden, H. H. Jensen, and J. L. Symonds. (*Proc. Phys. Soc.*, vol. 59, pp. 677–693; July 1, 1947.) The phase oscillations of an accelerated particle are analysed for the nonrelativistic and the relativistic cases. The influence and control of the eight significant forces on the oscillation amplitude are discussed. Injection and the consequent radial oscillations are considered. Numerical data and graphs for the case of the Birmingham synchrotron (208 above) are given.

621.385.832 210

A Memory Tube—Haeff. (*See* 326.)

621.385.833 211

The Design and Construction of an Electron Microscope—M. E. Haine. (*Engineering* (London), vol. 164, pp. 20–24; July 4, 1947.) Long summary of I.E.E. Measurements Section paper giving details of the Metropolitan-Vickers Type EM2 electron microscope. The general construction, the procedure for aligning the electron gun and magnetic lenses, and the operating and photographic techniques are described in detail. The instrument is continuously pumped, uses an accelerating voltage of 25–50 kv. and gives a magnification of 10,000 diameters.

621.385.833 212

Improvements in the Electrostatic Microscope—H. Bruck and P. Grivet. (*Ann. Radioélec.*, vol. 2, pp. 244–248; July, 1947. In English.) Details of a smaller power unit, a new design of Wehnelt cylinder and anode, and a focusing system involving no mechanical movement. See also 3706 of 1946 and 3236 of 1947.

621.385.833 213

A New Electron Microscope with Continuously Variable Magnification—J. B. le Poole. (*Philips Tech. Rev.*, vol. 9, pp. 33–45; 1947.) An electron microscope constructed at Delft in 1944 is fully described and compared with previous models. Its resolving power is 25 Å and its magnification is continuouslly variable from 1000 to 80,000 diameters. Various applications are mentioned.

621.385.833 214

Influence of Mechanical Defect of the Objectives on the Resolving Power of the Electrostatic Microscope—F. Bertein, H. Bruck, and P. Grivet. (*Ann. Radioélec.*, vol. 2, pp. 249–252; July, 1947. In English.) A mathematical analysis of the dependence of resolving power upon aberration constant, two values of which correspond to (a) ellipticity defects and (b) off-center defects. See also 3236, 3238, 3613, and 3614 of 1947.

621.385.833 215

A Space-Charge Lens for the Focusing of Ion Beams—D. Gabor. (*Nature* (London), vol. 160, pp. 89–90; July 19, 1947.) Suggested design for a powerful concentrating lens for positive ions, particularly those of extreme energy. Means are described for maintaining a suitable space charge inside a hollow cylinder using electrons derived from an auxiliary ring-shaped cathode. The focal length of the lens is expected to increase only linearly with the energy of the ion beam, and the design should enable lenses of relatively short focal length to be made.

621.385.833 216

Spherical Aberration of Compound Magnetic Lenses—L. Marton and K. Bol. (*Jour. Appl. Phys.*, vol. 18, pp. 522–529; June, 1947.)

621.386.1 217

X-Ray Tube with Very Bright Line Focus—M. Poittevin. (*Compt. Rend. Acad. Sci.* (Paris), vol. 224 pp 1709–1711; June 16, 1947.) Details of a tube with curved filament located in a groove cut across the face of a semicylindrical concentration piece. The apparent brightness is 30 k./mm.^{2} when the apparent dimensions of the focus are those of a square of side 0.1 mm.

621.396.9:623.26 218

Metal Locator with Remote Field Source—(*Beama Jour.*, vol. 54, p. 271; August, 1947.) Description and photograph of ERA Mine Locator No. 7. The magnetic field is generated by a cable fed by a.c. and laid on the ground in a large loop, instead of by the search unit. Therefore, its operating range is not limited by the magnetic properties of the ground.

621.396.9:623.454.25 219

The Radio Proximity Fuse—H. M. Bonner. (*Elec. Eng.*, vol. 66, pp. 888–893; September, 1947.)

623.978+550.838]:538.71 220

Air-Borne Magnetometers—E. P. Felch, L. G. Parratt, W. J. Means, L. H. Rumbaugh, T. Slonczewski, and A. J. Tickner. (*Elec. Eng.*, vol. 66, pp. 680–685; July, 1947.) An inductor with an open core of highly permeable and easily saturable material, such as permalloy, is placed in the unknown field, with a superposed sinusoidal magnetomotive force large enough to saturate the core. The time variation of the core flux induces an e.m.f. in a coil surrounding the core; this e.m.f. is fed into an electronic circuit and there analyzed. The sensitivity increases with the length of the core, but is limited by the highest impedance which can be maintained at the grid of the first tube with satisfactory stability. With a 1.5-inch length, the sensitivity exceeds 10 microvolts/γ ($1\gamma = 10^{-5}$ oersted). The detector-inductor is kept parallel to the magnetic field by the controlling action, through servomotors, of two auxiliary inductors. The apparatus records variations in the sum of the squares of the outputs of all three inductors, hence giving the variations of the unknown field. See also 3245 of 1947 (Shackelton).

621.365.5+621.365.92 221

Theory and Application of Radio-Frequency Heating [Book Review]—G. H. Brown, C. N. Hoyler, and R. A. Bierwirth. D. Van Nostrand, New York, 1947, 370 pp., $6.50. (*Electronics*, vol. 20, pp. 258, 260; September, 1947.)

621.38/.39].001.8 222

Electronic Developments [Book Review]—R. G. Britton. George Newnes, London, 206 pp., 7s. 6d. (*Electronic Eng.* (London), vol. 19, p. 268; August, 1947.) "This book will be of value even to those already acquainted with many applications of electronic science, and a well-balanced survey of such an important subject is something new in more than one sense."

PROPAGATION OF WAVES

538.566 223

Calculation of the Interaction between Two Particles from the Asymptotic Phase—C. E. Fröberg. (*Phys. Rev.*, vol. 72, pp. 519–520; September 15, 1947.) Proof that it is formally possible to calculate the potential from the asymptotic phase of a wave function. Convergence is not considered. A fuller account will appear in *Ark. Mat. Astr. Fys.*

538.566:621.396.11 224

The Field of a Microwave Dipole Antenna in the Vicinity of the Horizon—C. L. Pekeris. (*Jour. Appl. Phys.*, vol. 18, pp. 667–680; July, 1947.) Three cases are treated in which the transmitter or receiver is either on the ground or elevated. For very short waves, the field at points on the horizon approaches that of the direct wave diffracted by a straight edge at the point of tangency. The results are compared graphically with the exact theory of van der Pol and Bremmer (2249 of 1939 and back references). When both transmitter and receiver are on the ground, the potential can be expressed as the sum of a surface wave for a flat earth and an integral depending upon the earth radius, these two terms tending to cancel at large distances.

538.566.2 225

The Structure of an Electromagnetic Field in the Neighbourhood of a Cusp of a Caustic—T. Pearcey. (*Phil. Mag.*, vol. 37, pp. 311–317; May, 1946.) "A detailed mathematical and numerical study of the field structure at and near a line focus of a cylindrical electromagnetic wave train possessing any finite amount of cylindrical aberration of the first order."

621.396.11 226

A Method for Calculating Electric Field Strength in the Interference Region—H. E. Newell, Jr., (Proc. I.R.E., vol. 35, p. 777; August, 1947.) Brief summary only. For an interference region, over a spherical earth, which has an effective radius equal to four-thirds that of the earth. The accuracy is limited by the great number of graphical steps involved, but the procedure has given "very useful working estimates."

621.396.11 227

Circularly Polarized Waves Give Better F.M. Service Area Coverage—T. B. Friedman. (*Tele-Tech.*, vol. 6, pp. 26–30, 102; August, 1947.) A discussion of the theory and practical applications of circularly polarized radiation, and its advantages in certain cases of f.m. reception.

621.396.11:551.510.535 228
Some Observations of the Maximum Frequency of Radio Communication over Distances of 1000 km and 2400 km—W. J. G. Beynon. (*Proc. Phys. Soc.*, vol. 59, pp. 521–534; July 1, 1947. Discussion, p. 535.) The maximum usable frequencies for radio transmission from short-wave broadcasting stations near Berlin and Moscow were deduced from observations at Slough of the field strength variations around sunrise and sunset. The results were compared with theoretical values deduced from vertical-incidence ionospheric measurements at Slough and at Burghead (Scotland), and the mean discrepancies of the calculated values with respect to those observed were found to be −3 per cent for Berlin and −11 per cent for Moscow.

A discussion is given of the factors involved in applying vertical incidence ionospheric data to oblique incidence transmission, and it is concluded that the main source of the discrepancy lay in the inadequate knowledge of ionospheric conditions at the midpoint of the trajectory.

621.396.11:551.510.535 229
A Frequency Prediction Service for Southern Africa—F. J. Hewitt, J. Hewitt, and T. L. Wadley. (*Trans. S. Afr. Inst. Elec. Eng.*, vol. 38, part 7, pp. 180–193; July, 1947. Discussion, pp. 193–197.) A discussion of existing facilities and the proposed short-term predictions of ionospheric disturbances. The nature of the observed data and the prediction methods are described. As local data over a number of years do not exist, back data from Australian records are used, suitably modified according to present observations in South Africa. A new design of recorder uses a double superheterodyne transmitter-receiver. The frequency is swept from a few hundred kilocycles to 20 Mc. in one band; the only moving part is the rotor of the main sweeping oscillator. Automatic frequency calibration is provided. The complete sweep takes 10 seconds and the display on a long afterglow c.r. tube is suitable for visual or fully automatic photographic recording.

621.396.11:551.510.535 230
How Daytime Skywave Reflections Affect Cleared Channels—(*Tele-Tech*, vol. 6, pp. 45–47; August, 1947.) Report on a conference organized by the F.C.C. at which evidence was produced suggesting that day-time sky-wave reflections could cause interference in the 550 to 1600 kc. band. Little information was available as to why this occurred.

621.396.81:621.396.712 231
A Developmental F.M. Broadcast Station—Honnell. (*See* 269.)

621.396.812.3:621.397.5:551.594.21 232
Television and Thunderstorms—E. G. Hill. (*Wireless World*, vol. 53, p. 344; September, 1947.) Increased television signal intensity from a station 90 miles away, two or three hours prior to a thunderstorm, has been observed.

RECEPTION

621.396.61/.621:621.396.931 233
F.M. Receiver Design for Rail Radio Service—Martin. (*See* 309.)

621.396.61/.621].029.6 234
Transmitter-Receiver, 280–330 Mc/s.—Dieutegard. (*See* 308.)

621.396.619+621.396.621.54 235
Heterodyning and Modulation—C. J. Mitchell. (*Wireless World*, vol. 53, p. 359; October, 1947.) A simplified comparison of additive and multiplicative mixing, indicating that both frequency changing and modulation are multiplicative processes, irrespective of the method employed

621.396.619:621.396.662 236
Design of Tuners for A.M. and F.M.—L. M. Hershey. (*Tele-Tech*, vol. 6, pp. 58–59, 95; August, 1947.) "Automatic frequency control, using dual triode as oscillator and reactance tube corrects for mistuning and drift; push-button tuning." See also 237 below.

621.396.619.13:621.396.621 237
F.M. Reception Problems and Their Solution—(*Electronics*, vol. 20, pp. 108–113; September, 1947.) A summary of the following I.R.E. Section papers. Antennas for F.M. Receivers, by N. W. Aram. R.F., I.F. and A.F.C. Circuits, by L. M. Hershey. Limiters and Frequency Detectors, by M. Hobbs.

621.396.621+621.396.69 238
British Printed and Sprayed Circuits—(*Tele-Tech*, vol. 6, pp. 52–53, 97; August, 1947.) Summary of 1913 of 1947 (Sargrove).

621.396.621 239
Adjustable-Bandwidth F.M. Discriminator—W. G. Tuller and T. P. Cheatham, Jr. (*Electronics*, vol. 20, pp. 117–119; September, 1947.) The performance of a Foster-Seeley discriminator (2543 of 1937), in which the conventional pentode drive is replaced by a cathode follower, is analyzed and discussed. 4 to 1 variation of bandwidth is readily obtained, and the normalized output is independent of bandwidth. The arrangement is, however, liable to be less sensitive than the pentode drive for large derivations, and larger bandwidths are required for a given amount of distortion. Experimental results and a circuit operating on 60 Mc. are given.

621.396.621 240
Cathode-Coupled Converters for Surplus Receivers—J. H. Bender. (*QST*, vol. 31, pp. 37–42; August, 1947.) A single-tube crystal-controlled adaptor for 28 Mc.; the principle can be extended to higher frequencies. The tuning controls and calibration of the BC-779 receiver remain unaltered. A twin triode in the converter acts as a fixed tuned-oscillator mixer. Its output is cathode-coupled to the receiver, which then functions as a tunable i.f. amplifier.

621.396.621:371.3 241
Broadcast Reception for Schools—(*Wireless World*, vol. 53, pp. 327–329; September, 1947.) A description of an "approved" installation. The power amplifiers are capable of 20 watts output, although an output of 300 milliwatts is found to be sufficient for one classroom. The effective frequency range of the installation including the loudspeaker, is 60 to 8000 c.p.s.

621.396.621:629.114.6 242
Radio Receivers for Motor Vehicles—G. Giniaux. (*T.S.F. Pour Tous*, vol. 23, pp. 151–155; July to August, 1947.) A general account of typical rotary-converter and vibrator h.v. supplies, aerials, noise suppressors, etc., with brief particulars of a number of commercial sets.

621.396.621.001.4:621.317.755 243
Qualities and Defects of Alignment by the Oscilloscope—Bernhardt. (*See* 184.)

621.396.621.029.62+621.396.662.029.62 244
Design of F.M. Receiver Front Ends—A. R. Miccioli and D. Pollack. (*Tele-Tech*, vol. 6, pp. 40–43; July, 1947.) Development of tuners and methods of reducing frequency drift of local oscillators. See also 3259 of 1947 (Miner).

621.396.621.029.62 245
Experimental Findings in Connection with the Design of V.H.F. Frequency-Modulation Receivers—R. S. Zucker. (Proc. I.R.E. (Australia), vol. 8, pp. 19–24; June, 1947.) Data obtained from actual practical experience are applied to specific problems encountered in the various stages. No systematic general treatment is attempted.

621.396.621.029.62 246
Harvey Double Superheterodyne F.M. Receiver—B. J. Cosman and A. W. Richardson. (*FM and Telev.*, vol. 7, pp. 21–24, 52; June, 1947.) Circuit details and description of a commercial receiver covering the frequency range 85 to 115 Mc. with a bandwidth of 250 kc. Limiter action occurs at 1 microvolt aerial input and the i.f. frequencies are 10.7 Mc. and 4.6 Mc., the latter being crystal controlled. Audio amplifier response is linear from 20 to 15,000 c.p.s.

621.396.621.53 247
Simple Converter-Preselector—F. C. Jones (*CQ*, vol. 3, pp. 31–34, 70; June, 1947.) "A unit to give broadcast band, 15- 10- and 6-meter coverage, as well as preselection on other bands, for a receiver with limited tuning range."

621.396.622.71 248
Ratio Detector for F.M. Signals—(*Tele-Tech*, vol. 6, pp. 46–49; July, 1947.) Modifications to the balanced discriminator circuit for conversion from f.m. to a.m. are described which make it independent of input amplitude variations due to fading, to multipath reflection effects, to selectivity effects in the r.f. or i.f. stages or to unbalances in the detector itself. See also 3643 of 1947 (Seeley and Avins).

621.396.722 249
The Development of a Receiving Station for the B.B.C. Monitoring Service—R. D. A. Maurice and C. J. W. Hill. (*BBC Quart.*, vol. 2, pp. 105–128; July, 1947.) A detailed description with circuit diagrams and photographs of the war-time development of the B.B.C. monitoring receiving stations first at Evesham, and later at Caversham and Crowsley. The object of the service was to listen to all forms of foreign broadcast, and distribute the information obtained to Government departments. At Evesham the stronger signals were received by omnidirectional aerials, amplified, and conveyed by buried coaxial cables to receivers remotely located in a region relatively free from interference; directive aerials were used for the weaker, long-distance signals. At Caversham and Crowsley an improved "amplified aerial system" supplied over 100 receivers; 8 wide-band octave amplifiers fed 3 coaxial lines so that the frequency bands on any one line were at least 2 octaves apart.

621.396.722:621.396.65 250
A Traffic Receiver: The RECRO 451—Juillet. (*See* 264.)

621.396.822:538.523 251
Electromagnetic Background Noise due to Sea Waves—Y. Rocard. (*Compt. Rend. Acad. Sci.*, (Paris), vol. 225, pp. 50–51; July 7, 1947.) Sea waves may give rise to such noise owing to the periodic motion of their conductive elements in the earth's magnetic field. The effect may be appreciable for l.f. reception; its magnitude is calculated approximately.

621.396.822:621.317.755 252
Random Fluctuations in a Cathode Ray Oscillograph—N. R. Campbell and V. J. Francis. (*Phil. Mag.*, vol. 37, pp. 289–310; May, 1946.) A mathematical paper. The basis for the treatment employed is that noise is the resultant of superposed effects of events that occur at random times. The chance $W(y)dy$ is calculated that the deflection of the trace at a snap reading is between y and $y+dy$. The mean frequency with which the trace cuts a given level, and the mean frequency of "peaks" and "troughs" at a given level, are calculated. The intractable problem of determining the duration of a "hill" above a given level is discussed. A final section briefly indicates a possible method of representing the reaction between any steady signal present and the noise. See also 1037 of 1946.

621.396.823 253

Ignition Interference: Part 1. Its Nature, Magnitude and Measurement—W. Nethercot. (*Wireless World*, vol. 53, pp. 352–357; October 1947.) A comprehensive account of unpublished reports by the Electrical Research Association on the mechanism of the ignition spark and the field strength of the radiation. Curves and tables are given of the variation of field strength with frequency up to 650 Mc., distance, azimuth, and polarization. Factors affecting the fundamental radiation, such as the position and length of the ignition leads, are discussed. See also 4020 of January (Turney).

621.396.828 254

Curing Interference to Television Reception—M. Seybold. (*QST*, vol. 31, pp. 19–23, 110; August, 1947.) A detailed account of methods of harmonic suppression applied to a 14-Mc. transmitter to improve a neighbor's television reception. Full-power transmitter operation was subsequently possible.

621.396.828:621.396.1 255

Installations for Improved Broadcast Reception—P. Cornelius and J. Van Slooten. (*Philips Tech. Rev.*, vol. 9, pp. 55–63; 1947.) A method of diversity reception is used to eliminate selective fading. Three identical sets of receiving equipment are situated about 2 kilometers apart. Voltages E_1, E_2, and E_3, which increase with the signal strength, are fed from each of the receivers to the corresponding tubes V_1, V_2 and V_3 of a three-tube switching circuit of the Eccles-Jordan type, of which a diagram is given. If E_1 is the greatest of the voltages, the switching circuit is only stable with V_1 carrying a high anode current and V_2 and V_3 carrying practically no anode current.

Interference from other transmitters on neighboring frequencies is counteracted by using directive frame aerials. The freedom from disturbance thus obtained enables the bandwidth of the receiving set to be increased, thus improving the quality of the reproduction.

621.396.621.004.67 256

Most-Often-Needed 1947 Radio Diagrams and Servicing Information [Book Review]—M. N. Beitman (Ed.). Supreme Publications, Chicago, 1947, 189 pp., $2.00. (PROC. I.R.E., vol. 35, p. 806; August, 1947.) Continuation of 1056 of 1947. The period covered is the latter part of 1946 and early 1947.

STATIONS AND COMMUNICATION SYSTEMS

621.395.43:621.392.029.64 257

The Exploitation of Micro-Waves for Trunk Wave-Guide Multi-Channel Communications—H. M. Barlow. (*Jour. Brit. I.R.E.*, vol. 7, pp. 251–257; October, 1947. Discussion, pp. 257–258.) The use of the H_{01} waves in a cylindrical waveguide at 40,000 Mc. is suggested. Attenuation would be about 6 db per mile, making repeaters at 8-mile intervals necessary when using a 1.5-inch diameter copper waveguide. The repeaters would convert the carrier to a lower frequency and, after amplification, use this signal to remodulate a new carrier on 40,000 Mc. Thousands of speech channels on a single waveguide would be possible.

The waveguide might also be used as a 132-kv., 50-c.p.s. power line.

621.395.43:621.396.619.16 258

Pulse Code Modulation Method for Multi-Channel Telephony—R. R. Batcher. (*Tele-Tech*, vol. 6, pp. 28–33; July, 1947.) Description of a system of modulation in which the variations of amplitude of the speech wave control the amplitude of short pulses at a sampling rate that will give at least two pulses per cycle at the highest audio frequency, but many more at the lowest. The pulse amplitude variations are transmitted over the system by a special five-digit code permitting the handling of 32 levels. Coding and decoding methods are described. The system is stated to be distortionless and free from cumulative noise effects on long circuits. For another account of this system by H. S. Black, see *Bell Lab. Rec.*, vol. 25, pp. 265–269; July, 1947.

621.396(99) 259

Electronics in the Antarctic—H. C. Bailey. (*Electronics*, vol. 20, pp. 82–88; August, 1947.) An account of the apparatus used and the difficulties met on a United States Navy expedition. Includes radar and sonar for ships among icebergs, radar and G.C.A. (ground controlled approach) for air navigation, radio for communications and broadcasting, teletype and radio-photo and an airborne magnetometer for aerial surveying.

621.396.611.21:621.316.726.078.3:621.396.712 260

The Problem of Synchronization in Broadcasting Networks—M. Toussaint and A. Sev. (*Ann. Radioélec.*, vol. 2, pp. 253–269; July, 1947.) A general discussion, with a critical examination of the different factors affecting the stability of a quartz oscillator. The synchronization equipment of the Société Française Radioélectrique is described. This uses crystals of frequency between 90 and 130 kc. with suitable multiplication stages, and a frequency stability of the order of 10^{-8} is achieved by use of a novel thermostat. Control apparatus for aligning a slave station to the network master frequency with high accuracy uses a stroboscopic phase-meter.

621.396.619.11/.13:621.396.97 261

The Relative Merits of Frequency Modulation and Amplitude Modulation as Applied to a Broadcasting Service—B. J. Stevens and E. J. Middleton. (*Trans. S. Afr. Inst. Elec. Eng.*, vol. 38, pp. 141–157; May, 1947. Discussion, pp. 157–162.) A comprehensive review of the two types of modulation is followed by some details of the development of f.m. broadcast equipment by the South African Broadcasting Corporation.

621.396.65 262

Mobile V.H.F. Radio Telephone—(*Electrician*, vol. 139, p. 117; July 11, 1947.) A description of a single-unit transmitter-receiver having a maximum current consumption of 10 amperes from a 12-volt heavy duty battery and output of 6 watts on any limited frequency band in the v.h.f. range. Either a.m. or f.m. can be used. The equipment weighs 16 and two thirds pounds, and its overall dimensions are 9 and three quarter inches by 7 and three quarter inches by 8 inches.

621.396.65 263

A Frequency-Modulated Multi-Channel V.H.F. Radio Link—E. S. Teltscher. (*Electronic Eng.* (London), vol. 19, pp. 256–258; August, 1947.) A f.m. adaptor is used in place of the ordinary modulator, in order to obtain a higher degree of linearity and reduce cross talk between the channels.

621.396.65:621.396.722 264

A Traffic Receiver: The RECRO 451—M. Juillet. (*Ann. Radioélec.*, vol. 2, pp. 270–282; July, 1947.) The functions of a central receiving station for long-distance radiotelephony and radiotelegraphy are outlined and an account is given of diversity receiving equipment constructed by the Société Française Radioélectrique.

621.396.65:621.397.5 265

Television Extensions—(*See* 297.)

621.396.65.029.64 266

Early Centimetre-Wave Communication Systems—J. C. Dix. (*Engineering* (London), vol. 163, p. 489; June 13, 1947.) A brief outline of development up to 1941, including a 15-mile 9-centimeter R/T land link used for joint research by the Admiralty Signal Establishment and the G.E.C. in 1941, and Army Wireless Set No. 10.

621.396.712 267

Modern A.M. Broadcast Station Arrangement—(*Tele-Tech*, vol. 6, pp. 38–39; July, 1947.) Illustrations of the 50-kw. equipment at Omaha.

621.396.712:621.396.61 268

Mountain-Top F.M. Installation—M. Cady. (*Communications*, vol. 27, pp. 12–13, 39; July, 1947.) Description of the installation of a 3-kw. transmitting station with 3-bay turnstile aerial on top of a mountain. Results of preliminary trials are given.

621.396.712:621.396.81 269

A Developmental F.M. Broadcast Station—M. A. Honnell. (*Communications*, vol. 27, pp. 20–21; July, 1947.) A 1-kw. 99-Mc. experimental aerial was placed on a 45-foot tower 1080 feet above sea level. Propagation measurements to determine f.m. coverage are still in progress; the area is wooded and hilly.

621.396.721+621.395.623.8]:625.232 270

Passenger Entertainment Systems for Railroad Use—J. A. Curtis. (*Tele-Tech.*, vol. 6, pp. 34–37, 97; July, 1947.) Equipment giving radio or wire recorder programs and train announcements.

621.396.86:621.397 271

Secret Message Transmission by Facsimile—(*Telegr. Teleph. Age*, vol. 65, pp. 8–30; August, 1947.) Secrecy is achieved by "scrambling" the transmission, the scanning drum being driven at varying speeds by a synchronous motor which follows frequency variations in the supply current. The scrambler frequency generator consists of three chopper disks or wheels driven at constant but different speeds. Each chopper wheel has a series of perforations whose spacing determines the frequency of impulse pickup in associated photoelectric cells. The outputs from these cells are mixed and multiplied to obtain a mean frequency of 1800 c.p.s., giving a supply current which may be used to drive the scanning drum either for scrambling or unscrambling.

621.396.931/.932 272

Mobile Radio-Telephone—(*Wireless World*, vol. 53, p. 357; October, 1947.) For police and fire services. The compact a.m. unit receives power from a 12-volt car battery, and the transmitter has an output of 10 watts in the 78- to 100-Mc. band. The receiver is a pre-tuned double superheterodyne using the fundamental and the third harmonic of a crystal oscillator, the first i.f. being about 45 Mc. and the second i.f. 5 Mc.; bandwidth is 50 kc. at −3 db, to permit reception of transmissions from several headquarters in different locations on slightly different frequencies using a common modulation source. The same receiver with a different power unit is used for the fixed headquarters' installation, where the transmitter delivers about 50 watts r.f. to the aerial. See also *Elec. Rev.* (London), vol. 141, p. 174; August 1, 1947; *Engineering*, (London), vol. 164, p. 138; August 8, 1947, and 2246 of 1947 (Austin).

621.396.931/.932 273

Two-Way Broadcast Via Train-to-Station to Ship-at-Sea Link—D. E. Noble (*Communications*, vol. 27, pp. 8–11; July, 1947.) Description of a v.h.f. link used between a

train and a radio station for the purpose of a broadcast from the train to a ship at sea. A phase-modulated duplex system working on frequencies in the region of 160 Mc. was used and contact was maintained for distances up to 15 miles from the radio station.

621.396.931.029.62 274
Mobile F.M. Communications Equipment for 30 to 44 Mc/s: Part 2—R. B. Hoffman and E. W. Markow. (*Communications*, vol. 27, pp. 34–35; August, 1947.) Conclusion of 3665 of 1947.

621.396.933:621.398 275
Telecontrol of Aeradio Ground Station Receivers—J. E. Benson and W. A. Colebrook. (PROC. I.R.E. (Australia), vol. 8, pp. 8–15; June, 1947.) A general discussion of radio communication services for civil aviation was given by Newstead (3425 of 1946). A crystal locked 3-channel telecontroled receiver installation operating in the 0.3-, 3-, and 6-Mc. frequency bands is described. The outputs from the receivers are conveyed over three independent telephone lines which also serve for the d.c. potentials used for switching from c.w. to speech, and for switching on and off the power supply and preset test oscillator.

SUBSIDIARY APPARATUS

621-526:621.396.615.14 276
Automatic Frequency Control of Microwave Oscillators—V. C. Rideout. (PROC. I.R.E., vol. 35, pp. 767–771; August, 1947.) A technique applicable to any type of tunable microwave oscillator is described. In this method, a servomechanism is used which includes a waveguide discriminator circuit, a mercury-contact relay which vibrates at 60 c.p.s and is used to convert the discriminator output into 60-c.p.s. square waves, a 60-c.p.s. amplifier and a small 2-phase induction motor. A stability of 1 part in 50,000 is obtainable. The application of the technique to microwave repeater operation is described.

621.314.58 277
A D.C. Mains-Operated Vibratory Inverter—E. E. Cornelius. (PROC. I.R.E. (Australia), vol. 8, pp. 16–18; June, 1947.) Using the potential gradient across a charging capacitor in opposition to the applied voltage, and a suitable *LC* product to conform to the vibrator frequency, the potential applied across the contacts of a vibrator can be reduced to a low value before contact break, minimising arcing, and enabling vibrators to be used on power-supply voltages.

An interference-free unit has been constructed on this principle, to operate from 220-volts d.c. mains and to provide 500 watts of a.c. energy at 250 volts. The conversion efficiency was 65 to 80 per cent over the operating range of load resistance. R.f. interference was easily suppressed to a level adequate for the operation of a commercial communications receiver at maximum sensitivity on all bands, with the remaining noise down to residual receiver noise level.

621.317.722.1.076.8 278
An Inductively Coupled Degenerative High Voltage Stabilizer—R. Pepinsky and P. Jarmotz. (*Phys. Rev.*, vol. 72, p. 529; September 15, 1947.) Summary of Amer. Phys. Soc. paper. The d.c. connection between the series-tube grid circuit and the input error voltage leads to insulation problems in very-high-voltage supplies. These are overcome by allowing the control amplifier to modulate a 2-Mc. oscillator whose output passes through a transformer before being rectified and applied to the grid of the series tube. The transformer is designed to withstand the required high voltage across the windings.

621.318.572 279
An Electronic Multicircuit Breaker—G. D. Hanchett, Jr. (*QST*, vol. 31, pp. 34–36; August, 1947.) Simple overload protection for transmitting gear.

621.318.572:621.398 280
R.F. Operated Remote Control Relay—D. G. Fink. (*Electronics*, vol. 20, pp. 114–116; September, 1947.) The relay, which consumes no stand-by power, responds directly to the current in a receiving aerial. It closes on 8 to 10 mv., r.f. It is operated by a tuned circuit and crystal, and actuates a power relay. It can be used at unattended stations or as a carrier-failure alarm.

621.396.68 281
The Characteristics of Power Supplies for Radio Transmitters—W. E. Pannett. (*Marconi Rev.*, vol. 10, pp. 33–40; April to June, 1947.) "Discusses the nature of the load of a radio transmitter on the source of power supply, and the economics involved in the provision of power from supply mains or generating plant. An analysis is made of the effects of voltage and frequency variations and cyclic disturbance on the performance of transmitter equipment. From these considerations, suitable tolerances of the supply characteristics are deduced for various classes of transmission."

621.396.68:621.314.222 282
The Theory and Practice of Constant Voltage Transformers for Radio Power Supplies: Part 1—R. H. Burdick. (*Marconi Rev.*, vol. 10, pp. 59–71; April to June, 1947.) The reasons for using constant voltage transformers are discussed. The use of a bucking winding, to reduce the operating flux density for the saturated iron-cored reactors required for these transformers, is explained. The effect of the ratio of the bucking winding to the main winding on the stabilized output voltage is considered and a series capacitor scheme is outlined. For constant voltage operation, the product $\mu_{ac}H_{rms}$ is constant. For the stabilized condition, the secondary voltage is independent of the number of primary turns. The effect of frequency is indicated. Types of iron circuit and typical loss figures are reviewed. Power factor control is shown to depend on the number of primary turns.

621.396.682:621.316.722.1 283
Low-Voltage [high current] Regulated Power Supplies—F. W. Smith, Jr., and M. C. Thienpont. (*Communications*, vol. 27, pp. 22, 43; July, 1947.) Voltage regulation obtained by feeding the output voltage back through a d.c. amplifier to control a saturable reactor in the a.c. input circuit. Characteristics of a 6-volt, 14-ampere supply are given.

621.396.682:621.316.722.1 284
Design of Regulated Power Source—L. L. Helterline, Jr., (*Tele-Tech*, vol. 6, pp. 63–65, 107, July, 1947.) A description of the Sorensen Nobatron stabilized d.c. supply device. A bridge circuit incorporating a mains-heated, temperature-limited diode in one arm is used, and voltage variations of the a.c. supply cause changes of grid potential in a beam power tube. The corresponding anode current changes vary the impedance of a transformer winding connected as part of a potential divider regulating the input to the metal rectifier. 0.5 per cent regulation and 1 per cent ripple voltage are claimed.

621.396.682:621.316.722.1 285
Voltage-Regulated Power Supplies—L. Mautner. (*Elec. Eng.*, vol. 66, pp. 894–900; September, 1947.) The basic series-type regulator circuit is analyzed; it can be regarded as a cathode follower. Methods of obtaining low internal impedance and low output ripple are discussed. Various typical reference-voltage connections and the necessity for a stable feedback amplifier are considered. Five circuits for specific applications are given, together with calculated performance data. See also 4046 of January (Koontz and Dilatush).

621.396.682:621.397.62 286
[5-kv] E.H.T. Supply for Television Receivers—C. H. Banthrope. (*Electronic Eng.* (London), vol. 19, p. 245; 1947.) The line-scan sawtooth wave form is applied to the control grid of a pentode. The sudden cutting off of the anode current at flyback causes a coil in the anode circuit to ring. The high oscillatory voltage generated is rectified by a diode whose heater power is provided by a small coil coupled magnetically to the ringing coil.

621.396.69 287
Maintenance Masts for B.B.C.—(*Engineer*, (London), vol. 184, p. 110; August 1, 1947.) A description of two transportable masts which may be quickly erected near permanent masts for use while maintenance work is done on the main installation. They are triangular, parallel sided, 300 feet high and insulated for 20 kv. r.m.s. There are 18 sections of total weight 4 and one-quarter tons including fittings.

778:621.396.619.23:621.396.96 288
Photographing Pulse Wave Shapes of Radar Modulators—L. W. Marks. (*Tele-Tech*, vol. 6, pp. 60–62; 103; July, 1947.) Small variations from the required shape of the output pulse of radar modulators may cause serious loss of power, double moding, misfiring, and frequency modulation of the associated transmitter. In production testing, the pulse wave shape is photographed for comparison with a standard to diagnose possible sources of trouble. Equipment for this purpose is described.

TELEVISION AND PHOTOTELEGRAPHY

621.397(73) 289
Facsimile is Ready for Home Use—M. B. Sleeper. (*FM and Telev.*, vol. 7, pp. 19–20, 55; June, 1947.) In America, facsimile is now commercially practicable, and transmission standards are required. A definition of 103 lines per inch and a paper speed of 3.43 inches per minute have been agreed upon and paper widths of 4.1 and 8.2 inches are proposed. Recorders using a width of 8.2 inches are expensive and require a flat frequency response range beyond that of the average f.m. set. Once a public facsimile service has been instituted, its use will spread rapidly.

621.397.26 290
V.H.F. Link for Press Photos—(*Electronics*, vol. 20, pp. 100–102; August, 1947.) A mobile equipment for picture transmission scanning at 90 lines per minute and using an 1800-c.p.s.a.m. tone for the picture gradations. Transmission time for a 5-inch by 7-inch photograph is about six minutes.

621.397.331.2 291
Improvements in Electronic Television Cameras—P. Hémardinquer. (*T.S.F. pour Tous*, vol. 23, pp. 163–165 and 191–193; July, August, and September, 1947.) Descriptions of the iconoscope or emitron, the super-emitron, the orthiconoscope, the image orthiconoscope and their mode of operation; also of the isoscope of Barthélemy and a method of modulation resembling somewhat the superheterodyne method used in radio receivers.

621.397.335 292
Sync Generator Frequency Stability and TV Remote Pickups—W. J. Poch. (*Communications*, vol. 27, pp. 14–39; July, 1947.) Locking the synchronizing generator to the power-supply system has advantages where power-supply frequency variation is small.

The generator can also be locked to a crystal oscillator; in this case, wire or radio links may be needed for maintaining a close relationship between vertical blanking signals. Pulse timing and amplitude during switching are also considered.

621.397.5 293

The Verdict of the F.C.C.—(*Télév. Franç.*, Supplement *Électronique*, p. 17; June, 1947.) (a) No color television for 5 years. (b) Immediate start of black-and-white television on the present line standard. (c) Laboratories are invited to continue research in order to achieve an absolutely flawless color television system.

621.397.5 294

The French [line] Standard—(*Télév. Franç.*, Supplement *Électronique*, p. 17; June, 1947.) The Comité Mixte de Télévision, at the session of May 28, 1947, has decided (a) to maintain for 10 years the present line standard for the Paris district and (b) to put into service in about 2 years a high-definition standard of about 1000 lines.

621.397.5:535.88 295

A New Television Projection System—W. E. Bradley and E. Traub. (*Electronics*, vol. 20, pp. 84–89; September, 1947.) Combination of a Schmidt optical system, a new fluorescent phosphor, directional viewing screen, and keystone projection, produces at 15 inch by 20 inch picture of exceptional brightness and contrast.

621.397.5:535.88:532.62 296

Theoretical Studies of the Use of Quasi-Insulating Ediophors for Large-Screen Television Projection—H. Thiemann. (*Schweiz. Arch. Angew. Wiss. Tech.*, vol. 13, pp. 147–154, 175–182, 210–217, and 239–252; May to August, 1947.) A continuation of previous work (3080 of 1941 and 1736 of 1942). The term eidophor is applied to a thin layer of a viscous fluid whose surface deformation can be used for television projection. The wiping out of the surface charges on the eidophor with the help of secondary emission is fully discussed and a general theory is presented of the electrohydrodynamical problems associated with the deformation of the surface of liquid eidophors of finite thickness. Picture production methods are described and stability conditions considered. See also 554 of 1947.

621.397.5:621.396.65 297

Television Extensions—(*Elec. Times*, vol. 111, p. 675; June 12, 1947.) A brief general description of the 1000-Mc. link, now under construction to carry normal 405-line, 50-frame per second signals from the Alexandra Palace to the relay station in Birmingham.

Three successive optical paths will be used, one of 20 miles and two of 40 miles, with 80-foot towers at the intermediate stations. For another account see *Elec. Rev.* (London), vol. 140, p. 984; June 13, 1947.

621.397.5:621.396.65 298

F.C.C. Studies TV Relays for Inter-City Network Systems—(*Tele-Tech*, vol. 6, pp. 34–37; August, 1947.) Report of conference organized by the F.C.C. Several links are already in operation, and the system between New York, Philadelphia, Pittsburgh, and Washington is practically complete. The New York-Chicago link of 900 miles will use 35 repeaters, and an aerial system operating uniformly over the band 3700 to 4200 Mc.

621.397.5:621.396.812.3:551.594.21 299

Television and Thunderstorms—Hill. (*See* 232.)

621.397.62 300

The R.C.A. Television Receiver Type 630—M. Chauvierre. (*Radio Franç.*, pp. 12–17; July, 1947.) An account of some of the principal features, with a complete circuit diagram. 13 stations having frequencies between 44 and 216 Mc. can be received.

621.397.62 301

The Philips [television] Receiver with Screen Projection—(*Radio Franç.*, p. 18; July, 1947.) A short description of the projection system and the h.v. supply unit.

621.397.62 302

Bush Television Model T91—(*Wireless World*, vol. 53, pp. 323–326; September, 1947.) Straight circuit for vision: superheterodyne for sound. Picture size is 7 and one half inches by 6 inches.

621.397.62 303

Build your Own Television Receiver—L. S. Wecker and T. Gootée. (*Radio News*, vol. 38, pp. 45–48, 139; August, 1947.) The construction and adjustment of a receiver covering all channels from 44 to 88 Mc., which can be built from the components and chassis of a war-surplus oscilloscope, Type BC-412, with a Type 5BP4 c.r. tube.

621.397.62 304

Television Receiver Construction: Part 8—(*Wireless World*, vol. 53, pp. 391–396; October, 1947.) Construction and assembly details. For previous parts see 4056 of January and back references.

621.397.62:621.314.67 305

Pulsed Rectifiers for Television Receivers—Maloff. (*See* 311.)

621.397.62.001.4:621.317.79 306

Visual Alignment of Television Receivers—Kronenberg. (*See* 192.)

TRANSMISSION

621.396.61:621.396.41 307

An Inexpensive Rig for Local Duplex Operation—D. D. Ralston. (*QST*, vol. 31, pp. 52–53; August, 1947.) Low-power equipment for R/T on 11 meter.

621.396.61/.621].029.6 308

Transmitter-Receiver, 280–330 Mc/s.—Dieutegard. (*Toute la Radio*, vol. 14, pp. 246–251; September, 1947.) Three distinct units are included: (a) the oscillator-detector, (b) the amplifier-modulator and (c) the supply unit. The oscillator uses an acorn tube, Type 955, and tuning is effected by Lecher lines with a variable bridge, the whole system being enclosed in a metal tube, with suitable coupling for the doublet aerial. Constructional and circuit details are given.

621.396.931:621.396.61/621 309

F.M. Receiver Design for Rail Radio Service—D. W. Martin. (*Communications*, vol. 27, pp. 14–17, 37; August, 1947.) Circuit details of a f.m. receiver-transmitter for use in the band 152 to 162 Mc. The receiver has a modified single superheterodyne circuit using half-frequency mixing to reduce reradiation and spurious responses. Special cone-wound coils are used in the temperature-compensated i.f. transformers. Figures are given for sensitivity and selectivity.

VACUUM TUBES AND THERMIONICS

537.533.8 310

Present State of Knowledge of Secondary Electron Emission from Solids—Palluel. (*See* 89.)

621.314.67:621.397.62 311

Pulsed Rectifiers for Television Receivers—I. G. Maloff. (*Electronics*, vol. 20, pp. 110–111; August, 1947.) "Brief analysis of pulsed cascade rectifiers used in television receivers indicates that no component is subjected to potentials substantially higher than those encountered per section. In a doubler, this voltage is about half the output voltage from the rectifier."

621.383.5 312

The Photoelectric Mechanism of Selenium Barrier Layer Elements—A. E. Sandström. (*Phil. Mag.*, vol. 37, pp. 347–356; May, 1946.) Mott's theory of the e.m.f. of oxide photoelements is applied to *Se* elements. See also 3593 of 1945.

621.385+621.396.694 313

Tube Registry—(*Electronics*, vol. 20, p. 232; August, 1947.) Characteristics of the 6AS6G pentode voltage amplifier and the 5594 xenon-filled thyratron. See also 3711 of 1947 and back references.

621.385.1.032.216 314

Rectification Characteristics of an Oxide Cathode Interface—W. E. Mutter. (*Phys. Rev.*, vol. 72, p. 531; September 15, 1947.) Summary of Amer. Phys. Soc. paper.

621.385.1.032.216 315

Some Electrical Properties of an Oxide Cathode Interface—A. Eisenstein. (*Phys. Rev.*, vol. 72, p. 531; September 15, 1947.) Summary of Amer. Phys. Soc. paper.

621.385.2.032.216:546.841-3 316

Thermionic Properties of Thoria—Wright. (*See* 141.)

621.385.1.032.22:621.317.789 317

A Calorimetric Method for Direct Measurement of Plate Dissipation—Squier. (*See* 188.)

621.385.831:537.533.8:621.397.6 318

Secondary-Emission Amplifier Tube—M. Chauvierre. (*Tele-Tech*, vol. 6, pp. 69–105; July, 1947.) A description of the construction and mode of operation of the EE 50 (Philips) single-stage, secondary-emission tube. Electrons from the cathode impinge upon the secondary-emission cathode; the secondary electrons constitute the anode current. The transconductance (14,000 micromhos) is considerably greater than that of a conventional tube. To prevent disturbance of the secondary-emission process by volatilization of the cathode, a screen is interposed between it and the secondary-emission cathode. The use of the tube in wide-band amplifiers is mentioned.

621.385.832 319

A Memory Tube—A. V. Haeff. (*Electronics*, vol. 20, pp. 80–83; September, 1947.) Operation is based on secondary emission. A pattern is first produced, then stored, and later scanned on a dielectric screen, each operation being performed by a separate electron beam. Uses include the three-dimensional presentation of radar data and the automatic recording and reproduction of transients.

MISCELLANEOUS

621.396 320

British Research in the Radio Field [Book Review]—Institution of Electrical Engineers, London, 1s. (*Electrician*, vol. 139, p. 396; August 8, 1947: *Beama-Jour.* vol. 54, p. 298; September, 1947.) A review of work at present in progress. The importance of effective coordination is stressed and it is recommended that a bureau should be set up, possibly under the Department of Scientific and Industrial Research, to disseminate details of research work.